Isoform-specific Modulation of Ventricular L-type Calcium Channels by Gαi Proteins in a Murine Model of Heart Failure

Inaugural Dissertation

zur

Erlangung des Doktorgrades

philosophiae doctor (PhD) in Health Sciences

der Medizinischen Fakultät

der Universität zu Köln

vorgelegt von

Nour Katnahji

aus Aleppo

(Digital Express [24], Köln)

2024

Betreuerin / Betreuer:	Prof. Dr. Jan Matthes
Gutachterin / Gutachter:	Prof. Dr. Stephan Rosenkranz
	PD Dr. Filomain Nguemo
Datum der Mündlichen Prüfung:	22.07.2024

For

Those whose hearts failed to accept a world full of

injustice, discrimination, and survival brains,

but they never stopped chasing the stars!

Ph.D. Dissertation
Center for Pharmacology
Institutes of Pharmacology I & II
Director: Univ. Prof. Dr. Dietmar Fischer
Faculty of Medicine and University Hospital Cologne
© 2024 Nour Katnahji

Table of Contents

List of Abbreviations & Acronyms viii
List of Figures x
List of Tables i
Graphical Abstract ii
Abstract iii
Zusammenfassung iv
1 **Introduction** 1
1.1 Heart Failure 1
1.1.1 Classification of heart failure 1
1.1.2 Etiology and pathophysiology of heart failure 2
1.2 β-adrenergic signaling in the heart 3
1.2.1 Cardiac β-adrenoceptors 3
1.2.2 Cardiac β-adrenergic signaling in heart failure 5
1.3 Heterotrimeric G-proteins 7
1.3.1 G-protein structure and signaling 7
1.3.2 Inhibitory G-proteins (Gi) and heart failure 9
1.3.3 Isoform-specific functions of $G\alpha_{i2}$ and $G\alpha_{i3}$ 11
1.4 Voltage-gated Calcium Channels 13
1.4.1 Definition and classification 13
1.4.2 Cardiac L-type calcium channels: Structure and kinetics 14
1.4.3 β-adrenergic regulation of cardiac calcium channels 16
1.4.4 L-type calcium channels and heart failure 17
1.5 Mouse Models and Study Aims 20
2 **Methods** 22
2.1 Mouse Models 22
2.1.1 Animal Care and Ethical Statement 22
2.1.2 Transgenic and Knock-out Mouse Models 22
2.1.3 Mouse Genotyping 23
2.2 Isolation of primary ventricular cardiomyocytes 24
2.2.1 Materials and Solutions 24
2.2.2 Myocyte Isolation 27
2.3 Patch-Clamp Electrophysiology 30
2.3.1 Whole-Cell Recordings of $I_{Ca,L}$ 31
2.3.2 Test-pulse Protocols and Data Analysis 36
2.3.3 Statistic 42
3 **Results** 43

3.1 Effects of β_1-adrenoceptor overexpression on ventricular $I_{Ca,L}$ ... 43
3.1.1 Basic characterization of ventricular $I_{Ca,L}$ in β_1-tg myocytes ... 43
3.1.2 Voltage dependence and rate of $I_{Ca,L}$ inactivation in β_1-tg mice ... 46
3.1.3 $I_{Ca,L}$ recovery from inactivation in β_1-tg myocytes ... 48
3.1.4 $I_{Ca,L}$ responsiveness to acute β-AR agonist stimulation in β_1-tg mice ... 50
3.2 Effects of $G\alpha_{i3}$ deficiency on the kinetics of $I_{Ca,L}$ in β_1-tg mice ... 52
3.2.1 LTCC activation and inactivation properties in β_1-tg/$G\alpha_{i3}^{-/-}$ mice ... 52
3.2.2 $I_{Ca,L}$ response to acute β-AR agonist stimulation in β_1-tg/$G\alpha_{i3}^{-/-}$ mice ... 54
3.2.3 Time constants and rate of basal $I_{Ca,L}$ inactivation in β_1-tg/$G\alpha_{i3}^{-/-}$ mice ... 56
3.2.4 Effects of isoproterenol on $I_{Ca,L}$ inactivation properties in β_1-tg and β_1-tg/$G\alpha_{i3}^{-/-}$ mice ... 57
3.2.5 Effects of $G\alpha_{i3}$ deficiency on basal $I_{Ca,L}$ recovery from inactivation in β_1-tg mice ... 59
3.3 Effects of $G\alpha_{i2}$ deficiency on the kinetics of $I_{Ca,L}$ in β_1-tg mice ... 62
3.3.1 LTCC activation and inactivation properties in β_1-tg/$G\alpha_{i2}^{-/-}$ mice ... 62
3.3.2 $I_{Ca,L}$ response to acute β-AR agonist stimulation in β_1-tg/$G\alpha_{i2}^{-/-}$ mice ... 64
3.3.3 Time constants and rate of basal $I_{Ca,L}$ inactivation in β_1-tg/$G\alpha_{i2}^{-/-}$ mice ... 66
3.3.4 Effects of isoproterenol on the $I_{Ca,L}$ inactivation properties in β_1-tg and β_1-tg/$G\alpha_{i2}^{-/-}$ mice ... 67
3.3.5 Effects of $G\alpha_{i2}$ deficiency on basal $I_{Ca,L}$ recovery from inactivation in β_1-tg mice ... 70
3.4 Testing of GPM-1: New potential Gαi-protein modulator ... 72
4 **Discussion** ... 74
4.1 L-type calcium channels in β-AR mediated heart failure ... 75
4.1.1 Altered $I_{Ca,L}$ preceded cardiac failure in β_1-tg mice ... 75
4.1.2 Reduced β-adrenergic response of $I_{Ca,L}$ in β_1-tg mice ... 77
4.2 Gi proteins in β-AR mediated heart failure ... 79
4.2.1 From earlier hypotheses to Gαi isoform-specific functions ... 79
4.2.2 $G\alpha_{i3}$ deficiency restores basal $I_{Ca,L}$ in β_1-tg myocytes, while β-AR responsiveness remains blunted 80
4.2.3 $G\alpha_{i2}$ deficiency affects $I_{Ca,L}$ gating properties in β_1-tg myocytes ... 82
4.3 Inhibitory G protein as therapeutic targets ... 84
4.4 Limitations of the Study ... 86
4.5 Future directions and Conclusions ... 86
Bibliography ... 88
Appendix ... 102
Acknowledgment ... 111
Erklärung ... 114
Curriculum Vitae ... 113

List of Abbreviations & Acronyms

AC	Adenyl Cyclase
ACC	American College of Cardiology
ADP	Adenosine diphosphate
AHA	American Heart Association
AKAP	A-Kinase Anchoring Protein
ANP	Atrial natriuretic peptide
AP	Action Potential
APA	American Psychological Association
approx.	approximately
AfCS	Alliance for Cellular Signaling
AR	Adrenoceptor
BBs	Betablockers
BNP	Brain natriuretic peptide
CA	Catecholamine
cAMP	Cyclic Adenosine monophosphate
CAD	Coronary Artery Disease
CaMKII	Calcium/Calmodulin-Dependent Protein Kinase II
CDI	Calcium-Dependent Inactivation
CICR	Ca^{2+}-Induced Ca^{2+} Release
Conc.	Concentration
CTX	Cholera toxin
DAD	Delayed-after Depolarization
DAG	Diacylglycerol
DCM	Dilated Cardiomyopathy
DCT	Distal C-terminus
DHP	Dihydropyridine
DMSO	Dimethyl Sulfoxide
EAD	Early-after Depolarization
ECC	Excitation-Contraction Coupling
EF	Ejection Fraction
EDV	End-diastolic Volume
EGTA	Ethylene Glycol-bis(β-aminoethyl ether)
ERK	Extracellular Signal-Regulated Kinases.
ESC	European Society of Cardiology
ERP	Effective Refractory Period
ESV	End-systolic Volume
FCS	Fetal Calf Serum
FDA	Food and Drug Administration
FVB/N	Friend Virus B NIH (mice strain)
HVA	High-Voltage-Activated
HF	Heart Failure
HFrEF	Heart failure with reduced ejection fraction
HFpEF	Heart failure with preserved ejection fraction
HFimEF	Heart failure with improved ejection fraction
$I_{Ca,L}$	L-Type Calcium Current

i.p.	Intraperitoneal
IP_3	Inositol Trisphosphate
IR	Ischemia Reperfusion
Iso	Isoproterenol (Isoprenaline)
GDI	Guanine nucleotide Dissociation Inhibitor
GDP	Guanosine diphosphate
GEM	Guanine nucleotide Exchange Modulator
GEF	Guanine nucleotide Exchange Factor
GIRK	G Protein-Gated Inwardly Rectifying K^+ Channels
GPCR	G Protein Coupled Receptor
GPM	G Protein Modulator
GRKs	G-Protein Receptors Kinase
GTP	Guanosine triphosphate
LTCC	L-Type Calcium Channel
LV	Left Ventricle
LVA	Low-Voltage-Activated
M-AChR	Muscarinic Acetylcholine Receptor
MEK	Mitogen-Activated Protein Kinase Kinase
MHC	Myosin Heavy-Chain
NPs	Natriuretic Peptides
NYHA	New York Heart Association
ns	Not significant
PKA	Protein Kinase A
PLB	Phsopholamban
PLC	Phospholipase C
PTX	Pertussis Toxin
RAAS	Renin-Angiotensin-Aldosterone System
Raf	Rapidly Accelerated Fibrosarcoma
Rat	Rat Sarcoma
Ref.	Reference
RG	Research Group
RGS	Regulators of G-Protein Signaling
RyRs	Ryanodine Receptors
SNS	Sympathetic Nervous System
SR	Sarcoplasmic Reticulum
SERCA2a	Sarcoplasmic/endoplasmic reticulum calcium-transporting ATPase
SSA	Steady-state activation
SSI	Steady-state inactivation
Suppl.	Supplements
TnI	Troponin I
VGCC	Voltage-Gated Calcium Channels
VDI	Voltage-Dependent Inactivation
WHO	World Health Organization
WT	Wild-Type

List of Figures

Fig. 1-1	Dual coupling of β_2-AR to Gs and Gi proteins	4
Fig. 1-2	Cardiac β-AR signaling in physiology and heart failure	6
Fig. 1-3	Signaling with G-proteins	7
Fig. 1-4	Overview of G-protein related disease	9
Fig. 1-5	Phylogeny of voltage gated Ca^{2+} channel α_1 subunits	14
Fig. 1-6	Proposed transmembrane topology and subunit composition of cardiac LTCC	15
Fig. 1-7	L-type calcium channel gating states and cardiac action potential	19
Fig. 1-8	Comparison of previous *in vivo* studies of this project	20
Fig. 2-1	Summary of cardiomyocyte isolations steps	25
Fig. 2-2	Examples of isolated cardiomyocytes and criteria for parch-clamp measurements	29
Fig. 2-3	Different configurations of patch-clamp	30
Fig. 2-4	Principal steps in conventional patch-clamp electrophysiology experiments	31
Fig. 2-5	Patch-clamp rig used for whole-cell recordings	32
Fig. 2-6	Schematic illustration of the test pulses producing different current responses during the steps of a whole-cell voltage clamp recording.	35
Fig. 2-7	Whole-cell recording scheme with isoproterenol	35
Fig. 2-8	Simplified scheme of different states of voltage gated Ca^{2+}channels	36
Fig. 2-9	Test pulse protocol for recording the L-type current	37
Fig. 2-10	$I_{Ca,L}$ decay and fit analysis models	39
Fig. 2-11	Test pulse protocol to measure steady-state $I_{Ca,L}$ inactivation	40
Fig. 2-12	Test pulse protocol to measure $I_{Ca,L}$ recovery from inactivation	41
Fig. 3-1	Characterization of whole-cell $I_{Ca,L}$ in β_1-tg mice in two different age groups	45
Fig. 3-2	Voltage dependence and rate of $I_{Ca,L}$ inactivation kinetics	47
Fig. 3-3	$I_{Ca,L}$ recovery from inactivation in β_1-tg mice in two different age groups	49
Fig. 3-4	Evaluation of the $I_{Ca,L}$ response to β-adrenergic stimulation in β_1-tg mice	51
Fig. 3-5	Effects of $G\alpha_{i3}$ deficiency on the voltage dependence of $I_{Ca,L}$ gating	53
Fig. 3-6	Effects of $G\alpha_{i3}$ deficiency on the $I_{Ca,L}$ response to isoproterenol	55
Fig. 3-7	Effects of $G\alpha_{i3}$ deficiency on the time courses of $I_{Ca,L}$ inactivation	57
Fig. 3-8	Effects of Isoproterenol on the $I_{Ca,L}$ inactivation rate in old mice	58
Fig. 3-9	Effects of Iso on the steady-state voltage-dependent inactivation ($G\alpha_{i3}^{-/-}$ effect)	60
Fig. 3-10	Effects of $G\alpha_{i3}$-deficiency on basal $I_{Ca,L}$ recovery from inactivation	61
Fig. 3-11	Effects of $G\alpha_{i2}$ deficiency on the voltage dependence of basal $I_{Ca,L}$ gating	63
Fig. 3-12	Effects of $G\alpha_{i2}$-deficiency on $I_{Ca,L}$ response to isoproterenol	65
Fig. 3-13	Effects of $G\alpha_{i2}$-deficiency on the time courses of $I_{Ca,L}$ inactivation	67
Fig. 3-14	Effects of Isoproterenol on the $I_{Ca,L}$ inactivation rate in young mice	68
Fig. 3-15	Effects of Iso on the steady-state voltage-dependent inactivation ($G\alpha_{i2}^{-/-}$ effect)	69
Fig. 3-16	Effects of $G\alpha_{i2}$-deficiency on basal $I_{Ca,L}$ recovery from inactivation	71
Fig. 3-17	Effects of GPM-1 peptide on $I_{Ca,L}$ activation properties	73
Fig. S1	Exemplary PCR-genotyping results	103
Fig. S2	Human Gi-αlpha-subunit structure and its amino sequence	104
Fig. S3	List of chemicals and suppliers	105
Fig. S5	Statistical analysis of all mono vs. bi-exponential events (basal)	107
Fig. S6	Statistical analysis of all mono vs. bi-exponential events (Iso)	108
Fig. S7	Preliminary results of the effect of $G\alpha_{i3}$ deficiency in young mice	109
Fig. S8	Preliminary results of the effect of $G\alpha_{i3}$ deficiency in young mice (recovery)	110
Fig. S9	Preliminary results of from $G\alpha_{i3}^{-/-}$ knockout mice	110

List of Tables

Table 1- 1. G-protein Classical Effectors and Available Modulators 8

Table 1- 2. Literature Review: Distinct functions of $G\alpha_{i2}$ and $G\alpha_{i3}$ in Murine Models of Cardiomyopathy 12

Table 2- 1. Primers for Mouse Genotyping 23

Table 2- 2. Perfusion Buffer (1X) – Ca^{2+}-free for Cardiomyocytes Isolation 26

Table 2- 3. Myocyte Digestion Buffer (50 ml/Heart) for Cardiomyocytes Isolation 26

Table 2- 4. Myocyte Stopping Buffer (50 ml/Heart) and Calcium Reintroduction Solutions 27

Table 2- 5. Heparin for i.p. injection 27

Table 2- 6. Equipment and Supplies for Myocyte Isolation 29

Table 2- 7. Patch-Clamp Equipment & Computer Software 32

Table 2- 8. Whole-cell $I_{Ca,L}$ Recording Solutions 33

Table 2- 9. Isoproterenol Stock Solution I, 1 m*M* 36

Table 2- 10. BN6 (GMP-1), Stock Solution, 1 m*M* 36

Table 3- 1. Descriptive statistics for basal $I_{Ca,L}$ electrophysiological properities in β_1-tg mice 44

Table 3- 2. Descriptive statistics for the inactivation time constants in β_1-tg mice, young *vs.* old 46

Table 3- 3. Descriptive statistics for $I_{Ca,L}$ recovery parameters in β_1-tg mice, young *vs.* old 48

Table 3- 4. Descriptive statistics for $I_{Ca,L}$ gating parameters in old mice, 3 groups 54

Table 3- 5. Descriptive statistics for the inactivation time constants in old mice, 3 groups 56

Table 3- 6. Descriptive statistics for the $I_{Ca,L}$ recovery parameters, old mice, 3 groups 61

Table 3- 7. Descriptive statistics for $I_{Ca,L}$ gating parameters, young mice, 3 gropus 64

Table 3- 8. Descriptive statistics for the inactivation time constants, young mice 3 groups 66

Table 3- 9. Descriptive statistics for the $I_{Ca,L}$ recovery parameters, young mice, 3 groups 70

Table 3- 10. Descriptive statistics for GPM-1 effects on $I_{Ca,L}$ gating parameters 72

Graphical Abstract

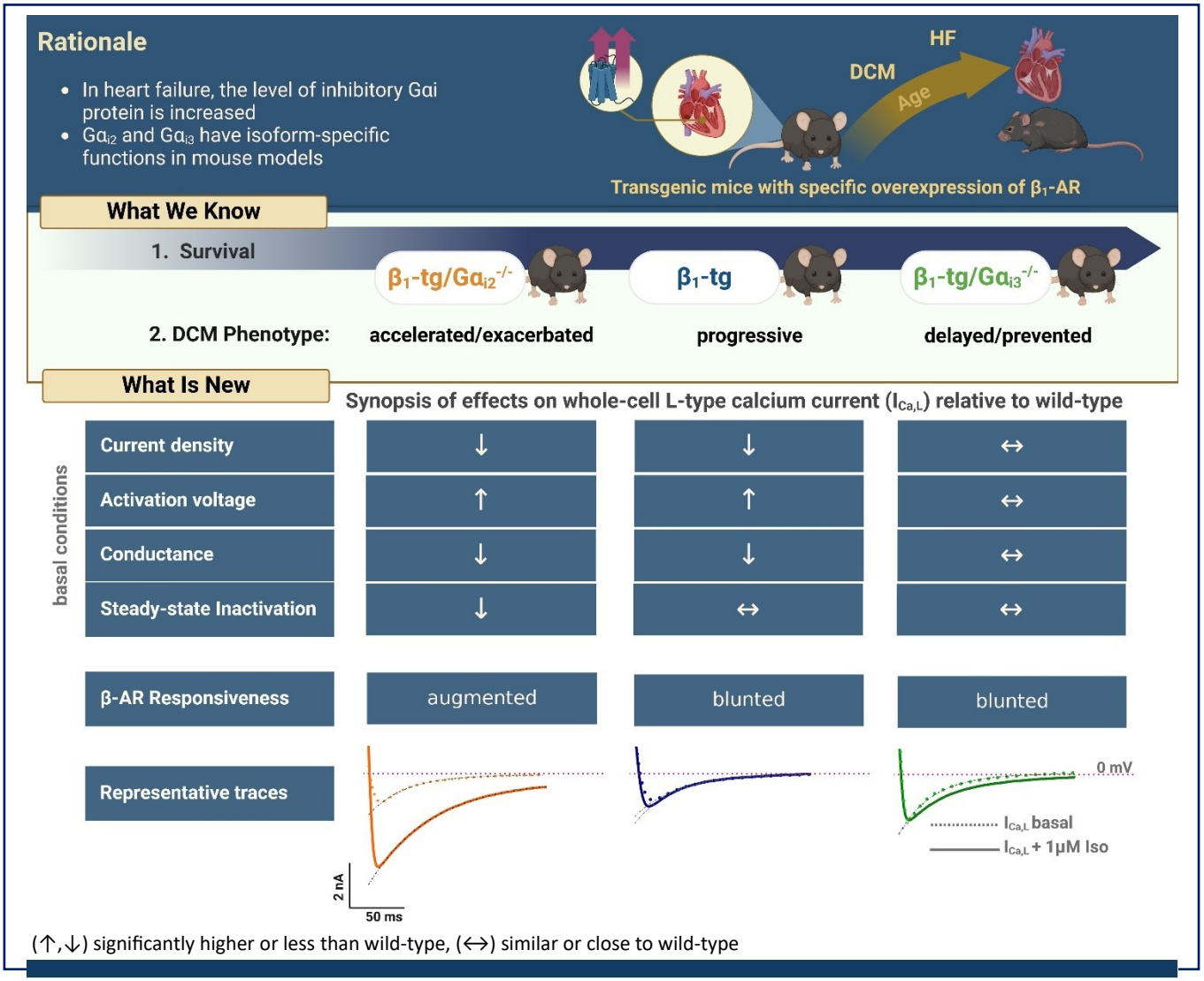

Keywords

● Inhibitory G protein (Gi) ● L-type calcium current ($I_{Ca,L}$) ● Heart failure (HF) ● Dilated cardiomyopathy (DCM) ● Isoproterenol (Iso)

Abstract

Background: Inhibitory G protein α-subunit is upregulated in heart failure (HF). In murine dilated cardiomyopathy induced by overexpression of the β_1-adrenoceptor in transgenic mice (β_1-tg), we have shown that $G\alpha_{i2}$ deficiency aggravated the cardiac dysfunction, while the absence of the closely related $G\alpha_{i3}$ had the opposite effect. The exact roles of these two Gi isoforms in failing cardiomyocytes are still unknown. As the L-type Ca^{2+} current ($I_{Ca,L}$) is altered in heart failure, this study aimed to investigate the effect of either $G\alpha_i$-isoform deficiency on modulation of ventricular $I_{Ca,L}$ in β_1-tg mice.

Methods: Ventricular $I_{Ca,L}$ was measured by whole-cell patch-clamp under basal conditions or after incubation with isoproterenol (Iso) in cardiomyocytes from male β_1-tg mice with or without specific $G\alpha_i$ expression. Absence of $G\alpha_{i2}$ (β_1-tg/$G\alpha_{i2}^{-/-}$) was studied at 4-5 months of age, while the absence of $G\alpha_{i3}$ (β_1-tg/$G\alpha_{i3}^{-/-}$) was studied at 10-11 months of age.

Results: Basal peak $I_{Ca,L}$ density was significantly reduced in β_1-tg myocytes (-5.5±1.5 pA/pF) compared to wild-type (-8.1±1.6 pA/pF). In β_1-tg/$G\alpha_{i3}^{-/-}$, $I_{Ca,L}$ was raised towards wild-type levels (-7.5± 1.6 pA/pF). The voltage of half maximal I_{CaL} activation was positively shifted in β_1-tg myocytes compared to wildtypes ($V_{0.5}$: -7.7±2.8 mV vs. -11.3±2.5 mV, p=01), whereas it was close to normal in β_1-tg/$G\alpha_{i3}^{-/-}$ myocytes (-10.6±4.3 mV). Iso (1μM) significantly increased $I_{Ca,L}$ density in wild-type (to +169±65%, p<.001) and caused a leftward shift of activation voltage ($V_{0.5}$ to -17.1±4.0 mV, p<.001). Both effects were attenuated in β_1-tg (133±34%, p<.01 and -9.7±4.6 mV, p=ns) and in β_1-tg/$G\alpha_{i3}^{-/-}$ myocytes (+127±48%, p=<.05 and -14.2±6.7 mV, p=ns). In young β_1-tg mice similar reduction in basal $I_{Ca,L}$ activity was observed, but an additional lack of $G\alpha_{i2}$ had no effect on this. However, there was a positive shift in the slope factor and voltage of basal steady-state of inactivation in β_1-tg/$G\alpha_{i2}^{-/-}$ myocytes (k_{inact}: -3.3±0.8 mV, $V_{0.5_inact}$ -21.4±1.7 mV) *versus* wild-type (-5.3±0.8 mV, -28.8±3.7 mV, p<.001) and β_1-tg (-5.1±1.1mV, -26.4±3.6 mV, p<.001). The $I_{Ca,L}$ recovery kinetics were also significantly enhanced. Interestingly, Iso-mediated stimulatory effects were augmented in β_1-tg/$G\alpha_{i2}^{-/-}$ myocytes (e.g., $I_{Ca,L}$ density was increased to +209±50%, p<.001).

Conclusions: These findings suggest isoform-specific modulation of ventricular $I_{Ca,L}$ by Gαi protein during cardiomyopathy progression. $G\alpha_{i3}$ deficiency is cardioprotective, likely due to the restoration of basal $I_{Ca,L}$ function and attenuation of adrenergic stimulatory effects. Conversely, $G\alpha_{i2}$ deficiency can be detrimental as it fails to restore $I_{Ca,L}$ or protect against intense β-adrenergic stimulation. It is also associated with unfavorable changes in $I_{Ca,L}$ inactivation and recovery gating. Pharmacological intervention in the Gi-dependent signaling pathway shows promise for developing cardioprotective therapeutics.

Zusammenfassung

Hintergrund: Die inhibitorische G-Protein-α-Untereinheit ist bei Herzinsuffizienz (HF) hochreguliert. In einer murinen dilatativen Kardiomyopathie, die durch Überexpression des β_1-Adrenozeptors bei transgenen Mäusen (β_1-tg) induziert wurde, haben wir gezeigt, dass ein Mangel an $G\alpha_{i2}$ die kardiale Dysfunktion verschlimmert, während das Fehlen des eng verwandten $G\alpha_{i3}$ den gegenteiligen Effekt hat. Die genauen Rollen dieser beiden Gi-Isoformen in versagenden Kardiomyozyten sind noch unbekannt. Da der L-Typ Ca^{2+}-Strom ($I_{Ca,L}$) bei Herzinsuffizienz verändert ist, hatte diese Studie zum Ziel, den Effekt eines Mangels an einer der Gαi-Isoformen auf die Modulation des ventrikulären $I_{Ca,L}$ bei β_1-tg-Mäusen zu untersuchen.

Methoden: Der ventrikuläre $I_{Ca,L}$ wurde mittels Whole-Cell-Patch-Clamp-Technik unter basalen Bedingungen oder nach Inkubation mit Isoproterenol (Iso) in Kardiomyozyten von männlichen β_1-tg-Mäuse mit oder ohne spezifische Gαi-Expression gemessen. Das Fehlen von $G\alpha_{i2}$ (β_1-tg/$G\alpha_{i2}^{-/-}$) wurde im Alter von 4-5 Monaten untersucht, während das Fehlen von $G\alpha_{i3}$ (β_1-tg/$G\alpha_{i3}^{-/-}$) im Alter von 10-11 Monaten untersucht wurde.

Ergebnisse: Die basale Spitzen- $I_{Ca,L}$ -Dichte war in β_1-tg -Myozyten (-5,5±1,5 pA/pF) im Vergleich zu Wildtypen (-8,1±1,6 pA/pF) signifikant reduziert. In β_1-tg/$G\alpha_{\mathbf{i3}}^{-/-}$ wurde $I_{Ca,L}$ auf Wildtyp-Niveau erhöht (-7,5±1,6 pA/pF). Die Spannung der halbmaximalen I_{CaL}-Aktivierung war in β_1-tg -Myozyten im Vergleich zu Wildtypen positiv verschoben ($V_{0.5}$: -7,7±2,8 mV vs. -11,3±2,5 mV, p=01), während sie in β_1-tg/$G\alpha_{i3}^{-/-}$ Myozyten nahezu normal war (-10,6±4,3 mV). Iso (1µM) erhöhte die $I_{Ca,L}$-Dichte in Wildtypen signifikant bis +169±65% (p<.001) und verursachte eine Linksverschiebung der Aktivierung ($V_{0.5}$ auf -17,1±4,0 mV, p<.001). Beide Effekte wurden in β_1-tg (133±34%, p<.01 und -9,7±4,6 mV, p=ns) und β_1-tg/$G\alpha_{i3}^{-/-}$ Myozyten (+127±48%, p=<.05 und -14,2±6,7 mV, p=ns) abgeschwächt. Bei jungen β_1-tg Mäusen wurde eine ähnliche Reduktion der basalen $I_{Ca,L}$-Aktivität beobachtet, jedoch hatte ein zusätzliches Fehlen von $G_{\alpha i2}$ keine Auswirkungen darauf. Allerdings gab es eine positive Verschiebung im Steigungs- und Inaktivierungsspannungsfaktor in β_1-tg/$G\alpha_{i2}^{-/-}$ Myozyten (k_{inact}: -3,3±0,8 mV, $V_{0.5_inact}$ -21,4±1,7 mV) im Vergleich zu Wildtyp (-5,3±0,8 mV; -28,8±3,7mV, p<.001) und β_1-tg (-5,1±1,1mV, -26,4±3,6 mV, p<.001). Die $I_{Ca,L}$ Wiederherstellungskinetik war ebenfalls signifikant erhöht. Interessanterweise wurden die Iso-vermittelten stimulierenden Effekte bei β_1-tg/$G\alpha_{i2}^{-/-}$ Myozyten verstärkt (z.B. wurde die $I_{Ca,L}$ Dichte auf +209±50%, p<.001 erhöht).

Schlussfolgerungen: Diese Ergebnisse legen eine isoformspezifische Modulation des ventrikulären $I_{Ca,L}$ durch Gαi-Protein während des Fortschreitens der Kardiomyopathie nahe. Das Fehlen von $G\alpha_{\mathbf{i3}}$ ist kardioprotektiv, wahrscheinlich aufgrund der Wiederherstellung der basalen $I_{Ca,L}$-Funktion und der Abschwächung adrenerger stimulierender Effekte. Im Gegensatz dazu kann ein Mangel an $G\alpha_{\mathbf{i2}}$ nachteilig sein, da er weder den $I_{Ca,L}$ wiederherstellt noch vor intensiver β-adrenerger Stimulation schützt. Er ist auch mit ungünstigen Veränderungen in der $I_{Ca,L}$-Inaktivierung und Recovery gating assoziiert. Pharmakologische Interventionen im Gi-abhängigen Signalweg zeigen Potenzial für die Entwicklung kardioprotektiver Therapeutika.

Gα$_i$

1

Introduction

"Although COVID is the most visible pandemic of our lifetime, it is neither the deadliest nor the most preventable. Cardiovascular disease has killed five times as many people"
WHO Europe, 2022

1.1 Heart Failure

Heart failure (HF) is the end stage of various cardiovascular diseases and is associated with significant morbidity and mortality, placing a global burden on healthcare systems.
According to the European Society of Cardiology (ESC) Guidelines 2021, HF is a clinical syndrome that presents with observable symptoms and/or signs due to structural and/or functional cardiac abnormalities. This results in reduced cardiac output and/or elevated intracardiac pressures at rest or during exercise (McDonagh et al., 2021).
The global burden of HF is estimated to affect around 64 million people worldwide. The incidence has remained stable or even slightly decreased due to improved treatment strategies in developing countries. However, the prevalence, which ranges from approx. 1% to 3% in adults, is projected to increase due to improved diagnostic tools and treatment options that extend the life expectancy of the population (Savarese et al., 2022).

1.1.1 Classification of heart failure

Heart failure can be classified based on various criteria, including severity, stage, and ejection fraction of the heart. The New York Heart Association (NYHA) functional classification measures the severity of HF, ranging from class I (no physical activity limitations) to class IV (symptoms at rest). The American Heart Association (AHA) and the American College of Cardiology (ACC) staging system decides the stage of HF, ranging from stage A (at risk for HF) to stage D (advanced HF). Based on the ejection fraction (EF) of the heart, which is the percentage of blood pumped out of the left ventricle (LV) with each contraction, HF can be

classified into three types: HF with reduced ejection fraction (HFrEF) with EF ≤ 40%, HF with mid-range ejection fraction (HFmrEF) with EF= 41- 49%, and HF with preserved ejection fraction (HFpEF) with EF ≥ 50% (McDonagh et al., 2021). Recently, a new type of heart failure called HF with improved EF (HFimEF) has been proposed based on the progression of EF over time. HFimEF is defined as HF with a baseline EF of ≤ 40%, with a ≥ 10-point increase in EF from baseline, and a second measurement of EF > 40% (Bozkurt et al., 2021). Identifying the causes of cardiac dysfunction and type of HF is crucial in diagnosing heart failure, as it can determine the proper treatment.

1.1.2 Etiology and pathophysiology of heart failure

Heart failure is often caused by myocardial dysfunction, which can be systolic, diastolic or both. This can have a variety of causes, including coronary artery disease (CAD), acquired or inherited cardiomyopathies, infections, hypertension, abnormalities in heart rhythm and conduction, as well as pathologies in the valves, pericardium, endocardium, and multisystem disease (McDonagh et al., 2021).The molecular and cellular mechanisms underlying HF are multifactorial and not yet fully understood. This includes activation of the neurohumoral system, specifically the sympathoadrenergic system and renin-angiotensin-aldosterone system (RAAS), the release of vasoactive peptides such as natriuretic peptides and nitric oxide, structural remodeling, and hemodynamic changes. While these mechanisms may provide short-term cardioprotection, they can become maladaptive over time and contribute to the progression and worsening of HF. This is due to potential adverse effects on the heart and circulation, including myocardial hypertrophy, fibrosis, apoptosis, arrhythmias, vasoconstriction, oxidative stress, and calcium mishandling, *see review* (Schwinger,2021). Furthermore, these mechanisms offer important diagnostic and prognostic implications. A good example is the endogenous hypotensive natriuretic peptides (NPs) that are used as biomarkers in cardiac hypertrophy. The levels of Brain-type (BNP) and N-terminal pro-BNP (NT-proBNP) are increased in cases of HF. They are commonly used in clinical practice, while atrial (ANP) is less often used (Kim & Januzzi, 2011; Pandey, 2021).

The present work focuses on three proteins that are crucial for cardiac function and contribute to the understanding of HF: **(1)** β-adrenoceptors, **(2)** inhibitory G proteins and their isoform-specific functions in HF, and **(3)** L-type calcium channels (LTCC), as they are essential for cardiac excitation-contraction coupling.

1.2 β-adrenergic signaling in the heart

1.2.1 Cardiac β-adrenoceptors

Beta-adrenergic receptors (β-ARs) are members of the G-protein coupled receptor (GPCR) family, which regulate cardiac function and adaptation to stress. β-ARs are composed of a conserved structure of seven transmembrane α-helices that signal primarily through interaction with intracellular heterotrimeric guanine nucleotide-binding regulatory proteins known as G proteins (Rockman et al., 2002).They mediate the effects of catecholamines (CA) on the heart and modulate cardiac contractility, heart rate, relaxation, metabolism, gene expression, and cell survival, (*review*, Rockman et al., 2002; de Lucia et al., 2018).

There are three subtypes of β-ARs in the heart: β_1-, β_2-, and the less expressed β_3-AR. β_1-AR is the predominant subtype accounting for approx. 70% to 80% of the total β-ARs depending on the species (Brodde, 1991). Both β_1- and β_2 -adrenoceptors can couple to the stimulatory G protein (G_s) and activate cAMP mediated signaling resulting in an increase inotropy (contractility), lusitropy (rate of relaxation) and chronotropy (frequency) effects (Brodde, 1991). The β_3-AR subtype is least expressed in the myocardium and is mainly present in adipose tissue (Krief et al., 1993). Unlike in adipose tissue, β_3-AR couple to Gi protein and mediate negative inotropic effects in the heart (Cheng et al., 2001; Kohout et al., 2001). However, the importance of this subtype has yet to be determined.

Pharmacological and genetic methods have revealed two primary aspects about the different subtypes of β-adrenoceptors coexisting in the heart. Firstly, β-AR subtypes have varying affinities for their respective ligands (Brodde, 1988), and recently reviewed by (Wu et al., 2021). Secondly, these receptors have specific subcellular localizations, resulting in distinct signaling pathways. While β_1-AR is primarily located on the sarcolemmal crest, β_2-AR is concentrated in the transverse tubules (T-tubules) (Nikolaev et al., 2006, 2010) and caveolae regions (Rybin et al., 2000) of healthy adult cardiomyocytes.

The classical signaling pathway for β-ARs involves the activation of adenyl cyclase (AC) by $G\alpha_s$, which increases cAMP levels and primarily activates protein kinase (PKA) Figure (1-1). In cardiomyocytes, PKA phosphorylates several downstream cytoplasmic proteins involved in cardiac excitation-contraction coupling (ECC), including the L-type calcium channels (Bers, 2002). However, in many mammalian species, including humans and rodents, β_2-AR stimulated cAMP signaling is functionally compartmentalized, while β_1-AR-activated cAMP signaling is more diffusible in cardiomyocytes (Zheng et al., 2005).

Furthermore, one of the key differences between β_1- and β_2-adrenoceptor is that β_2-AR can couple to both $G\alpha_s$ and $G\alpha_i$ proteins in human and rodent myocytes (Xiao et al., 1995, 1999; Kilts et al., 2000). The **β_2-AR-Gi coupling** has significant implications for the outcomes of Gs signaling, and it has been recognized to mediate antiapoptotic effects in cardiomyocytes Figure (1-1), *see review* (Xiao, 2001; Zheng et al., 2005; Woo et al., 2015). Activation of β_2-AR initiates cellular survival pathways, including the activation of the mitogen-activated protein kinase/extracellular signal–regulated protein kinase (MAPK/ERK) and the phosphoinositide 3-kinase (PI3K), which activates the Akt protein kinase (Communal et al., 1999; Chesley et al., 2000; Zhu et al., 2001). It has been found that phosphorylation of Akt was mediated by β_2-AR, but not by β_1-receptor, due to the activation of Gi (via the $G_{\beta\gamma}$ subunit) in mouse cardiac myocytes (Zhu et al., 2001). These studies concluded that signaling via β_2-AR may be cardioprotective, whereas sustained activation of β_1-ARs appears to be pro-apoptotic, e.g., through activation of Ca^{2+}/calmodulin dependent kinase II (CaMKII) (*review*, Feng & Anderson, 2017).

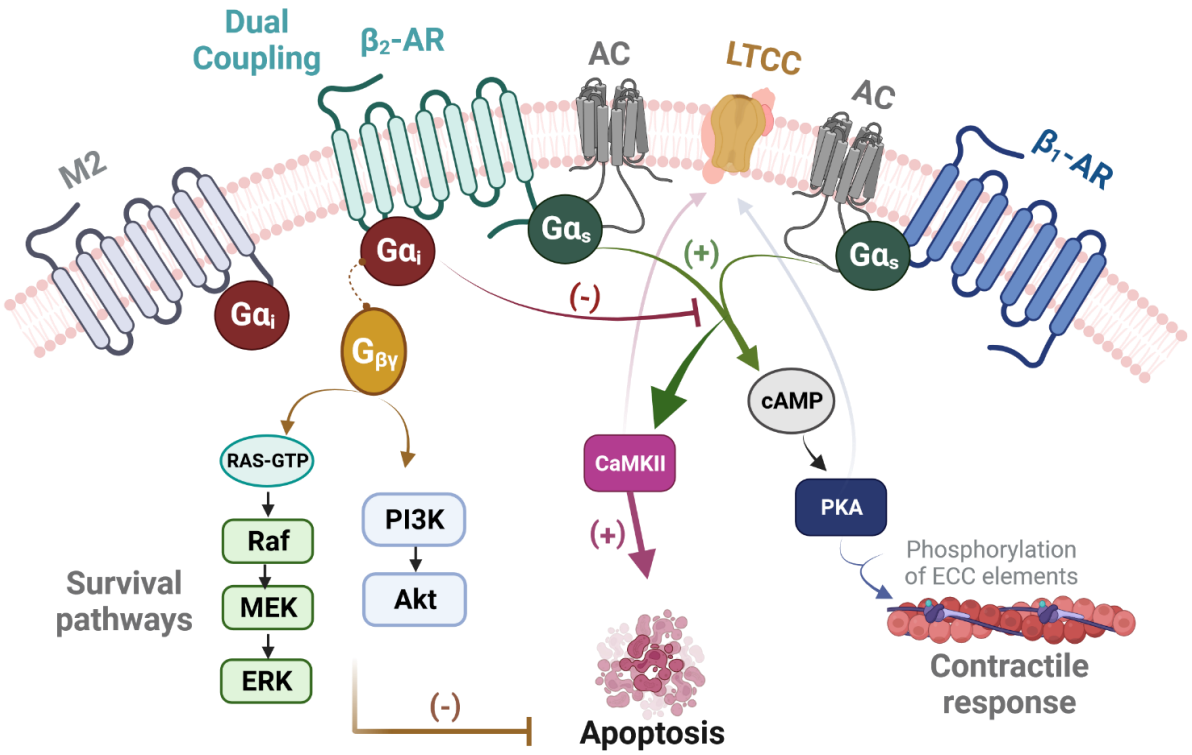

Fig. 1-1. Dual coupling of β_2-AR to Gs and Gi proteins in cardiac myocytes. The ability of β_2-AR to couple to Gi protein can activate survival pathway. Sustained activation of β_1-AR can enhance apoptosis. for details see text. Original figure, created with BioRender.com©, Ref. (Xiao, 2001; Xiao et al., 2006; Goldsmith & Dhanasekaran, 2007).

1.2.2 Cardiac β-adrenergic signaling in heart failure

Numerous studies have demonstrated chronic alterations of the cardiac β-adrenergic system during heart failure. These alterations are thought to be initially adaptive but can become maladaptive and mediate the progression of cardiomyopathy.

Following a cardiac insult, the sympathetic nervous system (SNS) is activated to compensate for depressed myocardial function and preserve cardiovascular homeostasis (Packer, 1988). This leads to a series of functional and structural changes that ultimately contribute to cardiac remodeling, decompensation, and failure, *see review* (Triposkiadis et al., 2009). A striking outcome of chronic SNS activation during HF is alteration in the β-ARs and their downstream signaling pathway. Figure (1-2) illustrates the primary changes observed in human HF including a reduction in β_1-AR density and mRNA levels, uncoupling of β_1-AR from Gs protein, and impaired compartmentalization of cAMP/PKA signaling (Bristow et al., 1986; Engelhardt et al., 1996; Böhm et al., 1997). Although the expression of β_2-ARs is not altered during HF, β_2-AR is also uncoupled from $G\alpha_s$, resulting in reduced efficiency in producing cAMP (Lohse et al., 2003). β_3-ARs are inactive under physiological conditions, while it has been shown that in human HF, they are upregulated and exert negative inotropic effects through activation of nitric oxide synthesis (Gauthier et al., 1998; Moniotte et al., 2001).

Desensitization of β-ARs is a characteristic of heart failure. This can be attributed to mechanisms that modify the expression or function of the receptors (*review,* Lohse et al. 1996; El-Armouche et al., 2003). On a functional level, receptors can be primarily altered by uncoupling from their G proteins. One of the most rapid and specific mechanisms for desensitizing G protein-coupled receptors is triggered by their phosphorylation through GPCR kinases (GRKs). This allows arrestins to bind to the phosphorylated receptor and terminate the G protein-mediated signaling. This process is typically initiated by agonist activation of the receptors to prevent overstimulation or to adapt to a persistent stimulus (*review,* Lohse et al., 1996; Woo et al., 2015). β_1-AR downregulation and enhanced activities of GRKs have been reported in human HF (Ungerer et al., 1993, 1994).

Furthermore, sustained β_1-AR stimulation in rat cardiomyocytes was reported to shift the classical cAMP-PKA signaling pathway to a CaMKII-dependent pathway (Wang et al., 2004). CaMKII is a protein kinase that is activated by calcium ions and the calcium-binding protein calmodulin, and it plays a crucial role in regulating various cellular processes. Although activation of CaMKII can have some beneficial and adaptive effects, prolonged and sustained activation can induce cardiotoxic and cardiac remodeling effects (Beckendorf et al., 2018).

Additionally, chronic activity of CaMKII is associated with arrhythmogenesis (Mustroph et al., 2017).

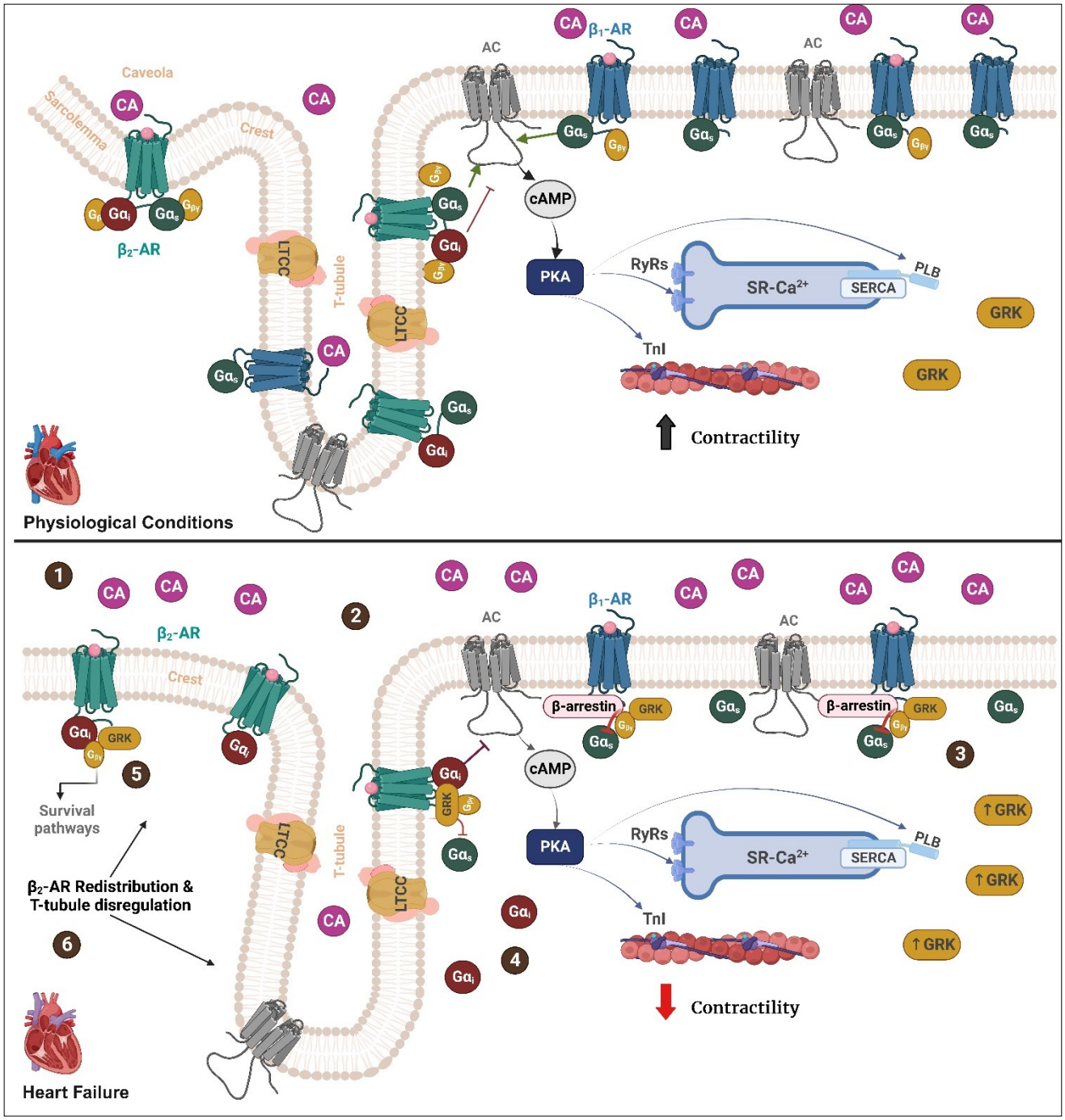

Fig. 1-2. Cardiac β-AR signaling in physiology and hear failure. In HF, there are changes in cardiac β-AR signaling. **(1)** The level of catecholamine (CA) increases. **(2)** The β_1-AR is hyperstimulated and downregulated, while β_2-AR remains unchanged. **(3)** GPCR kinase (GRK) is upregulated and binds to $G_{\beta\gamma}$ subunits. They are translocated to the plasma membrane and phosphorylate β-AR, thus increasing their affinity for β-arrestins protein, which prevents further G-protein signaling. **(4)** Gi proteins are upregulated, and **(5)** enhanced β_2-AR-Gi signaling leads to desensitization of AC signaling and activation of survival pathways. **(6)** The cardiac remodeling and structural derangements in the failing myocyte cause translocation of β_2-AR from T-tubules and caveola to the crests. Original illustration created with BioRender.com© – for details and ref. see text.

1.3 Heterotrimeric G-proteins

1.3.1 G-protein structure and signaling

Guanine nucleotide-binding regulatory proteins (G proteins) are a group of proteins that function as switches within the cells and transmit signals from various stimuli. The G protein-mediated signaling system is complex and includes a receptor, a heterotrimeric G protein, and an effector. This modular design allows for convergence and divergence at the receptor-G protein and G protein-effector junctions (*review*, Wettschureck & Offermanns, 2005).

The heterotrimeric G protein consist of an α-subunit that binds and hydrolyzes GTP, and β- and γ-subunit that form a non-dissociable complex. In the inactive state, the α-subunit of the G protein is bound to GDP. Upon ligand binding to a G protein-coupled receptor on the cell membrane, the receptor undergoes a conformational change, which activates the G protein by exchanging GDP with GTP (Figure 1-3). Upon receptor activation, the α-subunit and βγ-complex dissociate from it and interact with various effectors within the cell, such as enzymes or ion channels. Cellular signaling is terminated by the hydrolysis of GTP, which is inherent to the G protein α-subunit. When activated receptors are present, the resulting GDP-bound α-subunit re-associates with the βγ-complex to enter a new cycle (Gilman, 1987; Hepler & Gilman, 1992).

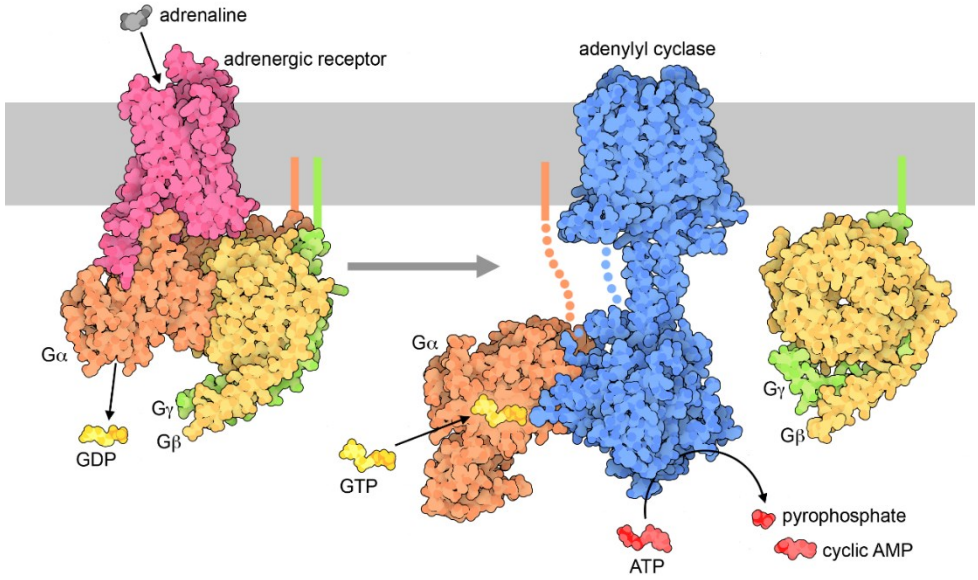

Fig. 1-3. Signaling with G-proteins. Hormones like adrenaline bind to a GPCR receptor (*left*), which binds to a heterotrimeric G-protein and releases GDP. Then the G-protein separates into two pieces, and the G-alpha subunit (Gα) binds to GTP and activates adenylyl cyclase (*right*) – *Source: PDB-101*

G-Protein – subtypes and pharmacological targeting

The G protein-mediated signaling system is highly versatile due to its modular architecture and the existence of multiple G protein subtypes. The α-subunits of a heterotrimeric G protein define its fundamental properties and can be categorized into four families: Gs, G_i/G_o, G_q/G_{11}, and G_{12}/G_{13}. Each family includes different G-protein isoforms that exhibit specific expression patterns. Members of the same family share structural similarities and often have similar functional properties. Li et al. recently reviewed the expression pattern of G protein and found that human genome contains 21 different Gα subunits (encoded by 16 genes), six different Gβ subunits (encoded by 5 genes), and twelve Gγ subunits (encoded by 12 genes) (Li et al., 2020).

Both the GTP-bound Gα and Gβγ subunits interact with diverse downstream effector proteins and transduce signals (Table 1-1). Due to their ubiquitous expression and involvement in multiple cellular processes, G proteins are significantly associated with the development and progression of several diseases (Figure 1-4). In certain diseases, the properties of G proteins differ from those in the normal state, as these proteins are either abnormally activated or overexpressed. Hence, direct targeting of G proteins represents an attractive therapeutic target. However, developing selective and effective G protein modulators for clinical use has been challenging. This is due to several reasons, including the fact that G proteins are intracellular molecules without well-defined pockets on their surface, making them difficult to target using conventional approaches (Nubbemeyer et al., 2021). In addition, they have a high degree of structural and sequence similarity, making specific pharmacological targeting challenging (Jones & Reed, 1987; Simon et al., 1991).

This dissertation focuses on the inhibitory G-proteins and on the isoform-specific functions of the two isoforms **$G\alpha_{i2}$** and **$G\alpha_{i3}$** and their role in cardiomyopathy.

Table 1- 1:
G-protein classical signaling pathway and available modulators

G protein	**$G\alpha_s$**	**$G\alpha_{i/o}$**	**$G\alpha_q/G\alpha_{11}$**	**$G\alpha_{12}/G\alpha_{13}$**	**$G\beta\gamma$**
Classical Signaling Pathway	AC ↑cAMP ↑PKA	AC ↓cAMP ↓PKA	PLC-β ↑$InsP_3$/↑$[Ca^{2+}]$ ↑DAG/PKC	Rho GTPases	Ion channels, protein kinases and small G-proteins
Selective Gα Modulators	CTX	PTX	YM-254890 FR900359	-	-

AC: adenyl cyclase, PLC: phospholipase, cAMP: cyclic adenosine monophosphate, PKA: protein kinase A, $InsP_3$: phosphoinositide 3-kinase, DAG: diacylglycerol, Rho: RAS homology. CTX: Cholera Toxin (inhibitor), PTX: Pertussis Toxin (inhibitor), YM-254890 and FR900359 are cyclic depsipeptides Gαq/Gα11 selective inhibitors (ref. McCudden et al.2005, Li et al. 2020).

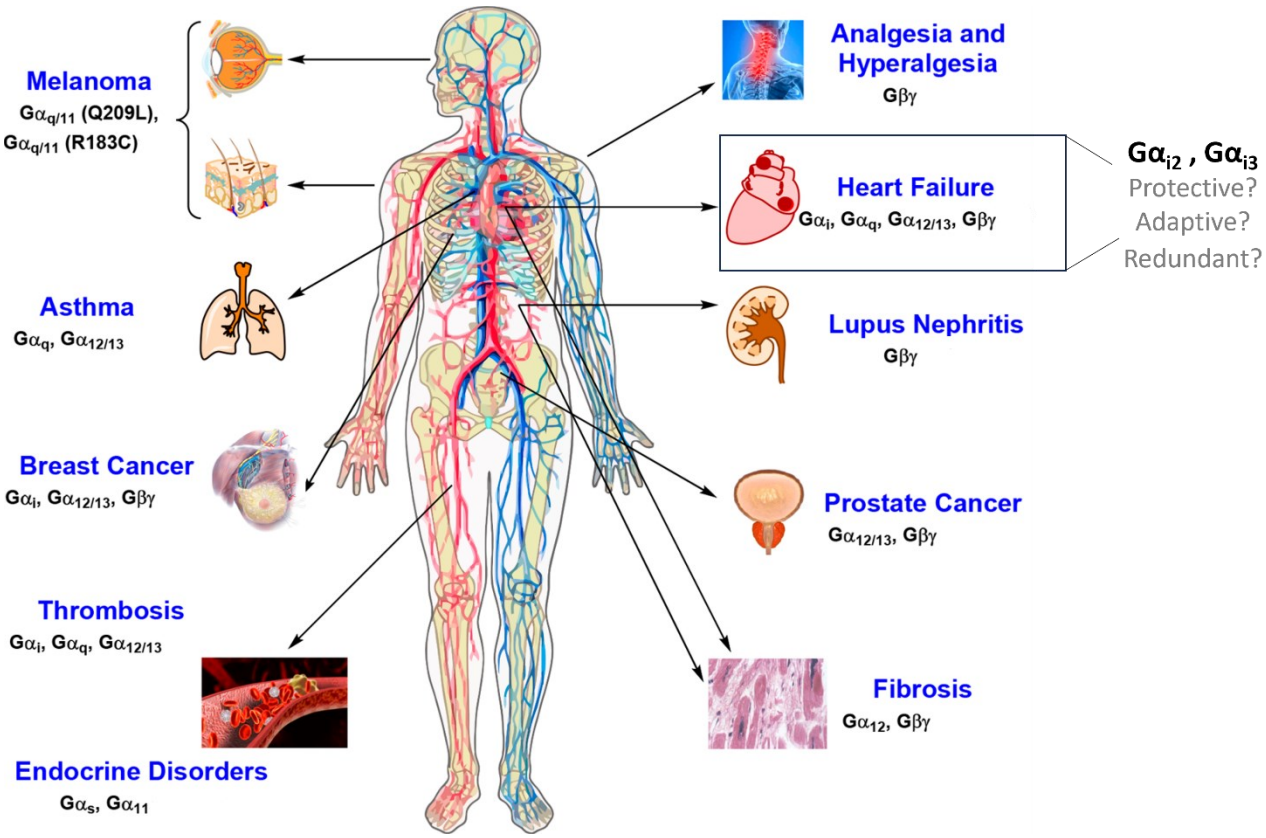

Fig. 1-4. Overview of G-protein related disease – modified after *Li et al. 2020*

1.3.2 Inhibitory G-proteins (Gi) and heart failure

Inhibitory G proteins ($G\alpha_i/G_o$) are a class of heterotrimeric G proteins that mediate the inhibitory regulation of several cell signaling pathways, including the AC pathway. This regulation is mediated by the adrenergic receptors β_2/β_3-AR in the heart and α_2-AR in coronary vessels, as well as the muscarinic receptors, specifically M2 receptors (Rockman et al., 2002). However, under basal conditions, the role of ventricular M2 receptors seems to be negligible and it may become significant when contractility is enhanced upon cAMP increase (Giessler et al., 1999).

The Gi/Go family of G proteins is widely expressed and there are several isoforms of the inhibitory G protein alpha subunit, namely **$G\alpha_{i1}$**, **$G\alpha_{i2}$**, **$G\alpha_{i3}$**, and the **$G\alpha o$**, which has two splice variants: $Go_{1\alpha}$ and $Go_{2\alpha}$ (Hepler & Gilman, 1992). They share considerable amino acid sequence identity and have similar structures, but they also have different tissue distribution and functional roles (Simon et al., 1991).

The function of these proteins has been extensively studied by researchers using pertussis toxin (PTX), a toxin from Clostridium botulinum that ADP-ribosylates most of the Gi/Go family

members close to their COOH termini. Gi/Go proteins that are ADP-ribosylated are unable to interact with the receptor, leading to their uncoupling from the receptors (Katada, 2012). The three $G\alpha_{i1\text{-}3}$ isoforms have structural similarity and share about 85-90% of amino acid sequence (Jones & Reed, 1987), suggesting partially overlapping functions. In contrast to other G proteins, Go, which is abundant in the nervous system, primarily mediates its effects through its βγ-complex. $G\alpha_z$, a less expressed member of the Gi family, is present in several tissues, including the nervous system and platelets. While this isoform shares functional similarities with other Gi-proteins, it has been found to interact specifically with various other proteins, such as certain regulators of G-protein signaling (RGS) (Wettschureck & Offermanns, 2005).

Gi-protein and their role in heart failure

Studies have shown that the activity and expression levels of $G\alpha_{i/o}$ are altered in the failing human heart. An increase of 40-90% of Gαi proteins, particularly the $G\alpha_{i2}$ isoform, was observed in the failing myocardium (A. M. Feldman et al., 1988; Neumann et al., 1988; Böhm et al., 1990; Eschenhagen, et al., 1992). This raises questions about the role of the Gi protein in HF and whether it has a protective function that could be targeted as a treatment. As previously mentioned, HF is characterized by the loss of responsiveness of β-adrenergic receptors. However, if the downregulation or uncoupling of these receptors is the only mechanism that causes desensitization of the adenylyl cyclase signaling pathway, agents that bypass the β-AR should retain their efficiency in the failing myocardium. Nevertheless, studies have shown that the positive effects of inotropic drugs were attenuated (M. D. Feldman et al., 1987; Böhm, 1995). There appears to be a second mechanism that contributes to the defective AC-cAMP signaling in HF.

Adenyl cyclase is regulated by Gαs and Gαi, as well as by the Gβγ subunits (Tang & Gilman, 1991; Taussig et al., 1993). In failing myocardium, levels of G(αs) and (β)-subunits were found unchanged (A. M. Feldman et al. 1988; Schnabel et al., 1990; Eschenhagen et al., 1992; Böhm, 1995). The catalytic subunits of AC and its total activity have also been reported to be unchanged (Böhm et al., 1994). In contrast, G(αi) protein subunits appear to play a role in desensitizing AC-signaling. Brown and Harding have shown that the inotropic effect of isoproterenol was restored when isolated myocytes from failing human hearts were treated with pertussis toxin (Brown & Harding, 1992). Enhanced Gαi expression that mediates AC desensitization was also confirmed in rat hypertrophic models, where no β-AR downregulation was detected (Böhm et al., 1992, 1994). This suggests a direct role of Gαi in

reducing AC activity, even in advance of overt HF. Several subsequent studies have provided evidence supporting the role of Gαi in the desensitization of cardiac AC, as reviewed by (El-Armouche et al., 2003). The question whether all Gαi isoforms have similar functions in the physiological and pathological regulation of the heart is still a matter of debate.

1.3.3 Isoform-specific functions of $G\alpha_{i2}$ and $G\alpha_{i3}$

Recent animal studies have shown that the closely related isoforms $G\alpha_{i2}$ and $G\alpha_{i3}$, which share about 85% identity (see Suppl.S2), have distinct functions in several different tissues, including the heart, when global or cell-specific Gαi deletion is involved. For example, $G\alpha_{i3}$ (but not $G\alpha_{i2}$) has been found to mediate insulin effects on hepatic autophagy (Gohla et al., 2007), regulate the size and density of melanosomes in the retinal pigment epithelium through the ocular albinism receptor (Young et al., 2011), play a crucial role in the hearing system (Mauriac et al., 2017; Beer-Hammer et al., 2018), and contribute to the development and normal patterning of the mammalian axial skeleton (Plummer et al., 2012). Furthermore, $G\alpha_{i2}$ and $G\alpha_{i3}$ were reported to exhibit distinct effects on ERK1/2 and Akt signaling in response to different growth factors (Z. Wang et al., 2014) and to differentially regulate the immune response (Thompson et al., 2007; Wiege et al., 2013; Kuwano et al., 2016).

Although it was confirmed that the activity and expression levels of $G\alpha_{i/o}$ protein increase in the failing human heart, the exact role of $G\alpha_{i/o}$ in the pathophysiology of heart failure is not yet fully understood. $G\alpha_{i2}$ is the most abundant $G\alpha_{i}$ isoform in the rodent heart, while other isoforms are less expressed (Jones & Reed, 1987; Asano et al., 1989; Foster et al., 1990).

Several studies have shown that $G\alpha_{i2}$ is essential in muscarinic signal transduction upon M-AChR (M_2) receptors, while $G\alpha_{i3}$ appears to be dispensable (Nagata et al., 2000; F. Chen et al., 2001; Zuberi et al., 2010). Moreover, $G\alpha_{i2}$ and $G\alpha_{i3}$ have been found to differentially modulate the function of cardiac ion channels. Nobles et al. have shown that in murine atrial cells, the lack of $G\alpha_{i2}$ resulted in an increase in I_{Kir} current, a measure of the activity of G-protein-gated inwardly rectifying K^+ channels (GIRK). Conversely, the double deletion of $G\alpha_{i1}/G\alpha_{i3}$ led to a reduction in I_{Kir} current (Nobles et al., 2018). In ventricular myocytes isolated from $G\alpha_{i2}$ knockout mice ($G\alpha_{i2}^{-/-}$), L-type calcium current was decreased, whereas it was increased in $G\alpha_{i3}^{-/-}$ mice (Dizayee et al., 2011). Enhanced β_2-AR-Gαi signaling has been suggested to have cardioprotective effects under pathological conditions. $G\alpha_{i2}$ and $G\alpha_{i3}$ appear to have opposing effects on the progression of cardiac diseases, with $G\alpha_{i2}$ exerting protective effects, while $G\alpha_{i3}$ appears to aggravate cardiac dysfunction (Table 1-2).

Table 1- 2: Literature Review
Distinct Functions of $G\alpha_{i2}$ or $G\alpha_{i3}$ Deficiency in Murine Models of Cardiomyopathy

Murine model of cardiomyopathy	Study Design	Gαi-isoform	Effects of inhibiting/deleting or enhancing $G\alpha_{ix}$	Ref.
Transgenic mice with cardiac specific β_2-AR - overexpression (β_2-tg) *(RG Herzig)*	β_2-tg mice with heterozygous $G\alpha_{i2}$ deletion*	$G\alpha_{i2}^{-/+}$	- Enhancement of the decrease in LTCC activity in β_2-tg mice - Enhancement of mortality	Foerster et al. 2003
	β_2-tg mice with homozygous $G\alpha_{i3}$ deletion	$G\alpha_{i3}^{-/-}$	- Increased LTCC activity in β_2-tg mice - No effect on lifespan	Klein 2009
Murine model of myocardial ischemic-reperfusion (I/R) injury	Transgenic mice with a targeted inhibition of cardiac $G\alpha_{i2}$ → (suppressed signaling)	$G\alpha_{i2}$	*Following I/R injury:* - Infarct size (↑) - Myocardial apoptosis (↑) - Contractility (↓)	DeGeorge# et al. 2008
	Mice expressing RGS-insensitive $G\alpha_{i2}$ → (enhanced signaling)	$G\alpha_{i2}$	*Following I/R injury:* - Infarct size (↓) - Post-ischemic recovery of contractile function (↑)	Waterson# et al. 2011
	Global specific Gαi knockout mice	$G\alpha_{i2}^{-/-}$ $G\alpha_{i3}^{-/-}$	*Following I/R injury:* - Infarct size (↑) - Infarct size (↓)	Köhler et al. 2014
Transgenic mice with cardiac specific β_1-AR overexpression *(RG Matthes)*	β_1-tg mice with global homozygous $G\alpha_{i2}$ knockout	$G\alpha_{i2}^{-/-}$	- Exacerbation of cardiac dysfunction - Enhancement of mortality - Enhancement of Hypertrophy	Keller et al. 2015
	β_1-tg mice with global homozygous $G\alpha_{i3}$ knockout	$G\alpha_{i3}^{-/-}$	- Prevention or delay of cardiac dysfunction - Prolongation of survival - Decreased hypertrophy	Schröper et al. 2024

Remarks: Mouse Models: Transgenic cardiac **β_2-AR** overexpression (~195-fold expression levels) leads to cardiomyopathy in mice aged 1 year. **I/R:** Ischemia reperfusion injury was induced using varying protocols in these studies, which were ranging from 30 to 60 min of ischemia followed by 2-3 hours of reperfusion. Transgenic overexpression of cardiac **β_1-AR** (at lower expression levels than β_2-AR) leads to a ventricular failure phenotype.
***** β_2-tg with homozygous $G\alpha_{i2}$ knockout died within few days after birth.
# This study did not make a direct comparison with data obtained using the $G\alpha_{i3}$ isoform.
LTCC: L-type Calcium Channel; **RGS**: regulatory-G-protein (it enhances G-protein deactivation).

However, it is important to note that not all studies endorse the concept that Gi proteins mediate the cardio-protective effects of β_2-adrenoceptor stimulation (Xiao et al., 2003; Ahmet et al., 2005), or that Gi-protein signaling is cardio-protective in general (Hussain et al., 2013).

1.4 Voltage-gated Calcium Channels

1.4.1 Definition and classification

Voltage-gated calcium channels (VGCCs), a subfamily of the superfamily of voltage-gated ion channels, are transmembrane ion channel proteins that selectively conduct calcium ions across the cell membrane in response to action potentials and subthreshold depolarizing signals. They are present in various cell types and play a critical role in the transduction of electrical signals. Signal transduction in different cell types involves specific molecular subtypes of VGCCs that mediate Ca^{2+} currents with distinct physiological, pharmacological, and regulatory properties, (*review,* Catterall, 2011; Zamponi et al., 2015).

VGCCs are multi-subunit protein complexes that were first characterized at the molecular level in skeletal muscle. They consist of a pore-forming **α_1** subunit along with auxiliary subunits **β**, **$\alpha_2\delta$**, and γ, but their subunit composition and properties differ in other tissue types. There are several types of calcium "currents" with distinct physiological and pharmacological properties. VGCCs are classified into two main groups based on their threshold of activation voltage and conductance: high-voltage-activated (HVA) and low-voltage-activated (LVA) calcium channels. These groups show different gating properties and pharmacological profiles. **HVA Ca^{2+} channels** include two primary types of channels: the L-type (long-lasting) or Dihydropyridine (DHP)-sensitive channels, and the non-L-type or DHP-insensitive channels, including P/Q- (Purkinje), N- (Neuronal) and R-type (Resistant). **LVA Ca^{2+} channels** conduct T-type (Transient) calcium current that is activated by mild depolarization (*review,* Hofmann et al., 1994; Catterall, 2000; Hoppe et al., 2005).

Mammalian **α_1**-subunits are encoded by at least ten different genes that define the subtype of a given calcium channel. These subunits can be grouped into three structurally and functionally related families (Ca_{V1}, Ca_{V2}, and Ca_{V3}). Figure (1-5) shows a phylogenetic tree of VGCCs based on the international nomenclature presented by (Ertel et al., 2000).
In the present work we focus on ventricular L-type calcium channel **($Ca_v1.2$)**. The $Ca_v1.2$ (α_1C)-subunit has several splice variants, including ($Ca_v1.2a$) found in the heart, ($Ca_v1.2b$) found in smooth muscle and lung, and $Ca_v1.2c$ found in neurons and heart (Hoppe et al., 2005).

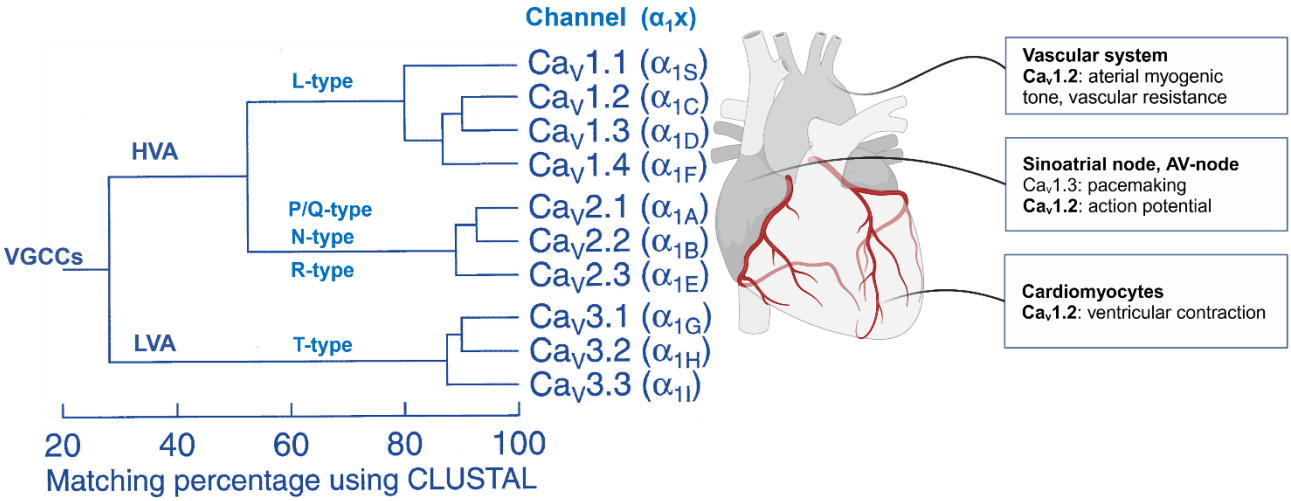

Fig. 1-5. Phylogeny of voltage gated Ca^{2+} channel α_1 subunits (right) according to the international classification presented by Ertel et al. 2000. Important cardiac calcium channels (left) and their primary function – (modified after Zamponi et al. 2015).

1.4.2 Cardiac L-type calcium channels: Structure and kinetics

Calcium ions influx through L-type ($Ca_V1.2$) calcium channels triggers muscle contraction, controls action potential duration, and regulates gene expression in the heart (Mangoni et al., 2006; Shaw & Colecraft, 2013). The $Ca_V1.2$ (α_1C) subunit is composed of four homologous domains (DI-DIV), each has six transmembrane α helices (segments S1-S6) connected by membrane-associated loops and flanked by cytosolic N and C termini. Segment S4 of each domain forms the voltage sensor for activation and initiation of a conformational change that opens the pore. Segments S5-S6 and the linking loop between them form the channel pore and have the selectivity filter (Figure 1-6). While all calcium channels share similar structural features, the Ca_V1 family, which conducts L-type Ca^{2+} currents, has specific amino acid residues that have a high affinity for the organic Ca^{2+} antagonists used in the treatment of cardiovascular disease (Catterall, 2011).

Under normal conditions, only the $Ca_V1.2$ (α_{1C}) subunit is expressed in adult ventricular myocytes (Shaw & Colecraft, 2013). The α_1 subunit primarily determines the kinetics and voltage dependence of VGCCs, as well as their pharmacology. The auxiliary subunits can induce changes in the physiological functions of the α_1 subunit. This can increase channel trafficking, enhance the expression of functional calcium channels at the plasma membrane, and affect the biophysical properties of the channels. The extent of these changes depends on the type and isoform of the auxiliary subunits expressed (Dolphin, 2012). There are four different isoforms of the $Ca_V\beta$ subunits (β_1-β_4), each with multiple splice variants, with β_2 being the predominant isoform in the heart (Dolphin, 2003).

The $Ca_V\alpha_2\delta$ subunit is encoded by a single gene and has four isoforms ($\alpha_2\delta$-1 - $\alpha_2\delta$-4) too, with the ($\alpha_2\delta$-2) isoform being expressed in the heart. The large α_2 protein is completely extracellular and bound to the plasma membrane via the δ subunit (Dolphin, 2018). The Ca_V γ-subunit family has eight different isoforms and consists of four transmembrane domains with intracellular N- and C-terminal ends (L. Yang et al., 2011). Four of these subunits (γ4, γ6, γ7, and γ8) have been identified in the human heart, but only γ6 expression has been confirmed at the protein level in rat heart. This subunit exerts different effects on $Ca_V1.2$ current amplitude and voltage dependence of gating, depending on the β-subunit isoform present in the channel complex. However, the impact of γ-subunit expression and diversity on $Ca_V1.2$ channel signaling in cardiac myocytes is not fully understood (L. Yang et al., 2011).

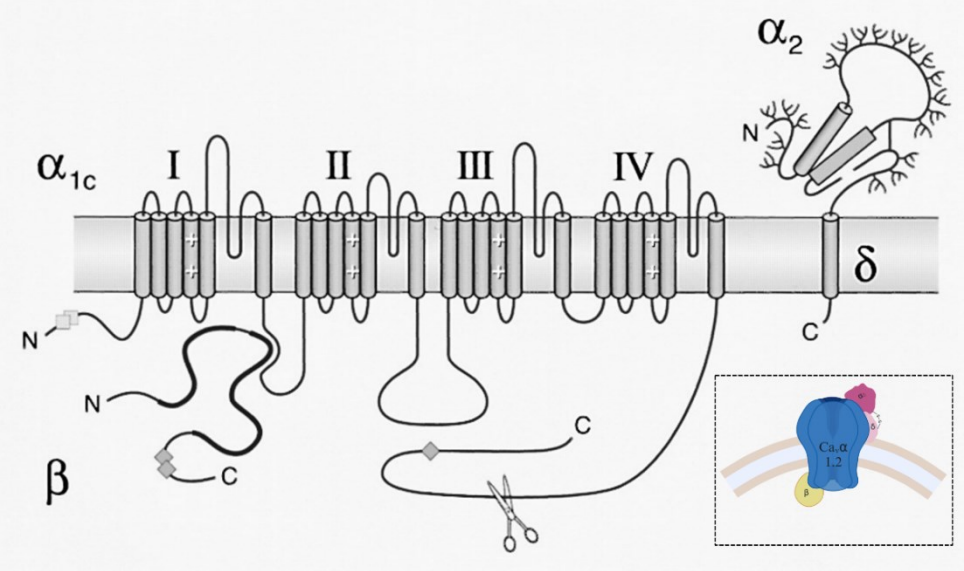

Fig. 1-6. Proposed transmembrane topology and subunit composition of cardiac L-type Ca^{2+} channel, modified after Kamp and Hell 2000, for details see text.

Kinetics properties of calcium channels

Voltage-gated calcium channels are activated by conformational changes in their positively charged transmembrane polypeptide regions. Upon depolarization, calcium current is rapidly activated, peaking within 2-7 ms, depending on temperature and membrane potential. The magnitude of the current across the membrane is determined by channel density, channel conductance, and open probability frequency (McDonald et al., 1994; Hoppe et al., 2005).

During prolonged depolarization, VGCCs undergo a transition to a non-conducting, inactivated state that prevents excessive calcium influx into the intracellular space. L-type current **($I_{Ca,L}$)** is inactivated by two different mechanisms: a fast, calcium-dependent (CDI) process regulated by calmodulin, and a slow, voltage-dependent (VDI) process (Peterson et al., 1999; Findlay, 2002). Channels must recover from inactivation, i.e., transition to the closed state, before being able to open again. The recovery from inactivation is also voltage- and calcium-dependent, Figure (1-7, B), (McDonald et al., 1994).

BOX 1

Basic Biophysical Properties of $Ca_V1.2$

- Mediate inward long lasting (L-type) Ca^{2+} current
- Contribute to plateau phase of cardiac AP
- Activation threshold at around (-20 and -30) mV
- Peak current at around (0 and +10) mV
- Relative slow inactivation kinetics
- Voltage (VDI) and calcium (CDI) -dependent inactivation kinetics
- Pharmacological blockers: DHPs
- Pharmacological agonist: S(–) Bay K 8644
- Resting membrane potential in vascular smooth muscle cells is -50 mV, while in the ventricles it is -80 mV

1.4.3 β-adrenergic regulation of cardiac calcium channels

β-adrenergic modulation of cardiac L-type Ca^{2+} current is the best known and most extensively studied example of Ca^{2+} current regulation. First experiments using voltage-clamp techniques on mammalian cardiac tissue had shown that β-adrenergic stimulation increases the L-type Ca^{2+} current (Reuter, 1979). This enhancement contributes significantly to the increase in heart rate, cardiac contractility, and cardiac action potential amplitude produced by β-adrenergic agonists. The potentiation of L-type Ca^{2+} current is mediated by cAMP and the consequent activation of protein kinase A (PKA). Activation of PKA and Ca^{2+} channel phosphorylation by β-AR agonists is a relatively slow process that requires activation of the Gs-AC pathway. This is different from the increased Ca^{2+} current occurred after direct activation of the channels, such as with BayK-8644 (Tsien et al., 1986; Trautwein & Hescheler, 1990).

The mechanisms underlying β-adrenergic activation of cardiac Ca^{2+} channels through the cAMP-dependent pathway at the single channel and whole cell levels are controversial. It is widely agreed that increased Ca^{2+} currents can result from an increase in the probability of channel opening (P_o) and/or an increase in the number of functional Ca^{2+} channels (Yue et al., 1990; Schröder & Herzig, 1999; G. Klein et al., 2000). Additionally, Isoproterenol (Iso), a

non-selective β-AR agonist, has stimulatory effects that are associated with changes in the voltage dependence of current activation. Typically, Iso causes a hyperpolarization shift in peak voltage (V_{peak}) by -5 to -10 mV and may also shift the inactivation-voltage relationship to less depolarizing voltages (McDonald et al., 1994). Although there is conflicting data on the effects of β-AR agonists on channel inactivation and recovery from inactivation kinetics, it is generally accepted that β-AR stimulation enhances calcium-dependent inactivation to prevent intracellular calcium overload (Tsien et al., 1986; Findlay, 2004). It is important to note that the effect of β-adrenergic stimulation on calcium current is determined by critical factors such as species, charge carriers used, and recording protocols.

The molecular basis for β-adrenergic modulation of cardiac calcium channels involves PKA phosphorylation sites on the Ca^{2+} channel subunits (α_{1C} and β_2). Adrenergic responsiveness is also modulated by the A-kinase anchoring protein (AKAP), which anchors the kinase to the distal C-terminus (DCT) of $Ca_V1.2$, *see review* (Papa et al., 2022). Mutations or disruption of the DCT can lead to loss of cAMP-mediated phosphorylation and loss of channel regulation, which is associated with impaired cardiac function, hypertrophy, arrhythmias, and heart failure (Fu et al., 2011, 2013). A recent study has shown that β-adrenergic stimulation can increase the abundance of sarcolemmal $Ca_V1.2$ in the t-tubule by increasing the insertion of channels in mouse ventricular myocytes, which was accomplished due to reduction in the colocalization of $Ca_V1.2$/endosomes (del Villar et al., 2021).

1.4.4 L-type calcium channels and heart failure

L-type calcium channels are essential to initiate excitation-contraction coupling (ECC) in the muscles. They are primarily located on the membrane of the T-tubules, which are closely associated with the sarcoplasmic reticulum (SR) (Scriven et al., 2000). Unlike $Ca_v1.1$ channels in the skeletal muscle, which interact directly with ryanodine-sensitive Ca^{2+} release channels (RyR_s) in the SR (Catterall, 1991), the initiation of ECC in the heart requires external Ca^{2+} entry through $Ca_v1.2$ channels. Activation of $Ca_v1.2$ channels initiates contraction directly by increasing cytosolic Ca^{2+} concentration and indirectly by activating Ca^{2+}-induced Ca^{2+} release (CICR) through RyR_s channels, (Bers, 2002).

Failing ventricular myocytes show impaired contractility and abnormal Ca^{2+} transients, making LTCC a prime suspect for contributing to ECC dysfunction. However, studies on properties of L-type calcium current in both human heart failure and animal models were

inconclusive regarding the role of LTCC in HF (*review*, Mukherjee & Spinale, 1998; Richard et al., 1998; Bénitah et al., 2002).

Several techniques have provided detailed information about the number and function of LTCC during the progression of cardiomyopathy. Biochemical methods have shown no change or decrease in protein abundance of channel subunits or DHP-binding sites in failing hearts (Mukherjee & Spinale, 1998; Tomaselli & Marbán, 1999).

Genetic alterations in Cav subunits have been associated with different forms of cardiac dysfunction in mice. Global knockout of $Ca_v\alpha_1$ or $Ca_v\beta_2$ is embryonically lethal due to impaired cardiac development (Seisenberger et al., 2000; Weissgerber et al., 2006). Deletion of the $Ca_v\alpha_1$ subunit or mutation in its C-terminus resulted in a reduction in $I_{Ca,L}$, which induced cardiomyopathy and death (Blaich et al., 2012; Goonasekera et al., 2012). On the other hand, overexpression of $Ca_v\alpha_1$ or $Ca_v\beta_2$ can lead to LTCC properties characteristic of heart failure (Beetz et al., 2009; Hullin et al., 2007; Muth et al., 1999). Furthermore, mutations in the gene that encodes $Ca_v\alpha_2\delta$ have been also associated with various forms of cardiac dysfunction and arrhythmias in humans, such as Brugada syndrome (Burashnikov et al., 2010), and short QT syndrome (Templin et al., 2011).

However, extrapolating functional sarcolemmal channels from subunit composition alone is challenging. Schröder et al. demonstrated increased single-channel activity in failing human left ventricular myocytes due to increased channel availability and open probability when Ba^{2+} was used as a charge carrier, despite no change in channel subunit expression or whole-cell current (Schröder et al., 1998).

The relationship between whole-cell current and number of LTCC can be described by the equation: $\boldsymbol{I=N*i*\ Po*f_{active}}$, where ($I$) is the whole-cell current, (N) is the number of channels, ,(i) it the unitary current of a single channel, (P_o) the probability that a functional channel is open and (f_{active}) fraction of active sweep per number of test pulses (McDonald et al., 1994). Therefore, modifications of individual channel gating parameters e.g., due to β-AR activation as mentioned above, may affect channel activity and influence Ca^{2+} hemostasis. Furthermore, when analyzing Ca^{2+} entry through LTCC, it is important to investigate at least two parameters: peak amplitude and decay kinetics which can affect Ca^{2+} release from the SR and contribute to the shape of the cardiac action potential (Tomaselli & Marbán, 1999). $I_{Ca,L}$ contributes to the plateau phase of the cardiac AP, which is a labile phase and any small current changes can affect the membrane balance leading to repolarization or maintained

depolarization. Thus, alterations in $I_{Ca,L}$ density or gating can predispose to early- (EAD) or delayed afterdepolarization (DAD), or both (Figure 1-7), for references see figure legend.

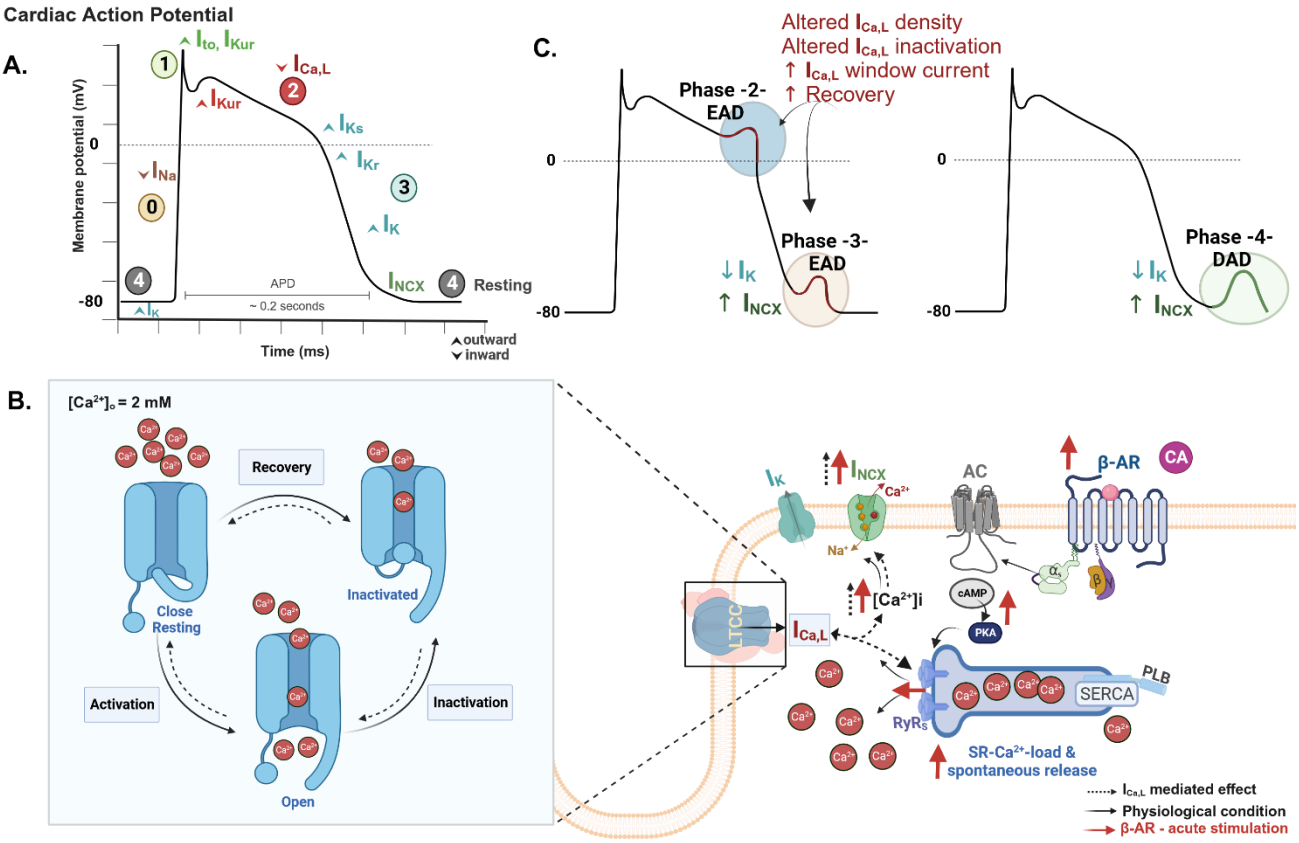

Fig. 1-7. L-type calcium current gating states and its contribution to cardiac action potential - Potential arrhythmogenic mechanisms in heart failure. A. Membrane currents that generate a normal action potential (AP): Resting (4), upstroke (0), early repolarization (1), plateau (2), and terminal repolarization are the phases of the action potential. Inward currents are sodium $\mathbf{I_{Na}}$, calcium $\mathbf{I_{Ca,L}}$, and the electrogenic sodium-calcium exchanger $\mathbf{I_{NCX}}$. Outward K^+ currents are $\mathbf{I_{to}}$ (transient fast/slow), $\mathbf{I_{Kur}}$ (delayed rectifier, ultrarapid), $\mathbf{I_{Ks}}$ (delayed rectifier, slow), $\mathbf{I_{Kr}}$ (delayed rectifier, fast), $\mathbf{I_K}$ (Kir current). **B.** $I_{Ca,L}$ contributes to ECC, directly by increasing cytosolic $[Ca^{2+}]i$, and indirectly by activating RyRs (dashed arrow). SR-Ca^{2+} load can affect $I_{Ca,L}$ decay (bidirectional dashed arrow) and I_{NCX}. **Inset:** different states of the voltage-gated Ca^{2+} channel. The resting state is defined when the membrane potential is negative. At a certain depolarization, the channels open and switch to the ion-conducting state. Prolonged depolarization can lead to inactivation of the channels (non-conducting). After repolarization, the channels can return to the resting state and thus become responsive again. Probabilities and rates of transition between states are not identical but modulated by factors like voltage or drugs. **C.** Action potential with early afterdepolarization (EAD) trigger activity due to electrophysiological changes in $I_{Ca,L}$, I_{NCX}, I_K currents or with delayed afterdepolarization (DAD) typically mediated by I_{NCX} due to SR-Ca^{2+} overload/spontaneous release i.e., following intense β-AR stimulation.

Original illustration, created with BioRender.com©; ref.: (Tomaselli & Marbán, 1999; Pogwizd & Bers, 2004; Grant, 2009; Weiss et al., 2010; Johnson & Antoons, 2018).

1.5 Mouse Models and Study Aims

Although several studies have documented alterations in the β-AR system in heart failure, the exact role of inhibitory G protein and whether long-term β-AR desensitization is beneficial or harmful remains uncertain. To address this question, gene-targeted mice can be employed to manipulate the expression of different components of the myocardial β-AR system.

In genetically modified mice, ventricular overexpression of either β_1- or β_2-AR resulted in distinct phenotypes, suggesting differences in their signaling and function in the myocardium. Overexpression (5- to 15-fold) of human β_1-AR resulted in dilated cardiomyopathy, even in young mice (Engelhardt et al., 1999; Bisognano et al., 2000), consistent with the pathology caused by chronic activation of catecholamines. Although, young mice with overexpression of β_2-AR did not exhibit significant cardiac pathology as first described by (Milano et al., 1994), similar levels of expression in older mice (Foerster et al., 2003) and overexpression at levels > 200-fold resulted in a progressive cardiac dysfunction (Liggett et al., 2000).

In our research, we have used transgenic mice with cardiac overexpression of β_1-AR to study the effects of $G\alpha_{i2}$ ($G\alpha_{i2}^{-/-}$) or $G\alpha_3$ ($G\alpha_{i3}^{-/-}$) deficiency on the cardiomyopathy phenotype. Our previous *in vivo* studies concluded that the lack of $G\alpha_{i2}$ has detrimental effects, while lack of $G\alpha_{i3}$ has beneficial effects in β_1-transgenic (β_1-tg) mice, as summarized in Figure (1-8):

Fig. 1-8. Summary of previous findings in the β_1-tg mouse model and the effects of additional deletion of a specific Gαi isoform

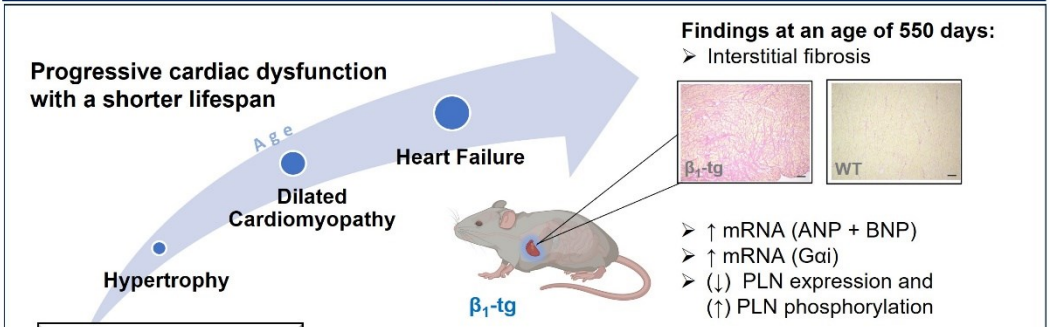

Alterations *versus* age-matched β_1-tg mice	Detrimental effects of $G\alpha_{i2}$ deficiency β_1-tg/$G\alpha_{i2}^{-/-}$	Protective effects of $G\alpha_{i3}$ deficiency β_1-tg/$G\alpha_{i3}^{-/-}$
• Compared age groups	300 days	550 days
• Lifespan	Shorter	Longer
• Ventricular hypertrophy	Exacerbated	Ameliorated
• ANP and BNP levels	Both markers increased	ANP decreased
• Ejection fraction (EF)	Decreased	Increased
• LVEDV & LVESV	Increased (significant)	Decreased (ns)
• Remaining Gαi isoform	Upregulation of $G\alpha_{i3}$ mRNA levels	Unchanged $G\alpha_{i2}$ mRNA levels

Fig. 1-8. Comparison of our two earlier *in vivo* studies that demonstrate the distinct functions of $G\alpha_{i2}$ and $G\alpha_{i3}$ in β_1-tg mice. We used the β_1-tg mouse model generated by Engelhardt et al. 1999. $G\alpha_{i2}$ deficiency caused early onset of cardiac dysfunction and accelerated the β_1-tg phenotype at 300 days of age (Keller et al. 2015). Conversely, $G\alpha_{i3}$ deficiency had a protective effect that was evident at an age of 550 days (Schröper et al. 2024). (LV) left-ventricular, EDV: end-diastolic volume, (LV) ESV: end-systolic volume. Brain-type (BNP) and Atrial-type (ANP) natriuretic peptides are hypertrophy markers, PLN, phsopholamban, a PKA-target.

Aims of the present study

Although our previous in vivo studies (Keller et al. 2015, Schröper et al. 2024) showed isoform-specific functions of $G\alpha_{i2}$ and $G\alpha_{i3}$ in β_1-tg mice, they could not explain the mechanistic basis for their distinct effects. Investigating the molecular and functional changes that occur downstream of Gi signaling at the myocyte level will help to gain a better understanding of their role in cardiomyopathy, therefore:

1) Considering the significance of LTCC for cardiac excitation-contraction coupling and the changes in I_{CaL} observed in human heart failure and various HF models, we examined the functional properties of $I_{Ca,L}$ in β_1-tg mice, and the $I_{Ca,L}$ responsiveness to acute β-adrenergic stimulation.

2) Given the detrimental effects of $G\alpha_{i2}$ deficiency but the beneficial effects of $G\alpha_{i3}$ deficiency in the murine HF model of cardiac β_1-AR overexpression, we analyzed ventricular I_{CaL} in the respective mouse models to identify putative differences that might hint at the mechanisms underlying the respective phenotypes.

3) Testing new Gαi modulator:

As previously stated, there is currently no effective selective G-protein modulator clinically available. In collaboration with the research group of Dr. Imhof at the University of Bonn, we conducted a proof-of-concept study to test a new Gαi modulator, labeled BN6 or recently published as G-protein modulator 1 (GPM-1) (Nubbemeyer et al., 2022). This peptide was developed through peptide library screening and is a small linear peptide consisting of nine amino acids (RWLRYLRYP). The aim of this study was to examine the effect of this peptide on whole-cell $I_{Ca,L}$ in wild-type myocytes. The experiments were performed blindly, without prior knowledge of its Gα subtype/isoform affinity.

2

Methods

2.1 Mouse Models

2.1.1 Animal Care and Ethical Statement

Animals were bred and maintained at the animal facilities of the Center for Molecular Medicine Cologne (CMMC), and of the Center for Pharmacology, Institute II, University Hospital Cologne. All mice were kept in individually ventilated cages with food and water ad libitum, maintained in a 12h/12h dark/light cycle. The animal breeding, maintenance and experiments were approved by the responsible federal state authority:

Landesamt für Natur-, Umwelt- und Verbraucherschutz Nordrhein-Westfalen; ref.: (84-84-02.04.2016.A422,and 81-02.04.2022.A141).

All procedures and experiments involving animals were conducted in accordance with the Guidelines 2010/63/EU of the European Communities Council Directives on the protection of animals used for scientific purposes.

2.1.2 Transgenic and Knock-out Mouse Models

Transgenic mice with a cardiac-specific overexpression of the human β_1-adrenoceptor (β_1-tg) were originally generated on an FVB/N background using a transgenic construct incorporating the coding sequence of the human β_1-adrenergic receptor under the control of the murine α-myosin heavy-chain (MHC) promotor, as described previously (Engelhardt et al., 1999). For β_1-tg mice used in this study, the FVB/N-based transgenic mice were backcrossed on a C57BL/6J background (10> generation) to allow mating with the Gαi-knockout mouse strains (Foerster et al., 2004). Mice ubiquitously lacking $G\alpha_{i2}$ ($G\alpha_{i2}^{-/-}$) or $G\alpha_{i3}$ ($G\alpha_{i3}^{-/-}$) were originally generated on a 129Sv background (Rudolph et al., 1993, 1995) and subsequently backcrossed to C57BL/6J strain (Keller et al., 2015; Schröper et al., 2024).

In this study, β_1-tg mice were crossbred with mice globally lacking $G\alpha_{i2}$ or $G\alpha_{i3}$ to produce β_1-tg mice lacking $G\alpha_{i2}$ (β_1-tg/$G\alpha_{i2}^{-/-}$), or lacking $G\alpha_{i3}$ (β_1-tg/$G\alpha_{i3}^{-/-}$). Only male mice were used, and two age groups were selected, (4-5) months and (10-11) months. Age-matched wild-type littermates served as controls. For the proof-of-concept study, 3-5 months wild-type animals of both sexes were used.

2.1.3 Mouse Genotyping[1]

For genotyping, ear- or tail-clips (stored at -20°C) from 14-20-weeks-old mice were used. For identifying the integration of the transgenic gene (β_1-AR-tg), singleplex PCR assays were performed with a sense primer located in the α-myosin heavy chain promoter, and an antisense primer located in β_1-receptor coding sequence (ADRB1). For Gαi genotyping, multiplex PCR assay could be used i.e., amplifying multiple target sequences such as mutant and wildtype in a single PCR reaction. However, for GNAI3 gene, a singleplex assay is recommended – Primers are listed in Table 2-1. Supplementary PCR-genotyping results, including a brief description of the PCR reaction and thermocycler programs, are provided[2], (suppl.-S1).

Table 2- 1
Primers for mouse genotyping

Gene	Oligo name	Primers
ADRB1	MHC 176+	**5`-ACA TGG AGT CCT GGT GGG AG-3`**
	HB1: 60-	**5`- TGC GGC CGA CGA CAG GTT AC-3`**
GNAI2	Gi2 Wt F	**5`- GAT CAT CCA TGA AGA TGG CTA CTC AGA AG -3`**
	Gi2 Wt R	**5`- CCC CTC TCA CTC TTG ATT TCC TAC TGA CAC -3`**
	Gi2 Mut F	**5`-CAG GAT CAT CCA TGA AGA TGG CTA C-3`**
	Gi2 Mut R	**5`-GCA CTC AAA CCG AGG ACT TAC AGA AC-3`**
GNAI3	I3Ex6 F1	**5`-GTG GCC AAA GAT CCG AAC GAA-3`**
	Neo F1	**5`- TGC CGA GAA AGT ATC CAT CAT G-3`**
	I3Ex7 R1	**5`- TTC ATG CTT TCA TGC ATT CGG TTC-3`**

ADRB1: gene coding β_1-adrenoceptor, MHC: myosin heavy-chain, HB1, human β_1, Wt: wild-type, Mut: mutant. GNAI2 gene coding $G\alpha_{i2}$. For GNAI3 gene coding $G\alpha_{i3}$: similar antisense primer was used for mutant and wild-type.

[1] Mouse Genotyping was performed by Mrs. Sigrid Kirchmann-Hecht and Ms. Cora Fried at the Center of Pharmacology, Institute II, University Hospital of Cologne.
[2] Detailed protocols for the isolation of genomic mouse DNA and PCR genotyping are available in the e-LabJournal, the electronic lab book of the University of Cologne - Group: Zentrum für Pharmakologie; Author: Katnahji.

2.2 Isolation of primary ventricular cardiomyocytes

Primary ventricular cardiomyocytes were isolated from the hearts of adult mice (22 to 35 grams) for electrophysiological patch-clamp measurements. The isolation procedure follows the AfCS protocol (ID: PP00000 125) originally described by (O'Connell et al., 2007).

Isolation of high-quality functional cardiomyocytes is dependent on various factors, such as mouse strain, age, genetic modifications, and applied procedures. Consequently, some modifications were made to the existing protocol to ensure optimal and reproducible cell isolation and to obtain crystal clear myocytes for the cell patch clamp. These modifications were made after a series of trial experiments carried out as part of this study. The isolation procedure can be divided into three main steps, preceded by a preparation step (Figure 2-1).

2.2.1 Materials and Solutions

All solutions and buffers must be prepared prior to isolation with distilled water and filtered before storage or use. The **perfusion buffer** (Table 2-2) is a calcium-free buffer that serves to wash out blood, remove extracellular calcium and provide a balanced electrolyte solution that mimics the physiological conditions of the heart. Additionally, it is supplemented with 2,3-butanedione monoxime (BDM), which is an inhibitor of myosin II ATPase that binds reversibly to cardiac myofilaments and prevents hypercontraction and cell death (KIVIST&Ouml et al., 1995). The **myocyte digestion buffer** (Table 2-3) is a collagenase-based enzyme solution that contains a low calcium concentration to allow for adequate enzyme activity. This buffer is essential for the breakdown of the extracellular matrix and intercellular junctions that hold the cardiomyocytes together in the cardiac tissue, thus allowing them to be dispersed into single cells. Both perfusion and myocyte digestion buffer were kept at 37°C shortly before use.

The **myocyte stopping buffer** (Table 2-4) is required to stop the enzymatic digestion and avoid over-digestion; it contains calf serum to inactivate the enzymes. This buffer was derived from the perfusion buffer and served as the foundation for preparing the calcium gradient solutions.

Before starting isolation, all surgical instruments must be sterilized with alcohol and the perfusion system must be pre-rinsed, removing any existing air bubbles. The necessary equipment and supplies for isolation are listed in (Table 2-6).

Step 1: Heart Removal and Cannulation

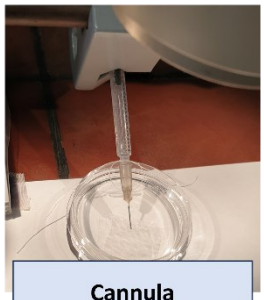

Cannula

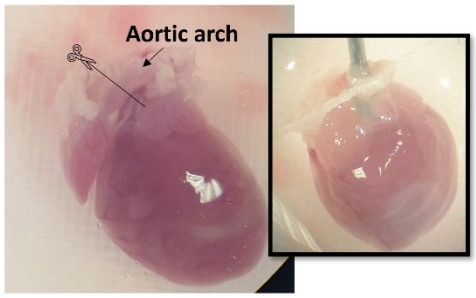

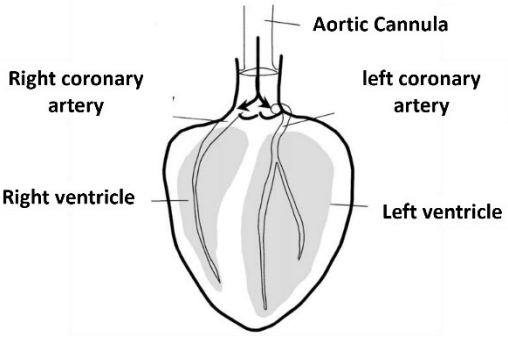

Step 2: Heart Perfusion and Digestion

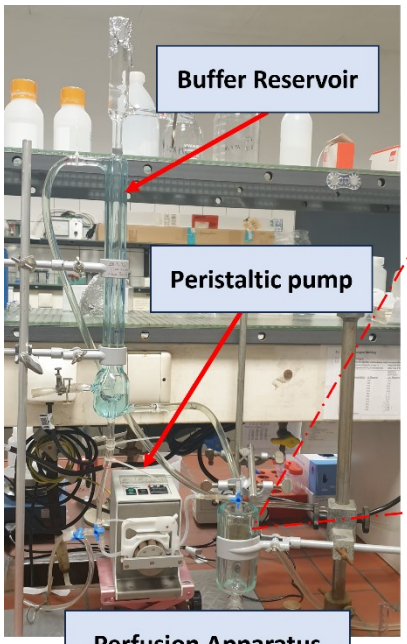

Perfusion Apparatus

Heart in organ bath

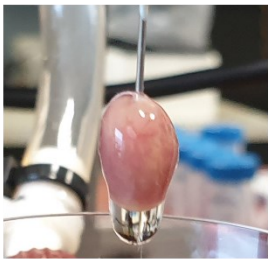

Successful enzymatic digestion
Swollen, pale heart

Step 3: Myocyte Dissociation

Dissociated myocytes

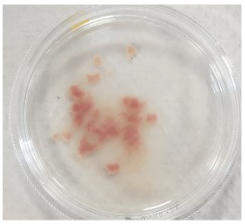

Ca^{2+} Reintroduction

Fig. 2-1. Original pictures summarize the primary steps for cardiomyocytes isolation.
The schematic illustration of the isolated perfused heart* (*in step 1*) is based on the Langendorff heart to show the correct position of the cannula over the valve for proper perfusion.

**Practical Method in Cardiovascular Research by Dhein Mohr Delmer (2005).*

Table 2- 2
Perfusion Buffer (1X) – Ca^{2+}-free

Compound – Stock Buffer	Mol. wt (g/mol)	For 1Liter (g)	Final conc. (m*M*)
Sodium chloride (NaCl)	58.4	6.6	113
Potassium chloride (KCl)	74.55	0.35	4.7
Potassium phosphate monobasic (KH_2PO_4)	136.09	0.0816	0.6
Sodium phosphate dibasic ($Na_2HPO_4)_2H_2O$	177.99	0.1067	0.6
Magnesium sulfate heptahydrate ($MgSO_4$-$7H_20$)	246.48	0.2957	1.2
Sodium bicarbonate ($NaHCO_3$)	84.01	1.0081	12
Potassium bicarbonate ($KHCO_3$)	100.12	1.0012	10
HEPES	238.30	2.383	10
Taurine	125.1	3.75	30
Compound – Perfusion Buffer pH 7.46	**Mol. Wt (g/mol)**	**For 1Liter**	**Final conc. (mM)**
Stock Buffer 1X	-	980 ml	0.98 X
500 m*M* 2,3-Butanedione monoxime (BDM)	101.1	20 ml	10 mM
Glucose	180.2	1 g	5.5 mM

For 1 Liter stock buffer (1X), dissolve ingredients in 990 ml dd H_2O, stir until all components are thoroughly dissolved, then adjust final volume to 1L in graduated cylinder. BDM and glucose are added to 980 ml of stock, and pH is adjusted with 10N NaOH to 7.46. Final volume should be adjusted to 1L with the stock buffer and sterile-filtered with a 0.22-µM filter. Perfusion buffer (1X) can be stored at -20°C up to 3 weeks.[3]

Table 2- 3
Myocyte Digestion Buffer (50 ml/Heart)

Compound	#Lot	Amount	Final conc.
Perfusion Buffer, pH 7.46	made in lab	50 ml	1X
Collagenase Type II (4°C) ACT: 305 u/mg dw ACT: 320 u/mg dw	 # S5B15572 # 41B21028	 59 mg* 46 mg	300 U/ml
Protease Type XIV (-20°C)	-	2 mg	0.04 µg/ml
100 m*M* Calcium Chloride ($CaCl_2$); (4°C)	made in lab	6.25 µl	12.5 µM

* The absolute amount of collagenase will vary based on the total activity (ACT) from lot to lot, and from different providers. Digestion buffer must be freshly prepared for each heart, max. 1 hour before use. This recipe was originally adapted from RG: Hofmann - Technical University of Munich, after personal communication.

[3] The suppliers and order numbers of all chemicals used in this study are listed alphabetically in the appendix (**S3-list of chemicals**).

Table 2- 4
Myocyte Stopping Buffer (50 ml/Heart)
and Calcium Reintroduction

Stopping Buffer (basic solution)	Amount	Final conc.
Perfusion Buffer, pH 7.46	45 ml	-
Fetal Calf Serum (FCS)	5 ml	10%

Solution	Stopping Buffer (ml)	100 m*M* $CaCl_2$ (µL)	Final Ca^{2+} conc.
I	20 ml	2.5 µl	12.5 µM
20 min*			
II	10 ml	10 µl	100 µM
20 min			
III	10 ml	40 µl	400 µM
20 min			
IV	10 ml	90 µl	900 µM

Myocyte stopping buffer is prepared as a basic solution (50 ml) containing 10% FCS (Biochrome – S05615). Solutions I-IV are then made with gradually increasing calcium concentration. The cells are allowed to settle via gravity. After each 20-minute time interval, the supernatant is discarded, and the next solution is carefully added to the pellet. This process is repeated until the maximum calcium concentration is achieved. The first step is repeated twice, adding 10 ml of solution I each time.

Table 2- 5
Heparin for i.p. injection

Compound	Source	Stock conc.	Amount	Final conc.
Heparin-Natrium	B-Braun	25000 IU/ 5 ml	1 ml	500 IU/ml
NaCl 0.9%	Fresenius Kabi	9 mg/ml	9 ml	8 mg/ml

For intraperitoneal injection, 10 µl (heparin 500 IU/ml) per gram of body weight is required. Both heparin and NaCl are stored at 4°C and diluted heparin can be stored for a maximum of 3 weeks.

2.2.2 Myocyte Isolation

1. Removal and cannulation of the heart:

Mice were injected with heparin to prevent blood clotting in the coronary arteries. After 30 minutes, the mouse was killed by cervical dislocation and then secured in the supine position by gently attaching the front and hind paws to the operation surface near the perfusion system. The chest and abdomen were wiped with 70% isopropyl alcohol and a midline skin incision was made to separate the fur and open the chest. Using small scissors and fine forceps, the diaphragm was cut, and the rib cage was pulled back to expose the heart. The heart was gently lifted, the pulmonary vessels were cut, and the aorta was to be cut about 2 mm from its entry into the heart (below the aortic arch, Fig. 2-

1).The heart was immediately transferred to a 60-mm dish containing 10 ml of ice-cold perfusion buffer for a quick wash step, and then transferred to another dish containing 10 ml of perfusion buffer at room temperature under a dissecting microscope. Extraneous tissues were removed, and the heart was cannulated by sliding the aorta onto a cannula, which is pre-attached to 1-ml syringe filled with perfusion buffer. The blunted tip of the cannula should be just above the aortic valve. Silk threads were used to tie the aorta to the cannula to prevent the heart from falling during the perfusion process.

2. **Heart perfusion and enzyme digestion:**

The perfusion apparatus used in this experiment was a modified Langendorf system, consisting of a water-jacketed reservoir connected to a water bath, with a circulating system to warm solutions (37°C). The solutions were pumped through a peristaltic pump to the cannulated heart, which was kept in an organ bath chamber to maintain temperature. The heart was perfused at a rate of 3ml/min for 4-6 minutes, depending on its size. Afterwards, the buffer was switched to myocyte digestion buffer for 8-10 minutes until the heart became swollen, pale, and flaccid.

3. **Myocyte dissociation and calcium reintroduction:**

After enzymatic digestion, heart was carefully removed from the cannula and placed in a sterile 60 mm dish containing 5 ml of myocyte digestion buffer. The atria and aorta were removed with a scalpel, and the ventricles were then transferred to a new, sterile 60 mm dish containing 2.5 ml of myocyte stopping digestion buffer (solution I, Table 2-4). Using two fine forceps, the ventricles were carefully picked into smaller pieces. Subsequently, 5 ml of solution I was added, and the cells were gently dissociated using a Pasteur pipette for 60-90 seconds. The cell suspension was then transferred and filtered through a 0.22 μM mesh filter into a 50 ml falcon tube. The dish was rinsed with solution I and combined with the cell suspension to a final volume of 10 ml. The cells were allowed to settle under gravity and the procedure was repeated until solution IV. The final calcium concentration will be 1.2 m*M*. The cells were then kept in the tube for at least 2 hours at room temperature before being subjected to electrophysiological experiments.

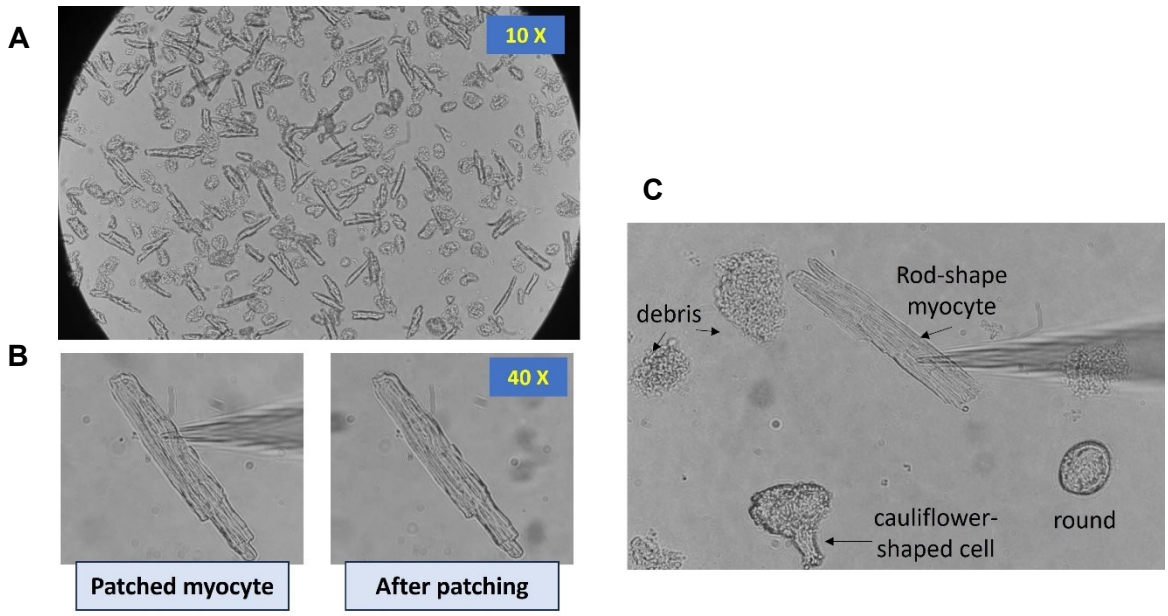

Fig. 2-2. Examples of isolated ventricular cardiomyocytes and criteria for cells selected for parch-clamp measurements. **A.** Myocytes observed in brightfield 10x **B.** Excellent-quality myocyte that kept intact for a few minutes after removing the patch-pipette. **C.** Only myocytes with an overall rod shape with a clear striation pattern (without granulation and without cauliflower-shaped cell edges), and quiescent cells in the absence of electrical stimulation or isoproterenol were used.

Table 2- 6
Equipment and Supplies for Myocyte Isolation

Item	Description/Supplier
Water bath with circulating pump	Thermo Scientific
Langendorff Column	Self-supplied
Dissecting Microscope	Olympus
Peristaltic pump	Istatec
Lighting and Imaging	Schott, KL1500 HAL
Cannula (blunted injection cannula)	20-22 g sized for heart canulation
Mesh filter 250 µm (polyamide 6.6+Nylon)	RCT Reichelt Chemitechnik GmbH
Seven Easy pH-meter	Mettler Toledo
Surgical instruments - Scissors (curved, straight) - Dumont fine-tip forceps - Serrated forceps - Tissue forceps - Miniature scissor - Lorna towel clamp	Fine Science Tools (F.S.T)
Cell culture dishes (35, 60 mm)	Lab consumables
Falcon tubes, 15 and 50 ml	
Filter 0.2 µM, 500 ml, for solutions	
Plastic transfer pipette, 5 mm	
Serological glass pipette (5,10, 25 ml)	
Sterile scalpel	
Syringes (1 ml, sterile)	

2.3 Patch-Clamp Electrophysiology

Patch clamp is a technique that enables the measurement of the current flowing through ion channels present in the membranes of excitable cells such as cardiomyocytes. It was developed by Neher and Sakmann in 1976, based on the initial voltage-clamp experiment that was described by Cole and Marmont in 1949, and refined by Hodgkin and Huxley in the early 1950s to elucidate the time- and voltage-dependent properties of the ionic conductance underlying action potential generation in the squid giant axon (Yang et al., 2014; Brackenbury, 2021).

Voltage patch-clamp allows the measurement of ion currents through individual ion channels **(Single-channel)** or the entire cell membrane **(Whole-cell)**. The technique involves applying negative pressure to establish a high-resistance seal (giga-ohm seal) between a glass micropipette and a cell membrane. The pipette's electrode can regulate the voltage across the membrane patch, and the channel current can be detected and measured. Various recording configurations can be achieved depending on how the pipette is positioned and retracted, such as cell-attached, inside-out, whole-cell, outside-out, or perforated patch (Hamill et al., 1981), Figure 2-3. Furthermore, this technique allows the manipulation of intra- and extracellular solutions as well as the application of pharmacological agents to activate or inhibit the channel of interest. This enables the study of a specific type of ion channel and various biophysical properties by selecting appropriate recording settings relevant to the research question.

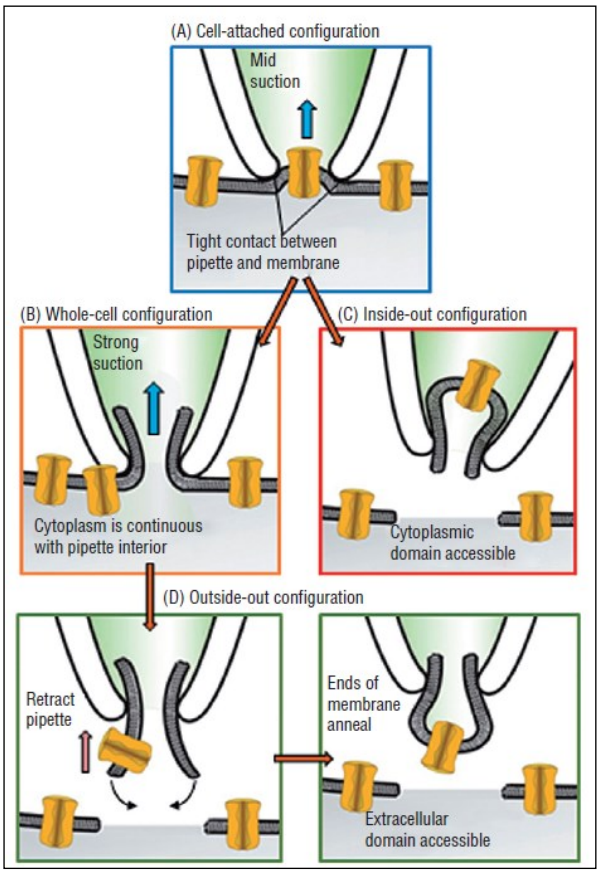

Fig. 2-3. Patch-Clamp Configurations. For both whole-cell and single-channel current recordings, a gigaohm GΩ tight seal must be established between the cell membrane and the recording pipette. The seal is formed by applying suction to the pipette after it comes into contact with the cell membrane. Once the seal resistance is high enough, single-channel recordings can be made in the "cell-attached" configuration ***(A)*.** By applying additional suction to the pipette, the membrane patch ruptures, which allows for whole-cell recording ***(B)*.** Alternatively, retracting the pipette in "cell-attached" mode allows single channel recordings in "inside-out" configuration***(C)*.** Retracting the pipette while in "whole-cell" mode creates "outside-out" configuration with annealed membrane ***(D)*.** Adapted from Yang et al. 2014.

2.3.1 Whole-Cell Recordings of $I_{Ca,L}$

In this study we used conventional whole-cell patch-clamp configuration in voltage-clamp mode to record the macroscopic L-type Ca^{2+} current ($I_{Ca,L}$) under basal conditions or after incubation with the non-selective β-AR agonist isoproterenol (Iso). Every conventional patch clamp experiment follows the main steps illustrated in Figure 2-4:

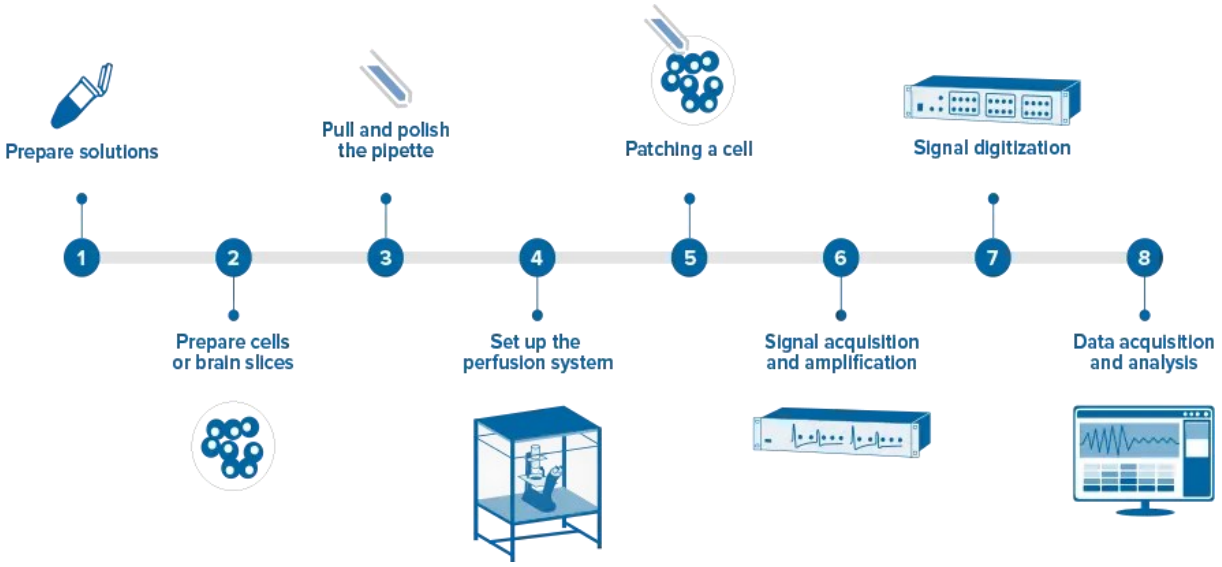

Fig. 2-4. The principal steps in conventional patch-clamp electrophysiology experiments for recording single cells or tissue slices – adapted from Molecular Devices, LLC©

2.3.1.1 Patch Clamp Rig

The patch-clamp setup consisted of an amplifier, a digitizer, a glass micropipette mounted on a preamplifier circuit built into a headstage, and a computer with pClamp software (an interface program that controls the amplifier and the digitizer, as well as performs data analysis and visualization). The headstage was mounted on an inverted microscope and placed on an anti-vibration table in a Faraday cage to eliminate noise and isolate mechanical vibrations (Fig 2-5, Table 2-7).

A 1-mm silver wire was used for the connection between the patch pipette solution and the preamplifier circuit. This wire was coated with silver chloride to minimize the polarization of the electrode, i.e., the accumulation of electrical charge at the interface between the electrode and the solution. This helps to improve the accuracy and stability of the measurements. To coat the wire with silver chloride, an electrochemical process was applied, in which a 0.3 mA current (for 1 cm of a 1 mm wire) is passed through the wire in a solution of 3*M* potassium chloride (KCl) until the wire is coated with a light gray to purple-gray layer of silver chloride (AgCl). Likewise, the bath solution was grounded by a reference electrode made of a silver-

silver-chloride wire. A hydraulic micromanipulator was used to control fine movement of the micropipette.

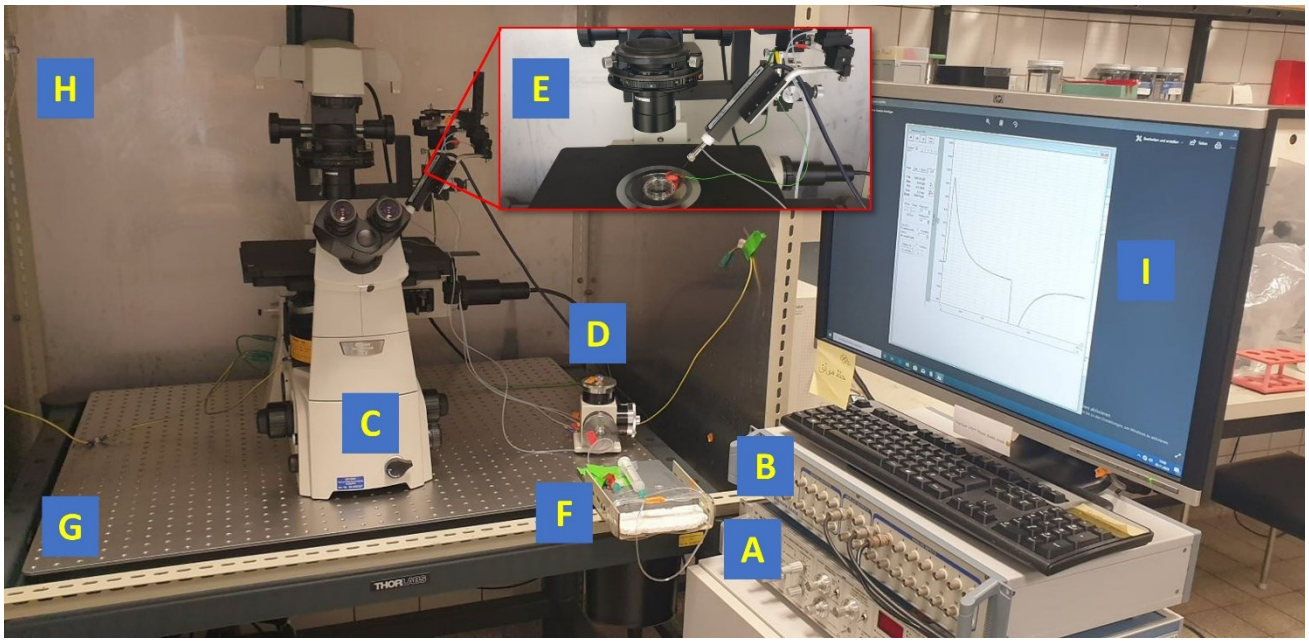

Fig. 2-5. **The patch-clamp rig used for whole-cell recordings. A.** amplifier, **B**. digitizer, **C**. microscope, **D**. hydraulic micromanipulator, **E.** headstage with a pipette holder, recording dish is also shown, **F.** 10-ml syringe connected to the holder for pressure application, **G**. anti-vibration table, **H**. faraday cage, **I.** PC/monitor.

Table 2- 7
Patch-Clamp Equipment & Computer Software

Item/Description	Supplier/Manufacturer
Antivibration Table + air compressor	Thoralabs
Axopatch 200B amplifier	Axon-CNS Molecular Devices
Computer assembled with a mointer	HP – KR1002149*
CV 203BU Headstage	Axon Instruments
Digidata 1440A A/D-converter	Axon-CNS Molecular Devices
Faraday Cage	Self-supplied
Microscope Nikon Eclipse	Nikon Instruments
Micromanipulator MHW-103	Narishige International
Pipetboy acu	Integra Biosciences
Pipette Puller P-97	Sutter instruments
Seven Easy pH-meter	Mettler Toledo
Silver wire (recording/reference electrode)	Science Products - Hofheim
Computer Software	
Clampex 10.3 and Clampfit 10.7	Molecular Devices – Free licence
Graphpad Prism 10	Personal licence: GPS-2420391-TFTL-7C5B5
Microsoft Office 365	Personal licence: 10032001D2289052

*The ID number of the computer (identified by the IT department of the University Hospital Cologne) on which the row data were generated and stored.

2.3.1.2 Fabrication of Patch-Pipette

In whole-cell recordings, high-frequency noise is mainly caused by the combination of the pipet resistance and the whole-cell capacitance. Unlike single-channel pipettes, factors such as the dissipation factor and the glass's dielectric constant are less significant in this application. To optimize the noise level of the whole-cell current recording, the best approach is to use pipettes with the lowest possible resistance (Rae & Levis, 2004).

In this study, we used thin Borosilicate glass capillaries (OD/ID: 1.7/1.3 mm, wall thickness: 0.283 mm; without filament - Hilgenberg®). Briefly, long glass capillaries were initially cut into individual 7-10 cm pieces and then pulled using a horizontal puller (P-97 Sutter) to create two identical patch-pipettes. The pulling-program was written in three lines, and fixed values were set for the following parameters: Pull: 0, Time: 250, and Pressure: 500. The heat and velocity of the pulling process were regularly adjusted in accordance with the ramp and mid-velocity tests.

Patch pipettes with a resistance of 3-5 mΩ when filled with the intracellular solution were used. Only newly fabricated pipettes were utilized, and a stable seal was established without the need to fire-polish the pipette tips.

Table 2- 8
Whole-cell $I_{Ca,L}$ Recording Solutions

Bath Solution, pH: 7.4		
Compound	**Mol. Wt (g/mol)**	**Final conc. (m*M*)**
NaCl	58.44	137
CsCl	168.36	5.4
$CaCl_2$* 2 H2O	147.02	2
$MgCl_2$* 6 H2O	203.30	1
Glucose	180.16	10
HEPES	238.30	10

This solution must be freshly prepared with dd H_2O on the day of the experiment. The pH value was adjusted with NaOH. The solution was used at room temperature and filtered directly with a 0.2 µm Luer lock filter before being added to the recording dish.

Pipette Solution, pH: 7.2		
Compound	**Mol. Wt (g/mol)**	**Final conc. (m*M*)**
CsCl	168.36	120
Mg-ATP	507.18	4
$MgCl_2$*$6H_2O$	203.30	1
EGTA	380.35	10
HEPES	238.3	5

This solution can be prepared, filtered, and stored at -20°C. The pH value was adjusted with CsOH. As this solution contains Mg-ATP, it is recommended to keep it on ice during the experiment. It was filtered again using a 0.2 µm Luer lock filter before being filled into the pipette.

2.3.1.3 Recording Procedure and Data Acquisition

Freshly isolated ventricular cardiomyocytes that met certain criteria (Figure 2-2) were selected for the measurements. Whole-cell $I_{Ca,L}$ was recorded in a bath solution containing a physiological Ca^{2+} concentration [2 m*M*] at room temperature; 2-10 hours after myocyte isolation. Table 2-8 lists the components of the bath and pipette solution that mimic the extra- and intracellular milieu, with two key points to note: Cesium chloride (CsCl) was used to block the potassium current, while EGTA serves as a Ca^{2+} buffer to prevent changes in Ca^{2+} concentration.

As mentioned above, the cells were maintained in a Falcon tube at room temperature until use. 30 µL of the cell suspension was transferred to a 35-mm cell culture dish (used as a recording chamber) containing 3 ml of a filtered bath solution, mixed gently and then allowed to settle for 2-3 minutes. During this time, the patch pipette was filled with a pipette solution in two steps (tip filling and back filling), and bubbles were completely removed by gentle tapping. The pipette was then mounted on the pipette holder, which contains the recording electrode that was plugged into the head stage. To prevent the pipette tip from clogging, a gentle positive pressure was applied to the pipette via a 10-ml plastic syringe connected to the electrode holder.

Once the pipette is immersed in the bath solution, the pipette resistance can be determined. Test pulses generate different current responses while proceeding to establish a whole-cell configuration (Figure 2-6). As the pipette tip approaches the cell surface, the pipette resistance increases, and the giga-ohm seal can be established by releasing the positive pressure. When the seal is achieved (Figure 2-6, C), the electrode transient should be cancelled by adjusting the pipette offset in the amplifier, so that the test impulse response is like that shown in (Figure 2-6, D). At this stage, the holding potential (HP) should be -80 mV, which corresponds to the resting potential of the cardiomyocytes, to avoid a large change in the membrane potential when the cell membrane bursts.

Whole-cell configuration was achieved by applying a strong suction via the 10-ml syringe, which should rupture the membrane patch without destroying the cell. In most cases, it was necessary to carefully pull the syringe throughout the recording to maintain a negative pressure and keep the cell open. Afterwards, the membrane capacitance (Cm), the membrane resistance (Rm) and the access resistance (Ra) were automatically determined by the pClamp software. However, it is necessary to compensate for cell capacitance and

series resistance (Rs) to reduce errors and artifacts during voltage clamp recording. Recordings were taken approximately 4-5 minutes after establishing the whole cell configuration, and cell compensation was monitored continuously throughout the recording i.e., before applying new test-pulse protocol.

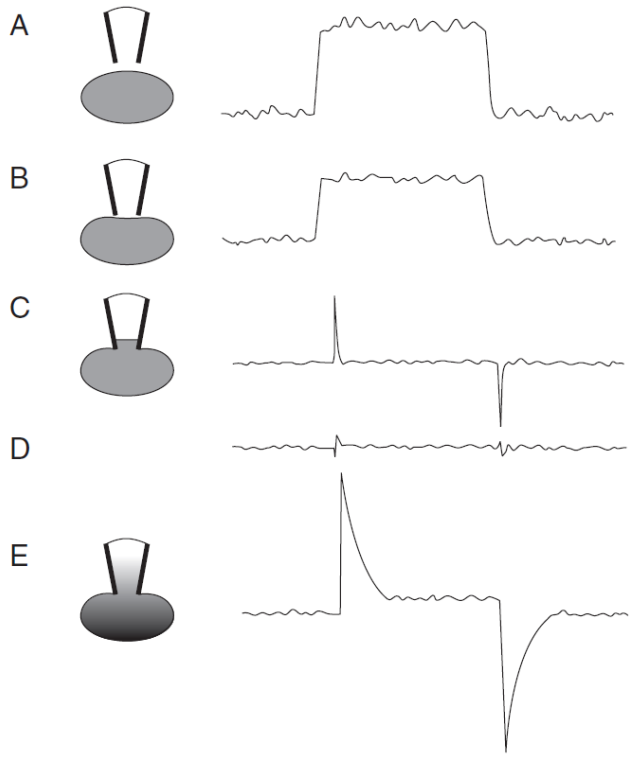

Fig. 2-6. Schematic illustration of the test pulses producing different current responses during the steps of a whole-cell voltage clamp recording. The physical relationship between the patch pipette and the cell is illustrated schematically on the left. (**A-B**) as the resistance across the patch pipette tip goes up, the size of the current change produced by the test pulse decreases. Thus, a reduction in test-pulse current indicates closer contact between the electrode tip and the cell. **(C)** A gigaseal has formed (cell-attached mode) as the result of gentle suction, which pulls a small patch of membrane up into the electrode tip. **(D)** The electrode capacitance transient is nulled. **(E)** The break-in is achieved by strong suction, which removes the membrane patch in the electrode tip but leaves the seal and the cell intact. The resistance decreases and large capacitive transients occur. Adapted from (Jackson, 1997).

2.3.1.4 Pharmacology

- To activate protein kinase A (PKA) signaling pathways, myocytes were exposed to the non-selective beta-adrenergic receptor agonist isoproterenol (Iso), also known as isoprenaline. Myocytes were placed in a 3-ml bath containing 1 μM Iso (Table 2-9), and the first $I_{Ca,L}$ measurement was performed 8±2 minutes after Iso exposure, as depicted in

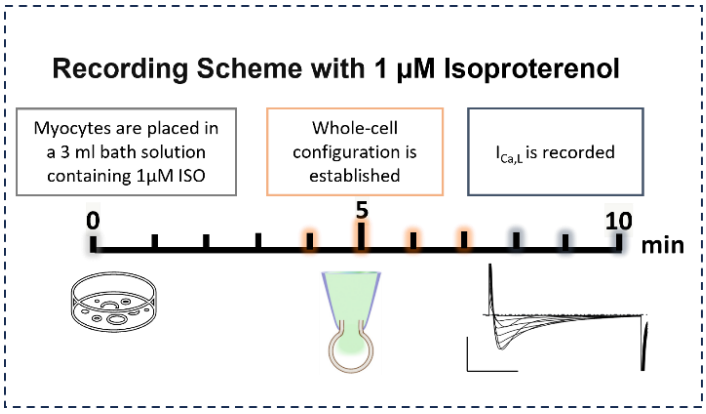

Fig. 2-7. Schematic representation of the protocol used for the whole-cell measurements of $I_{Ca,L}$ in myocytes incubated with 1 μM Isoproterenol.

❖ To test the effect of the new peptidyl-Gαi/s modulator BN6, recently identified as GPM1 (Nubbemeyer et al., 2022), on calcium channel activity, whole-cell measurements were performed by adding the peptide to the pipette solution, because it is not membrane permeable. The peptide was dissolved in 0.1 % DMSO, a concentration considered safe for patch-clamp measurements (Table 2-10).

Table 2- 9
Isoproterenol Stock Solution I, 1 m*M*

Compound	Mol. Wt (g/mol)	Amount (*g*)	Final conc.
Isoproterenol	247.7	0.01239	1 mM
Ascorbic acid	176.12	0.5	0.1 %

First, an Iso-stock solution I (1 mM) was prepared and then diluted 10-fold with dd H_2O to obtain a stock solution II (0.1 mM). The latter can be stored at +4°C for max. 6 weeks protected from light (aluminum foil). For a working concentration of 1 µM, a 30 µl of stock solution II was added to 3 ml of bath solution.

Table 2- 10
BN6 (GPM-1), Stock Solution, 1 m*M,* in 248 µl total volume

Compound	Mol. Wt (g/mol)	Amount	Final conc.
BN6	1321.57	328 µg	1 mM
DMSO	78.13	24.8 µl	10%

To fully dissolve the peptide, it is important to use 100% DMSO. Therefore, the peptide was first dissolved in the calculated amount of DMSO (100%) to prepare the stock solution, then the final volume was adjusted using dd H_2O. The stock solution was stored at -80°C. On the day of the experiment, the peptide concentration was diluted by a factor of 1:100 in the pipette solution to obtain a working concentration of 10µM – Calculations and adjustments were made after personal communication with RG Imhof.

2.3.2 Test-pulse Protocols and Data Analysis

Extensive electrophysiological characterization of cardiac L-type channels was performed using various pulse protocols that included measurements of activation, inactivation, and recovery kinetics (Figure 2-8). For whole-cell recordings, the front panel controls of the amplifier (Axopatch 200B) were set as follows: ● Mode: v-clamp ● Confg.: whole-cell β=1 ● Headstage Cooled: Vm ● Output gain (α): 2 ● Lowpass bessesl filter: 2 kHz. Other parameters were turned off or nulled as an initial setting.

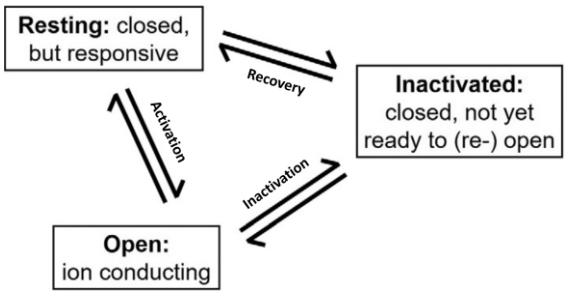

Fig. 2-8. Simplified scheme of different states of voltage-gated Ca^{2+} channels – adapted from (Matthes, 2022)

2.3.2.1 Current-Voltage (I-V) Relationship

- **I-V pulse protocol:**

To study the voltage dependence of $Ca_V1.2$ activation, $I_{Ca,L}$ was measured, and the current-voltage relationship was obtained using the I-V protocol shown in Figure 2-9. To isolate $I_{Ca,L}$ from other contaminating currents, I_{Na} and T-type $I_{Ca,T}$ (if present) were inactivated by a 45 ms prepulse to -40 mV (holding potential: HP -80 mV), and K^+ currents were blocked by substituting K^+ with Cs^+ (refer to Table 2-8). Then, test pulses with voltages ranging from -40 mV to +50 mV with a 10-mV increment were applied for 150 ms, and the cell was repolarized to -80 mV after each pulse. The pulse interval was set to 3 seconds and the stimulation frequency was set to 5 kHz.

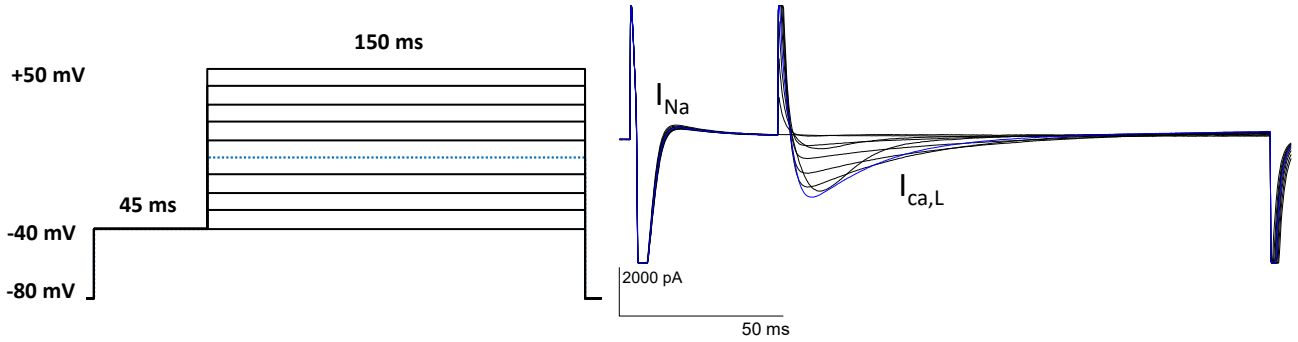

Fig. 2-9. Test pulse protocol (left) for recording the L-type current (example traces, right). In blue, the test pulse at 0 mV (dashed line) at which the peak current was typically reached in wild-type myocytes under basal conditions. For a detailed description of the protocol see text.

- **I-V curves and $I_{Ca,L}$ analysis:**

For data analysis, only good-quality recordings from stable patches with a minimal access resistance (Ra) i.e., ~10% ≤ of the membrane resistance (Rm), and a full inactivated sodium channels were considered.

Peak current amplitude was determined as the difference between the peak inward current and the current at the end of the depolarizing pulse. To account for variabilities in cell size, current density was determined by dividing the absolute current amplitudes (in pA) by the respective cell capacitance (in pF). Current density was plotted against voltage to have the I-V activation curves.

BOX 2 - Software

To calculate $I_{Ca,L}$ and subtract the leak in each individual recording, we used a Microsoft Excel© Template with fixed programmed functions (Designed in our lab – RG Herzig). For data analysis and transfer, Clampfit© 10.7 was used. Statistics and Fits of theoretical equations to the experimental data were performed using GraphPad Prism©.

- **$I_{Ca,L}$ activation parameters analysis:**

The biophysical properties of the calcium channels, such as their maximal conductance, activation threshold, steepness of activation, and equilibrium potential, were determined by fitting the activation curves to a combined Boltzmann-Ohm equation. This equation is a mathematical model that describes the shape of these curves by considering the voltage-dependent gating and the ohmic conductance of the channels.

The Boltzmann-Ohm equation is given by:

$$I(v) = Gmax \frac{V - Vrev}{(1 + exp\frac{(V0.5 - V)}{k})}$$

***Iv**: current density at certain test potential (v); **G_{max}**: the maximum conductance, **$V_{0.5}$**: the half maximal activation potential, **V_{rev}**: the reversal potential, and **k** the slope factor for activation.*

- **Time constants of $I_{Ca,L}$ decay (Tau, τ) analysis:**

The macroscopic cardiac $I_{Ca,L}$ activated by step depolarization decays over time during depolarization. In cardiomyocytes, the $I_{Ca,L}$ decay near V_{peak} might be described with a monoexponential or double-exponential function (McDonald et al., 1994). The decaying part is identified as the phase in which the current amplitude decreases over time after reaching its peak value until the end of the depolarization step (Figure 2-10).

Under our experimental conditions, the $I_{Ca,L}$ decay was best fitted with a mono-exponential fit, while in a few cases a bi-exponential fit was possible. Both fitting algorithms were first applied to the decaying part of the individual $I_{Ca,L}$ traces, and the fit quality was assessed. The maximum of $I_{Ca,L}$ was taken as time "0" and the fit was performed until the end of the depolarization step. The best fit was assessed by examining the confidence intervals (CI) of the fitted parameters (95% confidence level) and the goodness of fit, i.e., the R-squared value (R^2), as specified in GraphPad Prism for fitted curves with nonlinear regression.

The Mono- (single) exponential equation is given by:

$$Y=Y_0 + (Plateau\text{-}Y_0) * (1\text{-}exp\ (\text{-}K*\tau))$$

***Y**: current values (pA); **Y_0**: is the Y value when X (time) is zero, **Plateau**: is the Y value at infinite times, K: is the rate constant, **τ**: is the time constatnt.*

The Bi- (double) exponential equation is given by:

$$Y=Y_0+ SpanFast*(1-exp\ (-K_{Fast}* \tau_{fast})) + SpanSlow*(1-exp\ (-K_{Slow}* \tau_{slow}))$$

- *SpanFast=(Plateau-Y_0)*PercentFast*.01*
- *SpanSlow=(Plateau-Y_0)*(100-PercentFast)*.01*

PercentFast is the fraction of the span (from Y0 to Plateau) accounted for by the faster of the two components (see figure below).

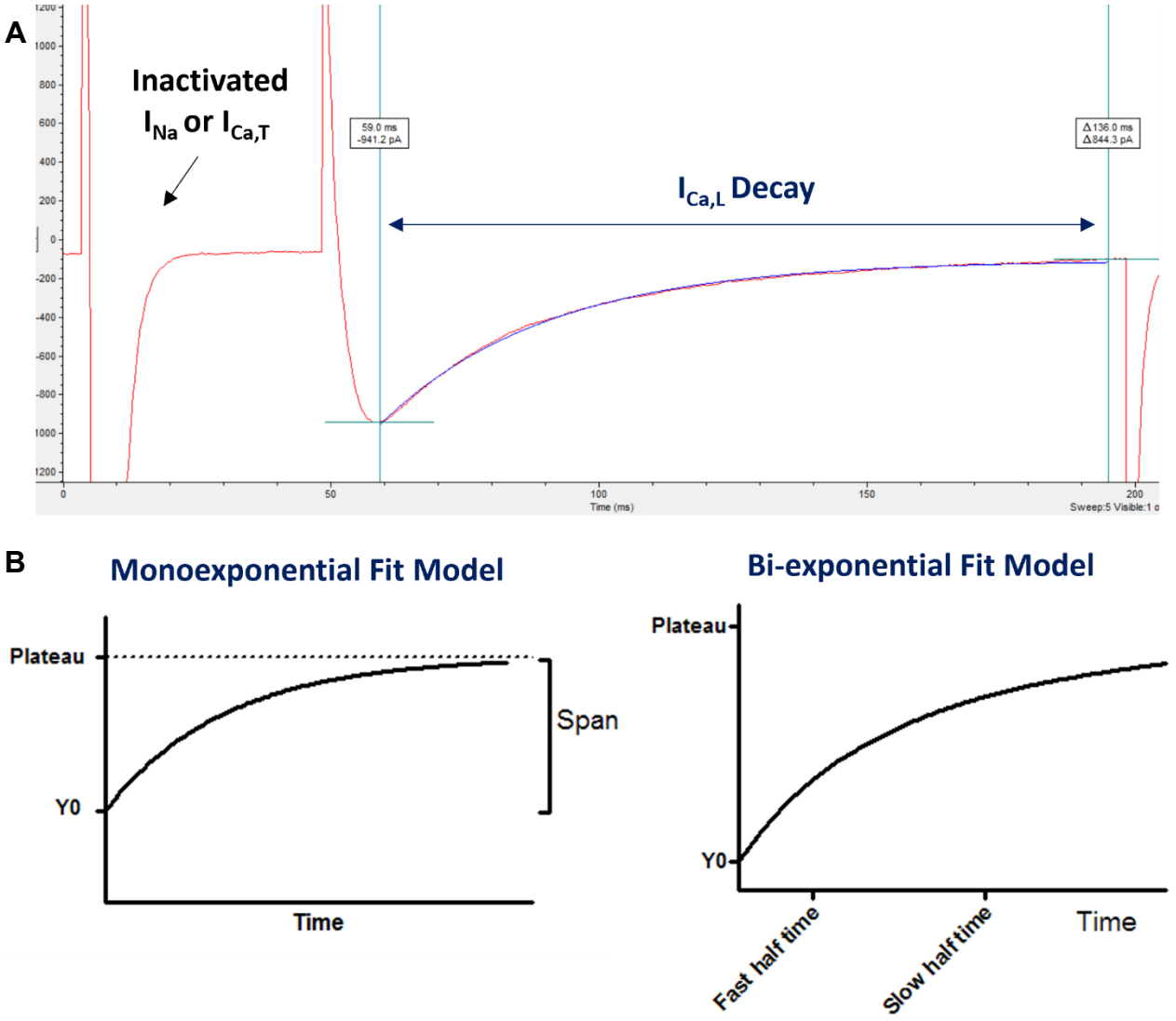

Fig. 2-10. $I_{Ca,L}$ decay and fit analysis models used to calculate the time constants of $I_{Ca,L}$ inactivation. **A.** Exemplary $I_{Ca,L}$ trace, at a voltage of 0 mV. The $I_{Ca,L}$ decay phase is shown in blue between the two cursors, where the data was extrapolated and fitted. At current peak (first cursor) the start time base was set to zero. **B.** Exponential fitting models used to calculate the time constants of $I_{Ca,L}$ decay (inactivation). The Plateau parameter in the fitting equations was constrained to a constant value of zero, as time zero was considered at peak current after subtracting the background signal. These fit model curves are adapted from GraphPad Prism's Curve Fitting Guide - last accessed in November 2023.

2.3.2.2 Steady-state voltage dependence of Inactivation

- **Steady-state inactivation (SSI) pulse protocol:**

To measure steady-state inactivation, myocytes were stimulated by a double-pulse protocol[4] (Figure 2-11). First, a prepulse was applied (HP of -80 mV), which involved a 25 ms short depolarization step to -40 mV to inactivate sodium channels, followed by a 200 ms depolarization step to 0 mV to elicit maximal $I_{Ca,L}$ (I_1). Then, 2-second conditioning potentials ranging from -60 to +60 mV were applied to induce steady-state inactivation of calcium channels. A test pulse at 0 mV was subsequently applied to measure the current (I_2) through the remaining available channels. The pulse interval was set to 10 seconds and the stimulation frequency was set to 2 kHz.

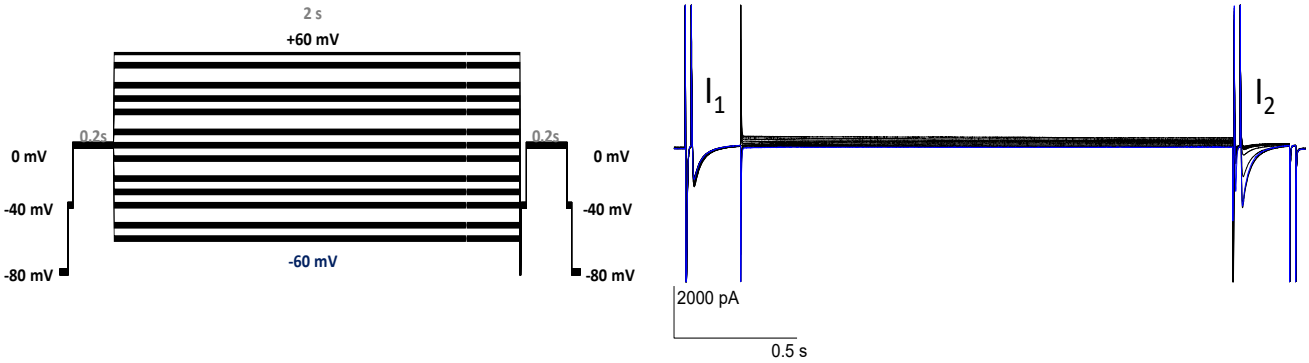

Fig. 2-11 Test pulse protocol (left) to measure steady-state $I_{Ca,L}$ inactivation (exemplary traces, right) - For a detailed description see text.

- **SSI data analysis:**

The steady-state inactivation curve was obtained by normalizing the current (I_2) to the current I_2 obtained with the most negative prepulse, i.e., -60 mV, which does not inactivate any channels, and plotted against the preconditioning voltages. Steady-state inactivation curves were fitted with a sigmoidal Boltzmann equation to obtain the gating parameters of channel's inactivation:

$$I/Imax = \frac{1}{1 + \exp\left(\frac{V0.5 - x}{k}\right)}$$

I/I*$_{max}$:** *I is peak current I2 in (pA), Imax: is I2 at -60 mV,* ***V*$_{0.5}$: the half maximal inactivation potential,* ***x****: the test potential, and* ***k*** *the slope factor for inactivation.*

[4] This protocol was adapted from the dissertation by (Köth, 2017) - RG Matthes, which was originally adapted by the research group: Hofmann (Poomvanicha et al., 2011) - Technical University of Munich.

2.3.2.3 Recovery from inactivation

- **$I_{Ca,L}$ recovery protocol:**

A standard two-pulse protocol was used to study channels' recovery from inactivation (Figure 2-12). A 100 ms prepulse (HP of - 45 mV) was applied at 0 mV to activate the channels. After this prepulse and full inactivation of $I_{Ca,L}$, the membrane potential was returned to the holding potential, and 50 ms test pulses (at 0 mV) were applied for varying time intervals ranging from 25 to 375 ms, with a time increment of 25 ms. The pulse interval was set to 3 seconds, and the stimulation frequency was set to 2 kHz.

- **Recovery curves and time constants:**

The peak current elicited by test pulses at a given time interval ($I_{@\,\Delta t}$) was normalized by dividing it by the peak current elicited by the prepulse ($I_{control}$), and the resulting ratio ($I_{@\,\Delta t}$ / $I_{control}$) represents the fraction of channels that recovered from inactivation (Fig. 2-12). The fraction of channels recovery could be fitted by a single or a double exponential function. In this study, $I_{Ca,L}$ recovery was best fitted with a monoexponential function and the time constant of recovery τ_{rec} was obtained.

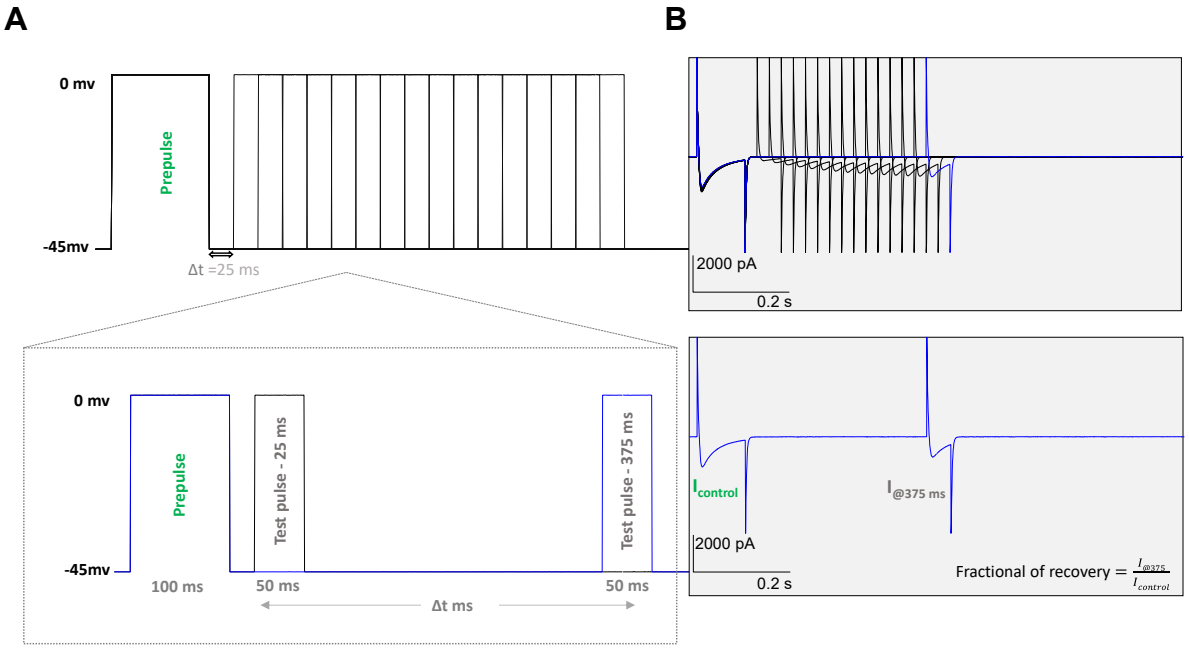

Fig. 2-12. Pulse protocol for $I_{Ca,L}$ recovery from inactivation. **A**. Schematic representation of the test pulse protocol, in the inset the first and last test pulse at 25 and 375 ms are shown. **B.** The upper traces show the original complete recovered $I_{Ca,L}$, while the lower traces show $I_{Ca,L}$ after 375 ms of recovery. The fractional recovery was calculated by dividing the current I at a certain time interval by the control current, for example, $I_{375}/I_{control}$.

2.3.3 Statistics

Electrophysiological data were expressed as mean ± standard deviation (SD) unless otherwise stated. Statistical tests and methods were carefully selected based on the experimental design, the number of groups, and whether or not the data followed a normal distribution. For multiple comparisons, an appropriate statistical hypothesis test, i.e., a post-hoc test, was performed.

Statistical analysis was performed using GraphPad Prism version 10. The significance level was set at $p < .05$ and only pairwise comparisons with *p-value* less than or equal to 0.05 were displayed. Statistical analysis specifications were given for each data set in the table or figure legend.

- Old β_1-tg mouse -

3

Results

IN THIS CHAPTER

3.1 Effects of β_1-adrenoceptor overexpression on ventricular $I_{Ca,L}$

3.2 Effects of $G\alpha_{i3}$-deficiency on the kinetics of $I_{Ca,L}$ in β_1-tg mice

3.3 Effects of $G\alpha_{i2}$-deficiency on the kinetics of $I_{Ca,L}$ in β_1-tg mice

3.4 New Gαi-protein modulators – proof-of-concept study

3.1 Effects of β_1-adrenoceptor overexpression on ventricular $I_{Ca,L}$

3.1.1 Basic characterization of ventricular $I_{Ca,L}$ in β_1-tg myocytes

To evaluate the effect of cardiac β_1-adrenoceptor overexpression on the function of L-type calcium channel, we measured whole-cell $I_{Ca,L}$ in β_1-tg ventricular cardiomyocytes. This mouse line was originally generated on an FVB/N background and as such developed cardiac dysfunction at a rather young age (<12 Mo). For our studies, we have backcrossed the mice to a C57BL/6 background, leading to a later onset of the cardiac phenotype (about 550d of age). Thus, were interested whether putative alterations at the level of ventricular $I_{Ca,L}$ would precede the “clinical” phenotype. We determined basal $I_{Ca,L}$ densities, I-V curves, and their fitting parameters as a basic characterization of $I_{Ca,L}$ (Figure 3-1 and Table 3-1).

The cell capacitance, which measures the surface area of the cell membrane, was comparable in all groups. In both age groups of β_1-tg mice, the I-V curves showed typical bell-shaped profiles, with elicited $I_{Ca,L}$ density reaching its maximum value between 0 and +10 mV. We observed changes in $I_{Ca,L}$ activation gating properties in β_1-tg myocytes, with this effect being more prominent in older mice, the peak $I_{Ca,L}$ density was reduced in β_1-tg myocytes over the entire voltage range from -40 to +50 mV (Figure 3-1, B).

In myocytes from young β_1-tg mice, peak $I_{Ca,L}$ density was significantly lower by 29.0±1.9% (-5.8±1.8 pA/pF, n=11) compared to wild-type (-8.1±1.9, n=15, p=.001), and from old β_1-tg mice,

it was significantly lower by 32.0±1.6% (-5.5±1.5 pA/pF, n=17) compared to wild-type (-8.1±1.6 pA/pF, n=18, p<.001; Figure 3-1, C). The voltage at which the half-maximal $I_{Ca,L}$ activation occurs ($V_{0.5_act}$) was shifted to more positive potentials in both young and old β_1-tg mice, as the absolute change was 3.83 mV (p=.007), and 3.63 mV (p=.003), respectively, compared to age-matched wild-type (Figure 3-1, D). Additionally, we observed a slight but significant increase in the activation slope factor k_{act} in β_1-tg myocytes (e.g., by 1.24 mV, in young; p=.002; and by 1.34 mV, in old; p<.001) compared to age-matched wild-type Table 3-1. The interaction factor was insignificant for all compared parameters in all groups as indicated by two-way ANOVA.

These results indicate that cardiac overexpression of β_1-AR leads to reduced current density and altered LTCC gating kinetics. This occurred already at a rather young age of 4-5 months.

Table 3-1. Electrophysiological properties of $I_{Ca,L}$ recorded in ventricular myocytes from wild-type and β_1-tg mice

Parameter	[4-5] months		[10-11] months	
	Wild-type	β_1-tg	Wild-type	β_1-tg
Basal $I_{Ca,L}$ Kinetics				
Number of animals, N	5	3	6	6
Number of cells, *n*	10-15	11-14	15-18	16-17
Cm (pF)	209.4±41	212.4±56.6	225.3±50.2	220.4±.59.5
Peak $I_{Ca,L}$ (pA/pF)	-8.1±1.9	-5.7±1.8	-8.1±1.6	-5.5±1.5
V_{rev} (mV)	50.8±3.6	49.1±4.8	55.5±6.1	49.9±4.6
$V_{0.5_act}$ (mV)	-13.3±4.7	-9.4±3.6	-11.3±2.5	-7.6±2.8
***k* $_{act}$ (mV)**	4.1±0.6	5.1±0.8	3.9±0.7	5.3±0.9
$V_{0.5_inact}$ (mV)	-28.8±3.7	-26.4±3.6	-26.0±3.1	-26.0±3.2
***k* $_{inact}$ (mV)**	-5.3±0.8	-5.2±1.0	-4.6±0.8	-5.0±0.6

Table 3- 1. Descriptive statistics showing values as mean ± SD for wild-type and β_1-tg mice at two ages. The analyzed parameters are: **$I_{Ca,L}$,** peak calcium current density normalized to cell capacitance (**Cm**); **V_{rev}** reversal potential; **$V_{0.5_act}$** voltage of half-maximal activation; ***k_{act}*** activation slope factor; **$V_{0.5_inact}$** voltage of half-maximal inactivation; ***k_{inact}*** inactivation slope factor. **N** indicates the number of animals; **n** indicates the number of cells per group.

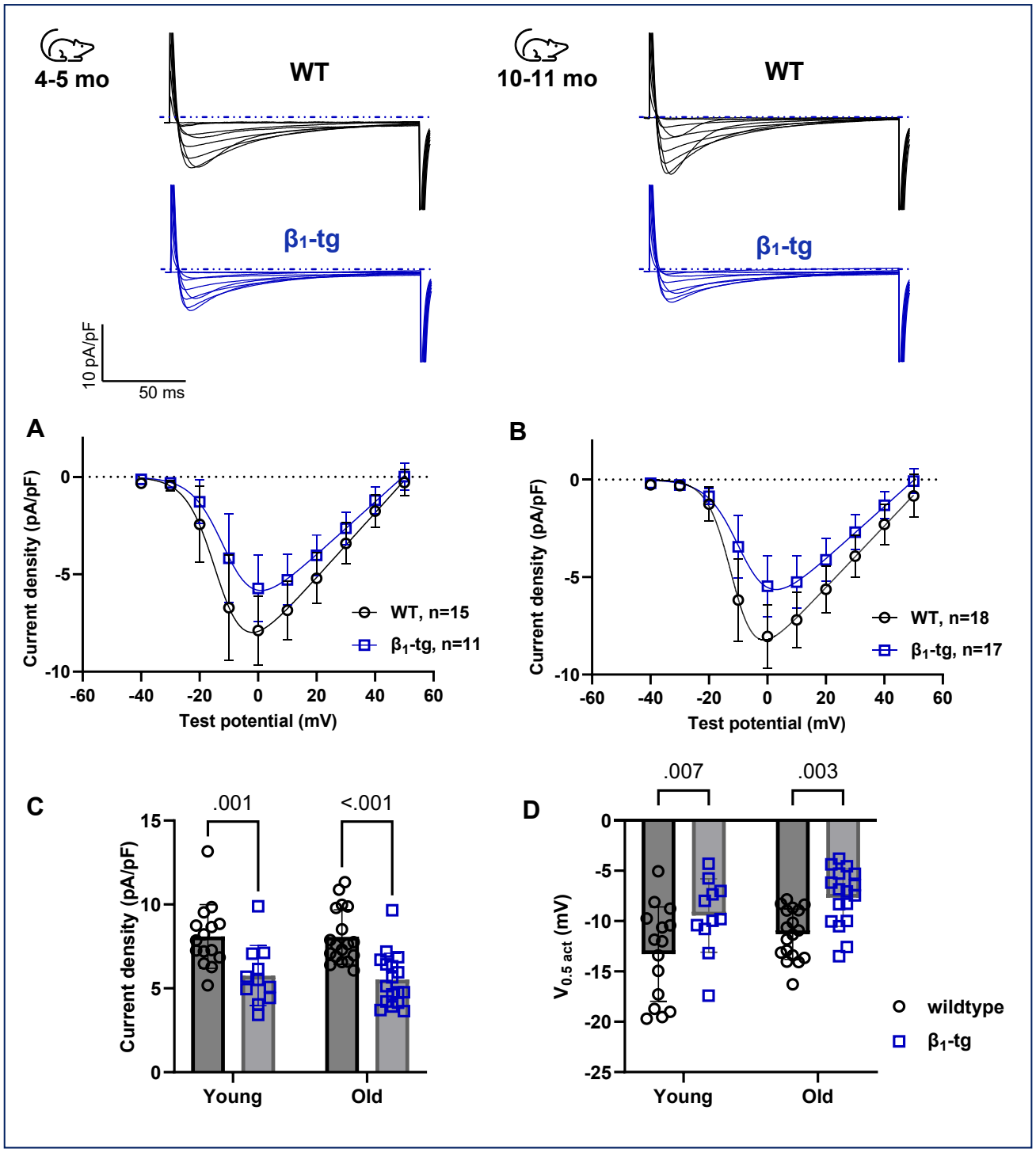

Fig. 3-1. Characterization of whole-cell $I_{Ca,L}$ in β_1-tg mice at two different ages. $I_{Ca,L}$ was recorded using voltage-clamp mode in freshly isolated ventricular myocytes. The upper traces show representative $I_{Ca,L}$ traces normalized by the cell-capacitance from 4-5 (left) and 10-11 (right) months old, male β_1-tg and wild-type mice. **A-B.** Current-voltage relationships of $I_{Ca,L}$ with the solid lines representing the fit of the curves to Boltzmann-Ohm function. **C.** Average peak $I_{Ca,L}$ density, and **D.** The half-maximal activation voltage $V_{0.5_act}$**.** Data are presented as mean ± SD from (N=3-5) young and (N=6) old animals per group. Each symbol represents a cell in the scatter box plots. Multiple unpaired *t-tests* were used to compare $I_{Ca,L}$ density at different test potentials (A-B). Two-way ANOVA with Fisher's test was used to compare the effect of genotype, age, and their interactions on peak $I_{Ca,L}$ and $V_{0.5_act}$ (C-D); interaction factor was insignificant in both. Experiments with poor voltage clamp were excluded from the analysis.

3.1.2 Voltage dependence and rate of $I_{Ca,L}$ inactivation in β_1-tg mice

We investigated the effects of cardiac β_1-AR overexpression on the inactivation gating kinetics of $I_{Ca,L}$. The steady-state of $I_{Ca,L}$ inactivation and time constants for $I_{Ca,L}$ decay were measured. There was no statistically significant difference in the steady-state voltage dependence of $I_{Ca,L}$ inactivation between β_1-tg and wild-type myocytes in any age group. The inactivation curves overlapped, and the values for the voltage half-maximal inactivation ($V_{0.5_inact}$) and the slope factor for inactivation (k_{inact}) were similar (Figure 3-2, A-B, Table 3-1).

The rate of inactivation was estimated by analyzing the time constants for $I_{Ca,L}$ decay, by fitting the decaying $I_{Ca,L}$ with a mono and/or bi-exponential function. Over the voltage range from -10 mV to +40 mV, the $I_{Ca,L}$ decay was best fitted with a monoexponential function, yielding the inactivation monophasic time constant **(τ_{inact})**, which was plotted as a function of voltage[5]. In β_1-tg myocytes, except for data obtained at +40 mV i.e., the reversal potential, the inactivation rate was faster throughout the whole potential range, but differences are not statistically significant compared to age-matched wild-type (Figure 3-2, C). Under basal conditions, the $I_{Ca,L}$ decay at 0 mV could be described with a bi-exponential algorithm in a good fraction of cells[6], allowing for a rough estimation of the early, fast component (τ_{fast}) and the late, slow component (τ_{slow}) of $I_{Ca,L}$ inactivation (Figure 3-2, D-E). However, like the results obtained from mono-exponential fit, no significant changes were observed. The values for inactivation time constants are summarized in Table 3-2.

These results indicate that cardiac overexpression of β_1-AR does not affect the voltage dependence of basal $I_{Ca,L}$ inactivation during this stage i.e., the adaptive/ non-failing phase.

Table 3-2. Time constants of $I_{Ca,L}$ decay at 0 mV under basal conditions in β_1-tg and wild-type myocytes

	n	τ_{inact} (ms)	n	τ_{fast} (ms)	τ_{slow} (ms)
Wildtype					
young	12	37.4±2.4	6	30.1±4.4	167.0±49.1
old	18	31.4±0.8	8	24.6±2.3	98.0±32.8
β_1-tg					
young	10	32.9±1.2	7	24.1±2.9	139.7±42.1
old	17	31.6±1.1	10	22.5±2.2	101.7±24.3

Table 3- 2. Descriptive statistics (as mean ± SEM) for the inactivation monophasic time constant (τ_{inact}) and the biphasic time constants, fast (τ_{fast}) and slow (τ_{slow}) measured at 0 mV. Two-way ANOVA indicates no significant changes in all groups. At least three animals were used per group.

[5] For detailed information on the fitting procedure, see methods 2.3.2.1/Fig. 2-10.
[6] Statistical analysis of frequency of occurrence (mono- *versus* bi-exponential fit) are provided in the supplements S5.

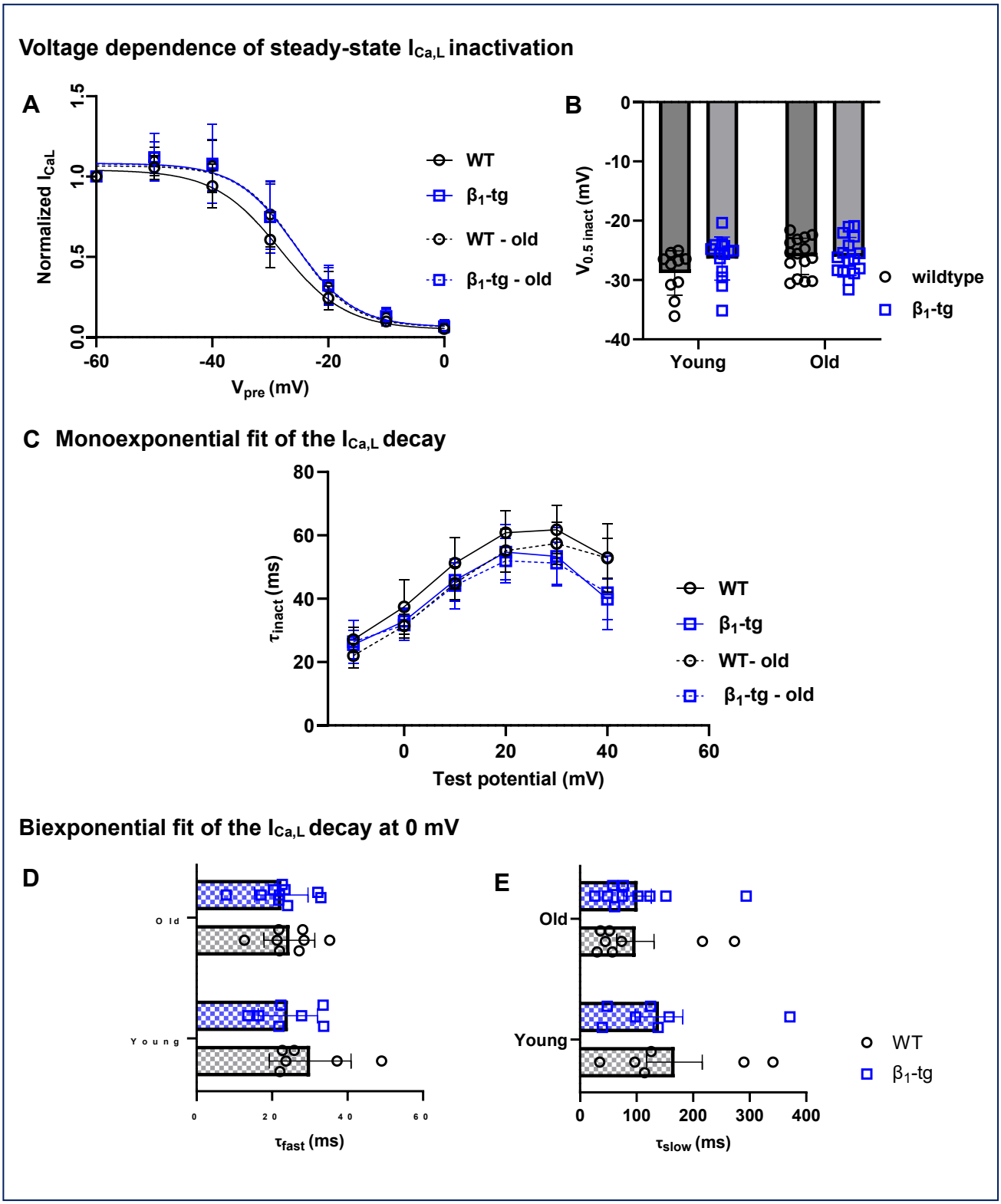

Fig. 3-2. Voltage dependence and rate of $I_{Ca,L}$ inactivation for wild-type (○) and β1-tg (□) at 4-5 (solid-lines) and 10-11(dashed-lines) months old. **A.** The steady-state inactivation curves were obtained by applying a series of 2-second conditioning pulses from -60 to +60 mV, followed by a test pulse at 0 mV. These curves were fitted with a Boltzmann-Sigmoidal function. **B.** The half-maximal voltage of inactivation ($V_{0.5_inact}$). **C.** The inactivation time constant of the monoexponential component of $I_{Ca,L}$ decay (τ_{inact}) measured in the voltage range from -10 to +40 mV. **D-E.** The inactivation time constants of the bi-exponential components of $I_{Ca,L}$, the fast (τ_{fast}) and slow (τ_{slow}) time constants at 0 mV. Data are presented as mean ± SD. Two-way ANOVA with Fisher's test was

Fig.3-2 continued; used to compare the effects of genotype, age, and their interactions, no significant differences were found. Each symbol represents a cell in the scatter box plots.

3.1.3 $I_{Ca,L}$ recovery from inactivation in β_1-tg myocytes

The interrelated processes of inactivation and recovery from inactivation are essential determinants of the channel availability and calcium influx. The balance between these processes is crucial for maintaining normal cardiac function and rhythm. In this study, we examined the kinetics of $I_{Ca,L}$ recovery from inactivation in β_1-tg myocytes. The recovery rate was estimated by fitting the fractional recovery curves of $I_{Ca,L}$ amplitudes at different time intervals with a monoexponential function, yielding the time constants for recovery from inactivation (τ_{rec}).

The $I_{Ca,L}$ recovery from inactivation in β_1-tg myocytes was time-dependent, similar to that of wild-type. At the last time intervals tested (375 ms), all groups showed an average of approximately 70% recovery (Figure 3-3, A). In the young mice group, $I_{Ca,L}$ showed faster recovery kinetics in β_1-tg myocytes (219.2±32.6, n=12) compared to age-matched wild-type (289.0±58.3, n=10, p=.002, Figure 3-3, B), while no significant differences were observed in the older group. This was consistent with an increased fraction of $I_{Ca,L}$ recovery in β_1-tg myocytes (Table 3-3). However, the interaction effect for age and genotype on the rate of $I_{Ca,L}$ recovery from inactivation was significant (p=.002). Specifically, $I_{Ca,L}$ in wild-type myocytes from older animals had a faster rate of recovery compared to younger ones (Table 3-3), This implies that the aging process may affect the L-type calcium channel or its regulatory proteins differently in β_1-tg and wild-type.

Table 3-3. Monophasic time constants for $I_{Ca,L}$ recovery from inactivation under basal conditions in β_1-tg and wild-type myocytes

	n	τ_{rec} (ms)	Half-life ($t_{1/2}$) (ms)	Fractional Recovery at 375 ms (%)
Wildtype				
young	10	289.1 ± 58.3	200.4 ± 40.4	64.1 ± 7.6
old	14	228.5 ± 56.9**	158.4 ± 39.5**	77.7 ± 6.7***
β_1-tg				
young	11	212.0 ± 21.9$^{\#\#}$	147.0 ± 15.2$^{\#\#}$	74.1 ± 6.5$^{\#\#}$
old	17	251.2 ± 49.9	174.1 ± 34.6	73.9 ± 5.8

Table 3- 3. Descriptive statistics for parameters of $I_{Ca,L}$ recovery from inactivation, with values as mean ± SD. (τ_{rec}) Monophasic time constant for recovery. (375 ms) is the last time interval at which the $I_{Ca,L}$ recovery was measured. Two-way ANOVA with Fisher's test was used to compare the effect of genotype, age, and their interactions on recovery kinetics under basal conditions ($^{\#\#}$:p<.01 vs. wild-type) (** p<.01, *** p<.001 vs. young group).

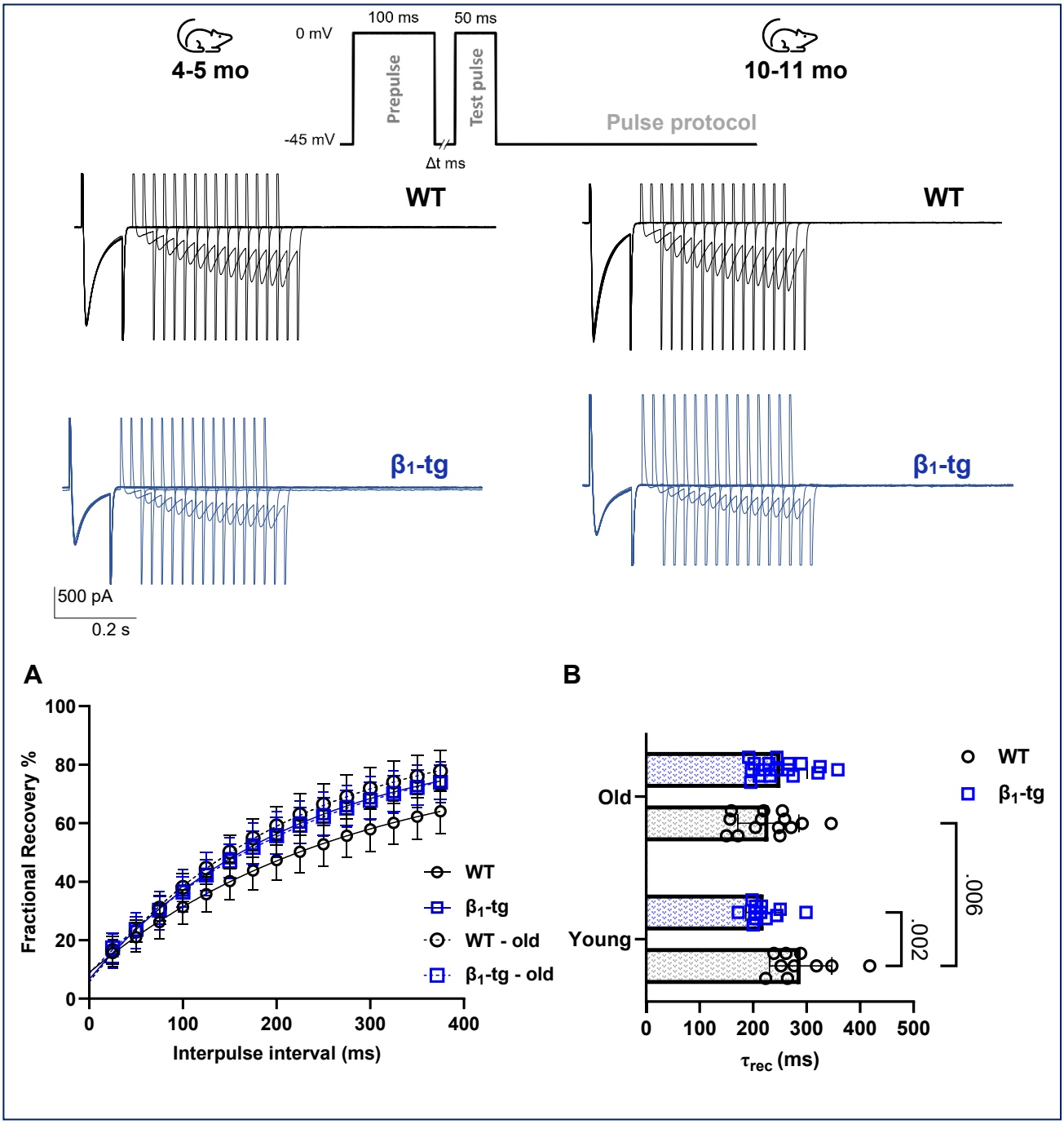

Fig. 3-3. Recovery of $I_{Ca,L}$ from inactivation in β_1-tg mice at two different ages. The upper traces show representative original traces. A two-pulse protocol (inset) was used with a 100 ms pre-pulse at 0 mV followed by a test pulse of 50 ms at different recovery intervals (Δt) in 25 ms increment. **A.** Mean fractional recovery from inactivation as a function of the time intervals; the lines represent the fit of the curves to a monoexponential function for wildtype (○) and β_1-tg (□) at 4-5 (solid-lines) and 10-11 (dashed-lines) months of age. **B.** The time constants for $I_{Ca,L}$ recovery from inactivation (τ_{rec}). Data are presented as mean ± SD of 10-17 myocytes per group. Two-way ANOVA with Fisher's test was used to compare the effects of genotype, age, and their interactions on τ_{rec}. Interaction effect was significant, p=.002. Each symbol represents a cell in the scatter box plots.

3.1.4 $I_{Ca,L}$ responsiveness to acute β-AR agonist stimulation in β_1-tg mice

To challenge intracellular Ca^{2+} handling and to simulate acute sympathetic activation, i.e., to mimic the effects of stress or exercise, we examined the responsiveness of calcium channels to acute stimulation with the non-selective beta-adrenergic agonist isoproterenol (Iso) in β_1-tg myocytes and compared it with that of wild-type cardiomyocytes.

It is well established that isoproterenol stimulation increases the amplitude of $I_{Ca,L}$ at the whole-cell level by increasing the channels' open probability (P_o) and/or number of active channels. Additionally, Iso increases the channels' sensitivity to depolarizations, resulting in a negative shift in the voltage dependence of activation (Tsien et al., 1986; McDonald et al., 1994). Accordingly, to assess the responsiveness of $I_{Ca,L}$ to stimulation with Iso, we analyzed the percentage increase in peak current density and the change in $I_{Ca,L}$ activation voltage relative to basal conditions. To ensure maximum effects, cells were incubated with 1µM Iso for 8±2 minutes.

As expected, peak $I_{Ca,L}$ density was significantly increased, and $V_{0.5_act}$ shifted to more negative potentials in wild-type myocytes Figure 3-4 (A,C for young, and B,D for old). In contrast, the $I_{Ca,L}$ response to Iso was notably attenuated in β_1-tg myocytes from both age groups. For instance, in old β_1-tg mice, the percentage increase in peak $I_{Ca,L}$ density was to +133±34% (-7.36±1.9 pA/pF, n=12) of the basal value (-5.5±1.5 pA/pF, n=17, p=ns), while in wild-type, it was to +169±65% (-13.6±5.2 pA/pF, n=12) of the basal value (-8.06±1.6 pA/pF, n=18, p<.001). Consistent with this observation, there was only a slight change in the half-maximal voltage of activation in β_1-tg myocytes treated with Iso (-9.7±4.6 mV, n=12) *versus* basal (-7.6±2.8 mV, n=17, p=ns), whereas in wild-type, $V_{0.5_act}$ was significantly more negative by -5.7mV (-17.0±4.0 pA/pF, n=12) *versus* basal (-11.3±2.5 pA/pF, n=18, p<.001). Similar observations were seen in the young group[7] (Figure 3-4).

These results indicate that overexpression of β_1-adrenoceptor leads to a decrease in the response to isoproterenol stimulation of $I_{Ca,L}$, regardless of the age of the mice.

[7] For descriptive statistics (mean ± SD) on isoproterenol effects on different parameters in wild-type and β_1-tg myocytes refer to suppl. S4(I-II).

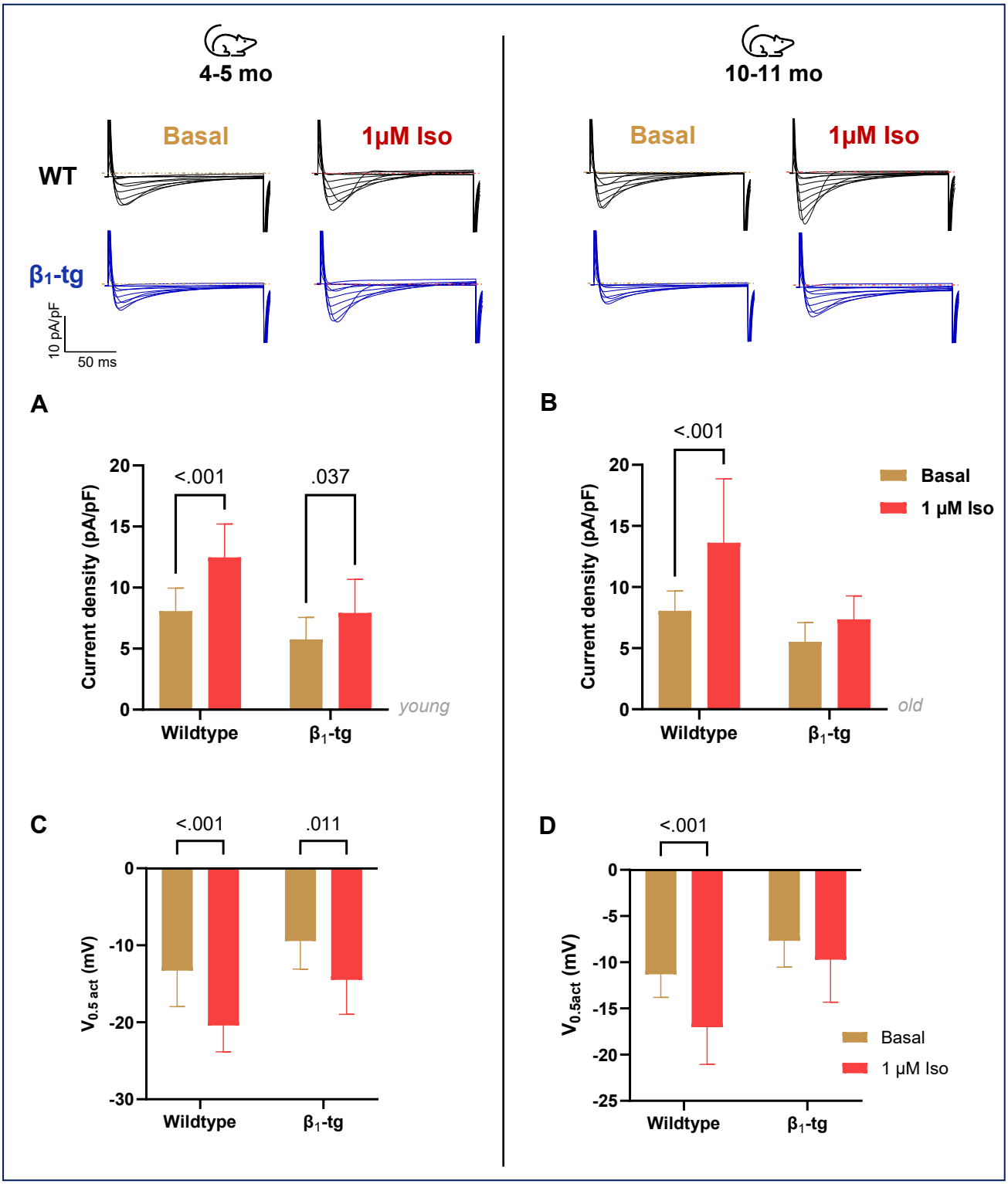

Fig. 3-4. Evaluation of the $I_{Ca,L}$ response to β-adrenergic stimulation. The upper traces show representative whole cell traces of $I_{Ca,L}$ recorded from wild-type and β_1-tg mice at 4-5 (left) and 10-11 (right) months of age, under basal conditions and after treatment with 1 μM Iso. **A-B**: Peak $I_{Ca,L}$ density; and **C-D**: Half-maximal activation voltage $V_{0.5_act}$. Data are presented as mean ± SD of 7-18 myocytes per group (see text). Two-way ANOVA with Fisher's test was used to compare the effects of genotype, isoproterenol treatment, and their interaction. Interaction factor was insignificant in all comparisons.

3.2 Effects of $G\alpha_{i3}$ deficiency on the kinetics of $I_{Ca,L}$ in β_1-tg mice

We previously reported that $G\alpha_{i3}$ deficiency prevented or delayed diastolic dysfunction in aged β_1-tg mice i.e., during the maladaptive stage. We now investigate the potential effects of $G\alpha_{i3}$ deficiency at the myocyte level, using the age range of 10-11 months for electrophysiology studies.

3.2.1 LTCC activation and inactivation properties in β_1-tg/$G\alpha_{i3}^{-/-}$ mice

Figure 3-5 summarizes the activation and inactivation parameters of $I_{Ca,L}$ in myocytes from old wild-type, β_1-tg and β_1-tg lacking $G\alpha_{i3}$ (β_1-tg/$G\alpha_{i3}^{-/-}$). Table 3-4 provides a statistical comparison between these groups under basal conditions or after stimulation with 1 µM Iso. We found that $G\alpha_{i3}$ deficiency partially normalized the reduced $I_{Ca,L}$ density in β_1-tg myocytes. Basal peak $I_{Ca,L}$ density was significantly higher in β_1-tg/$G\alpha_{i3}^{-/-}$ (-7.5±1.6 pA/pF, n=19) *versus* β_1-tg myocytes (-5.5±1.5 pA/pF, n= 17, p=.002), and no longer significantly different to wild-type levels (-8.1±1.6 pA/pF, p=.9, Figure 3-5, A/C). Additionally, the half-maximal activation voltage was shifted in β_1-tg/$G\alpha_{i3}^{-/-}$ (-10.6±4.3 mV) towards wild-type levels (-11.3±2.5 mV, p=ns), but was significantly more negative than in β_1-tg (p=.035) Figure 3-5, D. The slope factor of activation (k_{act}) in β_1-tg/$G\alpha_{i3}^{-/-}$ was comparable to those in wild-type and β_1-tg myocytes.

Figure 3-5, B shows the overlap of voltage dependence of $I_{Ca,L}$ steady-state activation (SSA) and inactivation (SSI). The conductance curve of $I_{Ca,L}$ was shifted to the right in β_1-tg myocytes compared to wild-type, implying that the channels required more depolarization steps to activate. This shift was not observed in β_1-tg/$G\alpha_{i3}^{-/-}$ myocytes. Specifically, at 0 mV, the conductance of $I_{Ca,L}$, measured as the ratio of the actual conductance (G) to the maximal conductance (G_{max}), was lower in β_1-tg (79.0±8.8%, n=17) than in wild-type (90.0±5.1%, n=18, p<.001) and β_1-tg/$G\alpha_{i3}^{-/-}$ (85.1±10.0%, n=19, p=.16).

The basal steady-state voltage dependence of $I_{Ca,L}$ inactivation was similar in all studied groups, as indicated by nearly overlapping inactivation curves and comparable values for the inactivation gating parameters, namely the $V_{0.5_inact}$ and slope factor for inactivation $k_{inact.}$ (Figure 3-5, B, E; Table 3-4).

Collectively, these results indicate that $G\alpha_{i3}$ deficiency largely restores reduced $I_{Ca,L}$ density in β_1-tg myocytes and normalizes the activation-gating properties of the channels. Inactivation kinetics were neither affected in β_1-tg myocytes nor by additional deletion of the $G\alpha_{i3}$ isoform.

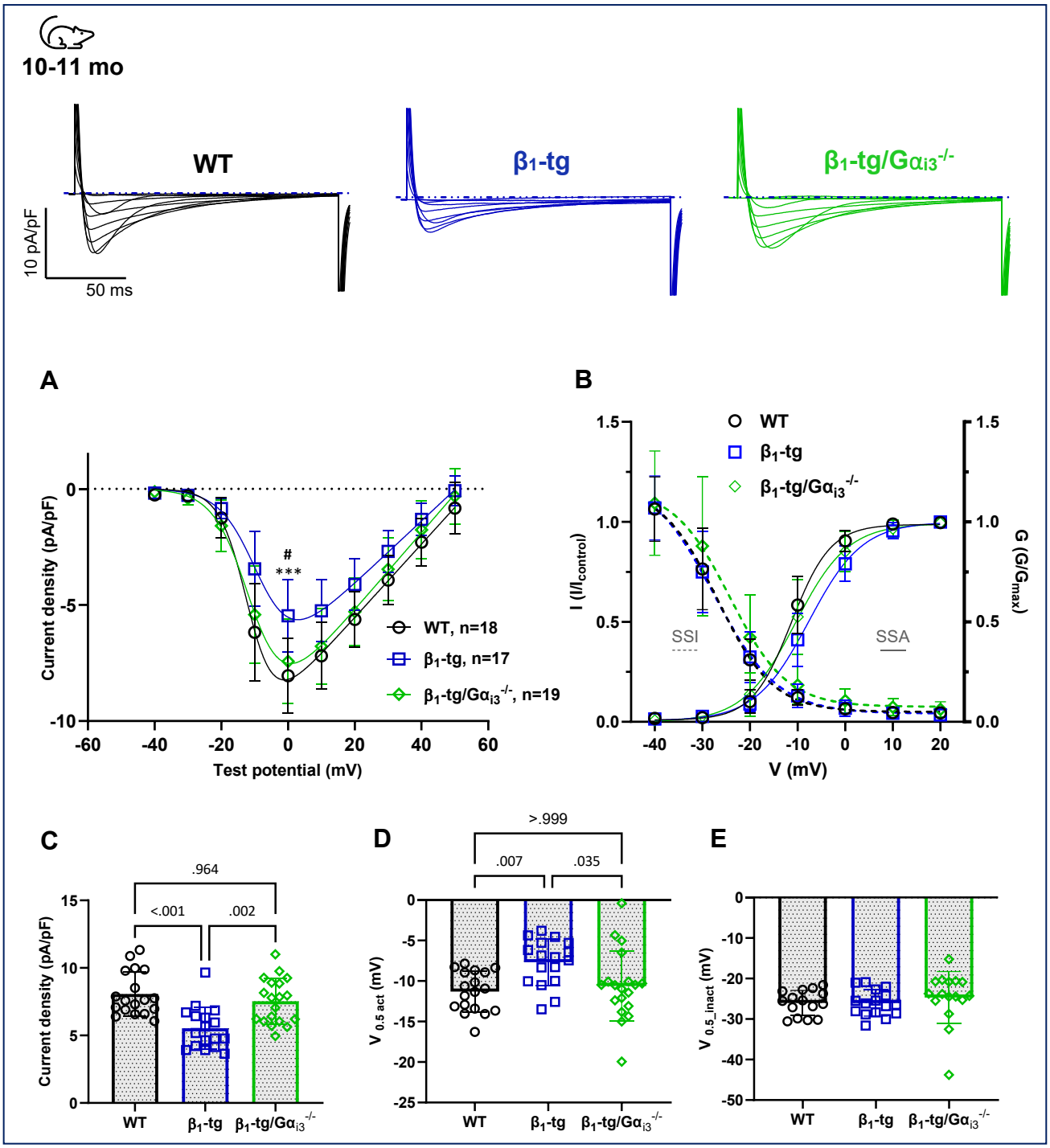

Fig. 3-5. Effects of Gα$_{i3}$ deficiency on the voltage dependence of basal $I_{Ca,L}$ activation and inactivation. $I_{Ca,L}$ was recorded in freshly isolated ventricular myocytes using voltage-clamp mode. Representative original $I_{Ca,L}$ traces normalized by the cell capacitance are superimposed **A.** Current-voltage relationships of $I_{Ca,L}$ with the solid lines representing the fit of the curves to Boltzmann-Ohm function from 10–11-month-old, male wild-type, β$_1$-tg, and β$_1$-tg/Gα$_{i3}^{-/-}$, where *n* is the number of cells. Basal $I_{Ca,L}$ density was significantly reduced in β$_1$-tg over the entire voltage range (***: p<.001 vs. WT), while it was nearly normal in β$_1$-tg/Gα$_{i3}^{-/-}$ (e.g., at 0 mV #: p=.002 vs. β$_1$-tg). **B.** Overlapping curves of steady-state activation (SSA - *solid lines*), and inactivation (SSI - *dashed lines*) of $I_{Ca,L}$. **C.** Average peak $I_{Ca,L}$ density; **D.** Half-maximal activation voltage ($V_{0.5_act}$), and **E.** Half-maximal voltage of inactivation ($V_{0.5_inact}$). Data are presented as mean ± SD and collected from 6-7 animals per group. Each symbol represents a cell in the scatter box plots. One-way ANOVA followed by Bonferroni's multiple comparisons tests was used to compare the three groups.

3.2.2 $I_{Ca,L}$ response to acute β-AR agonist stimulation in β_1-tg/$G\alpha_{i3}^{-/-}$ mice

In contrast to basal $I_{Ca,L}$, $G\alpha_{i3}$ deficiency did not restore response of $I_{Ca,L}$ to Iso in β_1-tg myocytes. Figure 3-6 shows the $I_{Ca,L}$ recorded under basal conditions and after stimulation with 1 μM Iso in the three groups. In particular, the percentage increase in peak $I_{Ca,L}$ density (pA/pF) was to +127.0±48% in β_1-tg/$G\alpha_{i3}^{-/-}$ and to +133.0±34% in β_1-tg myocytes compared to +169.0±65% in wild-type (Figure 3-6, B; Table 3-4). It is worth noting that in the wild-type group, most cells exhibited a "responsive" behavior under our experimental conditions. This was demonstrated by an increased peak $I_{Ca,L}$ occurring at more negative potentials, with 9 out of 12 cells reaching a peak current at -10 mV (in comparison to the typical basal peak that occurs between 0 and +10 mV). Conversely, the proportion of cells that showed a peak at -10 mV was lower in both age-matched β_1-tg/$G\alpha_{i3}^{-/-}$ (8 out of 18), and β_1-tg (0 out of 12) myocytes. The typical leftward shift in the I-V curve, was not present in β_1-tg/$G\alpha_{i3}^{-/-}$ and β_1-tg myocytes, and there were no significant differences in $V_{0.5_act}$ between basal and treated cells (Figure 3-6, C; Table 3-4).

These results indicate that $G\alpha_{i3}$ deficiency restores basal $I_{Ca,L}$ in β_1-tg mice, but does not restore current sensitivity to β-adrenergic stimulation. This implies that inhibiting the $G\alpha_{i3}$ isoform has minimal or no effect on the $I_{Ca,L}$ response mediated by β-AR stimulation.

Table 3-4. $I_{Ca,L}$ activation and inactivation parameters in wild-type, β_1-tg and β_1-tg/$G\alpha_{i3}^{-/-}$ cardiomyocytes (10-11 months-old)

	n	Peak $I_{Ca,L}$ (pF/pA)	$V_{0.5_act}$ (mV)	k_{act} (mV)	$V_{0.5_inact}$ (mV)	k_{inact} (mV)
Wildtype						
Basal	15-18	-8.1±1.6	-11.3±2.5	3.9±0.6	-26.0±3.1	-4.7±0.8
Iso	12-14	-13.6±5.2***	-17.1±4.0***	3.1±0.9*	-29.5±4.4*	-4.8±0.8
β_1-tg						
Basal	16-17	-5.5±1.5$^{\#\#\#}$	-7.7±2.8$^{\#\#}$	5.3±0.9$^{\#\#\#}$	-26.0±3.2	-5.0±0.9
Iso	12-14	-7.3±1.9**	-9.7±4.6	5.1±0.6	-26.9±4.5	-5.2±1.1
β_1-tg/$G\alpha_{i3}^{-/-}$						
Basal	16-19	-7.5±1.6††	-10.6±4.3†	4.7±1.2	-24.7±6.4	-4.6±1.3
Iso	12-18	-9.5±3.6*	-14.2±6.7	4.2±1.3	-29.9±4.8**	-4.9±0.7

Table 3- 4. Descriptive statistics for $I_{Ca,L}$ parameters are presented as mean ± SD. At least three animals per group were used, in the age range 10-11 months; *n* indicates the number of recorded cells. An unpaired t-test was used to compare basal values *versus* with 1μM Iso in each treated group (*p<.05,**p<.01, ***p<.001). One-way ANOVA with Bonferroni's multiple comparisons test was used to compare the three groups under basal conditions ($^{\#}$:p<.05, $^{\#\#}$:p<.01, $^{\#\#\#}$:p<.001 vs. wild-type) (†:p<.05, †††:p<.001 vs. β_1-tg).

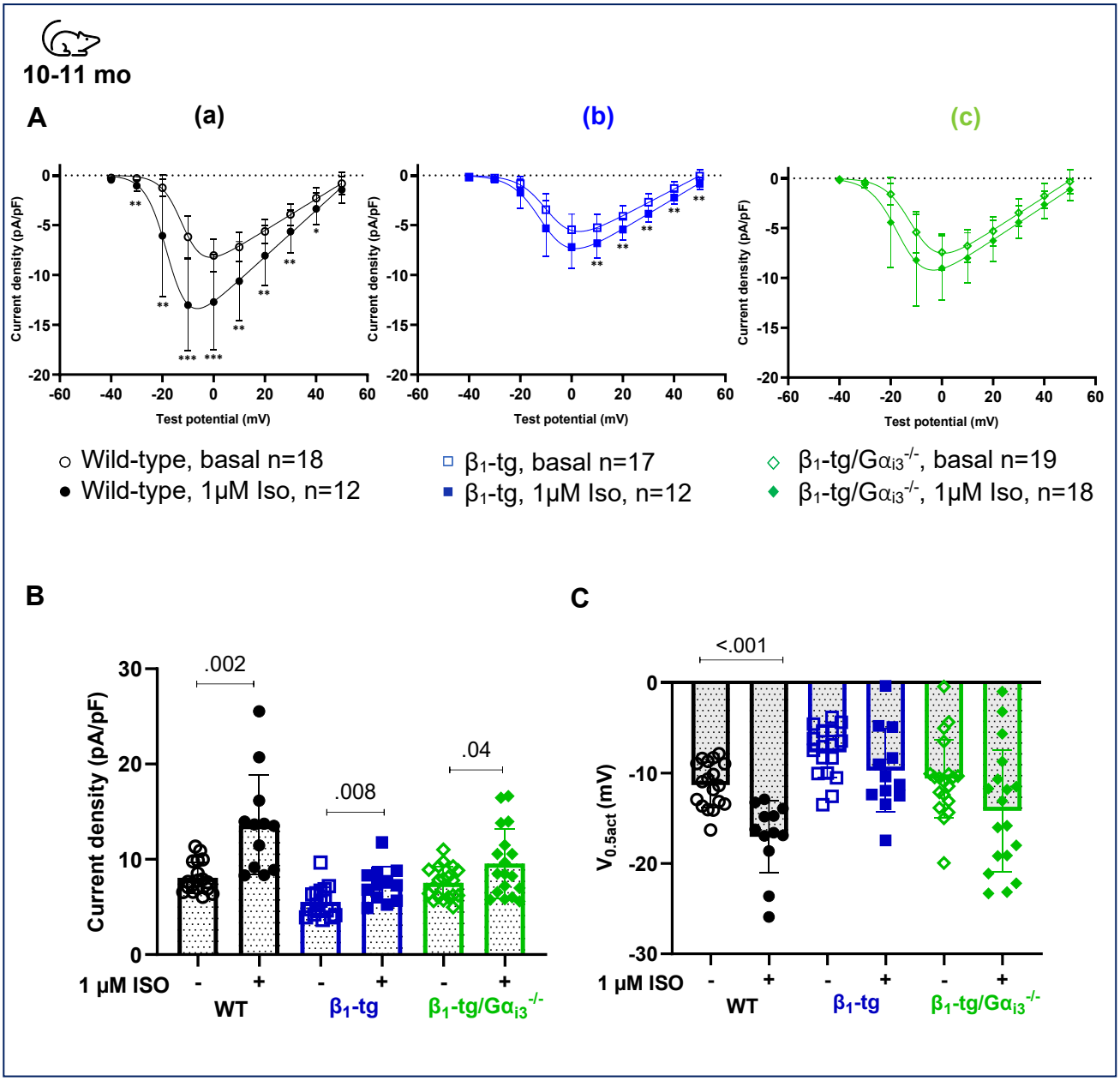

Fig. 3-6. Effects of $G\alpha_{i3}$ deficiency on the $I_{Ca,L}$ response to 1 µM isoproterenol (Iso, solid symbols versus basal, open symbols). A. Current-voltage relationships of $I_{Ca,L}$ show that in wild-type **(a),** Iso markedly increased the $I_{Ca,L}$ density over the entire voltage range and shifted the *I-V* curve to the left, as expected. In contrast**,** Iso had weaker effects on $I_{Ca,L}$ in β_1-tg and in β_1-tg/$G\alpha_{i3}^{-/-}$ myocytes **(b, c), *n*** indicates the number of cells. Iso-effects are further compared in **(B-C):** Peak $I_{Ca,L}$ density and the half-maximal activation voltage ($V0.5_{act.}$). Multiple unpaired *t-tests* were used in (A) to compare Iso effects on $I_{Ca,L}$ density at different test potentials; *p <.05, **p <.01, ***p <.001. Unpaired student *t-test* was used to compare Iso effect in each group (B+C). Data are presented as mean ± SD. Each symbol represents a cell in the scatter box plots.

3.2.3 Time constants and rate of basal $I_{Ca,L}$ inactivation in β_1-tg/$G\alpha_{i3}^{-/-}$ mice

As described above, the rate of $I_{Ca,L}$ inactivation was estimated by fitting the $I_{Ca,L}$ decay with a mono-exponential function. The resulting inactivation time constant (τ_{inact}) was then plotted against a voltage ranging from -10 mV to +40 mV (Figure 3-7, A).

The rate of inactivation tended to accelerate at more depolarized potentials (at +10 mV and above) in both β_1-tg and β_1-tg/$G\alpha_{i3}^{-/-}$ compared to wild-types myocytes. For instance, at +20 mV, the average τ_{inact} amounted to (55.2±6.7 ms, n=18) in wild-type, while to (51.9±7.0 ms, n=17, p=.59) in β_1-tg, and to (47.4±8.1 ms, n=19, p=.01) in β_1-tg/$G\alpha_{i3}^{-/-}$. The biphasic inactivation time constants determined at 0 mV showed comparable values for the slow τ_{slow} and fast τ_{fast} components in all groups (Figure 3-7, B-C; Table 3-5). These results suggest that the rate of $I_{Ca,L}$ inactivation is partially altered in the case of β_1-AR overexpression with or without $G\alpha_{i3}$ expression.

Table 3-5. Inactivation time constants at 0 mV under basal conditions – (10-11 months mice)

	n	τ_{inact} (ms)	n	τ_{fast} (ms)	τ_{slow} (ms)
Wildtype	18	31.4±0.8	8	24.6±2.3	98.0±32.8
β_1-tg	17	31.6±1.1	10	22.4±2.2	101.7±24.3
β_1-tg/$G\alpha_{i3}^{-/-}$	19	30.4±1.5	13	21.4±3.1	136.0±35.5

Table 3- 5. Descriptive statistics (as mean ± SEM) for the monophasic inactivation time constant (τ_{inact}), and the biphasic time constants, fast (τ_{fast}) and slow (τ_{slow}) at 0 mV. One-way ANOVA with Tukey or Dunnett's multiple comparisons test indicate no significant changes in any of the three groups. At least three animals per group were used.

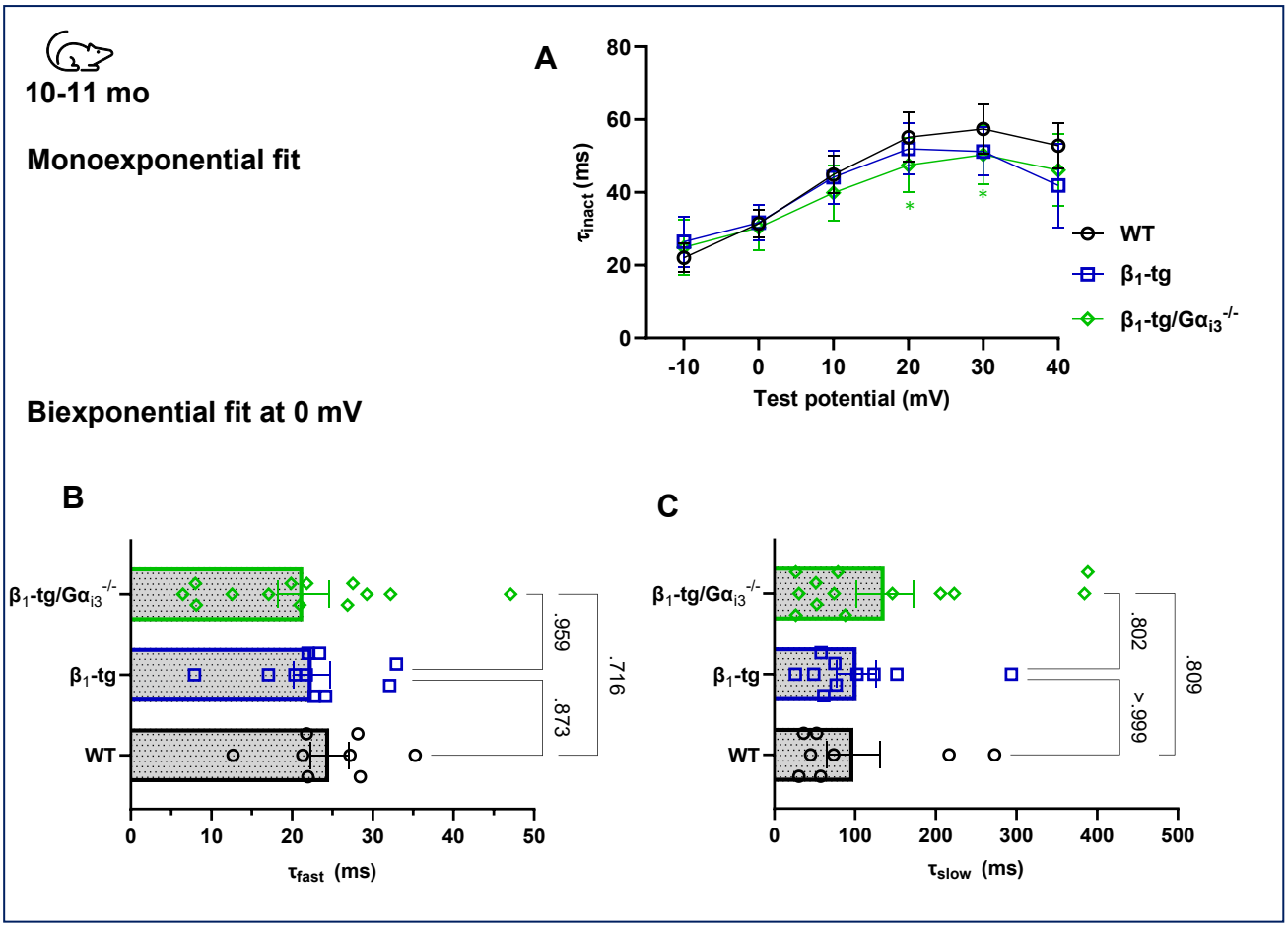

Fig. 3-7. Effects of $G\alpha_{i3}$ deficiency on the time courses of $I_{Ca,L}$ inactivation. A. The inactivation monophasic time constant (τ_{inact}) is plotted as a function of voltage and shows that the inactivation rate tended to increase at more depolarized potentials in β_1-tg (n=12-17) and β_1-tg/$G\alpha_{i3}^{-/-}$ (n=11-19) compared to wild-type (n=13-18). **B-C.** The time courses for fast (τ_{fast}) and slow (τ_{slow}) inactivation are obtained by biexponential function at 0 mV. Data are presented as mean ± SEM. *:p<.05 in one-way ANOVA followed by Bonferroni's multiple comparisons tests.

3.2.4 Effects of isoproterenol on $I_{Ca,L}$ inactivation properties in β_1-tg and β_1-tg/$G\alpha_{i3}^{-/-}$ mice

The analysis of $I_{Ca,L}$ activation properties showed that $I_{Ca,L}$ had a blunted responsiveness to β-AR agonist stimulation in cardiomyocytes from β_1-tg mice with or without $G\alpha_{i3}$ deletion. Subsequently, we analyzed the effects of Iso on the inactivation kinetics. The inactivation process is crucial in determining the duration and amplitude of the calcium influx during adrenergic stimulation to prevent excessive calcium load. To evaluate this process, we measured the rate of calcium current inactivation and the steady-state voltage dependence of inactivation after exposure to isoproterenol.

➢ Rate of $I_{Ca,L}$ inactivation in Iso treated myocytes – old mice:

Figure 3-8 demonstrates a comparison of the voltage dependence of inactivation time constants (τ_{inact}) under basal conditions and after exposure to 1µM Iso. There was a slight decrease in the rate of inactivation in Iso-treated wild-type and β_1-tg/$G\alpha_{i3}^{-/-}$ myocytes, and to a lesser extent in β_1-tg myocytes, but these differences were not statistically significant.

Of note, in stimulated myocytes from β_1-tg or in β_1-tg/$G\alpha_{i3}^{-/-}$ mice, in which Iso was less effective, $I_{Ca,L}$ decay was best fitted by a bi-exponential function in the voltage range of -10 to +10 mV. For example, the percentage of cells exhibiting a bi-fit at 0 mV was 75.0% and 61.1%, respectively. In contrast, in wild-type, where a pronounced response to Iso was observed, the $I_{Ca,L}$ decay was best fitted by a monoexponential fit (at 0 mV only 15.3% of cells showed bi-fit, see suppl.S5-S6). Therefore, it was not adequate to compare the inactivation fast and slow time constants at basal conditions and after stimulation with isoproterenol.

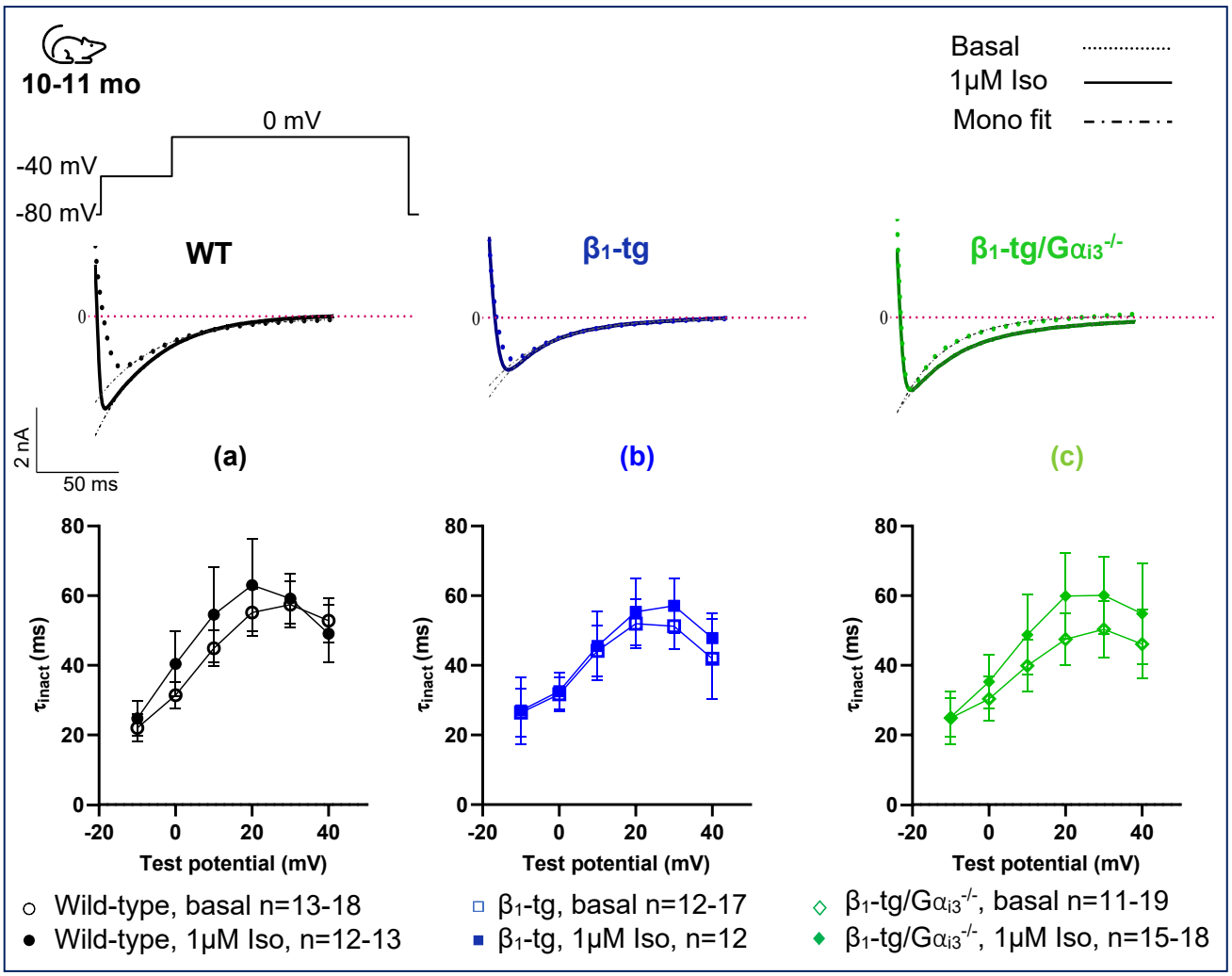

Fig. 3-8. Effects of 1 µM Isoproterenol on the $I_{Ca,L}$ inactivation rate in old mice. The upper traces show exemplary traces of $I_{Ca,L}$ (nA) at 0 mV under basal (dotted lines) and after treatment with 1µM Iso for 8±2 min (solid lines). Monoexponential fit of ICa,L decay from peak to the end of the test pulse is displayed as dashed lines. (a-c) $I_{Ca,L}$ inactivation time constants (τ_{inact}) are computed at voltages from -10 mV to +40 mV under basal conditions (open symbols) and after incubation with Iso (solid symbols). Data are presented as mean ± SD.

- Steady-state voltage dependence of $I_{Ca,L}$ inactivation after Iso treatment:

As previously stated, under basal conditions, the voltage dependence of steady-state $I_{Ca,L}$ inactivation remained unaltered in β_1-tg or β_1-tg/$G\alpha_{i3}^{-/-}$ compared to wild-type cardiomyocytes. However, β-AR stimulation with 1µM Iso caused a hyperpolarization shift in the $I_{Ca,L}$ inactivation curve in β_1-tg/$G\alpha_{i3}^{-/-}$ and wild-type but not in β_1-tg myocytes (Figure 3-9, A, c). This effect was underlined by a significant change in the half-maximal voltage of inactivation $V_{0.5_inact}$ towards more negative potentials in β_1-tg/$G\alpha_{i3}^{-/-}$ (-29.9±4.8 mV, n=12) *versus* basal (-24.7±6.4 mV, n=16, p=.003); and in wild-type (-29.5±4.4 mV, n=14) *versus* basal (-26.0±3.1 mV, n=15, p=.01), while in β_1-tg myocytes $V_{0.5_inact}$ did not significantly change (Figure 3-9, A, Table 3-4).

In summary, while β-AR stimulation has minimal effects on the activation gating characteristics of LTCC in β_1-tg/$G\alpha_{i3}^{-/-}$ mice, $G\alpha_{i3}$ deficiency appears to enhance the voltage-dependent of $I_{Ca,L}$ inactivation following acute adrenergic stimulation. This can enhance the channels' ability to inactivate upon phosphorylation, which may improve cardiac adaptation under stress conditions in β_1-tg mice.

3.2.5 Effects of $G\alpha_{i3}$ deficiency on basal $I_{Ca,L}$ recovery from inactivation in β_1-tg mice

In a previous section, it has been shown that in old β_1-tg mice, the rate of $I_{Ca,L}$ recovery from inactivation was comparable to age-matched wild-type. We next examined the effect of $G\alpha_{i3}$ deficiency on channels recovery. Under basal conditions, the recovery from inactivation was time-dependent and $I_{Ca,L}$ exhibited faster recovery kinetics in β_1-tg/$G\alpha_{i3}^{-/-}$ myocytes. This was evidenced by a significantly decreased recovery time constant (τ_{rec}) and half-life time ($t_{1/2}$) required for channels to reach 50% recovery after inactivation, compared to β_1-tg (p<.001) and wild-type (p<.03) (Figure 3-10, B; Table 3-6). However, there was no significant change in the fraction of current recovered at all time intervals among the three groups (Figure 3-10, A). This indicates that the absence of $G\alpha_{i3}$ under resting conditions increases the channels' susceptibility to recover from inactivation without increasing the net current influx in β_1-tg mice.

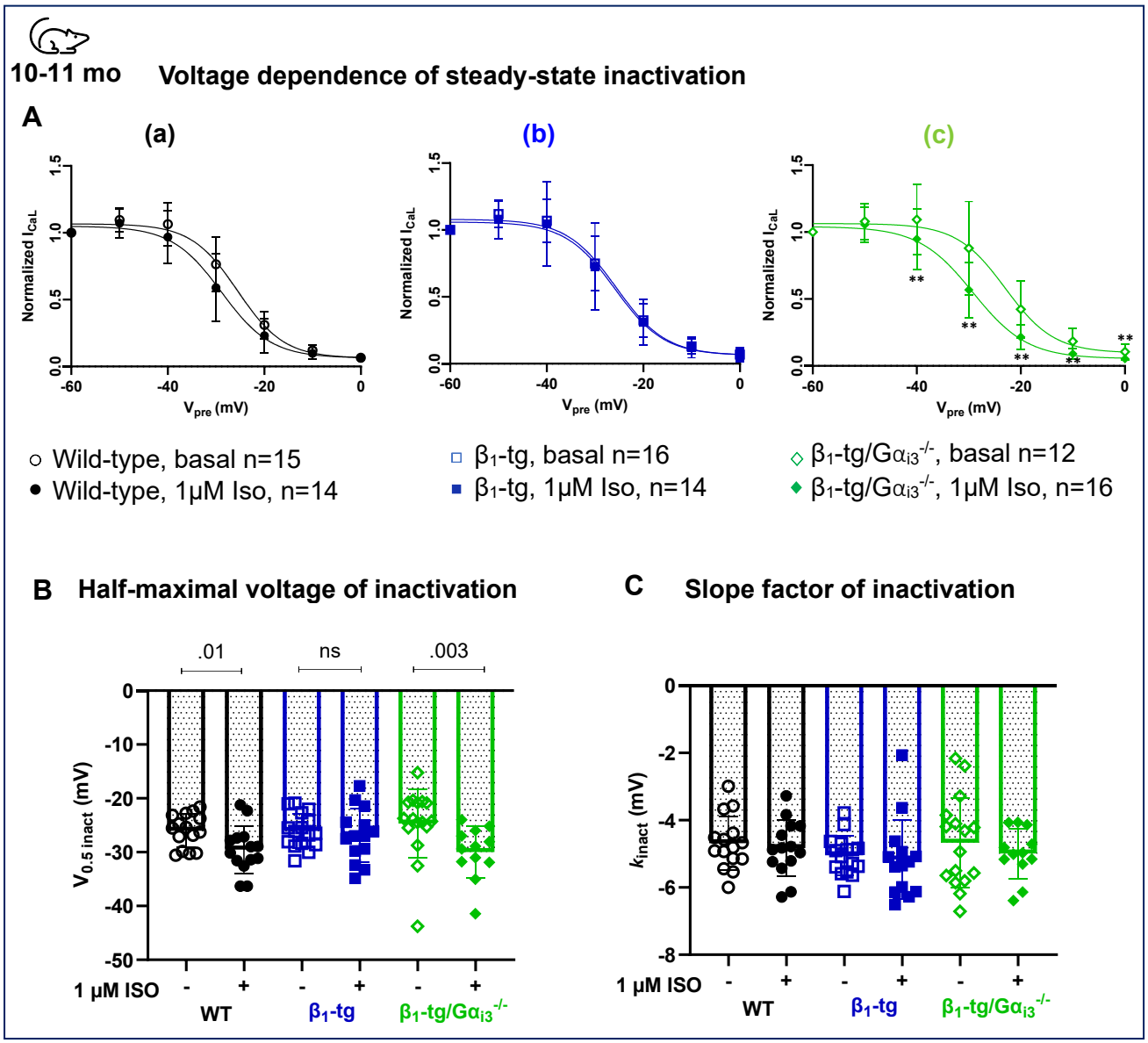

Fig. 3-9. Effects of 1 µM Isoproterenol on the steady-state voltage dependence of $I_{Ca,L}$ inactivation. (Iso, solid symbols *versus* basal, open symbols). The steady-state inactivation of $I_{Ca,L}$ is measured by applying conditioning pulses from -60 to +60 mV for 2-seconds followed by a test pulse at 0 mV. **A.** Normalized $I_{Ca,L}$ was fitted to a Boltzmann sigmoidal function and plotted as a function of conditioning voltages. In β_1-tg/$G\alpha_{i3}^{-/-}$ myocytes (c), 1 µM Iso induced a marked hyperpolarization shift in the $I_{Ca,L}$ inactivation curves within the voltage range from -30 to 0 mV (*vs.* basal **: p<.01 in Multiple unpaired *t-tests*), compared to slight shift in wild-type (a), while curves were almost identical in β_1-tg myocytes (b). The fitting parameters **B.** Half-maximal voltage of $I_{Ca,L}$ inactivation ($V0.5_{_inact.}$) and **C.** Slope factor of inactivation were compared with Student's t-test or Mann-Whitney test in each group. Data are presented as mean ± SD.

Table 3-6. $I_{Ca,L}$ recovery from inactivation parameters in cardiomyocytes from 10-11 m old mice

	n	τ_{rec} (ms)	Half-life ($t_{1/2}$) (ms)	Recovery at 375 ms (%)
Wildtype	14	228.5±56.9	158.4±39.5	77.7±6.7
β_1-tg	17	251.2±49.9	174.1±34.6	73.9±5.8
β_1-tg/G$\alpha_{i3}^{-/-}$	17	179.6±47.6$^{\dagger\dagger\dagger\#}$	124.5±33.0$^{\dagger\dagger\dagger\#}$	78.3±13.5

Table 3- 6. Descriptive statistics for the parameters of for $I_{Ca,L}$ recovery from inactivation, showing values as mean ± SD. τ_{rec}; Monophasic time constant for recovery, **375 ms**; the last time interval at which $I_{Ca,L}$ recovery was measured. One-way ANOVA with Bonferroni's multiple comparisons test was used to compare the three groups under basal conditions ($^{\#}p<.05$ vs. wild-type) ($^{\dagger\dagger\dagger}p<.001$ vs. β_1-tg).

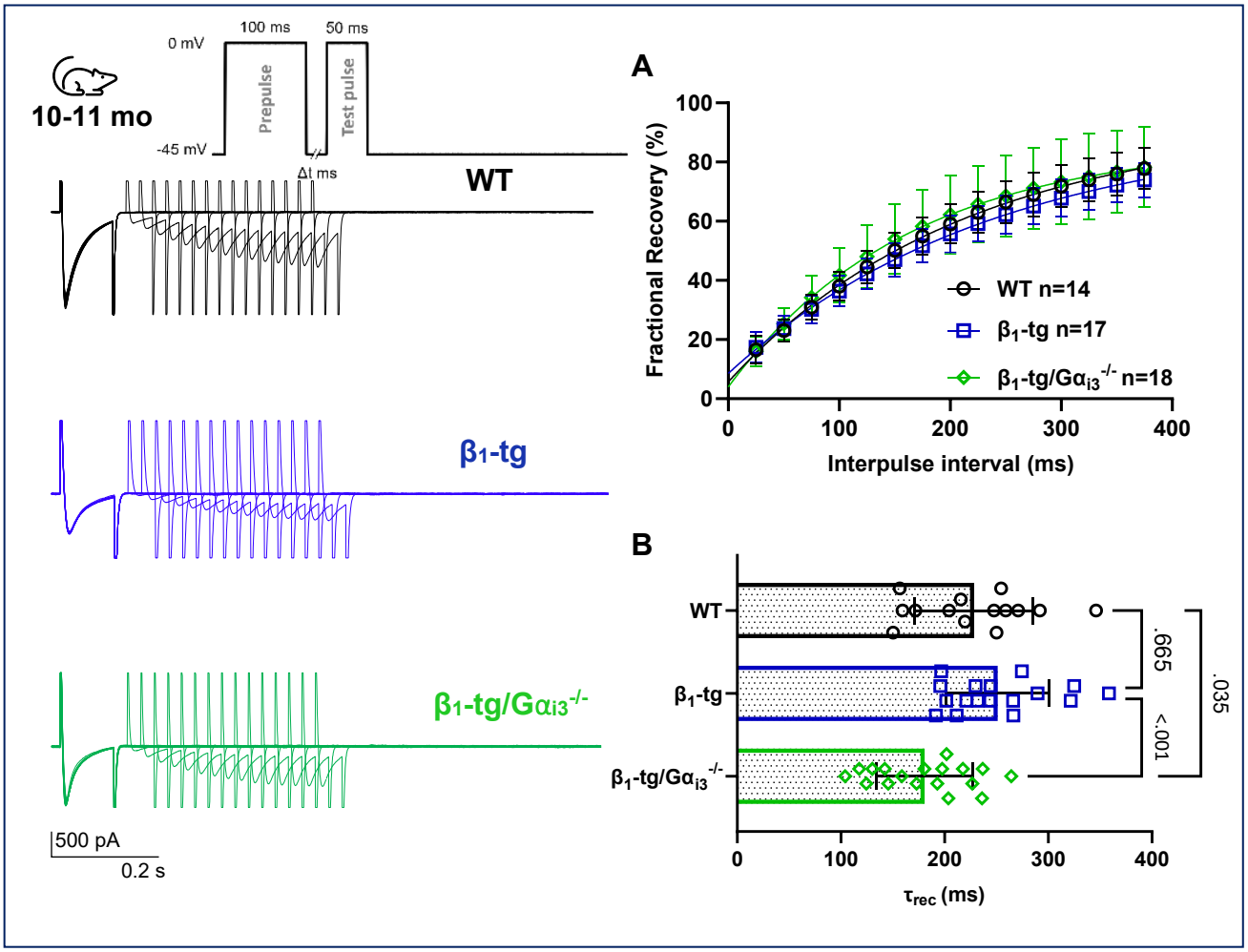

Fig. 3-10. Effects of Gα_{i3} deficiency on basal $I_{Ca,L}$ recovery from inactivation. The pulse protocol used to measure $I_{Ca,L}$ recovery is shown in the *inset*. Representative original traces are displayed on the left. **A.** The mean fractional recovery from inactivation is plotted as a function of the recovery intervals with the lines representing the monoexponential fit **B.** The time constants for $I_{Ca,L}$ recovery . Data are presented as mean ± SD. *p-values* obtained in one-way ANOVA followed by Bonferroni's multiple comparisons tests.

3.3 Effects of $G\alpha_{i2}$ deficiency on the kinetics of $I_{Ca,L}$ in β_1-tg mice

We next sought to delineate the effect of $G\alpha_{i2}$ deficiency on LTCC modulation in β_1-tg mice. Due to the frequent early lethality observed in β_1-tg/$G\alpha_{i2}^{-/-}$ mice, a direct comparison with aged β_1-tg mice lacking $G\alpha_{i3}$ was not feasible. However, our data suggest earlier alterations in ventricular $I_{Ca,L}$ in β_1-tg myocytes, and in another previous study, $G\alpha_{i2}$ deficiency led to early onset of heart failure in these mice, therefore we decided to investigate ventricular I_{CaL} at a younger age (4-5 months).

3.3.1 LTCC activation and inactivation properties in β_1-tg/$G\alpha_{i2}^{-/-}$ mice

We found that $I_{Ca,L}$ density was reduced, and channel activation kinetics were significantly altered in β_1-tg cardiomyocytes. However, in β_1-tg/$G\alpha_{i2}^{-/-}$ myocytes, the $I_{Ca,L}$ density and its activation properties were similar to those from age-matched β_1-tg myocytes (Figure 3-11, A-D). For a comprehensive analysis of the activation and inactivation parameters, and their statistical significance, see (Table 3-7).

Figure (3-11,E) shows the overlap of voltage dependence of $I_{Ca,L}$ activation and inactivation curves. The basal $I_{Ca,L}$ conductance (G/Gmax) was significantly lower in both β_1-tg and β_1-tg/$G\alpha_{i2}^{-/-}$ compared to wild-type myocytes. For instance, at 0 mV, the conductance was 91.6%±7.3 (n=15) in wild-type *versus* 82.6%±7.8 (n=11, p=.01) and 83.8±7.8 (n=17, p=0.2) in β_1-tg and β_1-tg/$G\alpha_{i2}^{-/-}$ myocytes, respectively. Surprisingly, additional deletion of $G\alpha_{i2}$ caused a noticeable shift in the steady-state inactivation curve in β_1-tg myocytes (dashed lines). There was a slight but significant increase in the slope factor for inactivation (k_{inact}) in β_1-tg/$G\alpha_{i2}^{-/-}$ (-3.3±0.8 mV, n=13) compared to both wild-type (-5.3±0.8 mV, n=10, p<.001) and β_1-tg (-5.2±1.1 mV, n=14, p<.001). Consequently, the half-maximal voltage of inactivation ($V_{0.5_inact}$) was more positive in β_1-tg/$G\alpha_{i2}^{-/-}$ (-21.4±1.7 mV, n=13) than in wild-type (-28.8±3.7 mV, p<.001) and β_1-tg (-26.4±3.6 mV, p<.001). This led to a distinct window current due to incomplete inactivation, where the areas of steady-state activation and inactivation overlapped. Of note, $G\alpha_{i3}$ deficiency in young β_1-tg mice seems to have similar effects on $I_{Ca,L}$ kinetics as those observed in older mice. However, only one young male β_1-tg/$G\alpha_{i3}^{-/-}$ animal was examined during this study (*see* *suppl. S7*).

Based on these findings, it appears that the lack of $G\alpha_{i2}$, as opposed to a $G\alpha_{i3}$ deficiency, does not affect the changes in $I_{Ca,L}$ activation kinetics observed in β_1-tg myocytes, at least not

at this stage. However, it does decrease the voltage dependence of $I_{Ca,L}$ inactivation and leads to a larger window current in β_1-tg myocytes.

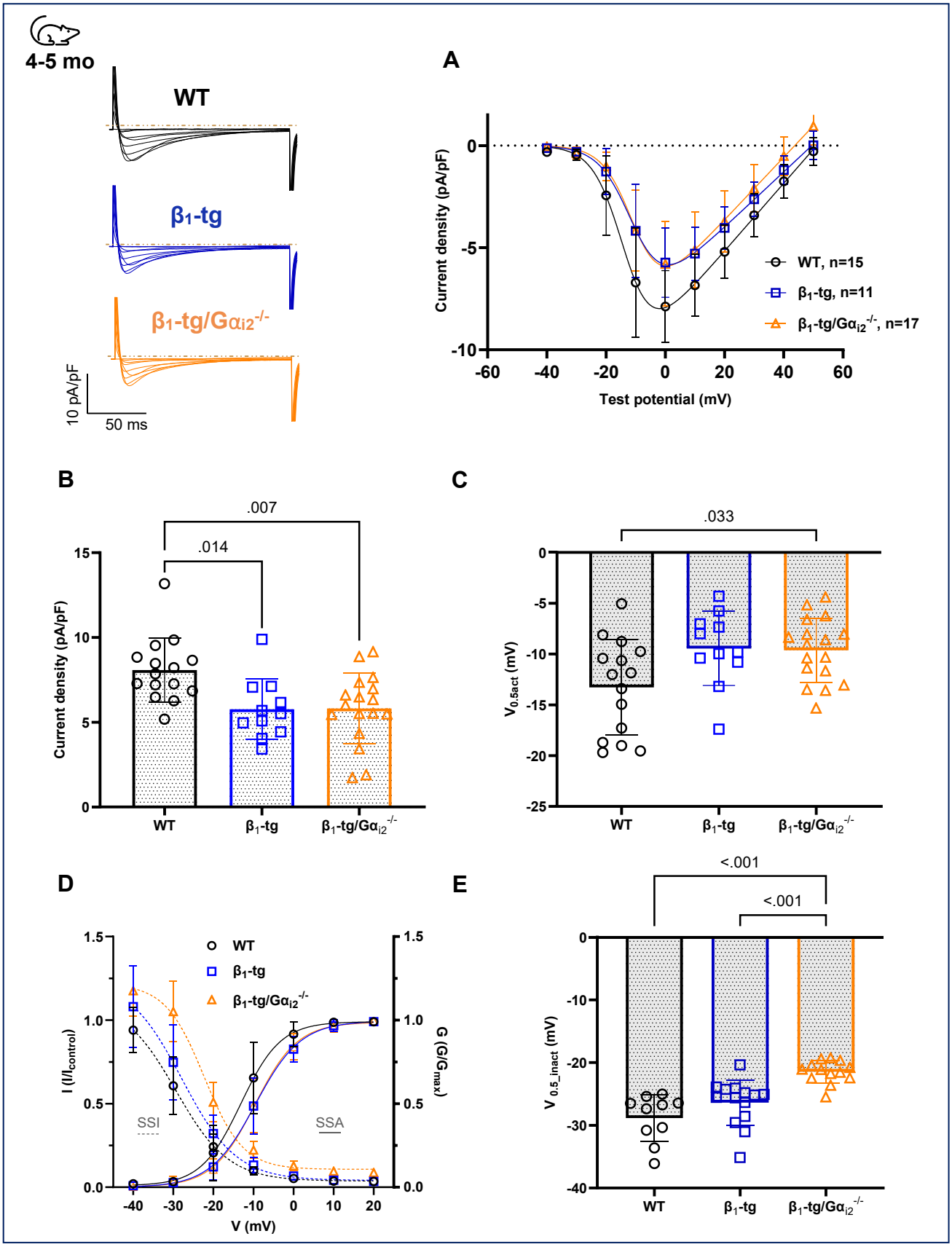

Fig. 3-11

Fig. 3-11. Effects of $G\alpha_{i2}$ deficiency on the voltage dependence of basal $I_{Ca,L}$ activation and inactivation in young mice. $I_{Ca,L}$ was recorded in freshly isolated ventricular myocytes using voltage-clamp mode. Representative original $I_{Ca,L}$ traces normalized by the cell-capacitance are shown on the top left **A.** Current-voltage relationships of $I_{Ca,L}$ with the solid lines representing the fit of the curves to Boltzmann-Ohm function from 4–5-month-old, male wild-type, β_1-tg, β_1-tg/$G\alpha_{i2}^{-/-}$ mice, where *n* is the number of cells. **B.** Peak $I_{Ca,L}$ density, **C.** The half-maximal activation voltage ($V_{0.5_act}$), **D.** Overlap of $I_{Ca,L}$ steady-state activation (SSA; *solid lines*), and inactivation (SSI; *dashed lines*) showing an elevated window current (the region where SSA and SSI are overlapping). **E.** Half maximal voltage of inactivation. One-way ANOVA with Bonferroni's multiple comparisons test was used in (B,C,E). Data are presented as mean ± SD, and each symbol in the scatter box plot represents a cell.

Table 3-7. $I_{Ca,L}$ activation and inactivation parameters of $I_{Ca,L}$ in wild-type, β_1-tg and β_1-tg/$G\alpha_{i2}^{-/-}$ cardiomyocytes (4-5 months)

	n	Peak $I_{Ca,L}$ (pF/pA)	$V_{0.5_act}$ (mV)	k_{act} (mV)	$V_{0.5_inact}$ (mV)	k_{inact} (mV)
Wildtype						
Basal	10-15	-8.1±1.9	-13.3±4.7	4.1±0.5	-28.8±3.7	-5.3±0.8
Iso	5-7	-12.4±2.7***	-20.4±3.4*	2.8±0.3***	-28.1±2.0	-4.5±0.3
β_1-tg						
Basal	11-14	-5.7±1.8$^{\#}$	-9.4±3.6	5.1±0.8$^{\#}$	-26.4±3.6	-5.1±1.1
Iso	9	-7.9±2.7*	-14.5±4.5*	3.9±0.9*	-25.6±3.1	-4.6±0.7
β_1-tg/$G\alpha_{i2}^{-/-}$						
Basal	13-17	-5.8±2.1$^{\#\#}$	-9.6±3.1$^{\#}$	4.9±1.1	-21.4±1.7$^{\#\#\#\dagger\dagger\dagger}$	-3.3±0.8$^{\#\#\#\dagger\dagger\dagger}$
Iso	8-9	-12.1±2.8***	-22.1±4.6***	2.3±0.4***	-19.8±2.6	-4.3±0.5*

Table 3- 7. Descriptive statistics for $I_{Ca,L}$ parameters showing values as mean ± SD. At least 3 animals per group were used in the experiments; *n* indicates the number of recorded cells. An unpaired *t-test* was used to compare basal values vs. with 1µM Iso in each group (*:p<.05, ***:p<.001). One-way ANOVA with Bonferroni's multiple comparisons test was used to compare the three groups at basal conditions ($^{\#}$:p<.05, $^{\#\#}$:p<.01, $^{\#\#\#}$:p<.001 vs. wild-type) (†:p<.05, †††:p<.001 vs. β_1-tg).

3.3.2 $I_{Ca,L}$ response to acute β-AR agonist stimulation in β_1-tg/$G\alpha_{i2}^{-/-}$ mice

We have shown that β-AR responsiveness was blunted in both β_1-tg and β_1-tg/$G\alpha_{i3}^{-/-}$ myocytes. Therefore, we wondered how the absence of $G\alpha_{i2}$ would affect the response to acute β-AR stimulation with isoproterenol.

In sharp contrast, $G\alpha_{i2}$ deficiency in β_1-tg myocytes resulted in restoration and enhancement of $I_{Ca,L}$ responsiveness to stimulation with Iso. There was a significant increase in peak $I_{Ca,L}$ density over the entire potential range and a marked leftward shift in $I_{Ca,L}$ activation voltage, which was even more prominent compared with wild-type Figure (3-12).

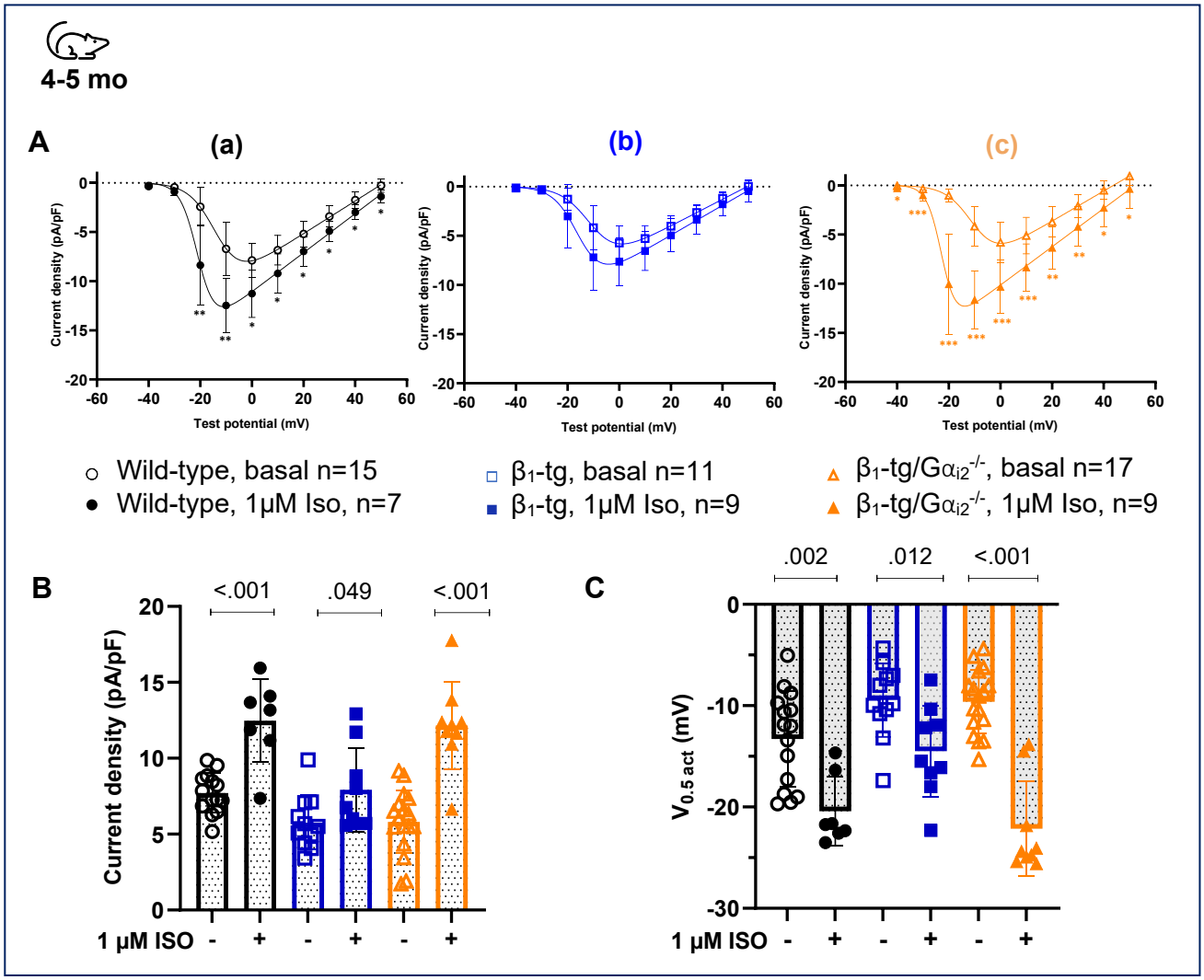

Fig. 3-12. Effects of $G\alpha_{i2}$ deficiency on $I_{Ca,L}$ response to 1 μM isoproterenol in young mice (Iso, solid symbols *versus* basal, open symbols). A. Current-voltage relationships for $I_{Ca,L}$ show that 1 μM iso caused a significant increase in the $I_{Ca,L}$ density over the entire voltage range and shifted the I-V curve to the left in wild-type (a) and β_1-tg/$G\alpha_{i2}^{-/-}$ (c). Both effects were blunted in β_1-tg myocytes (b). These observations are consistent with a marked increase in the average peak $I_{Ca,L}$ density (**B)** and more negative values for half maximal voltage of activation $V_{0.5_act}$ in wild-type and β_1-tg/$G\alpha_{i2}^{-/-}$**(C).** Multiple unpaired *t- tests* were used to compare Iso effects on $I_{Ca,L}$ density at different test potentials; *p <.05,**p <.01,***p <.001(A). Unpaired student *t-test* was used to compare Iso effects in each group (B+C). Data are presented as mean ± SD, and each symbol represents a cell in the scatter box plots.

In β_1-tg/$G\alpha_2^{-/-}$ myocytes, the maximal effect of Iso on $I_{Ca,L}$ exceeded that in age-matched wild-type. Specifically, the percentage increase in peak $I_{Ca,L}$ density was to +209.0±50% compared to +154.0±34% in wild-type myocytes (Figure 3-12, B; Table 3-7). Likewise, Iso caused a significant shift in the half-maximal voltage of activation to more negative values in β_1-tg/$G\alpha_2^{-/-}$ (to -22.1±4.6 mV *vs.* -9.6±3.1 mV basal, p<.001, Figure 3-12, C, Table 3-7). Of note, in all young wild-type myocytes stimulated with Iso, the peak of $I_{Ca,L}$ was observed at -10 mV, whereas in 66% of β_1-tg/$G\alpha_2^{-/-}$ myocytes, $I_{Ca,L}$ peaked at an even more negative potential, specifically at -20 mV.

Furthermore, stimulation with Iso resulted in a significant reduction in the activation slope factor (k_{act}) in wild-type (by 1.3 mV *vs.* basal, p<.001), in β_1-tg/$G\alpha_{i2}^{-/-}$ (by 2.6 mV, p<.001 *vs.* basal), and to a lesser extent in β_1-tg myocytes (by 1.2 mV, p=.005 *vs.* basal).

Preliminary data from young β_1-tg/$G\alpha_{i3}^{-/-}$ myocytes showed that neither $I_{Ca,L}$ nor $V_{0.5_act}$ was changed significantly after stimulation with 1µM Iso as shown (suppl. S7).

Collectively, these results indicate that in contrast to β_1-tg mice with or without $G\alpha_{i3}$ expression, the $I_{Ca,L}$ response to acute β-AR agonist stimulation is preserved in β_1-tg/$G\alpha_{i2}^{-/-}$ mice. This effect seems to be associated with more abrupt changes i.e., augmented current density and enhanced voltage sensitivity to activation following acute β-AR stimulation, which are more pronounced than in wild-type mice.

3.3.3 Time constants and rate of basal $I_{Ca,L}$ inactivation in β_1-tg/$G\alpha_{i2}^{-/-}$ mice

The inactivation time constant (τ_{inact}) indicates that the rate of $I_{Ca,L}$ inactivation was slightly faster in young β_1-tg myocytes. An additional deletion of $G\alpha_{i2}$ resulted in a significant acceleration of inactivation rate over the voltage range from -10 to +40 mV. For example, at +20 mV, τ_{inact} was (46.0±8.5 ms, n=17) *versus* wild-type (60.8±6.9 ms, n=12, p<.0001), and *versus* β_1-tg (54.7±8.7 ms, n=10, p=.03), Figure (3-13, A).

The bi-exponential fit of $I_{Ca,L}$ decay at 0 mV showed a significant reduction in the fast component of $I_{Ca,L}$ decay in β_1-tg/$G\alpha_{i2}^{-/-}$ myocytes compared to wild-type myocytes (p=.02). The slow component was also reduced, but changes were not statistically significant (Figure 3-13, B; Table 3-8). These results indicate that under basal conditions, $G\alpha_{i2}$ deficiency caused faster $I_{Ca,L}$ inactivation, likely by affecting the fast $I_{Ca,L}$ inactivation kinetics.

Table 3-8.
Inactivation time constants at 0 mV under basal conditions – (4-5 months)

	n	τ_{inact} (ms)	n	τ_{fast} (ms)	τ_{slow} (ms)
Wildtype	12	37.0±2.5	6	30.1±4.4	167.0±49.1
β_1-tg	10	33.0±1.3	7	24.1±2.9	139.7±42.0
β_1-tg/$G\alpha_{i2}^{-/-}$	17	28.0±1.3**	10	18.7±1.4*	97.1±12.6

Table 3- 8. Descriptive statistics (as mean ± SEM) for the monophasic time constant (τ_{inact}) of $I_{Ca,L}$ inactivation, and the biphasic time constants, fast (τ_{fast}) and slow (τ_{slow}) at 0 mV. One-way ANOVA with Bonferroni's multiple comparisons test was used to compare the three groups. (*:p<.05, **:p<.01 *vs.* wild-type).

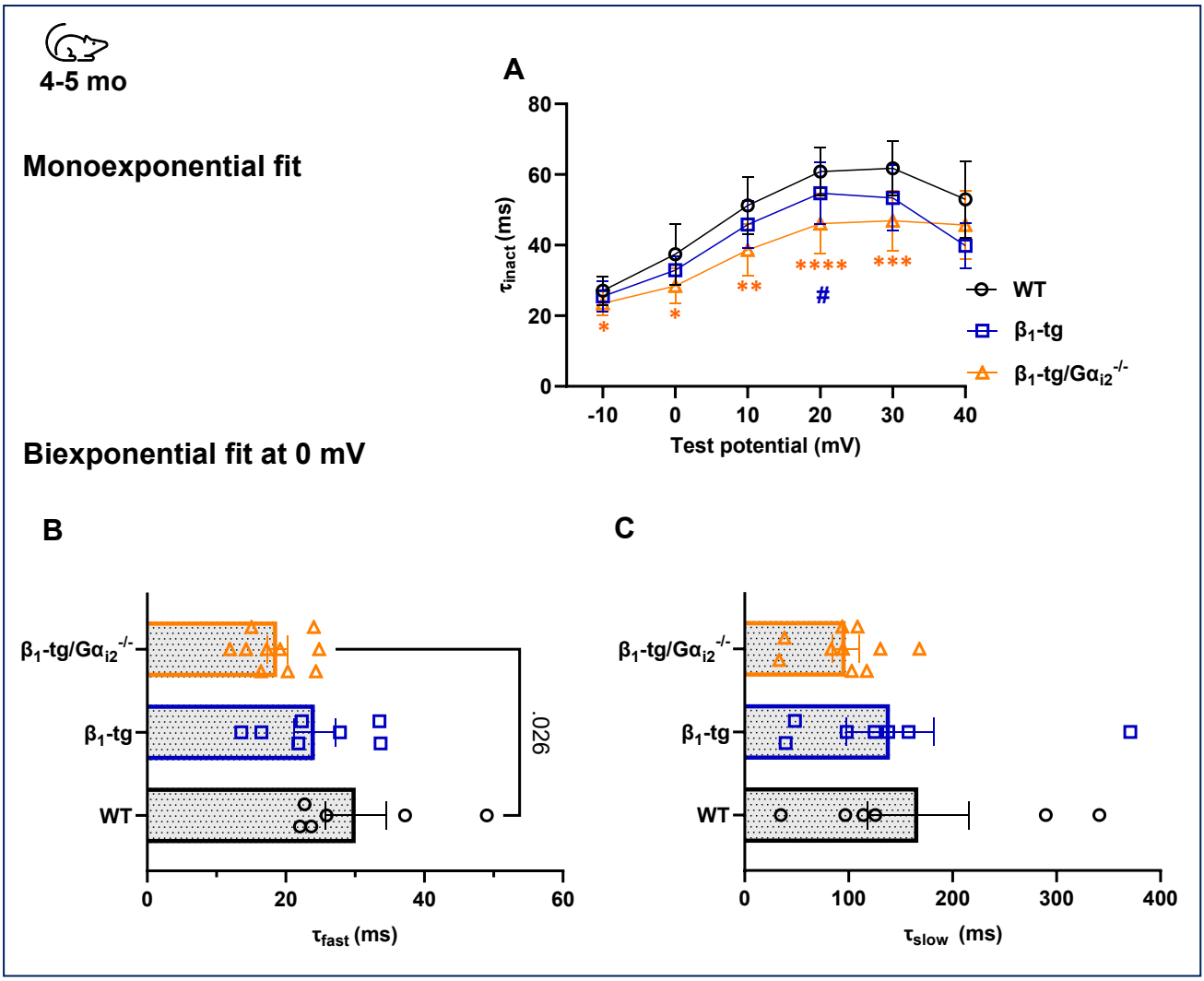

Fig. 3-13. Effects of $G\alpha_{i2}$ deficiency on the time course of $I_{Ca,L}$ inactivation. A. The monophasic time constant of $I_{Ca,L}$ inactivation (τ_{inact}) is plotted as a function of voltage and shows that the inactivation rate is significantly accelerated in β_1-tg/$G\alpha_{i2}^{-/-}$ (n=10-17) *versus* wild-type (n=10-12; *:p<.05, **:p<.01 ***:p<.001, ****:p<.001), and versus β_1-tg (n=6-10; #=.03) myocytes. **B-C.** The time courses for fast (τ_{fast}) and slow (τ_{slow}) inactivation are obtained by biexponential function at 0 mV. Data are presented as mean ± SEM. *p-values* in One-way ANOVA followed by Bonferroni's multiple comparisons test. The number of cells in plot (A) varies for each genotype depending on the test potential, whether $I_{Ca,L}$ could be fitted with a monoexponential function or not.

3.3.4 Effects of isoproterenol on the $I_{Ca,L}$ inactivation properties in β_1-tg and β_1-tg/$G\alpha_{i2}^{-/-}$ mice

Given the pronounced increase in peak $I_{Ca,L}$ density and enhanced activation kinetics observed in β_1-tg/$G\alpha_{i2}^{-/-}$ myocytes after stimulation with isoproterenol, one might expect $I_{Ca,L}$ inactivation to accelerate in order to counteract the increase in Ca^{2+} influx and prevent calcium overload. However, we observed the opposite effect.

Iso-stimulation resulted in a slower $I_{Ca,L}$ decay in β_1-tg/$G\alpha_{i2}^{-/-}$ myocytes, as τ_{inact} significantly increased in the voltage range from 0 to +40 mV compared to basal conditions, whereas no significant changes were observed in age-matched β_1-tg or wild-type myocytes (Figure 3-14). Consistent with the observations from older mice, $I_{Ca,L}$ decay in myocytes, where Iso had pronounced effects, was best fitted by a mono-exponential function in the voltage range of -10 to +10 mV. For example, at 0 mV, only 10% of myocytes in β_1-tg/$G\alpha_{i2}^{-/-}$ and 14.2% in wild-type exhibited a bi-fit, while 44.4% of β_1-tg myocytes did (see suppl.S6, for the percentage of occurrence).

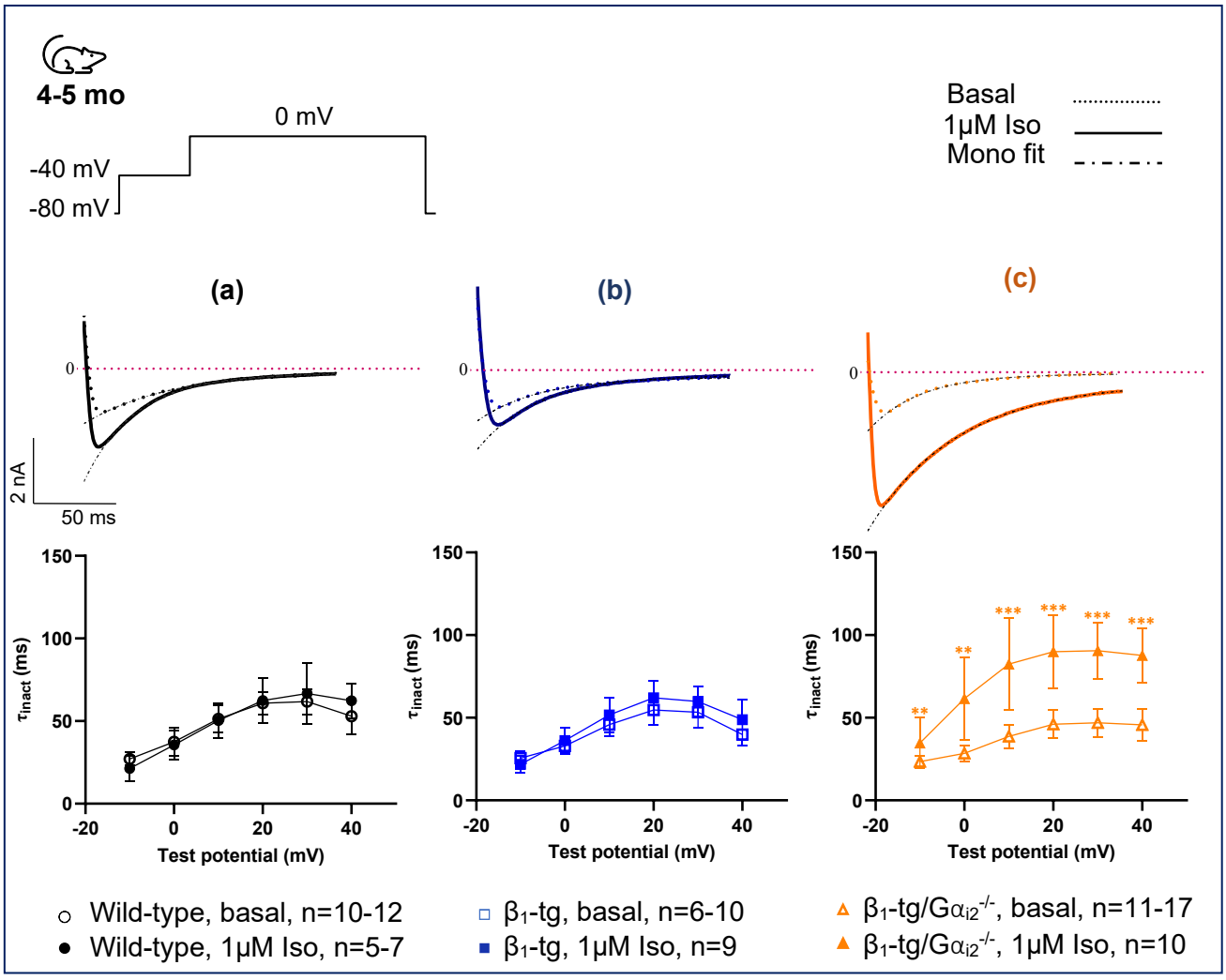

Fig. 3-14. Effects of 1 µM Isoproterenol on the $I_{Ca,L}$ inactivation rate in young mice. The upper traces show exemplary traces of $I_{Ca,L}$ (nA) at 0 mV under basal (dotted lines) and after treatment with 1µM Iso for 8±2 min (solid lines). Monoexponential fit of $I_{Ca,L}$ decay from peak to the end of the test pulse is displayed as dashed lines. (a-c) $I_{Ca,L}$ inactivation time constants (τ_{inact}) are computed at voltages from -10 mV to +40 mV under basal conditions (open symbols) and after incubation with Iso (solid symbols). Data are presented as mean ± SD.

Furthermore, stimulation with Iso led to a decrease in the voltage dependence of $I_{Ca,L}$ inactivation in β_1-tg/$G\alpha_{i2}^{-/-}$, as evidenced by a marked rightward shift in the steady-state inactivation curve at more depolarized potentials from -10 to +10 mV as shown in (Figure 3-

15, c). This shift was underlined by a significant decrease in the slope factor for inactivation (k_{inact}) in β_1-tg/G$\alpha_{i2}^{-/-}$ myocytes (to -4.3±0.5 mv, n=8 *vs.* basal: -3.3±0.8 mv, n=13; p=.008 in Mann Whitney Test; Figure 3-15,C). Neither in wild-type nor in β_1-tg myocytes, Iso affected the voltage dependence of inactivation. No significant differences were observed in the half-maximal inactivation voltage in all groups (Figure 3.15,B). However, basal $V_{0.5_inact}$ was already shifted to more positive potentials in β_1-tg/G$\alpha_{i2}^{-/-}$ myocytes as mentioned above.

These results suggest that the absence of Gα_{i2} leads to abnormal LTCC inactivation in both the basal and phosphorylated states. In contrast to Gα_{i3} deficiency, the $I_{Ca,L}$ decay was dramatically prolonged and $I_{Ca,L}$ voltage dependent inactivation was reduced following β-AR stimulation in β_1-tg/G$\alpha_{i2}^{-/-}$, which could lead to an excess of calcium in the heart muscle.

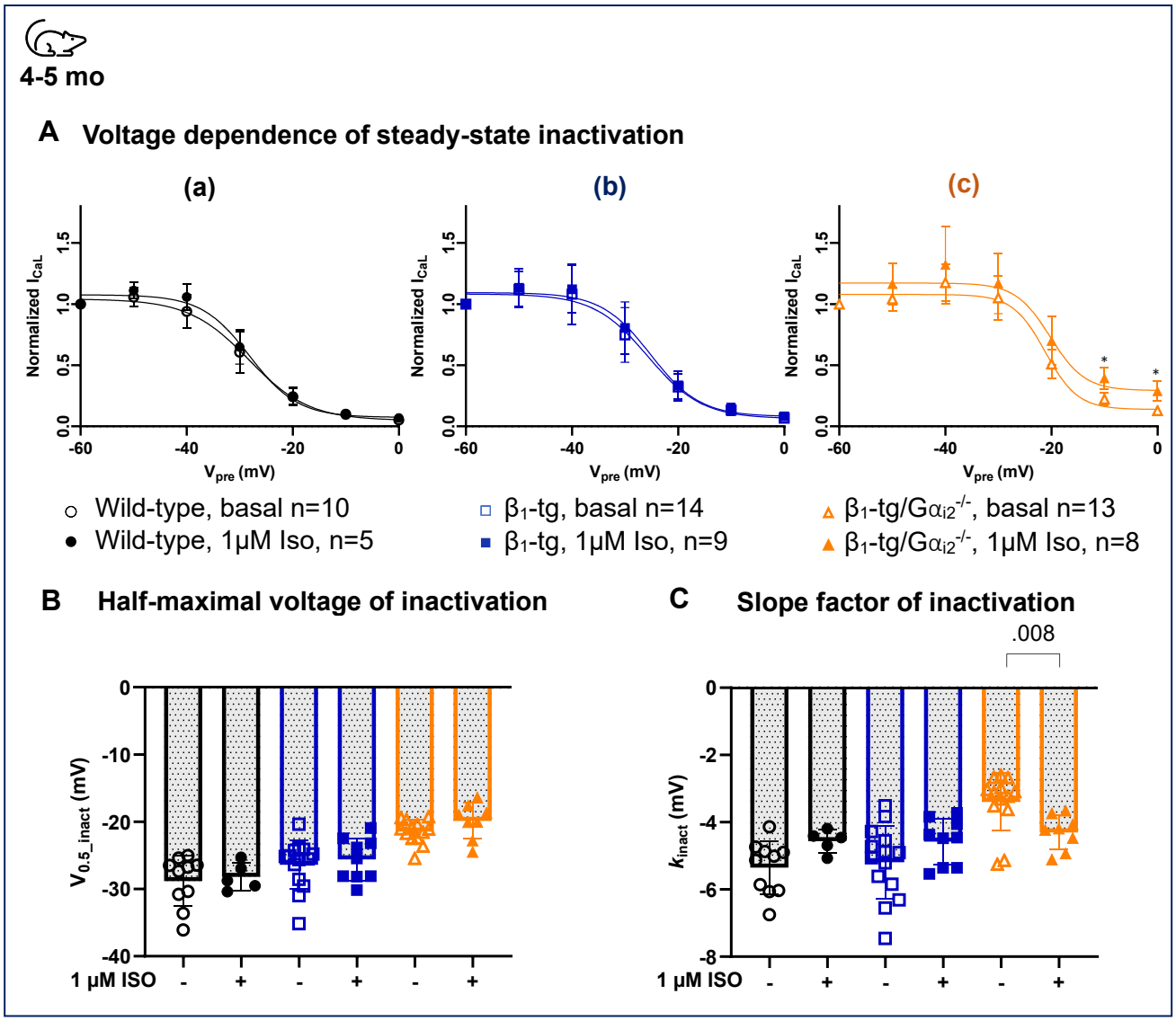

Fig. 3-15

Fig. 3-15. Effects of Isoproterenol on the steady-state voltage dependence of $I_{Ca,L}$ inactivation. (Iso, solid symbols *versus* basal, open symbols). The steady-state of $I_{Ca,L}$ inactivation is measured by applying conditioning pulses from -60 to +60 mV for 2-seconds followed by a test pulse at 0 mV. **A.** Normalized $I_{Ca,L}$ was fitted to a Boltzmann sigmoidal function and plotted as a function of conditioning voltages. In β_1-tg/$G\alpha_{i2}^{-/-}$ myocytes (c), voltage-dependence of $I_{Ca,L}$ inactivation was reduced i.e., curves were shifted to the right (*vs.* basal *: p<.05 in Multiple unpaired *t-tests*), while the curves were almost overlapped in wild-type (a) and, β_1-tg myocytes (b). The fitting parameters are **B.** Half-maximal voltage of $I_{Ca,L}$ inactivation ($V0.5_{_inact.}$) and **C.** Slope factor of inactivation compared by Student's *t-test* or Mann-Whitney test. Data are presented as mean ± SD and each symbol represents a cell in the scatter box plots.

3.3.5 Effects of $G\alpha_{i2}$ deficiency on basal $I_{Ca,L}$ recovery from inactivation in β_1-tg mice

$G\alpha_{i2}$ deficiency resulted in an accelerated rate of channel recovery in β_1-tg myocytes, as evidenced by a significantly decreased time constant for recovery (τ_{rec}) compared to wild-type and β_1-tg myocytes (Figure 3-16, B; Table 3-9). In contrast to $G\alpha_{i3}$ deficiency, there was a marked increase in the fraction of current recovered over the entire time intervals in β_1-tg/$G\alpha_{i2}^{-/-}$ myocytes (Figure 3-16, A). At this young age, preliminary data from β_1-tg/$G\alpha_{i3}^{-/-}$ myocytes indicated only a slight acceleration in recovery compared to β_1-tg or wild type (suppl. S8).

Collectively, these findings suggest that deficiencies in both $G\alpha_{i2}$ and $G\alpha_{i3}$ accelerate the $I_{Ca,L}$ recovery kinetics regardless of age, but the magnitude of this effect varies depending on the specific Gαi isoform.

Table 3-9. $I_{Ca,L}$ recovery from inactivation parameters in cardiomyocytes from 4-5 month-old mice

	n	τ_{rec} (ms)	Half-life ($t_{1/2}$) (ms)	Recovery at 375 ms (%)
Wildtype	10	289.1 ± 58.3	200.4 ± 40.4	64.1 ± 7.6
β_1-tg	11	212.0 ± 21.9	147.0 ± 15.2	74.1 ± 6.5
β_1-tg/$G\alpha_{i2}^{-/-}$	15	128.6 ± 13.8$^{\#\#\#\dagger\dagger}$	89.1 ± 9.5$^{\#\#\#\dagger\dagger}$	89.6 ± 4.9$^{\#\#\#\dagger\dagger}$

Table 3- 9. Descriptive statistics for the parameters of $I_{Ca,L}$ recovery from inactivation, showing values as mean ± SD. At least 3 animals per group were used in the experiments. n, indicates the number of recorded cells. Kruskal-Walli's test was used to compare the three groups under basal conditions *($^{\#\#\#}$:p<.001 vs. wild-type) (††:p<.01 vs. β_1-tg).*

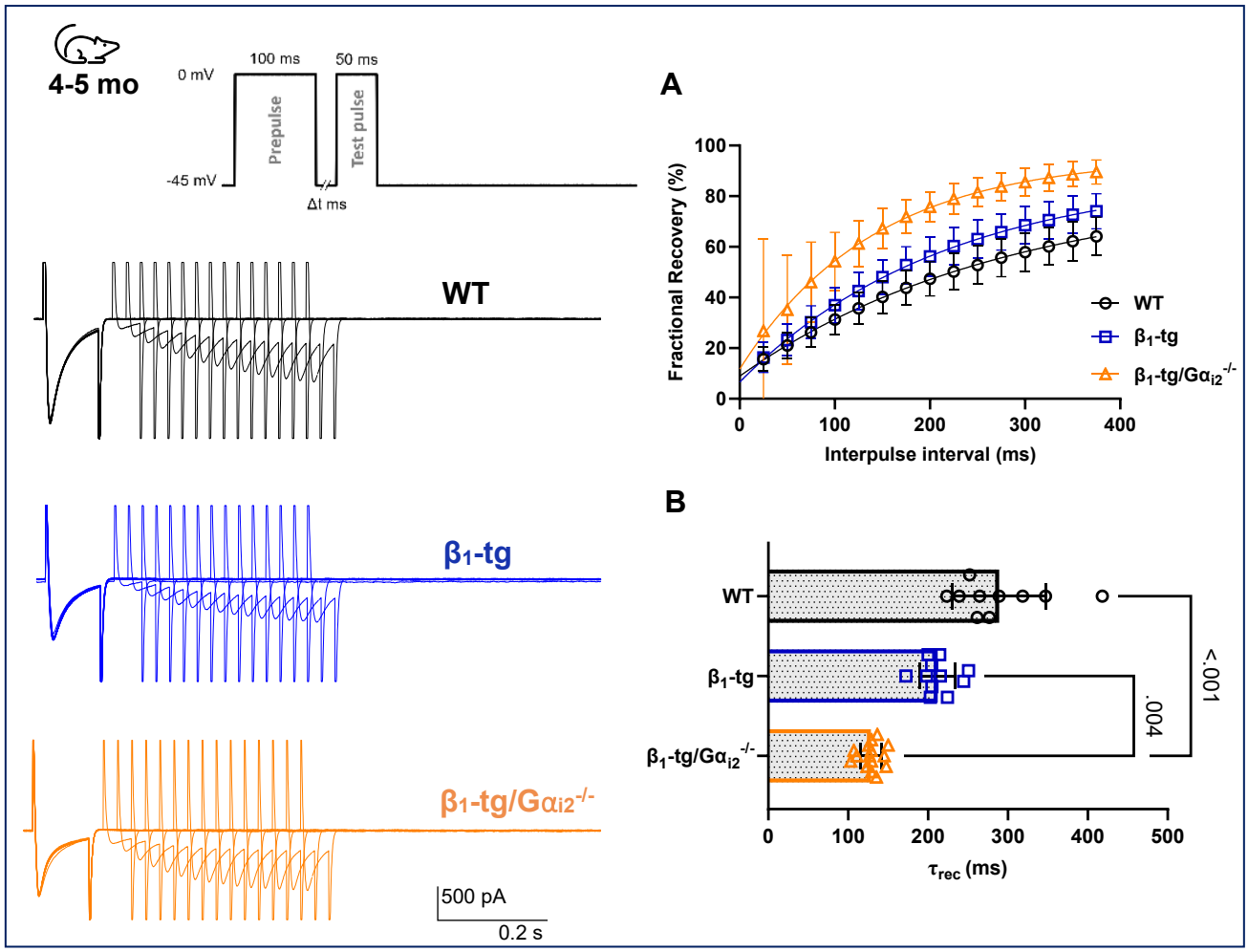

Fig. 3-16. Effects of $G\alpha_{i2}$ deficiency on basal $I_{Ca,L}$ recovery from inactivation in young mice. The pulse protocol used to measure $I_{Ca,L}$ recovery is shown in the inset. The upper traces show the representative original traces. **A.** The mean fractional recovery from inactivation is plotted as a function of the recovery intervals with the lines representing the monoexponential fit. **B.** Time constants for $I_{Ca,L}$ recovery. Data are presented as mean ± SD. p-values were obtained in Kruskal-Wallis test followed by Dunn's multiple comparisons test.

3.4 Testing of GPM-1: New potential Gαi-protein modulator

In this proof-of-concept study we tested a new Gαi modulator known as GPM-1 (G protein Modulator-1). GPM-1 is a linear peptide that lacks membrane 's permeability, therefore it was added to the patch pipette, and its putative effect on the $I_{Ca,L}$ was tested under basal conditions and after stimulation with 1 µM Iso in ventricular cardiomyocytes from young mice (3-5 months) of both sexes.

First, we assessed the feasibility of using this peptide for $I_{Ca,L}$ patch clamp measurements, specifically patch seal stability and $I_{Ca,L}$ properties. Using 10 µM GPM-1 dissolved in 0.1 % DMSO, we obtained typical $I_{Ca,L}$ current waveforms and bell-shaped *I-V* curves (Figure 3-17, A). The giga-seal formation was achieved successfully, and the cells remained intact during the recordings.

Under basal conditions, cardiomyocytes exposed to 10µM GPM-1 exhibited a slight reduction in current density over the voltage range of -40 to +50 mV (Figure 3-17, A). Though, the maximal $I_{Ca,L}$ density was significantly reduced (-7.4±2.4 pA/pF, n=22) compared to control (-8.9±1.8 pA/pF, n=31, p=.01). The reversal potential and the slope factor of activation were also slightly but significantly altered (Table-3-10). GPM-1 had no effect on $I_{Ca,L}$ responsiveness to 1µM Iso, as evidenced both by the increased peak $I_{Ca,L}$ and the negative shift in $V_{0.5_act}$ compared to the typical βAR response in the control (Figure 3-17, B-C).

These results indicate that $I_{Ca,L}$ in cardiomyocytes treated with 10 µM GPM-1 was slightly reduced, while response to Iso appears to be unaffected.

Table 3-10. Effects of 10 µM GPM-1 on $I_{Ca,L}$ activation parameters in ventricular cardiomyocytes from wild-type mice (3-5 months-old)

	n	V_{rev} (mV)	Peak $I_{Ca,L}$ (pF/pA)	$V_{0.5\text{-}act}$ (mV)	k_{act} (mV)
Control					
Basal	31	51.5±3.6	-8.9±1.8	-11.9±3.5	4.3±0.9
Iso	12	53.5±4.4	-12.6±2.3***	-19.6±4.0***	2.8±0.5***
GPM-1					
Basal	22	48.8±4.2$^{\#}$	-7.4±2.4$^{\#}$	-10.2±3.5	4.9±0.7$^{\#}$
Iso	6	50.6±6.0	-11.9±1.2***	-19.5±3.9***	3.1±0.8***

Table 3- 10. Descriptive statistics for $I_{Ca,L}$ parameters showing values as mean ± SD. At least 3 animals per group were used in the experiments; *n* indicates the number of recorded cells. Two-Way ANOVA with Fisher's LSD test was applied to compare the two groups under basal conditions ($^{\#}$:p<.05 vs. control), and after exposure to Iso (***:p<.001 vs. basal).

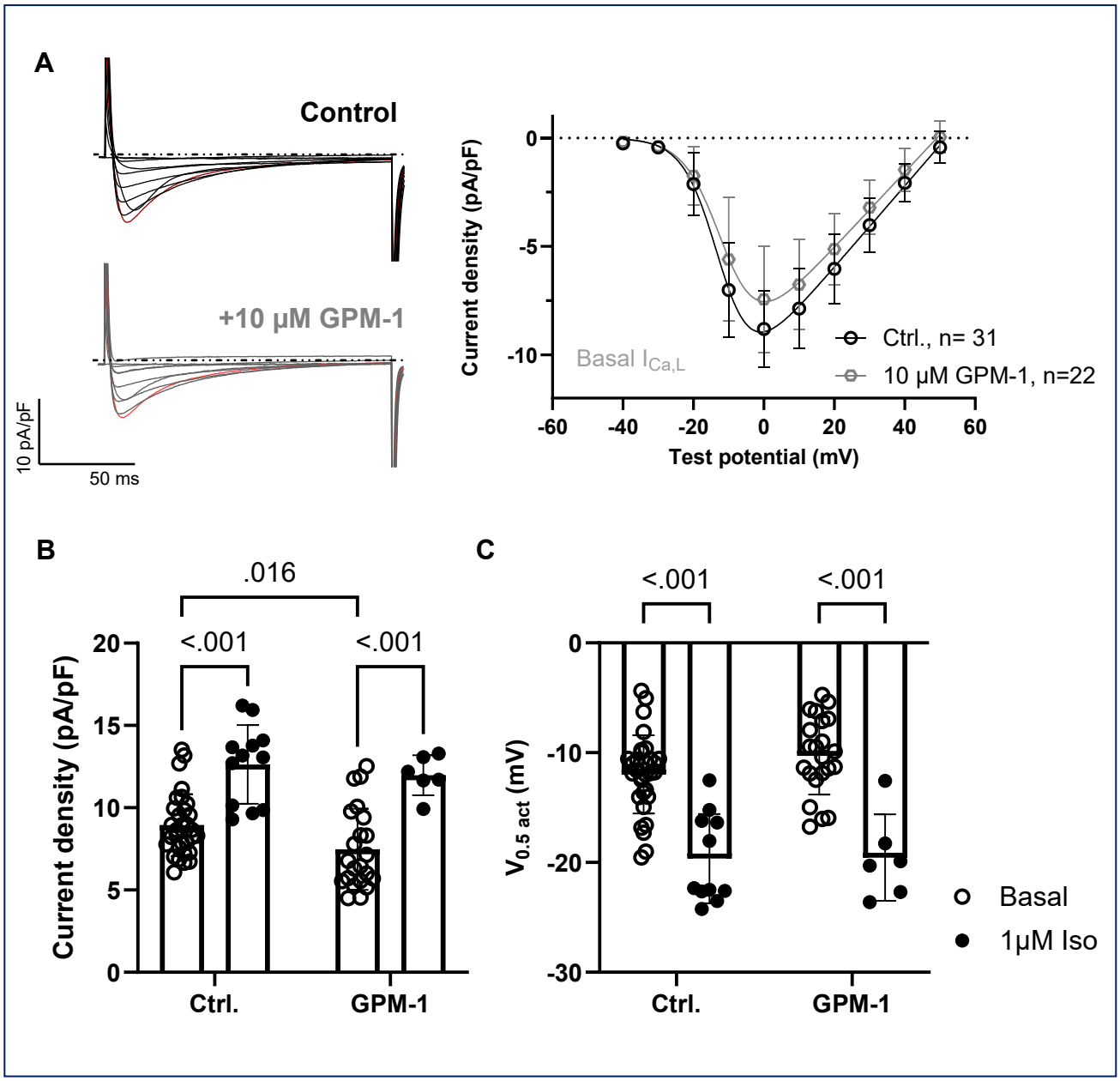

Fig. 3-17. Effects of GPM-1 peptide on $I_{Ca,L}$ activation properties. $I_{Ca,L}$ was recorded using voltage-clamp mode in freshly isolated ventricular myocytes. **A.** Representative $I_{Ca,L}$ traces normalized by the cell-capacitance are shown on the left. Current-voltage relationships of basal $I_{Ca,L}$ with the solid lines representing the fit of the curves to Boltzmann-Ohm function (traces in red represent $I_{Ca,L}$ at 0 mV). **B.** Average peak $I_{Ca,L}$ density, and **C.** Half-maximal activation voltage $V_{0.5_act}$ (basal versus 1µM Iso). Two-way ANOVA with Fisher's LSD test was used to compare the effect of peptide, Iso-treatment, and their interactions on peak $I_{Ca,L}$ and $V_{0.5_act}$. Interaction effects were insignificant. Data are presented as mean ± SD and each symbol represents a cell in the scatter box plots.

4

Discussion

Motivated by our previous studies highlighting the distinct roles of specific Gαi protein isoforms in transgenic mice with a cardiac overexpression of the human β_1-adrenoceptor (β_1-tg), in which deletion of $G\alpha_{i2}$ exacerbates (Keller et al., 2015), whereas deletion of $G\alpha_{i3}$ ameliorates the cardiac phenotype (Schröper et al., 2024), we now performed a series of *in vitro* patch-clamp experiments to investigate the biophysical properties of ventricular L-type calcium channels (LTCC) in these mouse models.

$G_{i/o}$-mediated signaling has been proposed to have potential cardioprotective benefits in cardiomyopathies. This effect has been primarily attributed to the $G\alpha_{i2}$ isoform (Foerster et al., 2003; DeGeorge et al., 2008; Waterson et al., 2011; Köhler et al., 2014; Keller et al., 2015). However, the precise mechanism underlying these protective effects and the role of other $G\alpha_i$-isoforms are yet to be fully understood and require further investigation.

The β_1-tg mouse model used in this study is known for developing a progressive cardiomyopathy that results in hypertrophy, contractile dysfunction, and ultimately heart failure (Engelhardt et al., 1999). This makes it a suitable model to study the long-term pathological changes associated with β-adrenergic receptor-mediated heart failure, and to test the effects of altered downstream effectors. Given the essential role of the L-type calcium current ($I_{Ca,L}$) in cardiac excitation-contraction coupling and its contribution to the pathophysiological changes in Ca^{2+} homeostasis in failing myocytes, this study aims to investigate its properties and modulation in β_1-tg mice, and to determine whether the absence of $G\alpha_{i2}$ or $G\alpha_{i3}$ has any additional effect in this murine model of heart failure.

The salient findings of the present study are as follows: **(i)** $I_{Ca,L}$ density was significantly reduced in β_1-tg mice, **(ii)** $G\alpha_{i3}$ deficiency largely restored alterations of basal $I_{Ca,L}$, **(iii)** $G\alpha_{i2}$ deficiency induced substantial changes in basal $I_{Ca,L}$ inactivation and recovery kinetics in β_1-tg mice, and **(iv)** the $I_{Ca,L}$ response to acute β-adrenergic stimulation was attenuated in β_1-tg and β_1-tg/$G\alpha_{i3}^{-/-}$ but augmented in β_1-tg/$G\alpha_{i2}^{-/-}$ mice. Preliminary results of this study have been published in abstract form (Katnahji & Matthes, 2023).

4.1 L-type calcium channels in β-AR mediated heart failure

4.1.1 Altered $I_{Ca,L}$ preceded cardiac failure in β_1-tg mice

In our previous study, β_1-tg mice were found to have a significantly shortened lifespan and impaired cardiac function, which was observed at around 18 months, specifically at 550 days of age (Schröper et al., 2024). Mice tested at 300 days of age showed no overt contractile dysfunction (Keller et al., 2015). However, earlier impairment of cellular Ca^{+2} handling and fibrosis that progressing to contractile dysfunction have been observed in this mouse model at even younger ages (Engelhardt et al., 2001). Several studies conducted in both animal models (Ming et al., 1994; Nakayama et al., 2007; Beetz et al., 2009) and diseased human hearts (Ouadid et al., 1995; Schröder et al., 1998; Chen et al., 2002, 2008) have shown that changes in ventricular $I_{Ca,L}$ during cardiomyopathy may lead to progression of heart failure. Therefore, we hypothesized that the cardiac phenotype of β_1-tg mice would be preceded by alterations in LTCC function and regulation. Indeed, we find altered properties of the ventricular $I_{Ca,L}$ in β_1-tg mice at an age when the contractile dysfunction was not yet impaired in our recent study.

While Engelhardt et al. reported no changes in I_{CaL} density in β_1-tg ventricular myocytes (Engelhardt et al., 2004), we have observed a significant reduction in current density. The mice used in their study were relatively young, only two months old, and they used the FVB/N based mouse line, which was backcrossed to a C57BL/6 background in our study.

The role of $I_{Ca,L}$ in the pathogenesis and progression of heart failure is still controversial. Several animal studies have reported conflicting results regarding the $I_{Ca,L}$ density, with some showing an increase, others a decrease, and others no change (*review*, Mukherjee & Spinale, 1998; Richard et al., 1998). These discrepancies are likely due to the use of different experimental models with varying genetic backgrounds and stages of cardiomyopathy induced by different methods. However, most studies have observed a reduction in $I_{Ca,L}$ density in severely hypertrophied hearts and/or end-stage heart failure. It is also important to point out that none of the studies cited in the aforementioned reviews were conducted on mice. Interestingly, Beetz et al. have demonstrated that induced alterations of L-type calcium channel gating in mice resulted in morph-histological changes, suggesting that altered $I_{Ca,L}$ may not only precede HF but also be causal (Beetz et al., 2009).

Furthermore, we observed fibrosis and elevated hypertrophy markers in aged β_1-tg mice (Schröper et al., 2024), while such changes were insignificant in younger mice (Keller et al., 2015). Earlier animal studies have suggested a potential association between the reduction in $I_{Ca,L}$ density and the progression of myocardial hypertrophy (Nuss & Houser, 1991; Bouron et al., 1992; de Brito Santos et al., 1995). A genetically induced reduction in the pore-forming subunit α_{1C} of LTCC resulted in a decreased $I_{Ca,L}$ density in mice, which was accompanied by hypertrophy and cardiac dysfunction (Goonasekera et al., 2012).The authors proposed that the reduced current density may increase the sensitivity of SR-Ca^{2+} release to maintain cardiac contractility, ultimately activating hypertrophic signaling if $I_{Ca,L}$ is sufficiently reduced. Indeed, Engelhardt and colleagues showed that isolated cardiomyocytes from β_1-tg mice exhibited altered calcium homeostasis. This was manifested by prolonged intracellular Ca^{2+} transients $[Ca^{2+}]_i$ at two months of age, prior to the development of structural changes and fibrosis at four months, and these changes were due to altered expression of the SR regulatory proteins (Engelhardt et al., 2001). Altered SR-Ca^{2+} release can indeed influence the time course of $I_{Ca,L}$ in myocytes (Bers, 2002). However, whether or not the reduction we observed in $I_{Ca,L}$ is secondary to changes in intracellular calcium levels requires further investigation.

Another possible explanation for reduced $I_{Ca,L}$ would be due to changes in single channel properties and/or a reduction in the abundance of calcium channels. The whole-cell current is a function of both the number of functional channels and their individual (single-channel) properties (McDonald, et al., 1994). In a previous study conducted in our lab, it was shown that the basal activity of single channel in myocytes from 3–5-month-old β_1-tg mice remained unchanged. In addition, no changes in the total number of calcium channels were detected by radiological binding of dihydropyridine (DHP) sites or western blot analysis (Foerster et al., 2004). Given that $I_{Ca,L}$ density was partially normalized by additional deletion of $G\alpha_{i3}$ in β_1-tg mice in this study, it is unlikely that the expression levels of LTCC were affected.

Moreover, we observed a depolarization shift in the voltage of $I_{Ca,L}$ activation and a decrease in the channel conductance in β_1-tg myocytes. These changes suggest altered LTCC gating kinetics and reduced voltage sensitivity for activation, which may account for the reduction in $I_{Ca,L}$ density. Interestingly, we have previously seen similar reduced current and gating abnormalities in mice lacking $G\alpha_{i2}$ ($G\alpha_{i2}^{-/-}$ knockout mice). In this mouse model, there were also changes in steady-state inactivation and recovery properties that may explain the reduced $I_{Ca,L}$ density (Dizayee et al., 2011). However, we did not observe dramatic changes

in the kinetics of $I_{Ca,L}$ decay, steady-state of inactivation or recovery from inactivation in β_1-tg mice.

The amplitude and gating kinetics of cardiac $I_{Ca,L}$ can be modulated by protein kinases (Bers & Perez-Reyes, 1999). Thus, it is possible that altered phosphorylation of the channels underlies the observed changes in $I_{Ca,L}$ gating. Although this idea can be challenged by the fact that basal function of cardiac LTCC does not require phosphorylation of their subunits, we cannot exclude the possibility that chronic β-AR activity might alter the basal level of LTCC phosphorylation. Moreover, PKA-mediated regulation of cardiac $I_{Ca,L}$ is influenced by the spatial localization of signaling, as highlighted by (Kamp & Hell, 2000). Redistribution of β-ARs with changes in cAMP compartmentalization was observed in a rat model of chronic heart failure (Nikolaev et al., 2010). Similar changes in cAMP signaling have been reported under post-myocardial infarction (*review*, Colombe & Pidoux, 2021). However, except for increased PLB phosphorylation (Schröper et al., 2024), the level of cAMP and the phosphorylation state of individual PKA downstream targets have not been fully investigated in our β_1-tg mouse model.

In summary, these findings suggest that a reduction in $I_{Ca,L}$ density and alterations in LTCC gating kinetics precede the onset of overt failure in β_1-tg mice. This reduction may be adaptive and prevent calcium overload, however, in the long term, it may contribute to the progression of hypertrophy and eventually lead to loss of pump function.

4.1.2 Reduced β-adrenergic response of $I_{Ca,L}$ in β_1-tg mice

Despite controversies surrounding changes in the L-type calcium current density, most studies have reported a decreased $I_{Ca,L}$ response to beta-adrenergic stimulation in heart failure animal models (Scamps et al., 1990; Böhm et al., 1992; Mukherjee et al., 1995, 1998; Zhang et al., 1995; Hegyi et al., 2019), as well as in clinical studies (Ouadid et al., 1995; Schröder et al., 1998; Chen et al., 2002).

Reduced β-adrenergic responsiveness is a characteristic of heart failure and results from the activation of several mechanisms to counteract the increased stimulation of the β-adrenergic system (Böhm & Maack, 2000). This can occur due to molecular and functional changes that lead to receptor desensitization, including selective downregulation of β_1-AR, upregulation of α-subunit of Gi protein, and phosphorylation of the β-ARs by the upregulated and enhanced GRKs kinases, thus resulting in inefficient receptor-effector coupling (*review,* Lohse et al., 1996; El-Armouche et al., 2003).

Stimulation through β-adrenergic- or cAMP-dependent pathways results in an increase in $I_{Ca,L}$ amplitude and a negative shift in the voltage dependence of activation and inactivation of $I_{Ca,L}$ (*review*, McDonald et al., 1994; Bers & Perez-Reyes, 1999). Both effects were observed in channels from our wild-type mice, but not in β_1-tg mice. Despite the overexpression of β_1-AR, the $I_{Ca,L}$ response to stimulation with 1μM isoproterenol was attenuated as evidenced by a lower percentage increase in peak $I_{Ca,L}$ density and an insignificant change in the activation voltage compared to those in wild-type. This finding is consistent with the results obtained at the single-channel level, where channels failed to respond to acute adrenoceptor stimulation by the same applied concentration of Iso in β_1-tg myocytes (Foerster et al., 2004).

Desensitization in β-adrenergic signaling occurs in aging and heart failure (de Lucia et al., 2018). However, its impact on the progression of heart failure remains elusive. This may depend on several factors, such as the subtype of β-AR involved and the stage and severity of heart failure. Reduced β-adrenoceptor function may serve as a protective mechanism to shield the heart from SNS-related adrenergic overactivity, which can have detrimental effects on the heart, such as increased oxygen demand, arrhythmias, apoptosis, hypertrophy, and fibrosis. In the long-term, however, this can lead to maladaptation and reduced contractile reserve and output (Lymperopoulos et al., 2013; de Lucia et al., 2018; Mahmood et al., 2022).

Interestingly, in this study we find a Gαi protein isoform-specific modulation of the $I_{Ca,L}$ response to β-AR stimulation in β_1-tg mice. Specifically, the lack of $G\alpha_{i2}$ resulted in a restoration of $I_{Ca,L}$ response to Iso, whereas the lack of $G\alpha_{i3}$ did not, as discussed in detail below. Given the respective *in vivo* detrimental effects of $G\alpha_{i2}$ deficiency, manifested by exacerbated failure phenotype and shortened lifespan, these results suggest that the attenuated β-AR responsiveness is rather beneficial in β_1-tg mice. This is in line with findings indicating that therapeutic approaches focused on increasing β-AR stimulation, such as β-AR agonists, are linked to higher mortality rates in HF (*review,* El-Armouche & Eschenhagen, 2009). Conversely, beta-blockers, which are an integral part of the first-line treatment for chronic heart failure, have been shown to reduce the risk of hospitalization and mortality rates, and lead to reverse ventricular remodeling (*review,* Böhm & Maack, 2000; Bristow, 2011; McDonagh et al., 2021). To sum up, these findings suggest that cardiac overexpression of β_1-AR in mice may lead to activation of adaptive mechanisms that result in β-AR desensitization. The attenuated β-AR-mediated activation may have protective effects against adrenergic overstimulation-induced cardiotoxicity.

4.2 Gi proteins in β-AR mediated heart failure

4.2.1 From earlier hypotheses to Gαi isoform-specific functions

In hypertrophied myocardium and failing human hearts, there is an increase in inhibitory Gi proteins (Feldman et al.,1988; Neumann et al., 1988; Böhm et al., 1990, 1992b; Eschenhagen, et al., 1992; Mittmann et al., 2003), which has been associated with the desensitization of β-adrenergic receptors in animal models and human HF (Brown & Harding, 1992). β_2-adrenoceptors couple to Gs and Gi protein in animals and human hearts (Xiao et al., 1995, 1999; Kilts et al., 2000). The β_2-AR-Gi signaling provides a mechanism to counteract adverse β_1-AR signaling in the heart, such as blunting β_1-AR activation of $I_{Ca,L}$ (Heubach et al., 2001), and activation of cell anti-apoptotic pathways e.g., PI3K/Akt and MAPK/ERK pathways (Communal et al., 1999; Chesley et al., 2000; Zheng et al., 2005).

The closely related $G\alpha_{i2}$ and $G\alpha_{i3}$ isoforms are expressed in the ventricular myocardium of mammals and show tissue-specific and developmental differences in expression within the heart (Foster et al., 1990; Eschenhagen et al., 1992). Recent studies in mouse models of cardiomyopathy have demonstrated isoform-specific functions of $G\alpha_{i2}$ and $G\alpha_{i3}$ (*refer to* table 1-2). Studies conducted by our group and others suggest that $G\alpha_{i2}$ has cardioprotective effects, whereas $G\alpha_{i3}$ has a negative impact on the progression of cardiac dysfunction.

A limited number of studies have investigated the modulation of cardiac L-type calcium channels by a specific Gαi isoform using global Gαi-knockout mouse models (Nagata et al., 2000; F. Chen et al., 2001; Zuberi et al., 2010; Dizayee et al., 2011). However, these studies were controversial in terms of the magnitude and direction of effects on the calcium current as well as whether the absence of a specific Gαi isoform alters β-adrenergic responsiveness.

Previous studies conducted by our group have reported opposite effects of $G\alpha_{i2}$ and $G\alpha_{i3}$ on $I_{Ca,L}$ at both single-channel and whole-cell levels, where deletion of $G\alpha_{i2}$ reduced channel activity, while deletion of $G\alpha_{i3}$ enhanced it (Foerster et al., 2003; Klein 2009; Dizayee et al., 2011). On the contrary, Zuberi et al., 2010 reported increased $I_{Ca,L}$ density in $G\alpha_{i2}$-knockout mice, while others observed no changes in $I_{Ca,L}$ regardless of the deleted $G\alpha_i$ isoform (Nagata et al., 2000; F. Chen et al., 2001; Jain et al., 2001). This controversy may be due to the use of different experimental conditions and mouse strains.

In the present study, the putative effects of $G\alpha_{i2}$ or $G\alpha_{i3}$ deficiency were studied in β_1-tg mice as a model of progressive dilated cardiomyopathy. Figure 1-8 summarizes our previously obtained *in vivo* data on echocardiography and molecular analysis of the Gαi protein transcriptional levels in β_1-tg mice, with or without the expression of either $G\alpha_{i2}$ (β_1-tg/$G\alpha_{i2}^{-/-}$) or $G\alpha_{i3}$ (β_1-tg/ $G\alpha_{i3}^{-/-}$). It is worth mentioning that $G\alpha_{i2}$/$G\alpha_{i3}$ double-deficient mice are not viable, which supports the hypothesis that the *in vivo* deletion of a single Gαi-isoform can be functionally compensated, at least in part, by the remaining Gαi-isoform (Gohla et al., 2007).

Based on our previous findings of isoform-specific effects of $G\alpha_{i2}$ and $G\alpha_{i3}$ on the modulation of ventricular $I_{Ca,L}$ in knockout models (Dizayee et al., 2011), we hypothesize that the genetic deletion of $G\alpha_{i2}$ or $G\alpha_{i3}$ may differentially modulate the function of LTCC and/or their response to acute β-AR stimulation.

4.2.2 $G\alpha_{i3}$ deficiency restores basal $I_{Ca,L}$ in β_1-tg myocytes, while β-AR responsiveness remains blunted

Recently, we found that $G\alpha_{i3}$ deficiency improved cardiac function, reduced hypertrophy, and enhanced survival of β_1-tg mice (Schröper et al., 2024). Thus, we sought to examine whether β_1-tg and β_1-tg/$G\alpha_{i3}^{-/-}$ mice also differed with respect to ventricular I_{CaL}. $G\alpha_{i3}$ deficiency largely normalized the abnormalities in $I_{Ca,L}$ gating kinetics observed in β_1-tg mice. Specifically, under basal conditions, the lack of $G\alpha_{i3}$ increased the reduced peak $I_{Ca,L}$ density and restored the activation voltage and channel conductance to nearly wild-type levels. This suggests an effect on $I_{Ca,L}$ gating rather than on their expression levels, agreeing with previous findings of unaltered ventricular protein expression of the pore-forming (α_{1C}) of LTCC in $G\alpha_{i3}^{-/-}$ mice (Dizayee et al., 2011). In that study, $G\alpha_{i3}^{-/-}$ also caused an increase in whole-cell $I_{Ca,L}$ density, which was confirmed again in the preliminary experiments of the present study (*Suppl. S9*).

Foerster and colleagues demonstrated that transgenic mice overexpressing β_2-adrenoceptor (β_2-tg mice) also develop a cardiac dysfunction. In this model, additional deletion of $G\alpha_{i2}$ exacerbated the phenotype as well as the reduction in calcium channel activity, possibly due to a compensatory increase in ventricular $G\alpha_{i3}$ expression (Foerster et al., 2003), whereas the opposite effect was observed in β_2-tg mice lacking $G\alpha_{i3}$ (Klein, 2009). These results suggest that $G\alpha_{i3}$ protein may act as a negative regulator of basal LTCC function under certain conditions that can affect its expression and/or regulation. In line with this hypothesis, we observed contractile dysfunction accompanied by a compensatory upregulation of ($G\alpha_{i3}$) in β_1-tg mice lacking $G\alpha_{i2}$ (Keller et al., 2015). Likewise, in a murine model of cardiac ischemia-

reperfusion injury, a genetic deletion of $G\alpha_{i2}$ resulted in a twofold compensatory upregulation of $G\alpha_{i3}$, which was associated with increased severity of the IR injury in $G\alpha_{i2}^{-/-}$ ventricles (Köhler et al., 2014).

Next, we tested whether the loss of a specific Gαi protein isoform would interfere with the β-adrenergic acute stimulation of LTCC. Neither the absence of $G\alpha_{i2}$ ($G\alpha_{i2}^{-/-}$) nor of $G\alpha_{i3}$ ($G\alpha_{i3}^{-/-}$) has been shown to affect the response of I_{CaL} to Iso (Nagata et al., 2000; Jain et al., 2001). In contrast, on the background of cardiac β_1-AR overexpression, we find significant differences depending on whether $G\alpha_{i2}$ or $G\alpha_{i3}$ is absent. The $I_{Ca,L}$ response to isoproterenol stimulation was blunted in β_1-tg/$G\alpha_{\mathbf{i3}}^{-/-}$ myocytes, similar to what was observed in β_1-tg mice. Conversely, the Iso stimulatory effects on $I_{Ca,L}$ were augmented and even exceeded wild-type levels in cardiomyocytes from β_1-tg/$G\alpha_{\mathbf{i2}}^{-/-}$ mice.

Brown and Harding have shown that pertussis toxin (PTX)-induced non-selective inhibition of the Gαi protein can restore the diminished responsiveness of β-adrenoceptor in failing rodent and human myocytes (Brown & Harding, 1992). Although several lines of evidence suggest that $G\alpha_{i2}$ is particularly involved in the desensitization of cardiac β-AR-mediated adenylyl cyclase signaling (Janssen et al., 2002; Rau et al., 2003), experimental evidence for the role of $G\alpha_{i3}$ is still lacking. Here we report for the first time a Gαi isoform-specific regulation of isoproterenol-mediated LTCC activation in murine myocytes. Our results suggest that $G\alpha_{i3}$ may have a redundant role in the β-AR desensitization mechanisms. Although we did not observe any upregulation of the remaining isoform ($G\alpha_{i2}$) in the cardiac tissues from β_1-tg/$G\alpha_{\mathbf{i3}}^{-/-}$ mice (Schröper et al., 2024), we believe that normal levels of $G\alpha_{i2}$ are sufficient to contribute to attenuation of β-AR response. Additionally, a lack of inhibitory regulation of $I_{Ca,L}$ by the cholinergic muscarinic agonist carbachol was observed in ventricles from $G\alpha_{i2}$-deficient mice, but not from $G\alpha_{i3}^{-/-}$ mice (Nagata et al., 2000, F. Chen et al., 2001). Attenuated effects of carbachol on cAMP levels (DeGeorge et al. 2008), heart rate regulation (Zuberi et al. 2008) and ERK1/2 activation (Dizayee et al., 2011) have also been reported in $G\alpha_{i2}$-deficient mice. Thus, it could be hypothesized that the enhanced β-AR response in β_1-tg/$G\alpha_{i2}^{-/-}$ mice may be due, in part, to the lack of muscarinic antagonistic effects on β-AR stimulation.

Taken together, our results suggest that $G\alpha_{i3}$ deficiency confers cardioprotection in β_1-tg mice, probably by restoring the ventricular $I_{Ca,L}$ characteristics, thereby enhancing the cardiac performance, and by attenuating the adverse effects that might result from excessive β-adrenergic stimulation.

4.2.3 $G\alpha_{i2}$ deficiency affects $I_{Ca,L}$ gating properties in β_1-tg myocytes

In a previous study, the absence of $G\alpha_{i2}$ was associated with a premature onset of heart failure in β_1-tg/$G\alpha_{i2}^{-/-}$ mice at an average age of 300 days, whereas, neither $G\alpha_{i2}^{-/-}$ nor β_1-tg mice showed cardiac malfunction in this age. The average lifespan of β_1-tg/$G\alpha_{i2}^{-/-}$ mice was around 363 days, and they were born at an approximate Mendelian ratio (Keller et al., 2015). However, in the current study, we observed frequent deaths among the β_1-tg/$G\alpha_{i2}^{-/-}$ mice before even reaching 300 days of age in most cases. Given that our data revealed changes in ventricular I_{CaL} in β_1-tg mice preceding the contractile dysfunction, we decided to investigate the ventricular I_{CaL} in β_1-tg/$G\alpha_{i2}^{-/-}$ mice at a younger age (4-5 months).

We find a reduction in basal $I_{Ca,L}$ density and a depolarization shift in the half-maximal voltage of activation in β_1-tg/$G\alpha_{i2}^{-/-}$ myocytes, but these changes were indistinguishable from those seen in myocytes from age-matched β_1-tg mice. This suggests that an additional deletion of $G\alpha_{i2}$ may not further affect the changes in the current activation properties, at least at this early stage. Studies using knockout mouse models have produced conflicting results regarding the effects of $G\alpha_{i2}^{-/-}$ on whole-cell $I_{Ca,L}$. For example, in $G\alpha_{i2}^{-/-}$ mice with a (129/Sv) background, $I_{Ca,L}$ density was found to be increased (Zuberi et al., 2010), while in $G\alpha_{i2}^{-/-}$ mice with a (C57BL6) background it was found to be decreased (Dizayee et al., 2011), Of note, we used the latter mouse line (Dizayee et al. 2011) to generate the β_1-tg/$G\alpha_{i2}^{-/-}$ genotype used in this study.

On the other hand, we find a significant reduction in steady-state inactivation of $I_{Ca,L}$ and faster recovery kinetics with increased fraction of current recovery in β_1-tg/$G\alpha_{i2}^{-/-}$ myocytes. In particular, there was a marked depolarization shift in the steady-state voltage dependence of current inactivation compared to that in age-matched β_1-tg and wild-type. Theoretically, this inactivation behavior may result in an increase in channel availability and a prolongation of the current duration. Ryder et al. found a similar shift in the steady-state inactivation curve of $I_{Ca,L}$ along with faster recovery kinetics in hypertrophied guinea pig left ventricular myocytes. They proposed that such changes in channel gating may contribute to the prolongation of action potential duration they observed in the hypertrophied cells (Ryder et al., 1993). We also observed a significant acceleration in the rate of basal $I_{Ca,L}$ decay in β_1-tg/$G\alpha_{i2}^{-/-}$ myocytes compared to wild-type and β_1-tg myocytes. This observation is intriguing since faster $I_{Ca,L}$ decay would typically be expected following β-AR activation due to enhanced calcium dependent inactivation (Findlay, 2004).

However, it is yet unclear why the absence of $G\alpha_{i2}$ caused these channel gating abnormalities. Although $I_{Ca,L}$ density was maintained in β_1-tg/$G\alpha_{i2}^{-/-}$ myocytes, this dysfunctional gating of LTCC may reflect impairments in calcium handling and/or affect the shape of cardiac action potential (*review*, Tomaselli & Marbán, 1999; Bénitah et al., 2002). A promising avenue for future research would be the examination of the CaMKII activity. CaMKII has been implicated in murine HF (Kreusser et al., 2014), and shown to modulate the $I_{Ca,L}$ inactivation and recovery properties in rat (Guo & Duff, 2006) and mice (Blaich et al., 2010).

Moreover, the frequent deaths observed in β_1-tg/$G\alpha_{i2}^{-/-}$ mice prompt us to reflect on possible reasons underlying the severity of the phenotype associated with $G\alpha_{i2}$ deficiency. Considering that all our animals were kept under the same and restricted stress- and pathogen-free conditions, exogenous factors are quite unlikely to contribute. Of note, unexpected sudden death was also reported in $G\alpha_{i2}$ deficient mice (Gohla et al., 2007; Zuberi et al., 2010). Given the rapid deterioration in cardiac function associated with signs of reduced cardiac output and increased ventricular congestion (Keller et al., 2015), these findings imply that premature progression to decompensated heart failure may underlie the mortality of these mice. On the other hand, the $I_{Ca,L}$ gating changes we have described in β_1-tg/$G\alpha_{i2}^{-/-}$ mice may be expected to increase the likelihood of arrhythmia activity in their cardiac tissue.

Previous studies have suggested a role of $G\alpha_{i2}$ deficiency in the development of arrhythmias. In $G\alpha_{i2}^{-/-}$ mice, evidence of unprovoked spontaneous ectopic activity was observed in the ventricles (Zuberi et al., 2010), while proarrhythmic events such as shortened effective refractory period (ERP) were seen in the atria (Nobles et al., 2018). Additionally, a clinical study had identified a focal somatic mutation in $G\alpha_{i2}$ in a patient with idiopathic ventricular tachycardia (Lerman et al., 1998).

Altered distribution and dysfunctional gating of LTCC have been linked to the formation of triggered activity in heart failure (*review*, Johnson & Antoons, 2018). Indeed, the distinct LTCC gating abnormalities identified in β_1-tg/$G\alpha_{i2}^{-/-}$ myocytes may be associated with the development of afterdepolarization activities. Specifically, we observed an increase in calcium window current with an enhanced current recovery. These gating changes have been suggested to underlie the mechanisms by which the $I_{Ca,L}$ current can contribute to the formation of early afterdepolarization (EAD) events (January et al., 1988; Zeng & Rudy, 1995). Patch-clamp modeling studies suggest that $I_{Ca,L}$ may become arrhythmogenic if it regenerates within the voltage range of its window current, thus increasing depolarization and

maintaining the AP plateau phase (Weiss et al., 2010; Madhvani et al., 2011). Under basal conditions, the window current was markedly increased in β_1-tg/$G\alpha_{i2}^{-/-}$ myocytes compared to wild-type, whereas this effect was negligible in β_1-tg or β_1-tg/$G\alpha_{i3}^{-/-}$ myocytes. Although the rate of $I_{Ca,L}$ recovery from inactivation tended to increase when $G\alpha_{i3}$ was not expressed, there was no change in the fraction of current recovery in β_1-tg/$G\alpha_{i3}^{-/-}$ myocytes. Furthermore, in Iso-treated β_1-tg/$G\alpha_{i2}^{-/-}$ myocytes, the $I_{Ca,L}$ decay and steady-state of inactivation were significantly reduced. This suggests that the absence of $G\alpha_{i2}$ may cause intracellular Ca^{2+} overload, leading to a production of complex Ca^{2+} transients that are known to trigger ventricular arrhythmias under intense β-AR stimulation (Yamada & Corr, 1992; Pogwizd et al., 2001; Venetucci et al., 2008). However, to explore and identify any potential arrhythmogenic activity, additional tests such as long-term electrocardiogram (ECG) and optical mapping of electrical activity are necessary.

We conclude that $G\alpha_{i2}$ deficiency (but not $G\alpha_{i3}$) alters the basal $I_{Ca,L}$ gating kinetics and leads to augmented response to acute β-adrenergic stimulation in β_1-tg mice. These alterations may compromise the Ca^{2+} homeostasis and increase the risk of arrhythmias under resting and/or stress conditions.

4.3 Inhibitory G protein as therapeutic targets

G-protein coupled receptors (GPCRs) are the largest receptor family and play a crucial role in regulating various physiological and pathological processes. More than 30% of the FDA-approved therapeutic drugs target GPCRs, highlighting the importance of the GPCR-G signaling pathway (Santos et al., 2017). Despite progress in GPCR drug discovery, G proteins, which are potential downstream targets, have received less attention. Currently, there are no drugs targeting G proteins that have been approved or undergone clinical trials. One of the major challenges in studying G proteins is the lack of modulators that can selectively and efficiently regulate G protein subfamilies and isoforms. Selective inhibitors have only been developed for $G\alpha_{q/11}$, which have shown great potential in several preclinical studies (Li et al., 2020).

In collaboration with the Imhof research group[8], we recently investigated the effects of a new Gα protein modulator, known as GPM-1 on calcium current properties using our whole-cell patch-clamp based assay. GPM-1 is a synthesized linear peptide proposed to possess

[8] Prof. Dr. Diana Imhof, Pharmaceutical Biochemistry and Bioanalytics, Pharmaceutical Institute, University of Bonn

guanine-nucleotide exchange modulator (GEM) activity (Nubbemeyer et al., 2022). The GEM activity was originally described for non-canonical cytosolic G protein modulators such as GIV/Giridin protein and other proteins containing the (GEM) motif. These modulators can bind to α-subunit of Gi/s protein and modulate their activity in different ways (Ghosh et al., 2017). GPM-1 was discovered in the Imhof lab by screening combinatorial peptide libraries. It has been suggested that GPM-1 may have bifunctional GEM activity with opposing actions on Gαi and Gαs. Specifically, GPM-1 was suggested to function as a guanine-nucleotide exchange factor (GEF) toward Gαi (activator) and as a guanine-nucleotide dissociation inhibitor (GDI) toward Gαs (inhibitor) (Nubbemeyer et al., 2022).

In the present study, we find that GPM-1, when used at a concentration of 10 μM, leads to a reduction in basal peak $I_{Ca,L}$ density in ventricular myocytes, but has no effect on isoproterenol modulation of $I_{Ca,L}$. Computational analysis of protein peptide interaction between Gαi/s and GPM-1 showed higher binding to Gαs, indicating a GDI-like action (Nubbemeyer et al., 2022). Due to its proteolytically instability and lack of membrane permeability, GPM-1 was only used in the pipette solution. Recently, new GPM-1 derivatives, namely GPM-1b and GPM-1c peptides, have been developed to improve cell stability and permeability. Both peptides showed improved biological activity compared to GPM1 (Nubbemeyer et al., 2022). Compounds that possess cell-membrane penetrating properties are better for patch-clamp experiments, as they can be added to the bath solution, allowing for more controlled electrophysiological experiments.

These findings are promising and represent a significant advancement in our understanding of the structure of G proteins and the potential interaction sites that could be targeted for the development of new selective modulators. Currently, studies are being conducted on modulators against $G\alpha_{i3}$ (as per personal communication with the Imhof lab). The development of selective modulators for $G\alpha_{i2}$ and $G\alpha_{i3}$ is promising as it will enable the study of their potentially different functions in specific tissues.

4.4 Limitations of the Study

This study was part of a long-term project that initially investigated the *in vivo* effects of $G\alpha_{i2}$ or $G\alpha_{i3}$ deficiency in β_1-tg mice. Specific-isoform functions of $G\alpha_i$ were detected at both the animal and single myocyte level. However, these studies remain extrapolative, and the underlying mechanisms still require further investigations.

One limitation of this study was the lack of comparison between the effects of the two Gαi isoforms in a cohort study, i.e., at the same age. To assess the outcomes of chronic β-AR-mediated heart failure, we had to study mice at advanced ages. $G\alpha_{i2}$- and $G\alpha_{i3}$ deficiency exhibited different age-dependent effects on the development of cardiomyopathy and the onset of failure. $G\alpha_{i2}$ deficiency correlated with frequent deaths that hindered the electrophysiology investigation in aged mice. Our experience showed that isolating cardiomyocytes from failing hearts with severe cardiac remodeling is challenging. Hence, taking these factors into consideration and animal welfare issues, we could not evaluate all genotypes simultaneously.

We used global knockout of a specific Gαi isoform in our mouse models. We acknowledge that systematic effects or upregulation of the other Gαi isoform may influence our findings. However, $G\alpha_{i2}$ and $G\alpha_{i3}$ knockout mouse models showed no changes in basal heart rate compared with respective wild-type (Jain et al., 2001). The β_1-tg mouse model is a well-established model for heart failure. However, it differs from human heart failure in some aspects, e.g., it has β_1-AR overexpression instead of downregulation. Nevertheless, this overexpression can be considered as a mimic of the chronically increased sympathetic stimulation observed in human heart failure (Engelhardt et al., 1999, Bisognano et al., 2000).

4.5 Future directions and Conclusions

Calcium-dependent $I_{Ca,L}$ inactivation is governed by LTCC gating kinetics and the SR-Ca^{2+} within the junctional regions of the T-tubules, owing to changes in local subsarcolemmal $[Ca^{2+}]_i$ during the CICR process (Bers, 2002). It would be interesting to evaluate the effect of intracellular $[Ca^{2+}]_i$ and examine the CICR contribution to the altered $I_{Ca,L}$ inactivation kinetics, especially in the case of $G\alpha_{i2}$ deficiency. This can be done by conducting whole-cell measurements with ryanodine, an inhibitor of SR-Ca^{2+} release. Another option would be to employ BAPTA as a Ca^{2+} chelator instead of EGTA in the pipette solution. BAPTA binds Ca^{2+} much faster than EGTA, and this compound is commonly used when strict control of

intracellular Ca^{2+} is required (Jackson, 1997). Additionally, we can use fluorescence microscopy and calcium imaging to measure the level of intracellular calcium.

Given the distinct effect of $G\alpha_{i2}$ and $G\alpha_{i3}$ on $I_{Ca,L}$ response to β-AR stimulation, it would be interesting to analyze the *in vivo* cardiac function of these mouse models with enhanced β-AR activity e.g., administration of β-AR agonists. Additional molecular analyses are needed to understand the mechanisms underlying the distinct effects of Gi isoforms. For example, it would be advantageous to evaluate cAMP levels and investigate the expression and phosphorylation of PKA targets that are involved in cardiac excitation-contraction coupling. Furthermore, it is useful to examine the distribution of Gαi compartmentalization by subcellular fractionation, which can be accomplished by western immunoblotting for the Gαi isoform. Investigating the role of muscarinic signaling, and the expression and activity of other G proteins or subunits, such as Gαq, which activate Ca^{2+} release from the sarcoplasmic reticulum, and the Gβγ subunit, which is involved in the activation of survival signaling pathways, would be of interest.

Conclusions

Cardiac-specific overexpression of the human β_1-AR in mice leads to functional changes in the LTCC that precede contractile dysfunction, and to blunted stimulatory effects of the β-AR agonist isoproterenol. In this mouse model of heart failure, the effects on LTCC regulation are differentially modulated by the absence of $G\alpha_{i2}$ or $G\alpha_{i3}$. Our findings suggest that $G\alpha_{i3}$ deficiency has protective effects by restoring channel function and protecting against intense β-AR activity. In contrast, $G\alpha_{i2}$ deficiency is detrimental as it alters channel gating and causes an augmented β-adrenergic response, which may raise the probability of $I_{Ca,L}$-associated arrhythmogenic effects. Developing selective Gαi-protein modulators can offer valuable tools to study cellular signaling of specific G proteins, paving the way to discover new strategies for cardio-protective therapies.

Bibliography

2021 ESC Guidelines for the diagnosis and treatment of acute and chronic heart failure. (n.d.). https://doi.org/10.1093/eurheartj/ehab368

Ahmet, I., Lakatta, E. G., & Talan, M. I. (2005). Pharmacological Stimulation of ß 2-adrenergic Receptors (ß 2 AR) Enhances Therapeutic Effectiveness of ß 1 AR Blockade in Rodent Dilated Ischemic Cardiomyopathy. In *Heart Failure Reviews* (Vol. 10). Springer Science + Business Media.

Asano, T., Morishita, R., Semba, R., Itoh, H., Kaziro, Y., & Kato, K. (1989). Identification of lung major GTP-binding protein as Gi2 and its distribution in various rat tissues determined by immunoassay. *Biochemistry*, *28*(11), 4749–4754. https://doi.org/10.1021/bi00437a035

Beckendorf, J., van den Hoogenhof, M. M. G., & Backs, J. (2018). Physiological and unappreciated roles of CaMKII in the heart. In *Basic Research in Cardiology* (Vol. 113, Issue 4). Dr. Dietrich Steinkopff Verlag GmbH and Co. KG. https://doi.org/10.1007/s00395-018-0688-8

Beer-Hammer, S., Lee, S. C., Mauriac, S. A., Leiss, V., Groh, I. A. M., Novakovic, A., Piekorz, R. P., Bucher, K., Chen, C., Ni, K., Singer, W., Harasztosi, C., Schimmang, T., Zimmermann, U., Pfeffer, K., Birnbaumer, L., Forge, A., Montcouquiol, M., Knipper, M., … Rüttiger, L. (2018). Gα i Proteins are Indispensable for Hearing. *Cellular Physiology and Biochemistry*, *47*(4), 1509–1532. https://doi.org/10.1159/000490867

Beetz, N., Hein, L., Meszaros, J., Gilsbach, R., Barreto, F., Meissner, M., Hoppe, U. C., Schwartz, A., Herzig, S., & Matthes, J. (2009). Transgenic simulation of human heart failure-like L-type Ca 2+-channels: Implications for fibrosis and heart rate in mice. *Cardiovascular Research*, *84*(3), 396–406. https://doi.org/10.1093/cvr/cvp251

Bénitah, J. P., Gómez, A. M., Fauconnier, J., Kerfant, B. G., Perrier, E., Vassort, G., & Richard, S. (2002). Voltage-gated Ca2+ currents in the human pathophysiologic heart: a review. *Basic Research in Cardiology*, *97*(1), I11–I18. https://doi.org/10.1007/s003950200023

Bénitah, J.-P., Kerfant, B. G., Vassort, G., Richard, S., & Gómez, A. M. (2002). Altered communication between L-type calcium channels and ryanodine receptors in heart failure. *FBL*, *7*(5), 263–275.

Bers, D. M. (2002). Cardiac excitation–contraction coupling. *Nature*, *415*(6868), 198–205. https://doi.org/10.1038/415198a

Bers, D. M., & Perez-Reyes, E. (1999). Ca channels in cardiac myocytes: structure and function in Ca influx and intracellular Ca release. *Cardiovascular Research*, *42*(2), 339–360. https://doi.org/10.1016/S0008-6363(99)00038-3

Bisognano, J. D., Weinberger, H. D., Bohlmeyer, T. J., Pende, A., Raynolds, M. V., Sastravaha, A., Roden, R., Asano, K., Blaxall, B. C., Wu, S. C., Communal, C., Singh, K., Colucci, W., Bristow, M. R., & Port, D. J. (2000). Myocardial-directed overexpression of the human β1-adrenergic receptor in transgenic mice. *Journal of Molecular and Cellular Cardiology*, *32*(5), 817–830. https://doi.org/10.1006/jmcc.2000.1123

Blaich, A., Pahlavan, S., Tian, Q., Oberhofer, M., Poomvanicha, M., Lenhardt, P., Domes, K., Wegener, J. W., Moosmang, S., Ruppenthal, S., Scholz, A., Lipp, P., & Hofmann, F. (2012). Mutation of the Calmodulin Binding Motif IQ of the L-type Cav1.2 Ca2+ Channel to EQ Induces Dilated Cardiomyopathy and Death*. *Journal of Biological Chemistry*, *287*(27), 22616–22625. https://doi.org/https://doi.org/10.1074/jbc.M112.357921

BIBLIOGRAPHY

Blaich, A., Welling, A., Fischer, S., Wegener, J. W., Köstner, K., Hofmann, F., & Moosmang, S. (2010). Facilitation of murine cardiac L-type Cav1.2 channel is modulated by Calmodulin kinase II–dependent phosphorylation of S1512 and S1570. *Proceedings of the National Academy of Sciences*, *107*(22), 10285–10289. https://doi.org/10.1073/pnas.0914287107

Böhm, M. (1995). Alterations of β-adrenoceptor-G-protein-regulated adenylyl cyclase in heart failure. In *Molecular and Cellular Biochemistry* (Vol. 147). Kluwer Academic Publishers.

Böhm, M., Flesch, M., & Schnabel, P. (1997). β-Adrenergic signal transduction in the failing and hypertrophied myocardium. *Journal of Molecular Medicine*, *75*(11), 842–848. https://doi.org/10.1007/s001090050175

Böhm, M., Gierschik, P., Jakobs, K. H., Pieske, B., Schnabel, P., Ungerer, M., & Erdmann, E. (1990). Increase of Gi alpha in human hearts with dilated but not ischemic cardiomyopathy. *Circulation*, *82*(4), 1249–1265. https://doi.org/10.1161/01.CIR.82.4.1249

Böhm, M., Gierschik, P., Knorr, A., Larisch, K., Weismann, K., & Erdmann, E. (1992). Desensitization of adenylate cyclase and increase of Gi alpha in cardiac hypertrophy due to acquired hypertension. *Hypertension*, *20*(1), 103–112. https://doi.org/10.1161/01.HYP.20.1.103

Böhm, M., & Maack, C. (2000). Treatment of heart failure with beta-blockers. Mechanisms and results. *Basic Research in Cardiology*, *95*(1), I15–I24. https://doi.org/10.1007/s003950070004

Böhm, M., Moll, M., Schmid, B., Paul, M., Ganten, D., Castellano, M., & Erdmann, E. (1994). Beta-adrenergic neuroeffector mechanisms in cardiac hypertrophy of renin transgenic rats. *Hypertension*, *24*(6), 653–662. https://doi.org/10.1161/01.HYP.24.6.653

Bouron, A., Potreau, D., & Raymond, G. (1992). The L type calcium current in single hypertrophied cardiomyocytes isolated from the right ventricle of ferret heart. *Cardiovascular Research*, *26*(7), 662–670. https://doi.org/10.1093/cvr/26.7.662

Bozkurt, B., Coats, A. J., Tsutsui, H., Abdelhamid, M., Adamopoulos, S., Albert, N., Anker, S. D., Atherton, J., Böhm, M., Butler, J., Drazner, M. H., Felker, G. M., Filippatos, G., Fonarow, G. C., Fiuzat, M., Gomez-Mesa, J. E., Heidenreich, P., Imamura, T., Januzzi, J., … Zieroth, S. (2021). Universal Definition and Classification of Heart Failure: A Report of the Heart Failure Society of America, Heart Failure Association of the European Society of Cardiology, Japanese Heart Failure Society and Writing Committee of the Universal Definition of Heart Failure. *Journal of Cardiac Failure*, *27*(4), 387–413. https://doi.org/10.1016/j.cardfail.2021.01.022

Brackenbury, W. J. (2021). “Patch Clamp Electrophysiology Methods and Protocols,” Editors Mark Dallas and Damian Bell. *Bioelectricity*, *3*(2), 154–155. https://doi.org/10.1089/bioe.2021.0015

Bristow, M. R. (2011). Treatment of Chronic Heart Failure With β-Adrenergic Receptor Antagonists. *Circulation Research*, *109*(10), 1176–1194. https://doi.org/10.1161/CIRCRESAHA.111.245092

Bristow, M. R., Ginsburg, R., Umans, V., Fowler, M., Minobe, W., Rasmussen, R., Zera, P., Menlove, R., Shah, P., & Jamieson, S. (1986). Beta 1- and beta 2-adrenergic-receptor subpopulations in nonfailing and failing human ventricular myocardium: coupling of both receptor subtypes to muscle contraction and selective beta 1-receptor down-regulation in heart failure. *Circulation Research*, *59*(3), 297–309. https://doi.org/10.1161/01.RES.59.3.297

Brodde, O. E. (1991). Beta 1- and beta 2-adrenoceptors in the human heart: properties, function, and alterations in chronic heart failure. *Pharmacological Reviews*, *43*(2), 203. http://pharmrev.aspetjournals.org/content/43/2/203.abstract

Brodde, O.-E. (1988). The functional importance of beta1 and beta2 adrenoceptors in the human heart. *The American Journal of Cardiology*, *62*(5), 24C-29C. https://doi.org/https://doi.org/10.1016/S0002-9149(88)80063-8

Brown, L. A., & Harding, S. E. (1992). The effect of pertussis toxin on β-adrenoceptor responses in isolated cardiac myocytes from noradrenaline-treated guinea-pigs and patients with cardiac failure. *British Journal of Pharmacology*, *106*(1), 115–122. https://doi.org/10.1111/j.1476-5381.1992.tb14302.x

BIBLIOGRAPHY

Burashnikov, E., Pfeiffer, R., Barajas-Martinez, H., Delpón, E., Hu, D., Desai, M., Borggrefe, M., Hissaguerre, M., Kanter, R., Pollevick, G. D., Guerchicoff, A., Laio, R., Marieb, M., Nademanee, K., Nam, G. B., Robles, R., Schimpf, R., Stapleton, D. D., Viskin, S., … Antzelevitch, C. (2010). Mutations in the cardiac L-type calcium channel associated with inherited J-wave syndromes and sudden cardiac death. *Heart Rhythm*, *7*(12), 1872–1882. https://doi.org/10.1016/j.hrthm.2010.08.026

Catterall, W. A. (1991). Excitation-contraction coupling in vertebrate skeletal muscle: A tale of two calcium channels. *Cell*, *64*(5), 871–874. https://doi.org/https://doi.org/10.1016/0092-8674(91)90309-M

Catterall, W. A. (2000). Structure and Regulation of Voltage-Gated Ca2+ Channels. *Annual Review of Cell and Developmental Biology*, *16*(1), 521–555. https://doi.org/10.1146/annurev.cellbio.16.1.521

Catterall, W. A. (2011). Voltage-gated calcium channels. *Cold Spring Harbor Perspectives in Biology*, *3*(8), 1–23. https://doi.org/10.1101/cshperspect.a003947

Chen, F., Spicher, K., Jiang, M., Birnbaumer, L., & Wetzel, G. T. (2001). Lack of muscarinic regulation of Ca2+ channels in Gi2α gene knockout mouse hearts. *American Journal of Physiology-Heart and Circulatory Physiology*, *280*(5), H1989–H1995. https://doi.org/10.1152/ajpheart.2001.280.5.H1989

Chen, X., Piacentino, V., Furukawa, S., Goldman, B., Margulies, K. B., & Houser, S. R. (2002). L-type Ca2+ channel density and regulation are altered in failing human ventricular myocytes and recover after support with mechanical assist devices. *Circulation Research*, *91*(6), 517–524. https://doi.org/10.1161/01.RES.0000033988.13062.7C

Chen, X., Zhang, X., Harris, D. M., Piacentino, V., Berretta, R. M., Margulies, K. B., & Houser, S. R. (2008). Reduced effects of BAY K 8644 on L-type Ca2+ current in failing human cardiac myocytes are related to abnormal adrenergic regulation. *American Journal of Physiology-Heart and Circulatory Physiology*, *294*(5), H2257–H2267. https://doi.org/10.1152/ajpheart.01335.2007

Cheng, H.-J., Zhang, Z.-S., Onishi, K., Ukai, T., Sane, D. C., & Cheng, C.-P. (2001). Upregulation of Functional β3-Adrenergic Receptor in the Failing Canine Myocardium. *Circulation Research*, *89*(7), 599–606. https://doi.org/10.1161/hh1901.098042

Chesley, A., Lundberg, M. S., Asai, T., Xiao, R.-P., Ohtani, S., Lakatta, E. G., & Crow, M. T. (2000). The β2-Adrenergic Receptor Delivers an Antiapoptotic Signal to Cardiac Myocytes Through Gi-Dependent Coupling to Phosphatidylinositol 3′-Kinase. *Circulation Research*, *87*(12), 1172–1179. https://doi.org/10.1161/01.RES.87.12.1172

Colombe, A.-S., & Pidoux, G. (2021). Cardiac cAMP-PKA Signaling Compartmentalization in Myocardial Infarction. *Cells*, *10*(4). https://doi.org/10.3390/cells10040922

Communal, C., Singh, K., Sawyer, D. B., & Colucci, W. S. (1999). Opposing Effects of β1- and β2-Adrenergic Receptors on Cardiac Myocyte Apoptosis. *Circulation*, *100*(22), 2210–2212. https://doi.org/10.1161/01.CIR.100.22.2210

de Brito Santos, P. E., BARCELLOS, L. C., MILL, J. G., & MASUDA, M. O. Y. A. (1995). Ventricular Action Potential and L-Type Calcium Channel in Infarct-Induced Hypertrophy in Rats. *Journal of Cardiovascular Electrophysiology*, *6*(11), 1004–1014. https://doi.org/https://doi.org/10.1111/j.1540-8167.1995.tb00377.x

de Lucia, C., Eguchi, A., & Koch, W. J. (2018). New insights in cardiac β-Adrenergic signaling during heart failure and aging. In *Frontiers in Pharmacology* (Vol. 9, Issue AUG). Frontiers Media S.A. https://doi.org/10.3389/fphar.2018.00904

DeGeorge, B. R., Gao, E., Boucher, M., Vinge, L. E., Martini, J. S., Raake, P. W., Chuprun, J. K., Harris, D. M., Kim, G. W., Soltys, S., Eckhart, A. D., & Koch, W. J. (2008). Targeted inhibition of cardiomyocyte Gi signaling enhances susceptibility to apoptotic cell death in response to ischemic stress. *Circulation*, *117*(11), 1378–1387. https://doi.org/10.1161/CIRCULATIONAHA.107.752618

del Villar, S. G., Voelker, T. L., Westhoff, M., Reddy, G. R., Spooner, H. C., Navedo, M. F., Dickson, E. J., & Dixon, R. E. (2021). β-Adrenergic control of sarcolemmal CaV1.2 abundance by small GTPase Rab

proteins. *Proceedings of the National Academy of Sciences*, *118*(7), e2017937118. https://doi.org/10.1073/pnas.2017937118

Dizayee, S., Kaestner, S., Kuck, F., Hein, P., Klein, C., Piekorz, R. P., Meszaros, J., Matthes, J., Nürnberg, B., & Herzig, S. (2011). Gα i2- and Gα i3-specific regulation of voltage-dependent L-type calcium channels in cardiomyocytes. *PLoS ONE*, *6*(9). https://doi.org/10.1371/journal.pone.0024979

Dolphin, A. C. (2003). β Subunits of Voltage-Gated Calcium Channels. *Journal of Bioenergetics and Biomembranes*, *35*(6), 599–620. https://doi.org/10.1023/B:JOBB.0000008026.37790.5a

Dolphin, A. C. (2012). Calcium channel auxiliary α2δ and β subunits: trafficking and one step beyond. *Nature Reviews Neuroscience*, *13*(8), 542–555. https://doi.org/10.1038/nrn3311

Dolphin, A. C. (2018). Voltage-gated calcium channel ?2? subunits: an assessment of proposed novel roles [version 1; peer review: 2 approved] . *F1000Research*, *7*(1830). https://doi.org/10.12688/f1000research.16104.1

El-Armouche, A., & Eschenhagen, T. (2009). β-Adrenergic stimulation and myocardial function in the failing heart. *Heart Failure Reviews*, *14*(4), 225–241. https://doi.org/10.1007/s10741-008-9132-8

El-Armouche, A., Zolk, O., Rau, T., & Eschenhagen, T. (2003). Inhibitory G-proteins and their role in desensitization of the adenylyl cyclase pathway in heart failure. *Cardiovascular Research*, *60*(3), 478–487. https://doi.org/10.1016/j.cardiores.2003.09.014

Engelhardt, S., Bohm, M., Erdmann, E., & Lohse, M. J. (1996). Analysis of Beta-Adrenergic Receptor mRNA Levels in Human Ventricular Biopsy Specimens by Quantitative Polymerase Chain Reactions: Progressive Reduction of Betal-Adrenergic Receptor mRNA in Heart Failure. In *J Am Coil Cardiol* (Vol. 27, Issue 1).

Engelhardt, S., Boknik, P., Keller, U., Neumann, J., Lohse, M. J., & Hein, L. (2001). Early impairment of calcium handling and altered expression of junctin in hearts of mice overexpressing the beta1-adrenergic receptor. *The FASEB Journal : Official Publication of the Federation of American Societies for Experimental Biology*, *15*(14), 2718–2720. https://doi.org/10.1096/fj.01-0107fje

Engelhardt, S., Hein, L., Dyachenkow, V., Kranias, E. G., Isenberg, G., & Lohse, M. J. (2004). Altered Calcium Handling Is Critically Involved in the Cardiotoxic Effects of Chronic β-Adrenergic Stimulation. *Circulation*, *109*(9), 1154–1160. https://doi.org/10.1161/01.CIR.0000117254.68497.39

Engelhardt, S., Hein, L., Wiesmann, F., & Lohse, M. J. (1999). Progressive hypertrophy and heart failure in β1-adrenergic receptor transgenic mice. *Proceedings of the National Academy of Sciences*, *96*(12), 7059–7064. https://doi.org/10.1073/pnas.96.12.7059

Ertel, E. A., Campbell, K. P., Harpold, M. M., Hofmann, F., Mori, Y., Perez-Reyes, E., Schwartz, A., Snutch, T. P., Tanabe, T., Birnbaumer, L., Tsien, R. W., & Catterall, W. A. (2000). Nomenclature of Voltage-Gated Calcium Channels. *Neuron*, *25*(3), 533–535. https://doi.org/https://doi.org/10.1016/S0896-6273(00)81057-0

Eschenhagen, T., Mende, U., Nose, M., Schmitz, W., Scholz, H., Haverich, A., Hirt, S., Döring, V., Kalmár, P., & Höppner, W. (1992). Increased messenger RNA level of the inhibitory G protein alpha subunit Gi alpha-2 in human end-stage heart failure. *Circulation Research*, *70*(4), 688–696. https://doi.org/10.1161/01.RES.70.4.688

Feldman, A. M., Cates, A. E., Veazey, W. B., Hershberger, R. E., Bristow, M. R., Baughman, K. L., Baumgartner, W. A., & Van Dop, C. (1988). Increase of the 40,000-mol wt pertussis toxin substrate (G protein) in the failing human heart. *The Journal of Clinical Investigation*, *82*(1), 189–197. https://doi.org/10.1172/JCI113569

Feldman, M. D., Copelas, L., Gwathmey, J. K., Phillips, P., Warren, S. E., Schoen, F. J., Grossman, W., & Morgan, J. P. (1987). Deficient production of cyclic AMP: pharmacologic evidence of an important cause of contractile dysfunction in patients with end-stage heart failure. *Circulation*, *75*(2), 331–339. https://doi.org/10.1161/01.CIR.75.2.331

BIBLIOGRAPHY

Feng, N., & Anderson, M. E. (2017). CaMKII is a nodal signal for multiple programmed cell death pathways in heart. *Journal of Molecular and Cellular Cardiology*, *103*, 102–109. https://doi.org/https://doi.org/10.1016/j.yjmcc.2016.12.007

Findlay, I. (2002). Voltage- and cation-dependent inactivation of L-type Ca2+ channel currents in guinea-pig ventricular myocytes. *Journal of Physiology*, *541*(3), 731–740. https://doi.org/10.1113/jphysiol.2002.019729

Findlay, I. (2004). Physiological modulation of inactivation in L-type Ca2+ channels: One switch. In *Journal of Physiology* (Vol. 554, Issue 2, pp. 275–283). https://doi.org/10.1113/jphysiol.2003.047902

Foerster, K., Groner, F., Matthes, J., Koch, W. J., Birnbaumer, L., & Herzig, S. (2003). Cardioprotection specific for the G protein Gi2 in chronic adrenergic signaling through β2-adrenoceptors. *Proceedings of the National Academy of Sciences*, *100*(24), 14475–14480. https://doi.org/10.1073/pnas.1936026100

Foerster, K., Kaeferstein, T., Groner, F., Engelhardt, S., Matthes, J., Koch, W. J., Lohse, M. J., & Herzig, S. (2004). Calcium channel function and regulation in β1- and β2-adrenoceptor transgenic mice. *Naunyn-Schmiedeberg's Archives of Pharmacology*, *369*(5), 490–495. https://doi.org/10.1007/s00210-004-0928-3

Foster, K. A., McDermott, P. J., & Robishaw, J. D. (1990). Expression of G proteins in rat cardiac myocytes: effect of KCl depolarization. *American Journal of Physiology-Heart and Circulatory Physiology*, *259*(2), H432–H441. https://doi.org/10.1152/ajpheart.1990.259.2.H432

Fu, Y., Westenbroek, R. E., Scheuer, T., & Catterall, W. A. (2013). Phosphorylation sites required for regulation of cardiac calcium channels in the fight-or-flight response. *PNAS*, *110*(48), 19621–19626. https://doi.org/10.1073/pnas.1319421110

Fu, Y., Westenbroek, R. E., Yu, F. H., Clark, J. P., Marshall, M. R., Scheuer, T., & Catterall, W. A. (2011). Deletion of the distal C terminus of Cav1.2 channels leads to loss of β-adrenergic regulation and heart failure in Vivo. *Journal of Biological Chemistry*, *286*(14), 12617–12626. https://doi.org/10.1074/jbc.M110.175307

Gauthier, C., Leblais, V., Kobzik, L., Trochu, J. N., Khandoudi, N., Bril, A., Balligand, J. L., & Le Marec, H. (1998). The negative inotropic effect of beta3-adrenoceptor stimulation is mediated by activation of a nitric oxide synthase pathway in human ventricle. *The Journal of Clinical Investigation*, *102*(7), 1377–1384. https://doi.org/10.1172/JCI2191

Ghosh, P., Rangamani, P., & Kufareva, I. (2017). The GAPs, GEFs, GDIs and…now, GEMs: New kids on the heterotrimeric G protein signaling block. *Cell Cycle*, *16*(7), 607–612. https://doi.org/10.1080/15384101.2017.1282584

Giessler, C., Dhein, S., Pönicke, K., & Brodde, O.-E. (1999). Muscarinic receptors in the failing human heart. *European Journal of Pharmacology*, *375*(1), 197–202. https://doi.org/https://doi.org/10.1016/S0014-2999(99)00261-7

Gilman, A. G. (1987). G PROTEINS: TRANSDUCERS OF RECEPTOR-GENERATED SIGNALS. *Annual Review of Biochemistry*, *56*(1), 615–649. https://doi.org/10.1146/annurev.bi.56.070187.003151

Gohla, A., Klement, K., Piekorz, R. P., Pexa, K., vom Dahl, S., Spicher, K., Dreval, V., Häussinger, D., Birnbaumer, L., & Nürnberg, B. (2007). An obligatory requirement for the heterotrimeric G protein Gi3 in the antiautophagic action of insulin in the liver. *Proceedings of the National Academy of Sciences*, *104*(8), 3003–3008. https://doi.org/10.1073/pnas.0611434104

Goldsmith, Z. G., & Dhanasekaran, D. N. (2007). G Protein regulation of MAPK networks. *Oncogene*, *26*(22), 3122–3142. https://doi.org/10.1038/sj.onc.1210407

Goonasekera, S. A., Hammer, K., Auger-Messier, M., Bodi, I., Chen, X., Zhang, H., Reiken, S., Elrod, J. W., Correll, R. N., York, A. J., Sargent, M. A., Hofmann, F., Moosmang, S., Marks, A. R., Houser, S. R., Bers, D. M., & Molkentin, J. D. (2012). Decreased cardiac L-type Ca 2+channel activity induces hypertrophy and heart failure in mice. *Journal of Clinical Investigation*, *122*(1), 280–290. https://doi.org/10.1172/JCI58227

BIBLIOGRAPHY

Grant, A. O. (2009). Cardiac Ion Channels. *Circulation: Arrhythmia and Electrophysiology*, *2*(2), 185–194. https://doi.org/10.1161/CIRCEP.108.789081

Guo, J., & Duff, H. J. (2006). Calmodulin kinase II accelerates L-type Ca2+ current recovery from inactivation and compensates for the direct inhibitory effect of [Ca2+]i in rat ventricular myocytes. *The Journal of Physiology*, *574*(2), 509–518. https://doi.org/https://doi.org/10.1113/jphysiol.2006.109199

Hamill, O. P., Marty, A., Neher, E., Sakmann, B., & Sigworth, F. J. (1981). Improved patch-clamp techniques for high-resolution current recording from cells and cell-free membrane patches. *Pflügers Archiv*, *391*(2), 85–100. https://doi.org/10.1007/BF00656997

Hegyi, B., Morotti, S., Liu, C., Ginsburg, K. S., Bossuyt, J., Belardinelli, L., Izu, L. T., Chen-Izu, Y., Bányász, T., Grandi, E., & Bers, D. M. (2019). Enhanced Depolarization Drive in Failing Rabbit Ventricular Myocytes. *Circulation: Arrhythmia and Electrophysiology*, *12*(3), e007061. https://doi.org/10.1161/CIRCEP.118.007061

Hepler, J. R., & Gilman, A. G. (1992). G proteins. *Trends in Biochemical Sciences*, *17*(10), 383–387. https://doi.org/https://doi.org/10.1016/0968-0004(92)90005-T

Heubach, J. F., Graf, E. M., Molenaar, P., Jäger, A., Schröder, F., Herzig, S., Harding, S. E., & Ravens, U. (2001). Murine ventricular L-type Ca2+ current is enhanced by zinterol viaβ1-adrenoceptors, and is reduced in TG4 mice overexpressing the human β2-adrenoceptor. *British Journal of Pharmacology*, *133*(1), 73–82. https://doi.org/https://doi.org/10.1038/sj.bjp.0704045

Hofmann, F., Biel, M., & Flockerzi, V. (1994). Molecular Basis for CA2+ Channel Diversity. *Annual Review of Neuroscience*, *17*(1), 399–418. https://doi.org/10.1146/annurev.ne.17.030194.002151

Hoppe, U. C., Brandt, M. C., Michels, G., & Lindner, M. (2005). L-Type Calcium Channel Recording. In S. Dhein, F. W. Mohr, & M. Delmar (Eds.), *Practical Methods in Cardiovascular Research* (pp. 324–354). Springer Berlin Heidelberg. https://doi.org/10.1007/3-540-26574-0_17

Hullin, R., Matthes, J., von Vietinghoff, S., Bodi, I., Rubio, M., D'Souza, K., Khan, I. F., Rottländer, D., Hoppe, U. C., Mohacsi, P., Schmitteckert, E., Gilsbach, R., Bünemann, M., Hein, L., Schwartz, A., & Herzig, S. (2007). Increased expression of the auxiliary β2-subunit of ventricular L-type Ca2+ channels leads to single-channel activity characteristic of the heart failure. *PLoS ONE*, *2*(3). https://doi.org/10.1371/journal.pone.0000292

Hussain, R. I., Aronsen, J. M., Afzal, F., Sjaastad, I., Osnes, J. B., Skomedal, T., Levy, F. O., & Krobert, K. A. (2013). The functional activity of inhibitory G protein (Gi) is not increased in failing heart ventricle. *Journal of Molecular and Cellular Cardiology*, *56*(1), 129–138. https://doi.org/10.1016/j.yjmcc.2012.11.015

Jackson, M. B. (1997). Whole-Cell Voltage Clamp Recording. *Current Protocols in Neuroscience*, *00*(1), 6.6.1-6.6.30. https://doi.org/https://doi.org/10.1002/0471142301.ns0606s00

Jain, M., Lim, C. C., Nagata, K., Davis, V. M., Milstone, D. S., Liao, R., & Mortensen, R. M. (2001). Targeted inactivation of Gαi does not alter cardiac function or β-adrenergic sensitivity. *American Journal of Physiology-Heart and Circulatory Physiology*, *280*(2), H569–H575. https://doi.org/10.1152/ajpheart.2001.280.2.H569

Janssen, P. M. L., Schillinger, W., Donahue, J. K., Zeitz, O., Emami, S., Lehnart, S. E., Weil, J., Eschenhagen, T., Hasenfuss, G., & Prestle, J. (2002). Intracellular β-blockade: overexpression of Gαi2 depresses the β-adrenergic response in intact myocardium. *Cardiovascular Research*, *55*(2), 300–308. https://doi.org/10.1016/S0008-6363(02)00406-6

January, C. T., Riddle, J. M., & Salata, J. J. (1988). A model for early afterdepolarizations: induction with the Ca2+ channel agonist Bay K 8644. *Circulation Research*, *62*(3), 563–571. https://doi.org/10.1161/01.RES.62.3.563

Johnson, D. M., & Antoons, G. (2018). Arrhythmogenic Mechanisms in Heart Failure: Linking β-Adrenergic Stimulation, Stretch, and Calcium. *Frontiers in Physiology*, *9*. https://www.frontiersin.org/articles/10.3389/fphys.2018.01453

Jones, D. T., & Reed, R. R. (1987). Molecular cloning of five GTP-binding protein cDNA species from rat olfactory neuroepithelium. *Journal of Biological Chemistry*, *262*(29), 14241–14249. https://doi.org/https://doi.org/10.1016/S0021-9258(18)47929-X

Kamp, T. J., & Hell, J. W. (2000). Regulation of Cardiac L-Type Calcium Channels by Protein Kinase A and Protein Kinase C. *Circulation Research*, *87*(12), 1095–1102. https://doi.org/10.1161/01.RES.87.12.1095

Katada, T. (2012). The Inhibitory G Protein G i Identified as Pertussis Toxin-Catalyzed ADP-Ribosylation. In *Biol. Pharm. Bull* (Vol. 35, Issue 12).

Katnahji, N., & Matthes, J. (2023). Differential modulation of ventricular Ca2+ currents by absence of Gαi2 or Gαi3 in a murine β1-transgenic heart failure model. *Naunyn-Schmiedeberg's Archives of Pharmacology*, *396*(1), S29–S29. https://doi.org/10.1007/s00210-023-02397-6

Keller, K., Maass, M., Dizayee, S., Leiss, V., Annala, S., Köth, J., Seemann, W. K., Müller-Ehmsen, J., Mohr, K., Nürnberg, B., Engelhardt, S., Herzig, S., Birnbaumer, L., & Matthes, J. (2015). Lack of Gαi2 leads to dilative cardiomyopathy and increased mortality in β1-adrenoceptor overexpressing mice. *Cardiovascular Research*, *108*(3), 348–356. https://doi.org/10.1093/cvr/cvv235

Kilts, J. D., Gerhardt, M. A., Richardson, M. D., Sreeram, G., Mackensen, G. B., Grocott, H. P., White, W. D., Davis, R. D., Newman, M. F., Reves, J. G., Schwinn, D. A., & Kwatra, M. M. (2000). β2-Adrenergic and Several Other G Protein–Coupled Receptors in Human Atrial Membranes Activate Both Gs and Gi. *Circulation Research*, *87*(8), 705–709. https://doi.org/10.1161/01.RES.87.8.705

Kim, H.-N., & Januzzi, J. L. (2011). Natriuretic Peptide Testing in Heart Failure. *Circulation*, *123*(18), 2015–2019. https://doi.org/10.1161/CIRCULATIONAHA.110.979500

KIVISTÖ, T., MÄKIRANTA, M., OIKARINEN, E.-L., KARHU, S., WECKSTRÖM, M., & SELLIN, L. C. (1995). 2,3-Butanedione Monoxime (BDM) Increases Initial Yields and Improves Long-Term Survival of Isolated Cardiac Myocytes. *The Japanese Journal of Physiology*, *45*(1), 203–210. https://doi.org/10.2170/jjphysiol.45.203

Klein, C. (2009). *Die Bedeutung des G-proteins Gαi3 für das Schaltverhalten kardialer L-Typ-Calciumkanäle in Kardiomyozyten sowie für die Entwicklung von kardialer Hypertrophie und Insuffizienz von Mäusen bei Überexpression des β2-Adrenorezeptors* [Dissertation]. University of Cologne.

Klein, G., Drexler, H., & Schröder, F. (2000). Protein kinase G reverses all isoproterenol induced changes of cardiac single L-type calcium channel gating. *Cardiovascular Research*, *48*(3), 367–374. https://doi.org/10.1016/S0008-6363(00)00194-2

Köhler, D., Devanathan, V., De Franz, C. B. O., Eldh, T., Novakovic, A., Roth, J. M., Granja, T., Birnbaumer, L., Rosenberger, P., Beer-Hammer, S., & Nürnberg, B. (2014). Gαi2 - and Gαi3-deficient mice display opposite severity of myocardial ischemia reperfusion injury. *PLoS ONE*, *9*(5). https://doi.org/10.1371/journal.pone.0098325

Kohout, T. A., Takaoka, H., McDonald, P. H., Perry, S. J., Mao, L., Lefkowitz, R. J., & Rockman, H. A. (2001). Augmentation of Cardiac Contractility Mediated by the Human β3-Adrenergic Receptor Overexpressed in the Hearts of Transgenic Mice. *Circulation*, *104*(20), 2485–2491. https://doi.org/10.1161/hc4501.098933

Köth, J. (2017). *Cardiac L-type calcium channels and expression of RGK proteins in mouse models associated with type 2 diabetes*. https://bonndoc.ulb.uni-bonn.de/xmlui/handle/20.500.11811/7284

Kreusser, M. M., Lehmann, L. H., Keranov, S., Hoting, M. O., Oehl, U., Kohlhaas, M., Reil, J. C., Neumann, K., Schneider, M. D., Hill, J. A., Dobrev, D., Maack, C., Maier, L. S., Gröne, H. J., Katus, H. A., Olson, E. N., & Backs, J. (2014). Cardiac CaM kinase II genes δ and γ contribute to adverse remodeling but redundantly inhibit calcineurin-induced myocardial hypertrophy. *Circulation*, *130*(15), 1262–1273. https://doi.org/10.1161/CIRCULATIONAHA.114.006185

Krief, S., Lönnqvist, F., Raimbault, S., Baude, B., Van Spronsen, A., Arner, P., Strosberg, A. D., Ricquier, D., & Emorine, L. J. (1993). Tissue distribution of beta 3-adrenergic receptor mRNA in man. *The Journal of Clinical Investigation*, *91*(1), 344–349. https://doi.org/10.1172/JCI116191

Kuwano, Y., Adler, M., Zhang, H., Groisman, A., & Ley, K. (2016). Gαi2 and Gαi3 Differentially Regulate Arrest from Flow and Chemotaxis in Mouse Neutrophils. *The Journal of Immunology*, *196*(9), 3828–3833. https://doi.org/10.4049/jimmunol.1500532

Lerman, B. B., Dong, B., Stein, K. M., Markowitz, S. M., Linden, J., & Catanzaro, D. F. (1998). Right ventricular outflow tract tachycardia due to a somatic cell mutation in G protein subunitalphai2. *The Journal of Clinical Investigation*, *101*(12), 2862–2868. https://doi.org/10.1172/JCI1582

Li, J., Ge, Y., Huang, J.-X., Strømgaard, K., Zhang, X., & Xiong, X.-F. (2020). Heterotrimeric G Proteins as Therapeutic Targets in Drug Discovery. *Journal of Medicinal Chemistry*, *63*(10), 5013–5030. https://doi.org/10.1021/acs.jmedchem.9b01452

Liggett, S. B., Tepe, N. M., Lorenz, J. N., Canning, A. M., Jantz, T. D., Mitarai, S., Yatani, A., & Dorn, G. W. (2000). Early and Delayed Consequences of β2-Adrenergic Receptor Overexpression in Mouse Hearts. *Circulation*, *101*(14), 1707–1714. https://doi.org/10.1161/01.CIR.101.14.1707

Lohse, M. J., Engelhardt, S., Danner, S., & Böhm, M. (1996). Mechanisms of β-adrenergic receptor desensitization: from molecular biology to heart failure. *Basic Research in Cardiology*, *91*(1), 29–34. https://doi.org/10.1007/BF00795359

Lohse, M. J., Engelhardt, S., & Eschenhagen, T. (2003). What Is the Role of β-Adrenergic Signaling in Heart Failure? *Circulation Research*, *93*(10), 896–906. https://doi.org/10.1161/01.RES.0000102042.83024.CA

Lymperopoulos, A., Rengo, G., & Koch, W. J. (2013). Adrenergic Nervous System in Heart Failure. *Circulation Research*, *113*(6), 739–753. https://doi.org/10.1161/CIRCRESAHA.113.300308

Madhvani, R. V, Xie, Y., Pantazis, A., Garfinkel, A., Qu, Z., Weiss, J. N., & Olcese, R. (2011). Shaping a new Ca2+ conductance to suppress early afterdepolarizations in cardiac myocytes. *The Journal of Physiology*, *589*(24), 6081–6092. https://doi.org/https://doi.org/10.1113/jphysiol.2011.219600

Mahmood, A., Ahmed, K., & Zhang, Y. (2022). β-Adrenergic Receptor Desensitization/Down-Regulation in Heart Failure: A Friend or Foe? *Frontiers in Cardiovascular Medicine*, *9*. https://www.frontiersin.org/articles/10.3389/fcvm.2022.925692

Mangoni, M. E., Couette, B., Marger, L., Bourinet, E., Striessnig, J., & Nargeot, J. (2006). Voltage-dependent calcium channels and cardiac pacemaker activity: From ionic currents to genes. *Progress in Biophysics and Molecular Biology*, *90*(1), 38–63. https://doi.org/https://doi.org/10.1016/j.pbiomolbio.2005.05.003

Matthes, J. (2022). 4.23 - Ca2+-Channel Inhibitors. In T. Kenakin (Ed.), *Comprehensive Pharmacology* (pp. 507–527). Elsevier. https://doi.org/https://doi.org/10.1016/B978-0-12-820472-6.00092-X

Mauriac, S. A., Hien, Y. E., Bird, J. E., Carvalho, S. D. S., Peyroutou, R., Lee, S. C., Moreau, M. M., Blanc, J. M., Geyser, A., Medina, C., Thoumine, O., Beer-Hammer, S., Friedman, T. B., Rüttiger, L., Forge, A., Nürnberg, B., Sans, N., & Montcouquiol, M. (2017). Defective Gpsm2/Gαi3 signalling disrupts stereocilia development and growth cone actin dynamics in Chudley-McCullough syndrome. *Nature Communications*, *8*. https://doi.org/10.1038/ncomms14907

McDonagh, T. A., Metra, M., Adamo, M., Baumbach, A., Böhm, M., Burri, H., Čelutkiene, J., Chioncel, O., Cleland, J. G. F., Coats, A. J. S., Crespo-Leiro, M. G., Farmakis, D., Gardner, R. S., Gilard, M., Heymans, S., Hoes, A. W., Jaarsma, T., Jankowska, E. A., Lainscak, M., … Koskinas, K. C. (2021). 2021 ESC Guidelines for the diagnosis and treatment of acute and chronic heart failure. In *European Heart Journal* (Vol. 42, Issue 36, pp. 3599–3726). Oxford University Press. https://doi.org/10.1093/eurheartj/ehab368

McDonald, T. F., Pelzer, S., Trautwein, W., & Pelzer, D. (1994). Regulation and modulation of calcium channels in cardiac, skeletal, and smooth muscle cells. *Physiological Reviews*, *74*(2), 365–507. https://doi.org/10.1152/physrev.1994.74.2.365

Milano, C. A., Allen, L. F., Rockman, H. A., Dolber, P. C., McMinn, T. R., Chien, K. R., Johnson, T. D., Bond, R. A., & Lefkowitz, R. J. (1994). Enhanced Myocardial Function in Transgenic Mice Overexpressing the β2-Adrenergic Receptor. *Science*, *264*(5158), 582–586. https://doi.org/10.1126/science.8160017

Ming, Z., Nordin, C., Siri, F., & Aronson, R. S. (1994). Reduced Calcium Current Density in Single Myocytes Isolated from Hypertrophied Failing Guinea Pig Hearts. *Journal of Molecular and Cellular Cardiology*, *26*(9), 1133–1143. https://doi.org/https://doi.org/10.1006/jmcc.1994.1132

Mittmann, C., Pinkepank, G., Stamatelopoulou, S., Wieland, T., Nürnberg, B., Hirt, S., & Eschenhagen, T. (2003). Differential coupling of m-cholinoceptors to Gi/Go-proteins in failing human myocardium. *Journal of Molecular and Cellular Cardiology*, *35*(10), 1241–1249. https://doi.org/https://doi.org/10.1016/S0022-2828(03)00235-9

Moniotte, S., Kobzik, L., Feron, O., Trochu, J.-N., Gauthier, C., & Balligand, J.-L. (2001). Upregulation of β3-Adrenoceptors and Altered Contractile Response to Inotropic Amines in Human Failing Myocardium. *Circulation*, *103*(12), 1649–1655. https://doi.org/10.1161/01.CIR.103.12.1649

Mukherjee, R., Hewett, K. W., & Spinale, F. G. (1995). Myocyte electrophysiological properties following the development of supraventricular tachycardia-induced cardiomyopathy. *Journal of Molecular and Cellular Cardiology*, *27*(6), 1333–1348. https://doi.org/https://doi.org/10.1016/S0022-2828(05)82396-X

Mukherjee, R., Hewett, K. W., Walker, J. D., Basler, C. G., & Spinale, F. G. (1998). Changes in L-type calcium channel abundance and function during the transition to pacing-induced congestive heart failure. *Cardiovascular Research*, *37*(2), 432–444. https://doi.org/10.1016/S0008-6363(97)00128-4

Mukherjee, R., & Spinale, F. G. (1998). L-type Calcium Channel Abundance and Function with Cardiac Hypertrophy and Failure: A Review. *Journal of Molecular and Cellular Cardiology*, *30*(10), 1899–1916. https://doi.org/https://doi.org/10.1006/jmcc.1998.0755

Mustroph, J., Neef, S., & Maier, L. S. (2017). CaMKII as a target for arrhythmia suppression. *Pharmacology & Therapeutics*, *176*, 22–31. https://doi.org/https://doi.org/10.1016/j.pharmthera.2016.10.006

Muth, J. N., Yamaguchi, H., Mikala, G., Grupp, I. L., Lewis, W., Cheng, H., Song, L.-S., Lakatta, E. G., Varadi, G., & Schwartz, A. (1999). Cardiac-specific Overexpression of the α1 Subunit of the L-type Voltage-dependent Ca2+ Channel in Transgenic Mice: LOSS OF ISOPROTERENOL-INDUCED CONTRACTION*. *Journal of Biological Chemistry*, *274*(31), 21503–21506. https://doi.org/https://doi.org/10.1074/jbc.274.31.21503

Nagata, K., Ye, C., Jain, M., Milstone, D. S., Liao, R., & Mortensen, R. M. (2000). Gαi2 but Not Gαi3 Is Required for Muscarinic Inhibition of Contractility and Calcium Currents in Adult Cardiomyocytes. *Circulation Research*, *87*(10), 903–909. https://doi.org/10.1161/01.RES.87.10.903

Nakayama, H., Chen, X., Baines, C. P., Klevitsky, R., Zhang, X., Zhang, H., Jaleel, N., Chua, B. H. L., Hewett, T. E., Robbins, J., Houser, S. R., & Molkentin, J. D. (2007). Ca2+- and mitochondrial-dependent cardiomyocyte necrosis as a primary mediator of heart failure. *The Journal of Clinical Investigation*, *117*(9), 2431–2444. https://doi.org/10.1172/JCI31060

Neumann, J., Scholz, H., Döring, V., Schmitz, W., Meyerinck, L., & Kalmár, P. (1988). INCREASE IN MYOCARDIAL Gi-PROTEINS IN HEART FAILURE. *The Lancet*, *332*(8617), 936–937. https://doi.org/https://doi.org/10.1016/S0140-6736(88)92601-3

Nikolaev, V. O., Bünemann, M., Schmitteckert, E., Lohse, M. J., & Engelhardt, S. (2006). Cyclic AMP Imaging in Adult Cardiac Myocytes Reveals Far-Reaching β1-Adrenergic but Locally Confined β2-Adrenergic Receptor–Mediated Signaling. *Circulation Research*, *99*(10), 1084–1091. https://doi.org/10.1161/01.RES.0000250046.69918.d5

Nikolaev, V. O., Moshkov, A., Lyon, A. R., Miragoli, M., Novak, P., Paur, H., Lohse, M. J., Korchev, Y. E., Harding, S. E., & Gorelik, J. (2010). β2-Adrenergic Receptor Redistribution in Heart Failure Changes cAMP Compartmentation. *Science*, *327*(5973), 1653–1657. https://doi.org/10.1126/science.1185988

Nobles, M., Montaigne, D., Sebastian, S., Birnbaumer, L., & Tinker, A. (2018). Differential effects of inhibitory G protein isoforms on G protein-gated inwardly rectifying K+ currents in adult murine atria. *Am J Physiol Cell Physiol*, *314*, 616–626. https://doi.org/10.1152/ajpcell.00271.2016.-G

BIBLIOGRAPHY

Nubbemeyer, B., Paul George, A. A., Kühl, T., Pepanian, A., Beck, M. S., Maghraby, R., Shetab Boushehri, M., Muehlhaupt, M., Pfeil, E. M., Annala, S. K., Ammer, H., Imhof, D., & Pei, D. (2022). Targeting Gαi/s Proteins with Peptidyl Nucleotide Exchange Modulators. *ACS Chemical Biology*, *17*(2), 463–473. https://doi.org/10.1021/acschembio.1c00929

Nubbemeyer, B., Pepanian, A., Paul George, A. A., & Imhof, D. (2021). Strategies towards Targeting Gαi/s Proteins: Scanning of Protein-Protein Interaction Sites To Overcome Inaccessibility. *ChemMedChem*, *16*(11), 1697–1716. https://doi.org/https://doi.org/10.1002/cmdc.202100039

Nuss, H. B., & Houser, S. R. (1991). Voltage dependence of contraction and calcium current in severely hypertrophied feline ventricular myocytes. *Journal of Molecular and Cellular Cardiology*, *23*(6), 717–726. https://doi.org/https://doi.org/10.1016/0022-2828(91)90981-Q

O'Connell, T. D., Rodrigo, M. C., & Simpson, P. C. (2007). Isolation and Culture of Adult Mouse Cardiac Myocytes. In F. Vivanco (Ed.), *Cardiovascular Proteomics: Methods and Protocols* (pp. 271–296). Humana Press. https://doi.org/10.1385/1-59745-214-9:271

Ouadid, H., Albat, B., & Nargeot, J. (1995). Calcium Currents in Diseased Human Cardiac Cells. *Journal of Cardiovascular Pharmacology*, *25*(2). https://journals.lww.com/cardiovascularpharm/fulltext/1995/02000/calcium_currents_in_diseased_human_cardiac_cells.14.aspx

Packer, M. (1988). Neurohormonal interactions and adaptations in congestive heart failure. *Circulation*, *77*(4), 721–730. https://doi.org/10.1161/01.CIR.77.4.721

Pandey, K. N. (2021). Molecular Signaling Mechanisms and Function of Natriuretic Peptide Receptor-A in the Pathophysiology of Cardiovascular Homeostasis. In *Frontiers in Physiology* (Vol. 12). Frontiers Media S.A. https://doi.org/10.3389/fphys.2021.693099

Papa, A., Kushner, J., & Marx, S. O. (2022). Adrenergic Regulation of Calcium Channels in the Heart. *Annual Review of Physiology*, *84*(1), 285–306. https://doi.org/10.1146/annurev-physiol-060121-041653

Peterson, B. Z., DeMaria, C. D., & Yue, D. T. (1999). Calmodulin Is the Ca2+ Sensor for Ca2+-Dependent Inactivation of L-Type Calcium Channels. *Neuron*, *22*(3), 549–558. https://doi.org/https://doi.org/10.1016/S0896-6273(00)80709-6

Plummer, N. W., Spicher, K., Malphurs, J., Akiyama, H., Abramowitz, J., Nürnberg, B., & Birnbaumer, L. (2012). Development of the mammalian axial skeleton requires signaling through the Gαi subfamily of heterotrimeric G proteins. *Proceedings of the National Academy of Sciences of the United States of America*, *109*(52), 21366–21371. https://doi.org/10.1073/pnas.1219810110

Pogwizd, S. M., & Bers, D. M. (2004). Cellular Basis of Triggered Arrhythmias in Heart Failure. *Trends in Cardiovascular Medicine*, *14*(2), 61–66. https://doi.org/https://doi.org/10.1016/j.tcm.2003.12.002

Pogwizd, S. M., Schlotthauer, K., Li, L., Yuan, W., & Bers, D. M. (2001). Arrhythmogenesis and Contractile Dysfunction in Heart Failure. *Circulation Research*, *88*(11), 1159–1167. https://doi.org/10.1161/hh1101.091193

Poomvanicha, M., Wegener, J. W., Blaich, A., Fischer, S., Domes, K., Moosmang, S., & Hofmann, F. (2011). Facilitation and Ca2+-dependent Inactivation Are Modified by Mutation of the Cav1.2 Channel IQ Motif*. *Journal of Biological Chemistry*, *286*(30), 26702–26707. https://doi.org/https://doi.org/10.1074/jbc.M111.247841

Rae, J. L., & Levis, R. A. (2004). Fabrication of Patch Pipets. *Current Protocols in Neuroscience*, *26*(1), 6.3.1-6.3.32. https://doi.org/https://doi.org/10.1002/0471142301.ns0603s26

Rau, T., Nose, M., Remmers, U., Weil, J., Weißmüller, A., Davia, K., Harding, S., Peppel, K., Koch, W. J., & Eschenhagen, T. (2003). Overexpression of wild-type Gαi-2 suppresses β-adrenergic signaling in cardiac myocytes. *The FASEB Journal*, *17*(3), 1–23. https://doi.org/https://doi.org/10.1096/fj.02-0660fje

Reuter, H. (1979). Properties of Two Inward Membrane Currents in the Heart. *Annual Review of Physiology*, *41*(1), 413–424. https://doi.org/10.1146/annurev.ph.41.030179.002213

Richard, S., Leclercq, F., Lemaire, S., Piot, C., & Nargeot, J. (1998). Ca2+ currents in compensated hypertrophy and heart failure. *Cardiovascular Research*, *37*(2), 300–311. https://doi.org/10.1016/S0008-6363(97)00273-3

Rockman, H. A., Koch, W. J., & Lefkowitz, R. J. (2002). Seven-transmembrane-spanning receptors and heart function. *Nature*, *415*(6868), 206–212. https://doi.org/10.1038/415206a

Rudolph, U., Brabet, P., Hasty, P., Bradley, A., & Birnbaumer, andLUTZ. (1993). Disruption of the Gi2(locus in embryonic stem cells and mice: a modified hit and run strategy with detection by a PCR dependent on gap repair. In *Transgenic Research* (Vol. 2).

Rudolph, U., Finegold, M. J., Rich, S. S., Harriman, G. R., Srinivasan, Y., Brabet, P., Boulay, G., Bradley, A., & Birnbaumer, L. (1995). Ulcerative colitis and adenocarcinoma of the colon in Gαi2-deficient mice. *Nature Genetics*, *10*(2), 143–150. https://doi.org/10.1038/ng0695-143

Rybin, V. O., Xu, X., Lisanti, M. P., & Steinberg, S. F. (2000). Differential targeting of β-adrenergic receptor subtypes and adenylyl cyclase to cardiomyocyte caveolae: A mechanism to functionally regulate the cAMP signaling pathway. *Journal of Biological Chemistry*, *275*(52), 41447–41457. https://doi.org/10.1074/jbc.M006951200

Ryder, K. O., Bryant, S. M., & Hart, G. (1993). Membrane current changes in left ventricular myocytes isolated from guinea pigs after abdominal aortic coarctation. *Cardiovascular Research*, *27*(7), 1278–1287. https://doi.org/10.1093/cvr/27.7.1278

Santos, R., Ursu, O., Gaulton, A., Bento, A. P., Donadi, R. S., Bologa, C. G., Karlsson, A., Al-Lazikani, B., Hersey, A., Oprea, T. I., & Overington, J. P. (2017). A comprehensive map of molecular drug targets. *Nature Reviews Drug Discovery*, *16*(1), 19–34. https://doi.org/10.1038/nrd.2016.230

Savarese, G., Becher, P. M., Lund, L. H., Seferovic, P., Rosano, G. M. C., & Coats, A. J. S. (2022). Global burden of heart failure: a comprehensive and updated review of epidemiology. In *Cardiovascular research* (Vol. 118, Issue 17, pp. 3272–3287). NLM (Medline). https://doi.org/10.1093/cvr/cvac013

Scamps, F., Mayoux, E., Charlemagne, D., & Vassort, G. (1990). Calcium current in single cells isolated from normal and hypertrophied rat heart. Effects of beta-adrenergic stimulation. *Circulation Research*, *67*(1), 199–208. https://doi.org/10.1161/01.RES.67.1.199

Schnabel, P., Böhm, M., Gierschik, P., Jakobs, K.-H., & Erdmann, E. (1990). Improvement of cholera toxin-catalyzed ADP-ribosylation by endogenous ADP-ribosylation factor from bovine brain provides evidence for an unchanged amount of Gsα in failing human myocardium. *Journal of Molecular and Cellular Cardiology*, *22*(1), 73–82. https://doi.org/https://doi.org/10.1016/0022-2828(90)90973-6

Schröder, F., Handrock, R., Beuckelmann, D. J., Hirt, S., Hullin, R., Priebe, L., Schwinger, R. H. G., Weil, J., & Herzig, S. (1998). Increased Availability and Open Probability of Single L-Type Calcium Channels From Failing Compared With Nonfailing Human Ventricle. *Circulation*, *98*(10), 969–976. https://doi.org/10.1161/01.CIR.98.10.969

Schröder, F., & Herzig, S. (1999). Effects of β2-adrenergic stimulation on single-channel gating of rat cardiac L-type Ca2+ channels. *American Journal of Physiology-Heart and Circulatory Physiology*, *276*(3), H834–H843. https://doi.org/10.1152/ajpheart.1999.276.3.H834

Schröper, T., Mehrkens, D., Leiss, V., Tellkamp, F., Engelhardt, S., Herzig, S., Birnbaumer, L., Nürnberg, B., & Matthes, J. (2024). Protective effects of Gαi3 deficiency in a murine heart-failure model of β1-adrenoceptor overexpression. *Naunyn-Schmiedeberg's Archives of Pharmacology*. https://doi.org/10.1007/s00210-023-02751-8

Schwinger, R. H. G. (2021). Pathophysiology of heart failure. In *Cardiovascular Diagnosis and Therapy* (Vol. 11, Issue 1). AME Publishing Company. https://doi.org/10.21037/CDT-20-302

BIBLIOGRAPHY

Scriven, D. R. L., Dan, P., & Moore, E. D. W. (2000). Distribution of Proteins Implicated in Excitation-Contraction Coupling in Rat Ventricular Myocytes. *Biophysical Journal*, *79*(5), 2682–2691. https://doi.org/https://doi.org/10.1016/S0006-3495(00)76506-4

Seisenberger, C., Specht, V., Welling, A., Platzer, J., Pfeifer, A., Kühbandner, S., Striessnig, J., Klugbauer, N., Feil, R., & Hofmann, F. (2000). Functional Embryonic Cardiomyocytes after Disruption of the L-type α1C (Cav 1.2) Calcium Channel Gene in the Mouse*. *Journal of Biological Chemistry*, *275*(50), 39193–39199. https://doi.org/https://doi.org/10.1074/jbc.M006467200

Shaw, R. M., & Colecraft, H. M. (2013). L-type calcium channel targeting and local signalling in cardiac myocytes. *Cardiovascular Research*, *98*(2), 177–186. https://doi.org/10.1093/cvr/cvt021

Simon, M. I., Strathmann, M. P., & Gautam, N. (1991). Diversity of G Proteins in Signal Transduction. *Science*, *252*(5007), 802–808. https://doi.org/10.1126/science.1902986

Tang, W. J., & Gilman, A. G. (1991). Type-specific regulation of adenylyl cyclase by G protein beta gamma subunits. *Science*, *254*, 1500–1503.

Taussig, R., Quarmby, L. M., & Gilman, A. G. (1993). Regulation of purified type I and type II adenylylcyclases by G protein beta gamma subunits. *Journal of Biological Chemistry*, *268*(1), 9–12. https://doi.org/https://doi.org/10.1016/S0021-9258(18)54106-5

Templin, C., Ghadri, J.-R., bastien Rougier, J.-S., Baumer, A., Kaplan, V., Albesa, M., Sticht, H., Rauch, A., Puleo, C., Hu, D., ctor Barajas-Martinez, H., Antzelevitch, C., Lü scher, T. F., Abriel, H., & Duru, F. (2011). Identification of a novel loss-of-function calcium channel gene mutation in short QT syndrome (SQTS6). *European Heart Journal*, *32*, 1077–1088. https://doi.org/10.1093/eurheartj/ehr076

Thompson, B. D., Jin, Y., Wu, K. H., Colvin, R. A., Luster, A. D., Birnbaumer, L., & Wu, M. X. (2007). Inhibition of Gαi2 Activation by Gαi3 in CXCR3-mediated Signaling*. *Journal of Biological Chemistry*, *282*(13), 9547–9555. https://doi.org/https://doi.org/10.1074/jbc.M610931200

Tomaselli, G. F., & Marbán, E. (1999). Electrophysiological remodeling in hypertrophy and heart failure. *Cardiovascular Research*, *42*(2), 270–283. https://doi.org/10.1016/S0008-6363(99)00017-6

Trautwein, W., & Hescheler, J. (1990). Regulation of Cardiac L-Type Calcium Current by Phosphorylation and G Proteins. *Annual Review of Physiology*, *52*(1), 257–274. https://doi.org/10.1146/annurev.ph.52.030190.001353

Triposkiadis, F., Karayannis, G., Giamouzis, G., Skoularigis, J., Louridas, G., & Butler, J. (2009). The Sympathetic Nervous System in Heart Failure. Physiology, Pathophysiology, and Clinical Implications. In *Journal of the American College of Cardiology* (Vol. 54, Issue 19, pp. 1747–1762). https://doi.org/10.1016/j.jacc.2009.05.015

Tsien, R. W., Bean, B. P., Hess, P., Lansman, J. B., Nilius, B., & Nowycky, M. C. (1986). Mechanisms of calcium channel modulation by β-adrenergic agents and dihydropyridine calcium agonists. *Journal of Molecular and Cellular Cardiology*, *18*(7), 691–710. https://doi.org/https://doi.org/10.1016/S0022-2828(86)80941-5

Ungerer, M., Böhm, M., Elce, J. S., Erdmann, E., & Lohse, M. J. (1993). Altered expression of beta-adrenergic receptor kinase and beta 1-adrenergic receptors in the failing human heart. *Circulation*, *87*(2), 454–463. https://doi.org/10.1161/01.CIR.87.2.454

Ungerer, M., Parruti, G., Böhm, M., Puzicha, M., DeBlasi, A., Erdmann, E., & Lohse, M. J. (1994). Expression of beta-arrestins and beta-adrenergic receptor kinases in the failing human heart. *Circulation Research*, *74*(2), 206–213. https://doi.org/10.1161/01.RES.74.2.206

Venetucci, L. A., Trafford, A. W., O'Neill, S. C., & Eisner, D. A. (2008). The sarcoplasmic reticulum and arrhythmogenic calcium release. *Cardiovascular Research*, *77*(2), 285–292. https://doi.org/10.1093/cvr/cvm009

BIBLIOGRAPHY

Wang, W., Zhu, W., Wang, S., Yang, D., Crow, M. T., Xiao, R.-P., & Cheng, H. (2004). Sustained β1-Adrenergic Stimulation Modulates Cardiac Contractility by Ca2+/Calmodulin Kinase Signaling Pathway. *Circulation Research*, *95*(8), 798–806. https://doi.org/10.1161/01.RES.0000145361.50017.aa

Wang, Z., Dela Cruz, R., Ji, F., Guo, S., Zhang, J., Wang, Y., Feng, G. S., Birnbaumer, L., Jiang, M., & Chu, W. M. (2014). Giα proteins exhibit functional differences in the activation of ERK1/2, Akt and mTORC1 by growth factors in normal and breast cancer cells. *Cell Communication and Signaling*, *12*(1). https://doi.org/10.1186/1478-811X-12-10

Waterson, R. E., Thompson, C. G., Mabe, N. W., Kaur, K., Talbot, J. N., Neubig, R. R., & Rorabaugh, B. R. (2011). Gαi2-mediated protection from ischaemic injury is modulated by endogenous RGS proteins in the mouse heart. *Cardiovascular Research*, *91*(1), 45–52. https://doi.org/10.1093/cvr/cvr054

Weiss, J. N., Garfinkel, A., Karagueuzian, H. S., Chen, P. S., & Qu, Z. (2010). Early afterdepolarizations and cardiac arrhythmias. *Heart Rhythm*, *7*(12), 1891–1899. https://doi.org/10.1016/j.hrthm.2010.09.017

Weissgerber, P., Held, B., Bloch, W., Kaestner, L., Chien, K. R., Fleischmann, B. K., Lipp, P., Flockerzi, V., & Freichel, M. (2006). Reduced Cardiac L-Type Ca2+ Current in Cavβ2−/− Embryos Impairs Cardiac Development and Contraction With Secondary Defects in Vascular Maturation. *Circulation Research*, *99*(7), 749–757. https://doi.org/10.1161/01.RES.0000243978.15182.c1

Wettschureck, N., & Offermanns, S. (2005). Mammalian G Proteins and Their Cell Type Specific Functions. *Physiological Reviews*, *85*(4), 1159–1204. https://doi.org/10.1152/physrev.00003.2005

Wiege, K., Ali, S. R., Gewecke, B., Novakovic, A., Konrad, F. M., Pexa, K., Beer-Hammer, S., Reutershan, J., Piekorz, R. P., Schmidt, R. E., Nürnberg, B., & Gessner, J. E. (2013). Gαi2 Is the Essential Gαi Protein in Immune Complex–Induced Lung Disease. *The Journal of Immunology*, *190*(1), 324–333. https://doi.org/10.4049/jimmunol.1201398

Woo, A. Y.-H., Song, Y., Xiao, R.-P., & Zhu, W. (2015). Biased β2-adrenoceptor signalling in heart failure: pathophysiology and drug discovery. *British Journal of Pharmacology*, *172*(23), 5444–5456. https://doi.org/https://doi.org/10.1111/bph.12965

Wu, Y., Zeng, L., & Zhao, S. (2021). Ligands of Adrenergic Receptors: A Structural Point of View. *Biomolecules*, *11*(7). https://doi.org/10.3390/biom11070936

Xiao, R. P., Zhang, S. J., Chakir, K., Avdonin, P., Zhu, W., Bond, R. A., Balke, C. W., Lakatta, E. G., & Cheng, H. (2003). Enhanced Gi signaling selectively negates β 2-adrenergic receptor (AR)- but not β1-AR-mediated positive inotropic effect in myocytes from failing rat hearts. *Circulation*, *108*(13), 1633–1639. https://doi.org/10.1161/01.CIR.0000087595.17277.73

Xiao, R.-P. (2001). β-Adrenergic Signaling in the Heart: Dual Coupling of the β2-Adrenergic Receptor to Gs and Gi Proteins. *Science's STKE*, *2001*(104), re15–re15. https://doi.org/10.1126/stke.2001.104.re15

Xiao, R.-P., Avdonin, P., Zhou, Y.-Y., Cheng, H., Akhter, S. A., Eschenhagen, T., Lefkowitz, R. J., Koch, W. J., & Lakatta, E. G. (1999). Coupling of β2-Adrenoceptor to Gi Proteins and Its Physiological Relevance in Murine Cardiac Myocytes. *Circulation Research*, *84*(1), 43–52. https://doi.org/10.1161/01.RES.84.1.43

Xiao, R.-P., Ji, X., & Lakatta, E. G. (1995). Functional coupling of the beta 2-adrenoceptor to a pertussis toxin-sensitive G protein in cardiac myocytes. *Molecular Pharmacology*, *47*(2), 322. http://molpharm.aspetjournals.org/content/47/2/322.abstract

Xiao, R.-P., Zhu, W., Zheng, M., Cao, C., Zhang, Y., Lakatta, E. G., & Han, Q. (2006). Subtype-specific α1- and β-adrenoceptor signaling in the heart. *Trends in Pharmacological Sciences*, *27*(6), 330–337. https://doi.org/https://doi.org/10.1016/j.tips.2006.04.009

Yamada, K. A., & Corr, P. B. (1992). Effects of β-Adrenergic Receptor Activation on Intracellular Calcium and Membrane Potential in Adult Cardiac Myocytes. *Journal of Cardiovascular Electrophysiology*, *3*. https://api.semanticscholar.org/CorpusID:72991663

BIBLIOGRAPHY

Yang, K.-C., Wang, W., & Nerbonne, J. M. (2014). Patch-Clamp Recordings from Isolated Cardiac Myocytes. In *Manual of Research Techniques in Cardiovascular Medicine* (pp. 50–59). https://doi.org/https://doi.org/10.1002/9781118495148.ch6

Yang, L., Katchman, A., Morrow, J. P., Doshi, D., & Marx, S. O. (2011). Cardiac L-type calcium channel (Ca v 1.2) associates with γ subunits. *The FASEB Journal • Research Communication*, *25*(3), 928–936. https://doi.org/10.1096/fj.10-172353

Young, A., Jiang, M., Wang, Y., Ahmedli, N. B., Ramirez, J., Reese, B. E., Birnbaumer, L., & Farber, D. B. (2011). Specific interaction of Gαi3 with the Oa1 G-protein coupled receptor controls the size and density of melanosomes in retinal pigment epithelium. *PLoS ONE*, *6*(9). https://doi.org/10.1371/journal.pone.0024376

Yue, D. T., Herzig, S., & Marban, E. (1990). Beta-adrenergic stimulation of calcium channels occurs by potentiation of high-activity gating modes. *Proceedings of the National Academy of Sciences*, *87*(2), 753–757. https://doi.org/10.1073/pnas.87.2.753

Zamponi, G. W., Striessnig, J., Koschak, A., & Dolphin, A. C. (2015). The Physiology, Pathology, and Pharmacology of Voltage-Gated Calcium Channels and Their Future Therapeutic Potential. *Pharmacological Reviews*, *67*(4), 821. https://doi.org/10.1124/pr.114.009654

Zeng, J., & Rudy, Y. (1995). Early afterdepolarizations in cardiac myocytes: mechanism and rate dependence. *Biophysical Journal*, *68*(3), 949–964. https://doi.org/10.1016/S0006-3495(95)80271-7

Zhang, X. Q., Moore, R. L., Tillotson, D. L., & Cheung, J. Y. (1995). Calcium currents in postinfarction rat cardiac myocytes. *American Journal of Physiology-Cell Physiology*, *269*(6), C1464–C1473. https://doi.org/10.1152/ajpcell.1995.269.6.C1464

Zheng, M., Zhu, W., Han, Q., & Xiao, R.-P. (2005). Emerging concepts and therapeutic implications of β-adrenergic receptor subtype signaling. *Pharmacology & Therapeutics*, *108*(3), 257–268. https://doi.org/https://doi.org/10.1016/j.pharmthera.2005.04.006

Zhu, W.-Z., Zheng, M., Koch, W. J., Lefkowitz, R. J., Kobilka, B. K., & Xiao, R.-P. (2001). Dual modulation of cell survival and cell death by. *Proceedings of the National Academy of Sciences*, *98*(4), 1607–1612. https://doi.org/10.1073/pnas.98.4.1607

Zuberi, Z., Birnbaumer, L., & Tinker, A. (2008). The role of inhibitory heterotrimeric G proteins in the control of in vivo heart rate dynamics. *American Journal of Physiology - Regulatory Integrative and Comparative Physiology*, *295*(6). https://doi.org/10.1152/ajpregu.90625.2008

Zuberi, Z., Nobles, M., Sebastian, S., Dyson, A., Lim, S. Y., Breckenridge, R., Birnbaumer, L., & Tinker, A. (2010). Absence of the inhibitory g-protein gαi2 predisposes to ventricular cardiac arrhythmia. *Circulation: Arrhythmia and Electrophysiology*, *3*(4), 391–400. https://doi.org/10.1161/CIRCEP.109.894329

Appendix

S1- Mouse Genotyping

- **DNA isolation**: genomic gDNA was isolated from mouse biopsies by using KAPA Express Extract Kit (from KAPABIOSYSTEMS- KR0383), a thermostable protease and buffer system that allows for the extraction of PCR-ready DNA from various tissue types.

- **Standard PCR reaction mix used for genotyping:**

Reagent	per 25 µl reaction	End Conc.
KAPA Taq Ready Mix (2X)*	12,5 µl	1X
Forward Primer (stock 10 µM)	1,25 µl	0.5 µM
Reverse Primer (stock 10 µM)	1,25 µl	0.5 µM
Template g-DNA	1 µl	-
dd H_2O	(up to 25µl)	-

* KAPA Taq Ready Mix PCR Kit (KR0354): is a ready-to-use cocktail containing all components for PCR, except primers and template. It contains KAPA Taq DNA Polymerase (0.5 U per 25 µL reaction), KAPA Taq Buffer, dNTPs (0.2 mM of each dNTP at 1X), MgCl2 (1.5 mM at 1X) and stabilizers.

- **Standard PCR thermocycler program for genotyping:**

Step	Temperature °C	Duration	Cycles
1. Hotstart (Hold)	95 °C	Hold	1
2. Initial Denaturation	95 °C	0:03:00	1
3. Denaturation	95 °C	0:00:15	35
4. Annealing	T_m – 5°C[1]	0:00:15[2]	35
5. Extension	72 °C	0:00:15[2]	35
► go to 3 rep. 32			
6. Amplification	72 °C	0:01:00	1
7. Hold	4 °C	Hold	1

1. The annealing temperature should be 5°C lower than the calculated melting temperature (Tm) of the primer.
2. The annealing and extension time is recommended to be 15 sec each when the targeted amplicons are less than 1 kb.

❖ Exemplary genotyping results

I. Transgenic gene, expected band: 300 bp

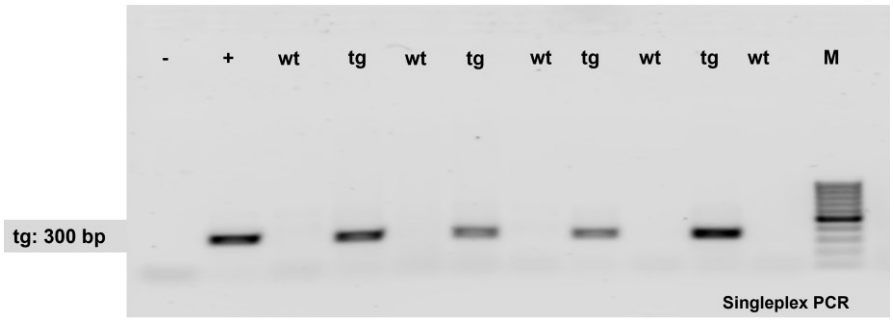

II. GNAI3 gene, expected bands: Wt: 805 bp, Mut: 500 bp

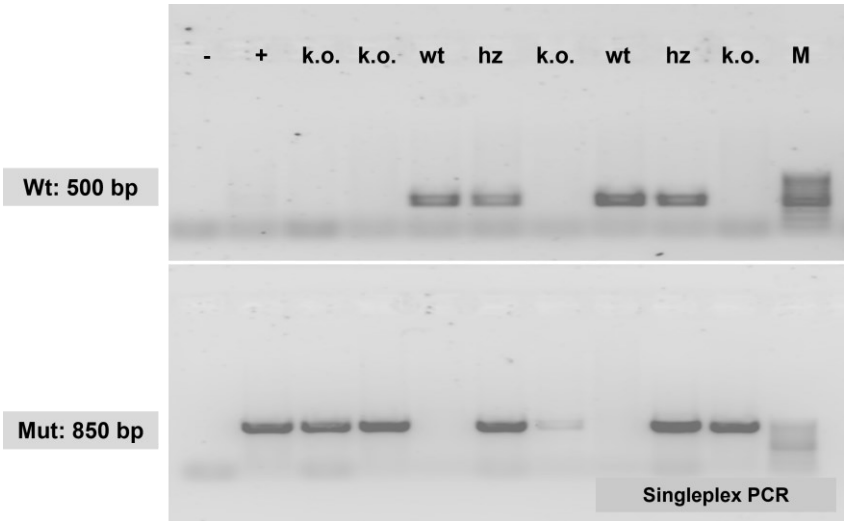

III. GNAI2 gene, expected bands: Wt: 500 bp, Mut: 850 bp

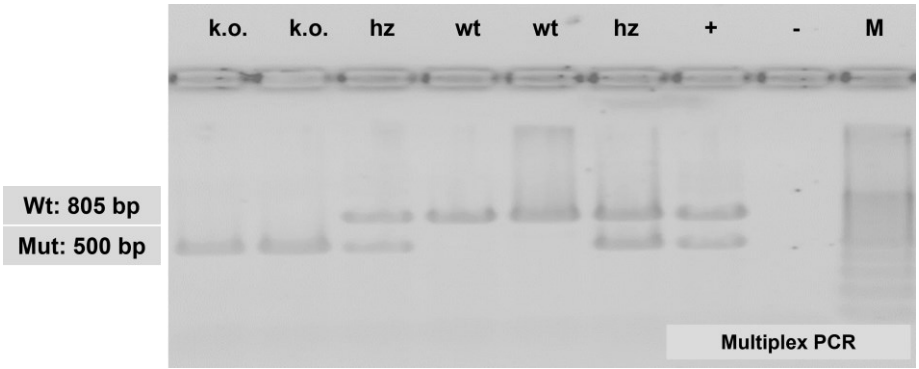

Fig. S1. Exemplary PCR-genotyping results for transgenic β_1-AR, GNAI3 (Gαi3), and GNAI2 (Gαi2) genes (wt: wild-type, k.o.: knock-out, hz: heterozygous, m: marker, bp: base pairs, "+" for positive and "–" for negative controls, respectively).

S2- Human Gα$_i$ structure and amino acid sequence

A

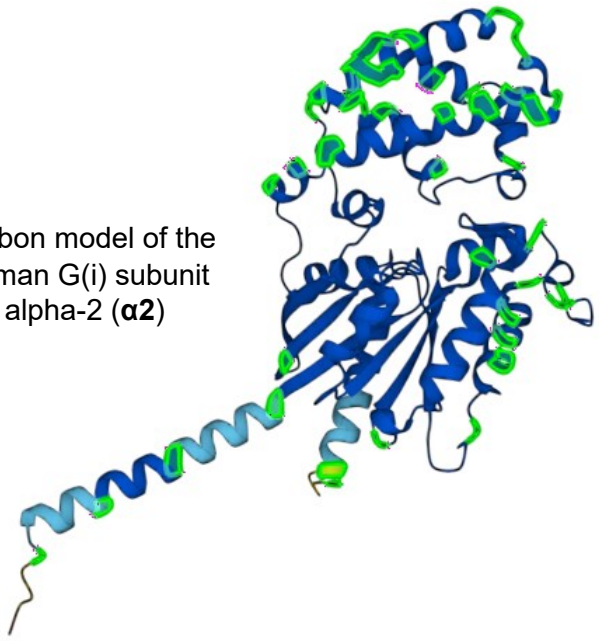

B

Fig. S2. Human Gα$_i$ structure and its amino acid sequence. (A) the structure of human G(i) subunit alpha-2 with the amino acid residues that differ from G(i) subunit alpha-3 indicated by the green label. This structure was generated and labelled using the AlphaFold Protein Structure Database (Code: AF-P04899-F1). **(B)** The protein sequences were identified and aligned using the Uniport data bank with the following entry codes: for human GNAI2 (P04899) and GNAI3 (P08754). The amino acid sequence similarity was found to be 85.88% based on the percent identity matrix (Last accessed on January 31, 2024, from https://www.uniprot.org/align).

S3- List of Chemicals and Suppliers

Item	Order No.	Supplier
Adenosin-5′-triphosphat Magnesium	A9187	Sigma-Aldrich (Merc)
2,3-Butanedione monoxime (BDM)	B0753	Sigma-Aldrich (Merc)
Calcium Chloride		Roth
Cesium chlorid	8627.3	Roth
Cesium hydroxid (CsOH)	232041	Sigma-Aldrich
Collagenase Type II	LS004176	Worthington-Biochem
Dimethyl sulfoxid (DMSO)	D8418	Sigma
Ethylene glycol tetra acetic acid (EGTA)	E4378	Sigma
Fetal Calf Serum	S05615	Biochrome
Glucose	G5767	Sigma-Aldrich (Merc)
HEPES	H3375	Sigma-Aldrich (Merc)
Isoprenalin hydrochloride	5627	sigma
L(+)-Ascorbic acid	6288.1	Roth
Magnesium Chloride	A1411533948	EMSURE
Magnesium sulfate heptahydrate	A172986	Sigma-Aldrich (Merc)
Protease Type XIV	P5147	Sigma
Potassium bicarbonate	P748	Roth
Potassium chloride	P4504	Sigma-Aldrich (Merc)
Potassium phosphate monobasic	4873	Sigma-Aldrich (Merc)
Sodium bicarbonate	6329	Sigma-Aldrich (Merc)
Sodium chloride	3957.2	Roth
Sodium phosphate dibasic	6580	Sigma-Aldrich (Merc)
Taurine	T0625	Sigma-Aldrich (Merc)

S4- Summary of Isoproterenol [1µM] effects on $I_{Ca,L}$ properties

S4- I

Wildtype	[4-5] months		[10-11] months	
	Basal	1µM ISO	Basal	1µM ISO
Parameters				
Number of animals	5	3	6	4
Number of cells, *n*	10-15	5-7	15-18	12-14
Cm (pF)	209.4±41	208.1±30.4	225.3±50.2	224.7±55.5
$I_{Ca,L\ peak}$ (pA/pF)	-8.09±1.9	-12.4±2.7	-8.06±1.6	-13.6±5.2
V_{rev} (mV)	50.8±3.6	56.1±4.3	55.5±6.1	56.2±6.6
$V_{0.5_act}$ (mV)	-13.3±4.7	-20.4±3.4	-11.30±2.5	-17.0±4.0
$k_{_act}$ (mV)	4.1±0.6	2.8±0.2	3.9±0.7	3.1±0.9
$V_{0.5_inact}$ (mV)	-28.8±3.7	-28.1±2.0	-26.0±3.1	-29.5±4.3
$k_{_inact}$ (mV)	-5.3±0.8	-4.5±0.3	-4.6±0.8	-4.8±0.8

S4- II

β_1-tg	[4-5] months		[10-11] months	
	Basal	1µM ISO	Basal	1µM ISO
Parameters				
Number of animals	3	3	6	3
Number of cells, *n*	11-14	9	16-17	12-14
Cm (pF)	212.4±56.6	226.0±61.6	220.4±59.5	206.7±51
$I_{Ca,L\ peak}$ (pA/pF)	-5.7±1.8	-7.9±2.7	-5.5±1.5	-7.3±1.9
V_{rev} (mV)	49.1±4.8	51.6±5.6	49.9±4.6	55.0±4.0
$V_{0.5_act}$ (mV)	-9.4±3.6	-14.49±4.4	-7.6±2.8	-9.7±4.6
$k_{_act}$ (mV)	5.1±0.8	3.9±0.9	5.3±0.9	5.1±0.6
$V_{0.5_inact}$ (mV)	-26.4±3.6	-25.6±3.1	-26.0±3.2	-26.8±4.9
$k_{_inact}$ (mV)	-5.19±1.0	-4.5±0.6	-5.0±0.6	-5.2±1.2

Data are presented as mean± SD.

S5- Mono *versus* Bi-exponential occurrence (Basal Conditions)

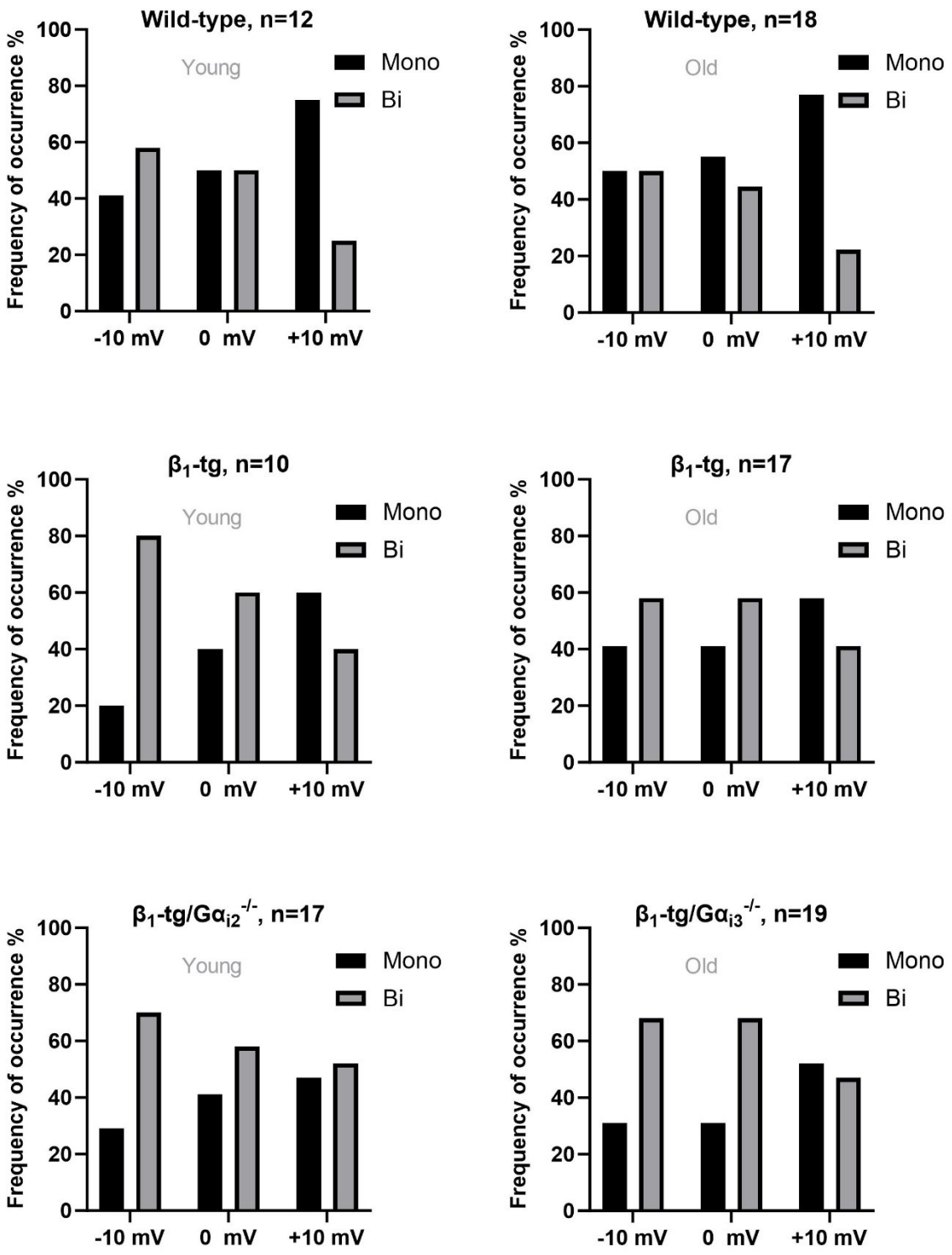

Fig. S5. Statistical analysis was conducted on all genotypes to determine the best fit for $I_{Ca,L}$ (under basal conditions) using either mono or bi-exponential algorithms. At voltages near V_{peak} (-10 to +10 mV), $I_{Ca,L}$ exhibited a bi-exponential decay, enabling the identification of fast and slow time constants. However, over the voltage range (-20 to +40 mV), $I_{Ca,L}$ decay was best described with a mono-exponential fit.

S6- Mono *versus* Bi-exponential occurrence (after exposure to 1 µM Iso)

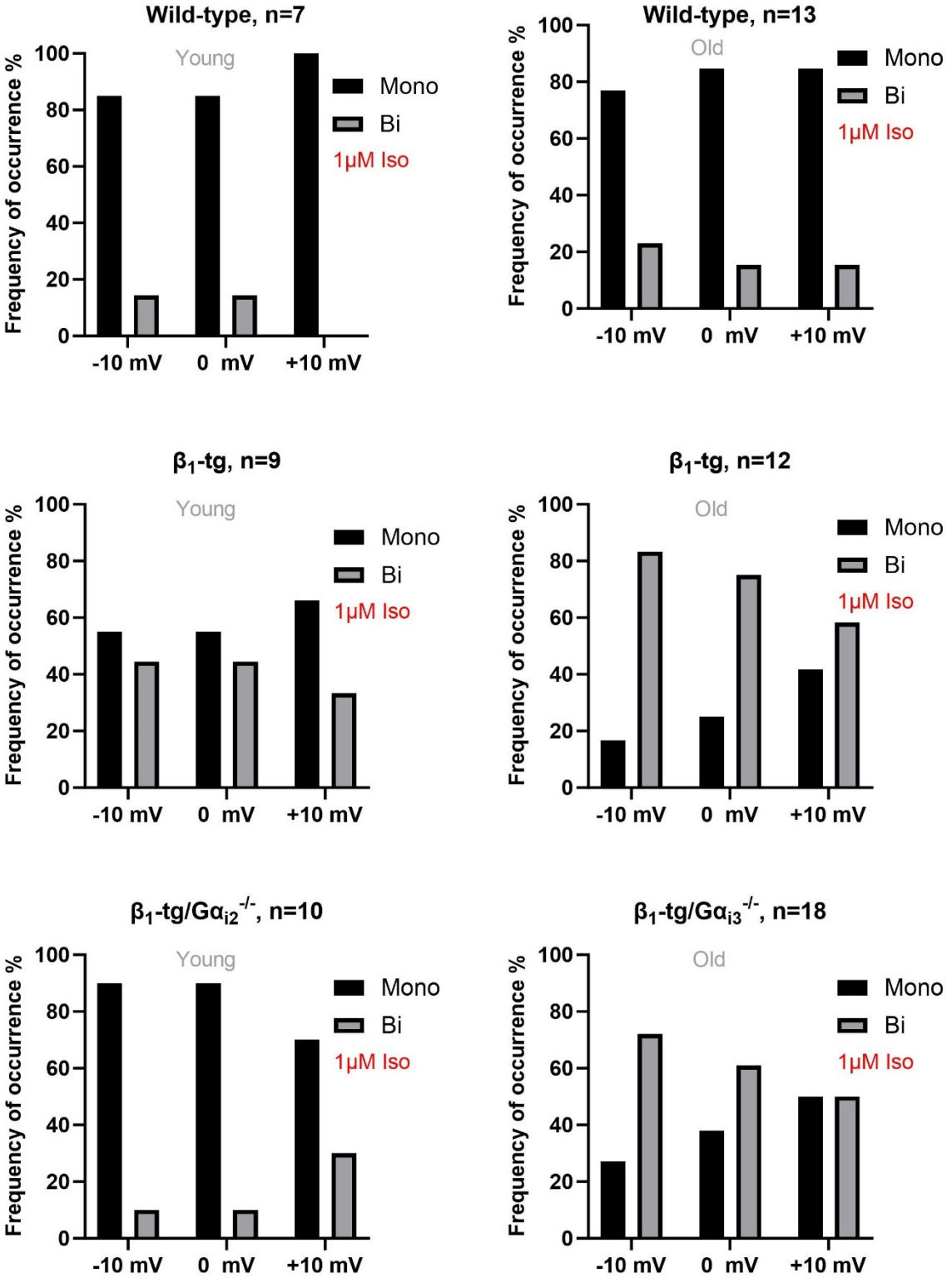

Fig. S6. Statistical analysis was conducted on all genotypes to determine the best fit for $I_{Ca,L}$ (under basal conditions) using either mono or bi-exponential algorithms. Unlike basal conditions, at voltages near Vpeak (-10 to +10 mV), $I_{Ca,L}$ decay was best described by a mono-exponential fit, particularly in genotypes with a pronounced response to Iso, i.e., wildtype and β_1-tg/$G\alpha_{i2}^{-/-}$.

S7- Preliminary results on the effect of lack of $G\alpha_{i3}$ in young mice

As the effect of $G\alpha_{i2}$ deficiency on $I_{Ca,L}$ was studied in young mice, it would be beneficial to examine the effect of $G\alpha_{i3}$ deficiency within the same age range. Unfortunately, due to technical problems encountered during the study, data could only be collected from one young β_1-tg/$G\alpha_{i3}^{-/-}$ animal (26 weeks). Therefore, the following results are preliminary data that compare effects in β_1-tg/$G\alpha_{i3}^{-/-}$ myocytes and young wild-type and β_1-tg myocytes.

Basal $I_{ca,L}$:

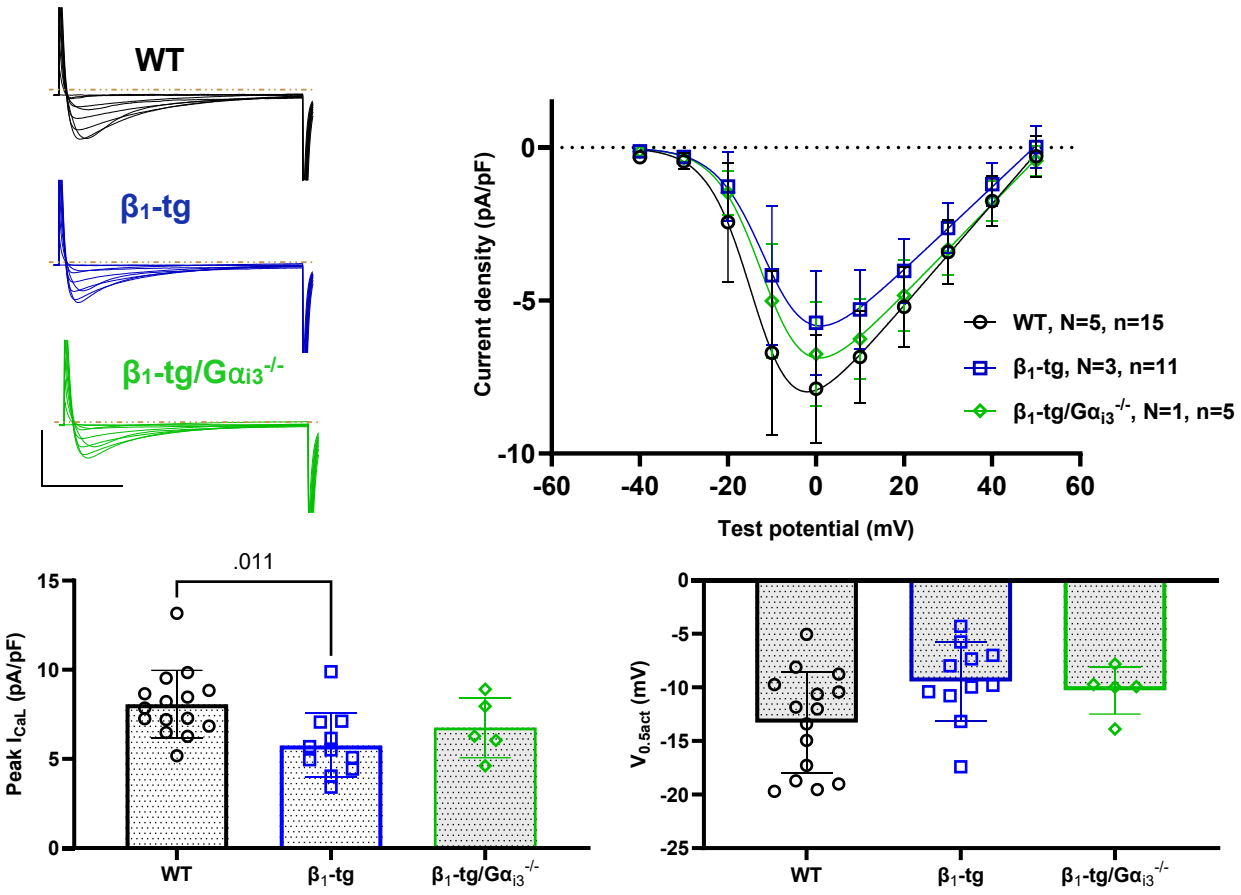

$I_{ca,L}$ with 1 µM Iso:

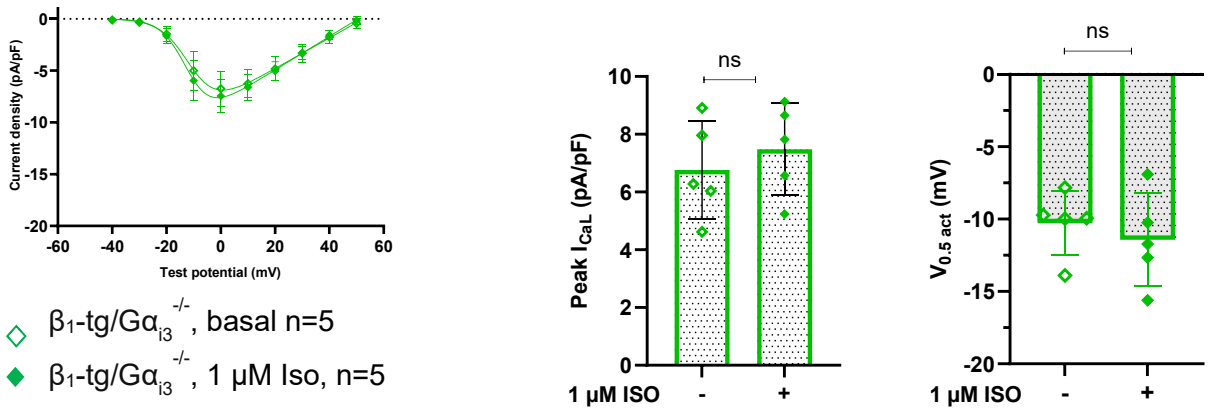

Data are presented as mean± SD.

S8- Preliminary results on the effect of $G\alpha_{i3}$ deficiency on $I_{Ca,L}$ recovery properties (young mice)

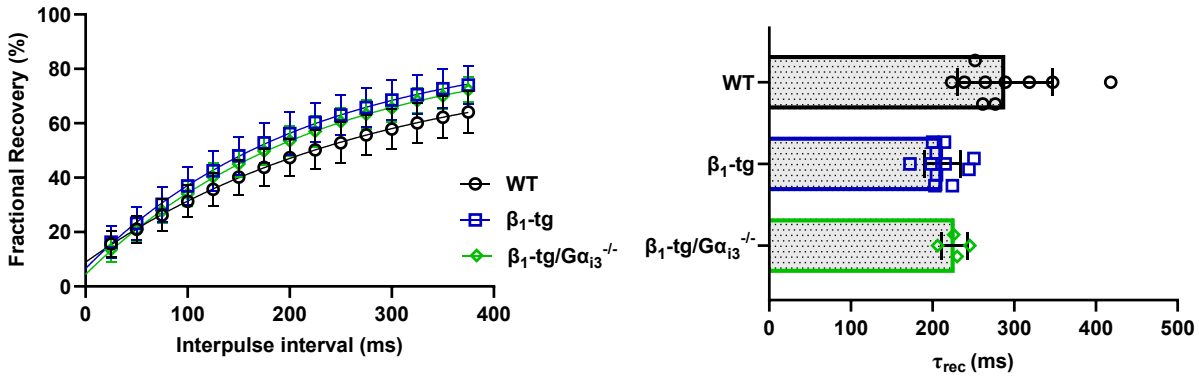

Table S-8. $I_{Ca,L}$ recovery from inactivation parameters in cardiomyocytes from 4-5 m old mice

	n	τ_{rec} (ms)	Half-life ($t_{1/2}$) (ms)	Recovery at 375 ms (%)
Wildtype	10	289.1 ± 58.3	200.4 ± 40.4	64.1 ± 7.5
β_1-tg	11	212.0 ± 21.9	147.0 ± 15.2	75.0 ± 6.5
β_1-tg/$G\alpha_{i3}^{-/-}$	4	227.0 ± 16.1	157.4 ± 11.2	72.2 ± 4.6

Data (mean ± SD). No significant differences

S9- Preliminary results on the effect of $G\alpha_{i3}^{-/-}$ on $I_{Ca,L}$ density

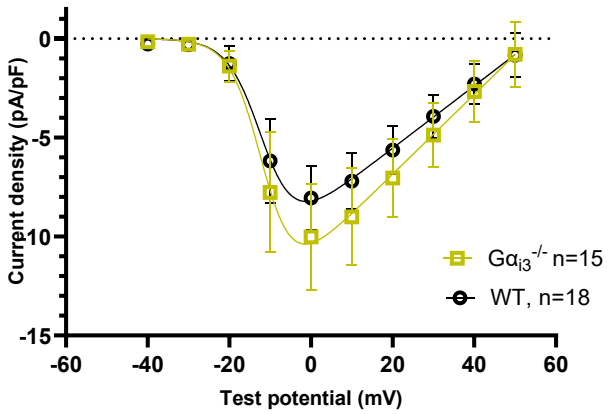

Effect of $G\alpha_{i3}$ deficiency on ventricular I_{CaL} density in murine ventricular myocytes. Whole-cell I_{CaL} density is increased in $G\alpha_{i3}^{-/-}$ mice compared to wildtype mice of the same age. Data are presented as mean ± SD.

●■■■●●■■■●

Acknowledgment

Thanks to …

My Doktorvater **Jan Matthes**, who gave me the chance to be part of his team. There will be no more "knocking on your door to say: the mouse is ready"...or late evenings to “pass by my door and say: see you tomorrow”, but there will be lifelong gratitude and fond memories.

Prof. Dr. **Rosenkranz** and Dr. **Nguemo**, who agreed to supervise my project and encouraged me from the first meeting to the last. I will always remember your valuable lesson, to embrace the challenges and move forward.

The **Animal Care Team** at Cologne University Hospital... one by one... you are great, and without you our work would not even be possible.

The IPHS Graduation Program Team, Dr. **Aszyk** and Ms. **Evers**, for their kindness and all the immediate actions and support they provide.

Members of the Center for Pharmacology, Dr. **Elza** Kuzmenkina, Ms. **Cora** Fried and for the “important” coffee time with Prof. Dr. **Markus** Pietsch.

The most valuable result I got during and from this journey… **Sarah**, **Verena**. and **Sigrid**.. our journey will never end.

My **besties**, my shadows on the earth when the sun is covered with clouds.

My **parents**... across thousands of miles of longing and empty pictures... wave to me with love and say: we are proud and if you would see tears in our eyes, it is just because we cannot be with you.

My beloved **husband**, from all my airs and graces to the little things I do... Everything is pointless without you ♡

Danke. شكرا. Merci

Curriculum Vitae

Nour Katnahji, M.Sc. (She/her)

09/2019 – 07/2024	**Doctoral Student** IPHS Graduation Program – (since July 2020) Medical Faculty - University of Cologne Center for Pharmacology - RG: Prof. Dr. Jan Matthes
09/2015 – 06/2018	**Biomedical Sciences (M.Sc.)** Bonn-Rhein-Sieg University of Applied Sciences Grade: Master of Science - good
09/2009 – 08/2014	**Pharmacy and Pharmaceutical Chemistry (B.Sc.)** Pharmacy Faculty - University of Aleppo Bachelor Project: "Cosmetics and pharmaceutical applications" Grade: Bachelor of Science/Diploma – very good
09/2006 – 07/2009	**General Secondary Education (Scientific Branch)** Al-Nil High School – Aleppo, Syria Grade: Higher Education Entrance Qualification

Scientific Contributions

- Katnahji, N., & Matthes, J. (2023). Differential modulation of ventricular Ca2+ currents by absence of Gαi2 or Gαi3 in a murine β1-transgenic heart failure model (**Abstract**); Naunyn-Schmiedeberg's Archives of Pharmacology, 396(1), S29–S29. https://doi.org/10.1007/s00210-023-02397-6

- Differential modulation of ventricular Ca^{2+} currents by absence of $G\alpha_{i2}$ or $G\alpha_{i3}$ in a murine β_1 transgenic heart failure model – Katnahji & Matthes, 2023, **(Poster Presentation)**; 8th German PHARM-TOX SUMMIT, Ulm, Germany

- Effect of $G\alpha_{i3}$-protein deficiency on ventricular Ca^{2+} currents in a β_1-adrenoceptor overexpressing mouse model of heart failure – Katnahji & Matthes, 2022, **(Poster Presentation)**; 4th European Calcium Channel Conference – Alpbach, Austria

- Modulation of action potential firing by the antiepileptic drug carbamazepine in human induced pluripotent stem cell (iPSC)-derived neurons *in vitro*" – **(Master Thesis, 2018)** – Bonn-Rhine-Sieg University of Applied Sciences

Funding and Award

DAAD Fellowship for Master Study in Germany (2015-2018)

Erklärung

Hiermit versichere ich an Eides statt, dass ich die vorliegende Dissertationsschrift selbstständig und ohne die Benutzung anderer als der angegebenen Hilfsmittel angefertigt habe. Alle Stellen - einschließlich Tabellen, Karten und Abbildungen -, die wörtlich oder sinngemäß aus veröffentlichten und nicht veröffentlichten anderen Werken im Wortlaut oder dem Sinn nach entnommen sind, sind in jedem Einzelfall als Entlehnung kenntlich gemacht. Ich versichere an Eides statt, dass diese Dissertationsschrift noch keiner anderen Fakultät oder Universität zur Prüfung vorgelegen hat; dass sie - abgesehen von unten angegebenen Teilpublikationen- noch nicht veröffentlicht worden ist sowie, dass ich eine solche Veröffentlichung vor Abschluss der Promotion nicht ohne Genehmigung der / des Vorsitzenden des IPHS-Promotionsausschusses vornehmen werde. Die Bestimmungen dieser Ordnung sind mir bekannt. Die von mir vorgelegte Dissertation ist von Prof. Dr. Jan Matthes betreut worden.

Darüber hinaus erkläre ich hiermit, dass ich die Ordnung zur Sicherung guter wissenschaftlicher Praxis und zum Umgang mit wissenschaftlichem Fehlverhalten der Universität zu Köln gelesen und sie bei der Durchführung der Dissertation beachtet habe und verpflichte mich hiermit, die dort genannten Vorgaben bei allen wissenschaftlichen Tätigkeiten zu beachten und umzusetzen.

Übersicht der Publikationen

Katnahji, N., & Matthes, J. (2023). Differential modulation of ventricular Ca2+ currents by absence of Gαi2 or Gαi3 in a murine β1-transgenic heart failure model **(Abstract)**; Naunyn-Schmiedeberg's Archives of Pharmacology, 396(1), S29–S29. https://doi.org/10.1007/s00210-023-02397-6

Ich versichere, dass ich alle Angaben wahrheitsgemäß nach bestem Wissen und Gewissen gemacht habe und verpflichte mich, jedmögliche, die obigen Angaben betreffenden Veränderungen, dem IPHS-Promotionsausschuss unverzüglich mitzuteilen.

27.08.2024
Datum

Nour Katnahji
Unterschrift